TECHNICAL REPORT STANDARD TITLE PAGE

1. Report No.	2. Government Accession No.	3. Recipient's Catalog No.
FHWA/TX-11/0-6022-2		

4. Title and Subtitle	5. Report Date
RECOMMENDATIONS FOR DESIGN, CONSTRUCTION, AND MAINTENANCE OF BRIDGE APPROACH SLABS	September 2011 Published: May 2012
	6. Performing Organization Code
7. Author(s)	8. Performing Organization Report No.
Anand J. Puppala, Ekarut Archeewa, Sireesh Saride, Soheil Nazarian and Laureano Hoyos	Report 0-6022-2
9. Performing Organization Name and Address	10. Work Unit No. (TRAIS)
Department of Civil Engineering The University of Texas at Arlington Arlington, Texas 76019	11. Contract or Grant No. Project 0-6022
12. Sponsoring Agency Name and Address	13. Type of Report and Period Covered
Texas Department of Transportation Research and Technology Implementation Office P. O. Box 5080 Austin, Texas 78763-5080	Technical Report: September 2007–August 2011
	14. Sponsoring Agency Code

15. Supplementary Notes

Project performed in cooperation with the Texas Department of Transportation and the Federal Highway Administration.

Project Title: Recommendations for Design, Construction, and Maintenance of Bridge Approach Slabs

URL: http://tti.tamu.edu/documents/0-6022-2.pdf

16. Abstract

Settlement and heave related movements of bridge approach slabs relative to bridge decks create a bump in the roadway. Several problems arise from these bumps, which include poor riding conditions, potential vehicle damage, loss of vehicle control causing injuries or even casualities, lowered perception of the department's road works, increased maintenance works, and constant delays to rehabilitate the distressed lanes. All these make this bump problem a major maintenance problem in Texas. Several mitigation methods have been employed, and the results are not always satisfactory. In the present research, two treatment methods are investigated for controlling settlements of approach slabs of new bridge construction. Researchers from UTA and UTEP performed two phases to accomplish these studies. During the first phase, the documented information that covers various methods used so far for approach slab settlement mitigation technologies is compiled and presented. The second and final phase focused on field evaluation studies of deep soil mixing and light weight embankment fill treatment methods in reducing settlements. A few other technologies were also evaluated for reducing settlements of existing bridge approach slabs. Both design and construction specifications of the new methods that provided effective treatments in field conditions are presented.

17. Key Word	18. Distribution Statement
Bridge Approach Settlements, Deep Soil Mixing, Expanded Clay Shale, Embankment, Clay	No restrictions. This document is available to the public through NTIS: National Technical Information Service Alexandria, Virginia 22312 http://www.ntis.gov

19. Security Classif. (of this report)	20. Security Classif. (of this page)	21. No. of Pages	22. Price
Unclassified	Unclassified	386	

Form DOT F 1700.7 (8-72)

RECOMMENDATIONS FOR DESIGN, CONSTRUCTION, AND MAINTENANCE OF BRIDGE APPROACH SLABS

by

Anand J. Puppala, Ph.D., PE
Professor
The University of Texas at Arlington

Ekarut Archeewa, Ph.D.
Former Doctoral Student
The University of Texas at Arlington

Sireesh Saride, Ph.D.
Former Post-Doctoral Fellow
The University of Texas at Arlington

Laureano Hoyos, Ph.D., PE
Associate Professor
The University of Texas at Arlington

and

Soheil Nazarian, Ph.D., PE
Professor
The University of Texas at El Paso

Project 0-6022
Report 0-6022-2
Project Title: Recommendations for Design, Construction, and Maintenance of Bridge Approach Slabs

Performed in cooperation with the
Texas Department of Transportation
and the
Federal Highway Administration

September 2011
Published: May 2012

The University of Texas at Arlington
Arlington, Texas 76019

DISCLAIMER

The contents of this report reflect the views of the authors/principal investigators who are responsible for the facts and the accuracy of the data presented herein. The contents do not necessarily reflect the views or policies of the Federal Highway Administration (FHWA) or the Texas Department of Transportation (TxDOT). This report does not constitute a standard, specification, or regulation.

The United States Government and the State of Texas do not endorse products or manufacturers. Trade or manufacturers' names appear here solely because they are considered essential to the object of this report.

ACKNOWLEDGMENTS

This study was supported by TxDOT under Research Project No. 0-6022. The authors acknowledge the following individuals and companies:

- Richard Williammee, Jr., Project Director, for his guidance and help.
- Several project management committee members including David Head, Dr. German Claros, Behman Afsheen, Bernie Holder, Darrell Anglin, Jon Holt, Mark McClelland, Stanley Yin, Taya Retterer, and Mark McDaniel.
- Graduate students, Raja Yenigalla, Varagorn Pulijan, Minh Le, and Dr. Bhaskar Chittoori for their help with research and report preparation.

TABLE OF CONTENTS

LIST OF FIGURES

LIST OF TABLES

EXECUTIVE SUMMARY

Bridge approach settlement is a common problem to the transportation departments nationwide. This uneven transition causes inconvenience to passengers and increases the cost of maintenance and repair of the distressed approach slabs. The Texas Department of Transportation spends millions of dollars annually to mitigate this problem across the state. The potential causes for this problem are numerous and purely site specific. Hence this settlement problem may not have a unique solution.

In this research, two methods were selected and evaluated to mitigate the approach slab settlements of new bridges. The first one is an improvement of ground foundation technique by using Deep Soil Mixing (DSM) columns to stabilize soft foundation soil. The second one is an improvement of fill material by using a lightweight fill material, Expanded Clay Shale (ECS), as a backfill in embankment construction. Therefore, this research was performed on two bridge sites: a DSM site on IH 30 and an ECS site on SH 360 sites located in the DFW metroplex. In order to study the effectiveness of the two mitigation methods, three tasks including laboratory studies, instrumentation and field monitoring, and numerical analysis were carried out.

The laboratory investigations were first conducted to study the properties of DSM samples prepared in the laboratory and the ECS. The test results show that the foundation soil gained more strength by the DSM technique and the ECS exhibited its high internal friction property. Both test sites with DSM and ECS treatments were instrumented with various sensors including vertical inclinometer, horizontal inclinometer, Sondex, and rod extensometers. Also, elevation surveys were performed to monitor soil movements in the vertical direction. Results from the field observations from two bridge sites showed that both the DSM and ECS techniques are effective to mitigate the settlement in both embankment and foundation subgrades.

In the DSM study, the settlement was reduced from 3.3 in. (85 mm) to 1.9 in. (49 mm) (measured in the control and test sections, respectively). On the ECS site, researchers found that to construct the embankment with the ECS, the settlement could be reduced from 3.36 in. (85.3 mm) that occurred in the control section to 1.4 in. (36.5 mm) in the test section. The monitored soil movement data from both test sites were then modeled using the numerical

models. The analysis results show that these methods can be modeled to decrease the settlements underneath the approach slabs.

A parametric study was conducted to investigate the parameters' influence on the amount of the settlement. The parameters in both the DSM and ECS studies include slope and height of the embankments and area-ratio between the DSM and foundation soil (only in the DSM study). The FEM results from both studies show that the embankment height mainly influences the amount of the settlement while the embankment slope has not shown to be controlling the settlement magnitudes. From the analyses, both DSM and ECS based design charts were developed to determine settlements for various heights, slopes, and area-ratios (only DSM study) for different bridge configurations and soil conditions.

Also, various other methods including urethane treatment, soil nailing, lightweight geofoam, and flowable fills to control bridge approach slab settlements of existing bridges are also summarized and reported. Recommendations of these methods and potential future research needs are also identified and discussed.

CHAPTER 1

INTRODUCTION

1.1 GENERAL

Bridge approach settlement and the formation of the bump are general problems found nationally. This problem usually emanates from soil settlement related problems arising from both embankment fill and subgrade foundation materials. Maintenance of these bridge approach slab settlements cost millions of dollars to repair annually and this mainly absorbs all the maintenance resources. Briaud et al. (1997) reported that 30% of bridges in Texas, i.e., 13,800 out of 46,000 bridges were subjected to the bump problem, while another study cited annual costs for bump repairs in Texas is around $7 million (Seo, 2003). These can signify that the bump is a major if not a premier maintenance problem in Texas.

There have been several research studies that investigated the bridge approach settlement problems, and these studies focused on causes of the bump problem and various techniques to mitigate the settlement problem. From the literature review conducted, researchers found that the causes of the bump are many and are sometimes too complex to identify. However, the primary sources of the settlement problems could be broadly divided into four categories: 1) properties of foundation and embankment materials, 2) design criteria for bridge foundation, abutment, and deck slabs, 3) construction methods adapted, and 4) maintenance criteria. Not all the factors contribute to the formation of the bump or differential settlement concurrently as one factor may be more problematic than the other. Also, one model cannot be used alone for capturing the response of settlements underneath the approach slabs.

For the settlement mitigation techniques, it was found that there have already been several methods employed to alleviate the bump problem, including 1) improvement of foundation soil, 2) improvement of backfill material, 3) design of bridge foundation, 4) design of approach slab, and 5) effective drainage and erosion control measures.

Two of the major contributors to settlements are weak subgrade conditions and the weight of the soil embankments. Hence, any mitigation techniques used need to address these conditions. This TxDOT funded research has been a comprehensive attempt to address the mitigation techniques using two methods, namely Deep Soil Mixing (DSM) columns and Expanded Clay and Shale (ECS) treatments. The first method was primarily used for stabilizing

weak subsoil conditions, and the second method was predominantly used as a lightweight embankment fill material. The present research work focused on many aspects including laboratory mix design to field construction and instrumentation, numerical modeling and validation, and design method development.

The DSM technique is used to enhance soil strength and compressibility properties, while the ECS is a lightweight granular material and is used as a backfill material for embankment construction. With its lightweight property, the ECS is expected to decrease the loads exerted on the soft foundation subgrade. As a consequence, the settlement due to the consolidation phenomenon will be drastically decreased. In addition to new bridge construction, several treatments have been used for repairing slabs of existing bridges. It is necessary to evaluate these and provide a few recommendations on these techniques.

1.2 RESEARCH OBJECTIVES

The main objectives of the research was to comprehensively evaluate the effectiveness of two different treatment methods: DSM columns for foundation treatment and ECS material for fill construction in alleviating the differential settlements of an approach slab of new bridge construction in the real field conditions. Although these methods have already been utilized in other places, they have not been employed in Texas conditions. If this study shows that the DSM and ECS techniques can be successful in mitigating the bump at the bridge approach problem, then the results will not only help agencies in lowering their maintenance and repair works of bridge embankments built with clayey soils but will also reduce traffic congestion problems arising due to constant repair works.

A secondary objective of this research was to investigate and study the effectiveness of existing and other techniques for mitigating settlements of slabs of existing bridges. Researchers explored the treatments that have been used in various other districts in TxDOT to repair the distressed slabs. Also, a few other methods that can be used for the same purpose are also explained.

1.3 RESEARCH REPORT ORGANIZATION

The research report consists of 10 chapters. The first chapter is an introduction, which presents the background, objectives, and tasks involved to accomplish this research.

Chapter 2 presents details of the review from available literature addressing the settlement at the bridge approach problem. In the chapter, definition of the bump and the causes of the bump are presented followed by viable techniques used to mitigate the settlement at the bridge approach, both for new bridge constructions and for distressed bridge approach mitigation measures.

The means of selecting mitigation methods for study in this research are presented in Chapter 3. Two tasks were performed in order to select practical techniques for this study. The first task was a survey questionnaire that was distributed to all TxDOT districts. The survey questionnaire and data collection were an attempt to understand the bump problems in Texas and to identify the solutions tried so far to minimize the bump at the approach slab problem. The second task was a ranking analysis of all viable techniques identified from Chapter 2. This analysis was performed by setting up criteria to rank methods feasible for Texas conditions.

Chapter 4 presents the design of Deep Soil Mixing technology for settlement mitigation under the slabs for new bridges. Since the DSM was selected as one of practical methods to mitigate the bump problem, the procedures used to predict soil settlements in the DSM section were studied and are presented in this chapter. The prediction of the settlement is based on the settlement prediction model originally proposed by Rao et al. (1988), which has included overburden pressures, thickness of soil layers, and properties of soil in each layer as the primary factors into the settlement calculation. By following the specifications of materials used in both the construction and design steps, DSM columns and related area ratio values can be determined.

Chapter 5 presents the laboratory results conducted on soil specimens collected from the DSM field site. The laboratory studies were carried out to evaluate the physical engineering properties of the representative soils that were used further as input data in the numerical analysis. A series of laboratory tests including Atterberg Limit tests, consolidation, and unconfined compression strength tests were performed on the field subsoil. All the tests were performed in compliance with the procedures outlined by TxDOT and the American Society of Testing Materials (ASTM) standards, whichever was applicable. Another site where a light weight Expanded Clay Shale was proposed for use in the study as an embankment fill material was also characterized using similar geotechnical tests.

Chapter 6 describes the construction practices of each mitigation method (DSM and ECS) along with field instrumentation details used in both field sites. In this chapter, the principle

mechanisms of each instrument and stepwise procedures of the instrument installation including horizontal inclinometer, vertical inclinometer, rod extensometer, and Sondex are presented.

Chapter 7 presents the details of data collected in the field monitoring studies. First, the procedures of the data collection are explained and then followed by presenting the values of collected field data. Settlement data analysis was performed to consider the efficiency of the mitigation methods by comparing settlements between both the test and control sections. The settlement data reported in this chapter are not only used for the aforementioned analysis but also used in the numerical modeling analyses that are presented in Chapter 8.

Chapter 8 presents the study results from the numerical analysis. The laboratory study results in Chapter 5 are used as input soil parameters in the numerical models and the model results were then compared with the monitored data. Settlements over the long-term condition are also evaluated and used in the comparisons. Design models and charts are provided to select any of these two methods for new bridge approach slab construction.

Chapter 9 presents various methods attempted to repair the distressed slabs. Summary and conclusions from this study, which include significant findings from the field and numerical analysis studies and also limitation of this research and future needs, are addressed in Chapter 10.

CHAPTER 2

LITERATURE REVIEW

2.1 INTRODUCTION

This chapter presents comprehensive information collected from available literature addressing the problem about the differential settlement at the bridge approach. As a part of this research, the literature review in this chapter was carried out to obtain comprehensive details in five sections. In the first part of this chapter, general information of the definitions of the bump at the end of the bridge and the tolerance of the bump are given. In the second part, the mechanisms causing the formation of the bump such as consolidation of foundation soil, poor compaction of the backfill material, poor water drainage and soil erosion close to the bridge abutments, types of bridge abutments, traffic volume passing over the bridge decks, age of the approach slab, design of the approach slab, skewness of the bridge, and seasonal temperature variations are mentioned and reviewed in detail. The third part presents the techniques used to mitigate the bump at the end of the bridge for a new bridge. In the fourth part, maintenance measures normally employed by highway agencies to alleviate distressed approach slabs are presented. The final section of the chapter is a summary.

2.1 DEFINITION OF THE BUMP AND THE BUMP TOLERANCE

2.1.1 Definition of the Bump

Generally, roadways and embankments are built on existing soil subgrade foundations and compacted fill materials, respectively, which undergo load induced compression and settlements with time. In contrast, the bridges typically need to rest on deep foundations such as piles, piers, or other types of deep foundation systems resting on a firm foundation material such as bedrock. By resting on a firm foundation, the total settlement of the bridge is usually much smaller than the total settlement of the roadway or adjacent embankment soil. As a result, a considerable differential settlement occurs at the area between the bridge and roadway interface and a noticeable bump can develop at the bridge ends.

The bump can affect drivers varying from feeling uncomfortable to being hazardous to their lives (Hopkins, 1969; Ardani, 1987). To eliminate the effects of the bump, approach slabs

are built to provide a smooth grade transition between these two structures (bridge and roadway). Another function of the approach slab is to keep the magnitude of differential settlement within a control limit (Mahmood, 1990; Hoppe, 1999). However, in practice it is found that the approach slabs also exceed differential settlements (Mahmood, 1990; Hoppe, 1999). In such cases, the approach slab moves the differential settlement problem at the end of the bridge to the end of the slab connecting with the roadway. Hence, the bump or approach settlement can be defined as the differential settlement or heave of the approach slab with reference to the bridge abutment structure.

2.1.2 Bump Tolerances

The differential settlement near the bridge approach is a common problem that plagues many bridges in the state of Texas (Jayawickrama et al., 2005). One of the major maintenance problems is to establish severity levels of the bump that require remedial measures. The differential settlement tolerances need to be established for consideration of when to initiate the repair works.

Walkinshaw (1978) suggested that bridges with a differential settlement of 2.5 in. (63 mm) or greater needs to be repaired. Bozozuk (1978) stated that settlement bumps could be allowed up to 3.9 in. (100 mm) in the vertical direction and 2.0 in. (50 mm) in the horizontal direction. Several researchers define the allowable bumps in terms of gradients as a function of the length of the approach slab. Wahls (1990) and Stark et al. (1995) suggested an allowable settlement gradient as 1/200 of the approach slab length. This critical gradient was also referred by Long et al. (1998) and was used by the Illinois DOT for initiating maintenance operations.

Das et al. (1990) used the International Roughness Index (IRI) to describe the riding quality. The IRI is defined as the accumulations of undulations of a given segment length and is usually reported in in./ft or mm/m. The IRI values at the bridge approaches of 3.9 (mm/m) or less indicates a very good riding quality. On the other hand, if the IRI value is equal to 10 or greater, then the approach leading to the bridge is considered as a very poor ride quality. Albajar et al. (2005) established a vertical settlement on the transition zone of 1.6 in. (4 cm) as a threshold value to initiate maintenance procedures on bridge approach areas. In Australia, a differential settlement or change in grade of 0.3% both in the transverse and the longitudinal direction and a

residual settlement of 4 in. (100 mm) (for a 40 year design period) are considered as limiting values for bridge approach settlement problems (Hsi and Martin, 2005; Hsi, 2007).

In Texas, the state of practice for repair strategies is different from district to district, and these repairs are typically based on visual surveys (Jayawickrama et al., 2005) and IRI values (James et al., 1991). James et al. (1991) indicated that several districts in Texas have reported bump problems and a few districts have explored methods such as urethane injection and moisture control to mitigate settlements. However, these methods have only provided temporary relief as the settlement continues to increase with the service life. As a part of the Jayawickrama et al. (2005) study, researchers visited three bridge sites in the Waco, Houston, and San Antonio Districts where urethane foam injection was used to mitigate approach settlement problems. Their findings are discussed in detail in the subsequent sections of this chapter.

2.2 MECHANISMS CAUSING THE FORMATION OF THE BUMP

Bridge approach settlement and the formation of the bump is a common problem that draws significant resources for maintenance and creates a negative perception of the state agencies in the minds of the roadway system users. From thorough studies compiled from the existing and on-going research studies on the bridge approach settlement, the causes of the problem can be highly variable and are still too complex to identify them easily. However, the primary sources of the problem are broadly divided into four categories: material properties of foundation and embankment, design criteria for bridge foundation, abutment and deck, construction supervision of the structures, and maintenance criteria. Not all the factors contribute to the formation of the bump concurrently.

There have been many studies employed across the United States to find the causes of the problem and the methodologies to solve it (Hopkins, 1969, 1985; Stewart, 1985; Greimann et al., 1987; Laguros et al., 1990; Kramer and Sajer, 1991; Ha et al., 2002; Jayawickrama et al., 2005; White et al., 2005, 2007).

White et al. (2005) define the term bridge approach, not just in terms of the approach slab alone, but in terms of a larger area, covering from the bridge structure (abutment) to a distance of about 100 ft (30.5 m) away from the abutment. This definition includes the backfill and embankment areas under and beyond the approach slab as significant contributors to the settlements in the bridge approach region.

Many factors are reported in the literature reports that explain the mechanisms causing the formation of bumps on the bridge transition (Hopkins, 1969; Stewart, 1985; Kramer and Sajer, 1991). According to Hopkins (1969), the factors causing differential settlement of the bridge approaches are listed as:

- Type and compressibility of the soil or fill material used in the embankment and foundation.
- Thickness of the compressible foundation soil layer.
- Height of the embankment.
- Type of abutment.

Kramer and Sajer (1991) and Briaud et al. (1997) concurred with these observations later based on extensive surveys of various state DOTs in the U.S. Stewart (1985) performed a research study for Caltrans and this study concurred with the finding reported by Hopkins (1969); in particular, the observations noting that the original ground and fill materials contribute the maximum settlement to the approach slab. Based on the results obtained from a field study performed at Nebraska, Tadros and Benak (1989) confirmed that the primary cause of this problem is due to the consolidation of the existing foundation soil but not the consolidation of the compacted embankment fill. The proper compaction of the embankment in accordance with the construction specifications has an important influence on the settlement of embankment fill material. Also, the swell and shrink behaviors of the foundation/backfill soil and vibration or movements of the backfill soil (in case of granular fill) due to moving traffic loads may significantly impact the development of the approach faults (Hopkins, 1969, 1985).

Ardani (1987), Wahls (1990), and Jayawickrama et al. (2005) also reported that both the time-dependent settlement (primary/secondary consolidation) of foundation soil beneath the embankment and the approach slab embankment as well as the poor compaction of embankment adjacent to the abutment and erosion of the soil at the abutment face and poor drainage system around the abutment are the major contributors to approach settlement problems.

Wahls (1990) stated that the approach slab design and the type of abutment and foundation can affect the relative settlement of the slab and bridge abutment. Abutments supported by shallow foundations and when these foundations lay within the approach embankment fill will settle along with the embankment. In addition, Wahls (1990) concluded

that the lateral creep of the foundation soils and the lateral movement of the abutments can potentially cause this problem.

Laguros et al. (1990) reported that factors including the age of the approach slab, height of embankment, skewness of the bridge and traffic volume influence the bridge approach settlement. The flexibility of the approach pavements has a considerable influence as well. Laguros et al. (1990) observed greater differential settlement in flexible pavements than rigid pavements during initial stages following construction (short term performance), while both pavement types performed similarly over the long term. More details are provided in later sections.

Other factors that influence the creation of the bump include the type of bridge abutment and approach slab design (Mahmood, 1990; Wahls, 1990). The design of abutment structures is not unique and varies as per the connection of the slab with the abutment. The abutments are characterized as mainly integral (movable) or non-integral (conventional or stub) type of abutments (Greimann et al., 1987). For an integral abutment, the bridge deck slab is monolithically connected to the abutment, and the abutment is allowed to move laterally along with the bridge deck slab; while for a non-integral one, the bridge deck is independent of the abutment, and the longitudinal movements of the bridge deck are taken care of by roller/pin-bearing plates.

Weather changes also contribute to the differential settlement between the bridge and the approach slab as in the case of integral abutments when seasonal temperature changes from summer to winter (Schaefer and Koch, 1992). Weather changes often lead to soil displacement behind the abutment eventually leading to void development under the approach slab (Schaefer and Koch, 1992; White et al., 2005). This creates water infiltration under the slab, which leads to erosion and loss of backfill material (Jayawickrama et al., 2005).

White et al. (2007) conducted a comprehensive field study of 74 bridges in Iowa to characterize problems leading to poor performance of bridge approach pavement systems. White et al. (2007) claimed that subsurface void development caused by water infiltration through unsealed expansion joints, collapse and erosion of the granular backfill, and poor construction practices were found to be the main contributing factors of the approach slab settlements in Iowa.

Other research studies from outside the U.S., primarily from Australia and China, show that the bump at the end of the bridge is a major concern in highway and freeway construction. Hsi and Martin (2005) and Hsi (2007) reported that the approach settlement problems were observed due to very soft estuarine and marine clays in subsoils at the construction of the Yelgun-Chinderah Freeway in New South Wales, Australia. Hsi (2007) reported that rapid construction of deep approach embankments over very soft clay subgrades often experienced the long-term settlement of the soft subgrade that attributed to causing settlements at the approach slabs.

In the following, three studies by Briaud et al. (1997), Seo (2003), and White et al. (2007) listed factors that contribute to bumps. Briaud et al. (1997) summarized various factors that contributed to the formation of bumps/settlements at the approach slabs in Figure 2.1. These factors were grouped and ranked in the following order in which they contribute to the soil movements: fill on compressible foundation, approach slab too short, poor fill material, compressible fill, high embankments, poor drainage, soil erosion, and poor joint design and maintenance.

Seo (2003) performed a circular track test involving the approach slab that was repeatedly loaded by a vehicle model. Seo (2003) listed the following observations:

1. Number of cycles of loading over the approach slab is proportional to the increase in the bump.
2. Shorter approach slabs result in higher displacements of the slab.
3. More highly compacted, stiffer soils result in less deflection of the slab.
4. The velocity of vehicles has an influence on the increase in magnitude of the bump.
5. The weight of vehicles relates to the degree of the settlement.

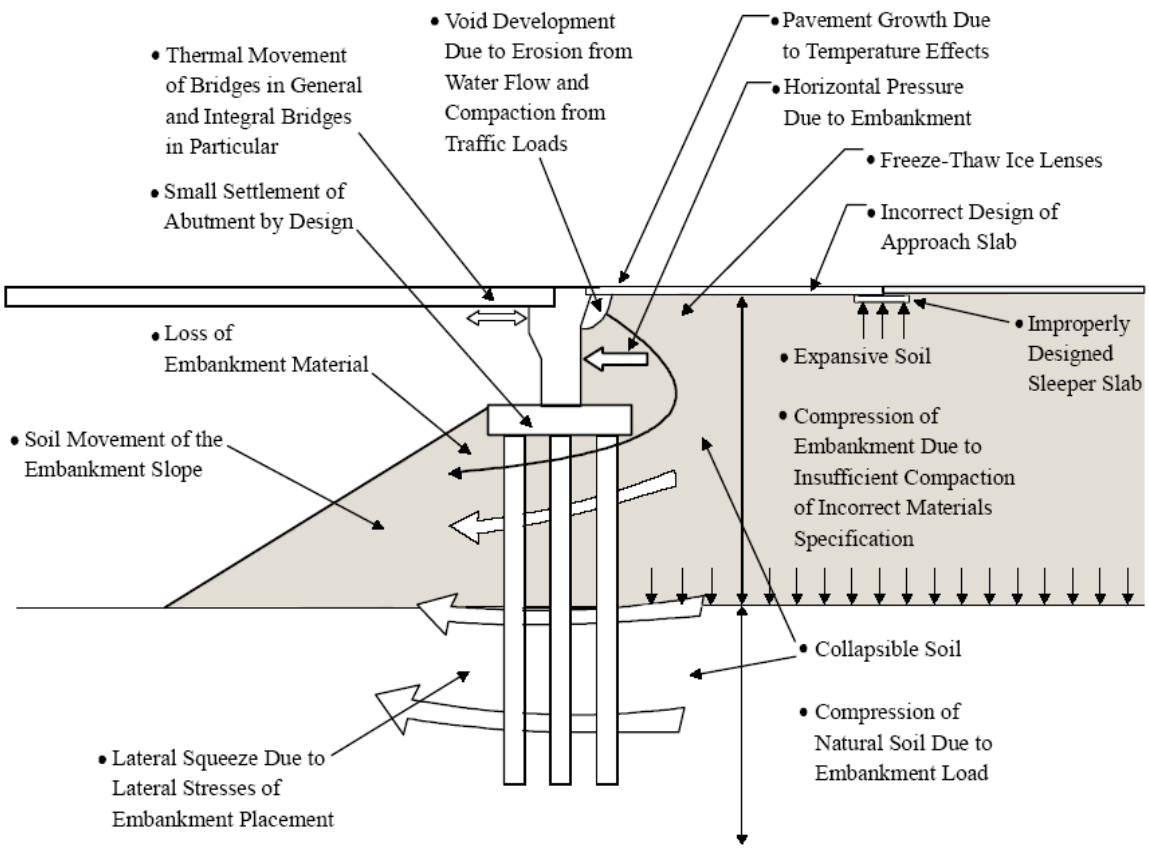

Figure 2.1. Schematic of Different Origins Lead to Formation of Bump at the End of the Bridge (Briaud et al., 1997).

A recent study conducted by White et al. (2007) summarized the following factors as contributors to differential settlements of the approach slab:

1. Backfill materials under poorly performing approach slabs are often loose and under-compacted.
2. The foundation soil or embankment fill settles.
3. Many bridge approach elevation profiles have slopes higher than 1/200, which is considered a maximum acceptable gradient for bridge approaches.
4. Voids develop under bridge approaches within one year of construction indicating insufficiently compacted and erodible backfill material.
5. Inadequate drainage is a major bridge approach problem. Many abutment subdrains are dry with no evidence of water, are blocked with soil and debris, or have collapsed.
6. Many expansion joints are not sufficiently filled, allowing water to flow into the underlying fill materials.

This chapter presents the following major factors that caused approach bumps by summarizing the above studies as well as a review of other investigations that addressed this bump problem:

1. Consolidation settlement of foundation soil.
2. Poor compaction and consolidation of backfill material.
3. Poor drainage and soil erosion.
4. Types of bridge abutments.
5. Traffic volume.
6. Age of the approach slab.
7. Approach slab design.
8. Skewness of the bridge.
9. Seasonal temperature variations.

Salient details of these factors are presented in the following subsections.

2.2.1 Consolidation Settlement of Foundation Soil

Consolidation of the foundation soil under an approach embankment is regarded as one of the most important contributing factors to bridge approach settlements (Hopkins, 1969; Wahls, 1990; Dupont and Allen, 2002). It usually occurs because of dynamic traffic loads applied at the embankment surface and static load due to the embankment weight itself (Dupont and Allen, 2002). However, this foundation settlement problem is difficult to address and repair in-situ because of the variability in the engineering properties of soils and the complexity of accessing the foundation after construction as it is buried deep below the roadway surface (Wahls, 1990).

Foundation problems usually are more severe in cohesive soils than in non-cohesive soils. Since consolidation occurs rapidly in non-cohesive soils, they do not normally represent a serious problem. On the other hand, cohesive soils, such as soft or high plasticity clays, represent a more critical situation because of their time dependent consolidation behavior. In addition, cohesive soils are more susceptible to lateral or permanent plastic deformation that can exacerbate the approach settlement problem.

Typically, settlement of soils is divided in to three different phases (Hopkins, 1969): initial, primary, and secondary consolidations, which are explained in the following subsections.

2.2.1.1 Initial Consolidation

The initial settlement is the short-term deformation of the foundation or embankment when a load is applied to a soil mass. This type of settlement does not contribute to the formation of bumps because it usually occurs before for the foundation soil or during for the construction of the approach embankment (Hopkins, 1969). The soil saturation level affects the total contribution of this settlement and for partially saturated soils; this initial settlement will be generally larger than that of saturated soils.

2.2.1.2 Primary Consolidation

Primary settlement is the main factor that contributes to the total settlement of soils. The gradual escape of water due to the compression of the loaded soil is believed to be the reason for this type of settlement. This primary settlement lasts from a few months for granular soils to a period of up to 10 years for some types of clay (Hopkins, 1973). This significant difference is attributed to the small void ratio and high permeability of granular soils.

2.2.1.3 Secondary Consolidation

This phase occurs as a result of changes in void ratio of the loaded soil after dissipation of excess pore pressure (Hopkins, 1969). In this case, soil particles in the soil mass readjust in a plastic way under a constant applied stress while the water and air are squeezed out. For the case of very soft, highly plastic or organic clays, secondary consolidation can be as large as the primary consolidation, while in granular soils, it is negligible (Hopkins, 1969).

To mitigate the settlement, a primary objective of any bridge construction project should include a complete or comprehensive investigation of the foundation soil before the construction of the approach embankment starts (Wahls, 1990). Previous studies have shown that the stresses applied to the foundation subgrades come primarily from the embankment loading rather than the bridge or traffic loads, except for shallow depths (less than 10 ft [3 m]) (Hopkins, 1969; Wahls, 1990; Dupont and Allen, 2002). Therefore, geotechnical studies have to be carried out with extensive foundation investigations, including laboratory tests, to evaluate compression and consolidation potential to better estimate the anticipated post-construction settlements (Dupont and Allen, 2002). It is also important to study the possible shear failures in the foundation that cause lateral deformations and surface settlement problems. This type of failure is more likely to appear in peat and other organic materials.

2.2.2 Poor Compaction and Consolidation of Backfill Material

To minimize construction costs, approach embankments are usually constructed with the most readily available material at or near the project site. But when low quality materials (such as locally available soft, cohesive, expansive soils and soils sensitive to freeze-thaw) are used, the approach settlements can be induced in terms of bigger bumps. In general, cohesive soils are more difficult to compact to their optimum moisture content and density when compared to coarser or granular fill materials (Hopkins, 1973).

Poor compaction control of the embankment material is found to be a factor, resulting in low density and highly deformable embankment mass (Lenke, 2006). Poor compaction can also be attributed to limited access or difficulty in access within the confined working space behind the bridge abutment (Wahls, 1990). Many highway agencies require only granular fills that can be better compacted and are able to reach their maximum consolidation in less time than more cohesive soils (Wahls, 1990; Lenke, 2006). The TxDOT Bridge Design Manual (2001) notes that either improper backfill materials used for mechanically stabilized earth (MSE) or the inadequate compaction of the backfill materials in the embankment are the contributing factors to the backfill failure.

Compaction type and project schedule are also of great importance (Dupont and Allen, 2002). Field inspectors should ensure that proper compactive effort and compaction levels of the fill material are reached during construction. It is common practice that bridge abutments are constructed before the embankment fill placement and compaction. This practice makes the compaction of the area closest to the bridge more difficult because the equipment access to this critical area becomes limited (Burke, 1987).

In addition to compression of the backfill material, lateral stability and shear strength are of great importance to the overall stability against the approach settlement. For the case of the foundation soil, lateral confining forces are significant, while on embankment fills, the confinement effects are much less pronounced (Wahls, 1990). Hence, slope design, material selection and loads applied to the backfill need to be carefully evaluated to anticipate or minimize the final settlement (Wahls, 1990).

2.2.3 Poor Drainage and Soil Erosion

Several researchers from different states including Texas, Virginia, Iowa, and Colorado reported the importance of the surface and subsurface drainage and soil erosion near the bridge abutment and embankment interface. Wahls (1990), Jayawickrama et al. (2005), Mekkawy et al. (2005), White et al. (2005), and Abu-Hejleh et al. (2006) identified the drainage system of the abutment and embankment as one of the most important factors that affect approach settlement. The dysfunctional, damaged, or blocked drainage systems cause erosion in the abutment and slope increasing soil erosion and void development. The dysfunctional drainage systems may be caused by either incorrect construction or improper design. Williammee (2008) observed that incorrect placement, such as the outlet flow line higher than the inlet flow line of the drainage pipes in the concrete riprap placed under the newly constructed bridge can make the drainage system ineffective. Briaud et al. (1997) explains how the poor joints between the pavement and the abutment structure as seen in Figure 2.2 can lead to soil erosion of embankment and abutment backfill.

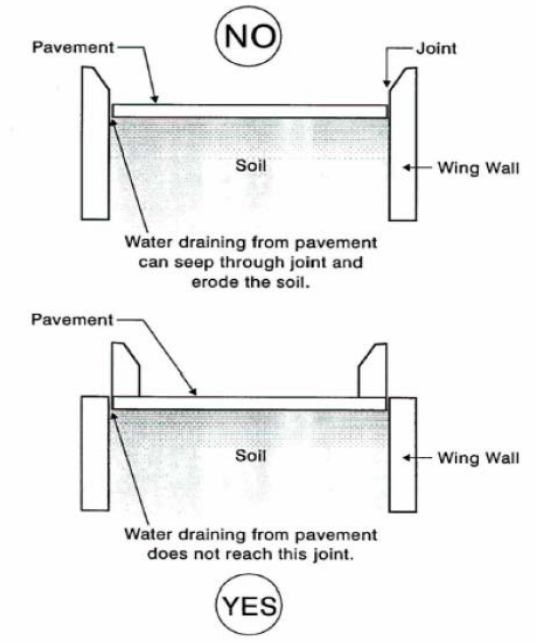

Figure 2.2. Cross Section of a Wingwall and Drainage System (Briaud et al., 1997).

Jayawickrama et al. (2005) noted that the erosion of soil at the abutment face and poor drainage material can induce serious approach settlement problems. This observation was based on the survey responses obtained from various TxDOT district officials. The intrusion of

surface water (rain) through weak expansion joints (openings) between the approach slab and bridge abutments can erode backfill material and further amplify the problem of approach slab settlements (Jayawickrama et al., 2005). Based on the detailed study of a few TxDOT bridges, they noted that these joint openings resulted from the construction practices such as poor compaction of backfill material near the abutments, poor construction of joint sealants, and poor design and construction of the surface and subsurface drainage systems.

In addition, the expansion joints should transfer traffic loads, prevent surface water from entering into the abutment, and allow pavement expansion without damaging the abutment structure (Wolde-Tinsae et al., 1987). Based on a comprehensive research study performed by White et al. (2005) on many bridges in Iowa, most of the expansion joints of the bridges inspected were not sufficiently filled allowing water to flow into the underlying fill materials. On the other hand, cracks were often encountered next to closed joints in bridge approaches because of expansion of the neighboring concrete allowing for leakage of water as well.

Similar observations were made by Mekkawy et al. (2005) that are discussed here. Based on field investigations in different states, Mekkawy et al. (2005) reported that inadequate drainage and subsequent severe soil erosion contributed to settlement problems on 40% of the bridge approach slabs that were surveyed by them. Moisture flow into the backfill coupled with poor drainage conditions can cause failure of the embankment, backfill, and bridge abutments either by excessive settlement or by soil strength failure. Typically, water can seep into the embankment fill material via faulty joints and cracked concrete pavement sections. The leaked water can soften the embankment fill and can cause internal erosion as the fines typically wash out from the fill material. Without approach slabs, water leakage will immediately induce settlement; with approach slabs, voids beneath the slab will form, amplifying the erosion by compression of the soil.

The erodability of soils is based on their grain size distribution. Some soil gradation guidelines can be found for soils that are erosion resistant and those that are prone to erosion (Briaud et al., 1997; Hoppe, 1999). As indicated in Figure 2.3, a gradation band of material in the sand to silt size materials is a bad choice for embankments and backfill unless additional preventive actions, such as providing appropriate drainage design or erosion control systems, are taken (Briaud et al., 1997).

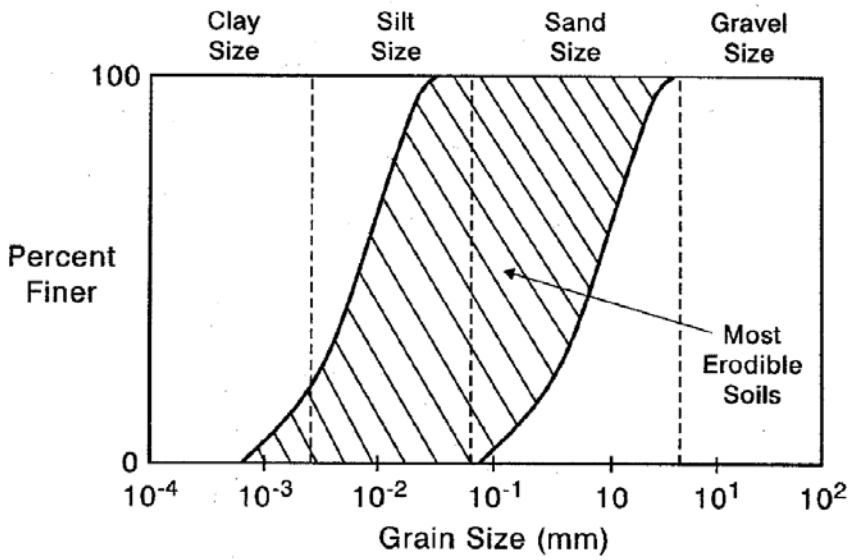

Figure 2.3. Range of Most Erodible Soils (Briaud et al., 1997).

2.2.4 Types of Bridge Abutments

Abutments must be compatible with the bridge approach roadway and they must have backwalls to keep the embankment from covering up the beam ends and to support possible approach slabs (Figure 2.4). They also usually have wingwalls to keep the side slopes away from the structure and to transition between the guard rail and the bridge rail as shown in Figures 2.4 and 2.5.

Abutments are characterized as integral (movable) or non-integral (conventional or stub) types (Greimann et al., 1987). In the integral type, the bridge deck slab is monolithically connected to the abutment, and the abutment is allowed to move laterally along with the bridge deck slab; in the non-integral type, the bridge deck is independent of the abutment and the longitudinal movements of the bridge deck are taken care of by roller/pin-bearing plates (Greimann et al., 1987). The advantages of integral bridge abutments are reduced construction and maintenance costs, minimum number of piles required to support the foundation and enhanced seismic stability (Greimman et al., 1987; Hoppe and Gomez, 1996). To avoid the use of the bearing plates and to reduce potential maintenance problems (such as frequent repair of bearing plates, expansion joint sealants) associated with non-integral bridge abutments, the use of integral bridge abutments has been increased since the 1960s (Horvath, 2000; Kunin and Alampalli, 2000). The following sections describe the advantages and disadvantages of both types of abutments.

2.2.4.1 Integral Abutments

Figure 2.4 shows a simplified cross section of an integral abutment bridge. The approach slab system of an integral bridge consists of the backfill, the approach fill, and the soil foundation. If an approach slab and a sleeper slab are used, they are also considered in the system. Integral abutment bridges are designed to carry the primary loads (dead and live loads) and also the secondary loads coming from creep, shrinkage, thermal gradients, and differential settlements. Integral abutments are rigidly connected to the bridge beams and deck with no expansion joint.

Even though integral abutments present structural advantages over non-integral abutments, they also introduce thermal movements in the approach system that can aggravate the bump problem on the approach system (Schaefer and Koch, 1992; White et al., 2005). Hence, special attention has to be paid in this type of abutment to the lateral loads imposed on the foundation piles due to horizontal movements induced by temperature cycles (Wahls, 1990).

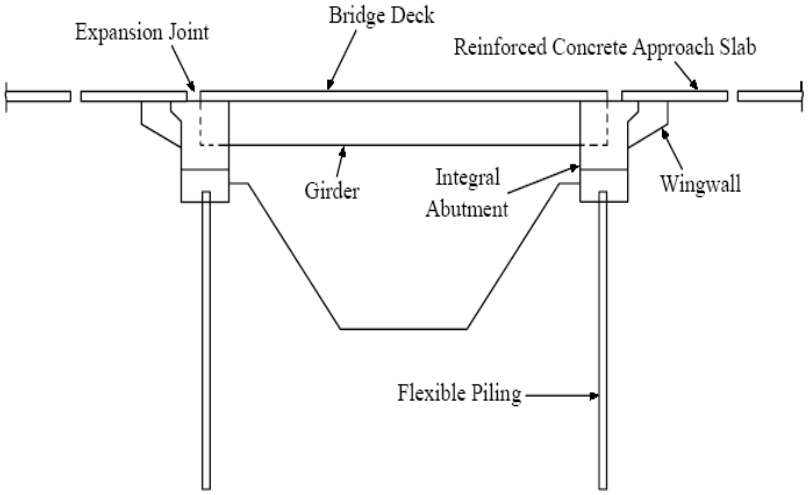

Figure 2.4. A Simplified Cross Section of an Integral Abutment Bridge (Greimann et al., 1987).

2.2.4.2 Non-Integral Abutments

Figure 2.5 shows a simplified cross-section of a non-integral abutment. In this case, abutments are supported on bearing connections that allow longitudinal movements of the superstructure without transferring lateral loads to the abutment. The non-integral bridge abutment is separated from the bridge beams and deck by a mechanical joint that allows for the thermal expansion and contraction of the bridge (Nassif, 2002).

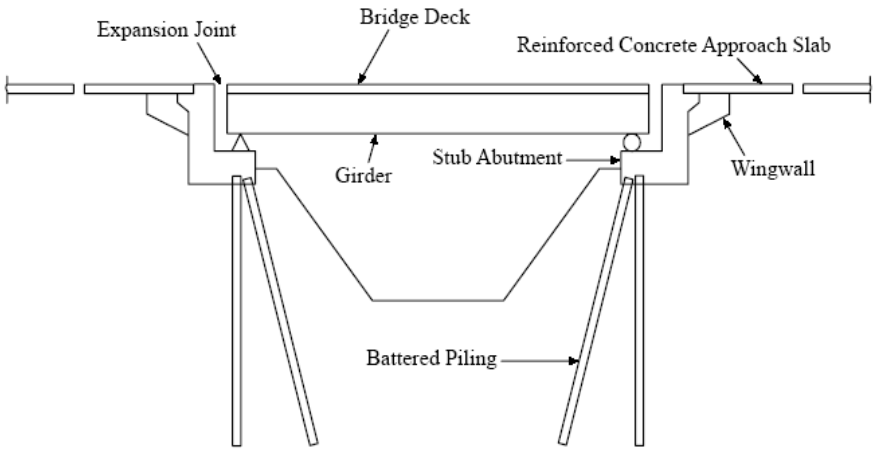

Figure 2.5 A Simplified Cross Section of a Non-Integral Abutment Bridge (Greimann et al., 1987).

Three major types of non-integral abutment bridges are found in the literature. These are: closed or U-type, spill-through or cantilever, and stub or shelf abutments (Hopkins and Deen, 1970; Timmerman 1976; Wahls 1990; TxDOT, 2001).

2.2.4.3 Closed Abutment or U-Type

Figure 2.6a shows a simplified cross-section of a closed abutment. The U-type abutments have two side walls and a front wall resting on spread footings below natural ground (TxDOT, 2001). For this type of abutment, the side walls are long enough to keep the embankment from encroaching on the bridge opening. In addition, the taller the abutment is, the longer the sidewalls will be. The compaction of the embankment fill is rather difficult in these abutments because of confined space near the abutment and due to the wall, which is extended over the whole height of the abutment (TxDOT, 2001). These abutments are also subjected to higher lateral earth pressures than other types.

2.2.4.4 Spill-through or Cantilever Abutment

Figure 2.6b shows a simplified cross-section of a spill-through abutment. A spill-through abutment is supported on the columns and hence, the compaction of the backfill material between the columns and near the abutment is very difficult. Cantilever type abutments have variable width rectangular columns supported on spread footings below natural ground (TxDOT, 2001). The fill is built around the columns and allowed to spill through, on a reasonable slope,

into the bridge openings. A great number of these types of abutments have been constructed in Texas, and they have performed well in the past (TxDOT, 2001). However, this type of abutment presents detailing and construction problems as well as high construction costs.

2.2.4.5 Stub or Shelf Abutment

Figure 2.6c shows a simplified cross-section of a stub type abutment. A stub abutment is constructed after the embankment so its height is directly affected by the embankment height. The compaction of the backfill material is relatively easier compared with the closed type except for the soil behind the abutment (TxDOT, 2001).

Most of the abutments in Texas are of the stub or shelf type, constructed by driving piling or drilling shafts through the compacted fill and placing a cap backwall and wingwalls on top. The header bank is sloped from the top of the wingwall through the intersection of the cap and backwall into the bridge opening. The bridge must be considerably longer than with U-type abutments but slightly shorter than the cantilever types. The extra length of this abutment is justified on the basis of cost and aesthetics (TxDOT, 2001).

Although more economical, stub abutments have maintenance problems. The bump at the beginning of the bridge caused by fill settlement is particularly noticed on stub type abutments (TxDOT, 2001).

From the past experiences with these non-integral abutment bridges, TxDOT officials attribute the approach settlements to the poor construction practices due to inaccessibility to compact the backfill/embankment fill near the vicinity of the abutment leading to the aggressive approach settlements (Jayawickrama et al., 2005).

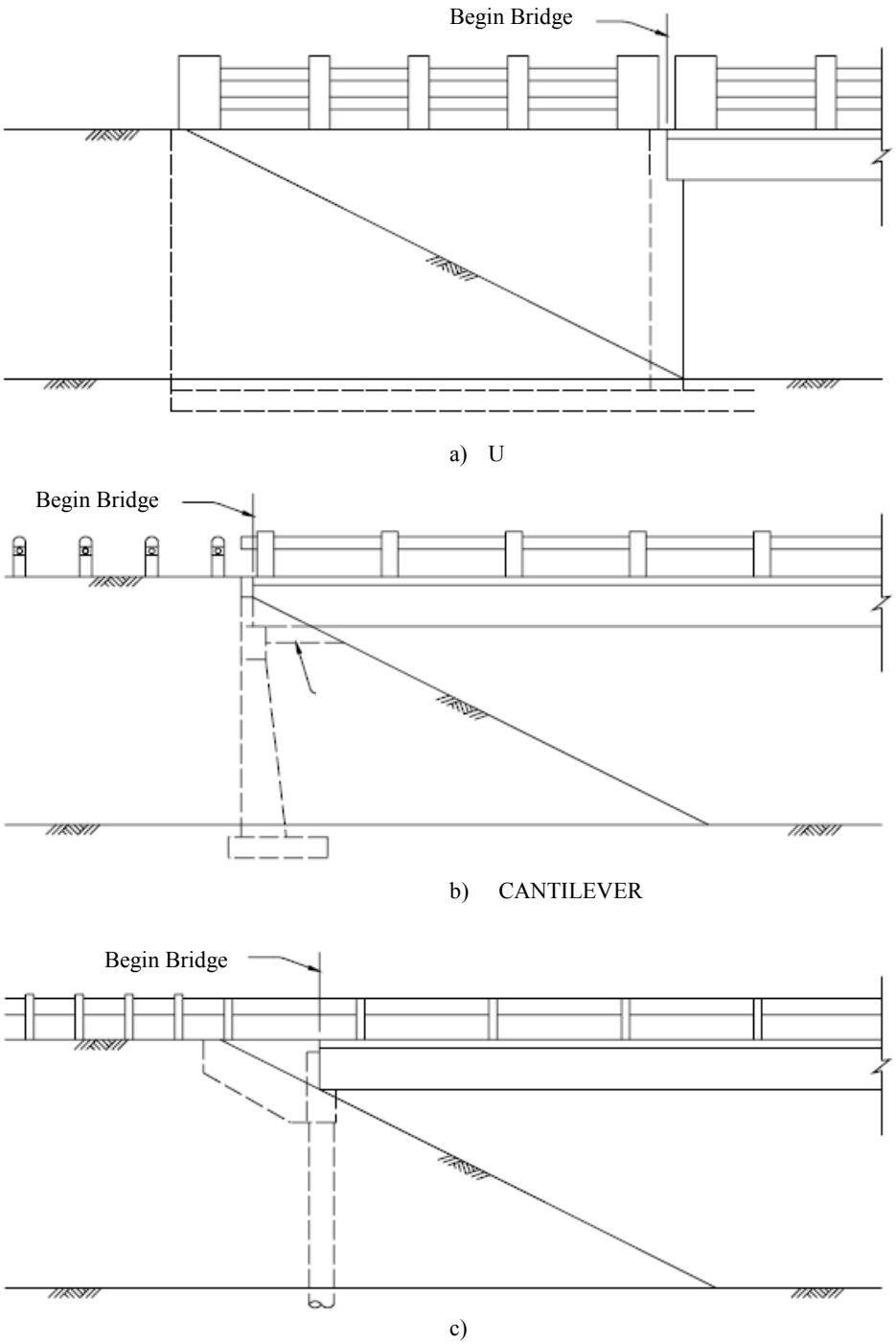

Figure 2.6. Non-Integral Abutment Types (TxDOT, 2001).

2.2.5 Traffic Volume

Heavy truck traffic has been found in some studies to be a major factor contributing to the severity of this bump along with the age of the bridge and approach, especially for the late 1970s or early 1980s (Wong and Small, 1994; Lenke, 2006). High-volume traffic has been found as a compelling reason for including approach slabs in the construction of both conventional and integral bridges. Lenke (2006) noted that the bump was found to increase with vehicle velocity, vehicle weight, especially heavy truck traffic, and number of cycles of repetitive loading, in terms of Average Daily Traffic (ADT). On the other hand, Bakeer et al. (2005) have concluded that factors such as speed limit and traffic count have no distinguishable impact on the performance of the approach slabs.

2.2.6 Age of the Approach Slab

The age of the approach slab is an important factor in the performance of different elements of the bridge structures, especially at the expansion joints next to the approach slab, which could negatively affect the backfill performance in terms of controlling settlements underneath the slab (Laguros et al., 1990; Bakeer et al., 2005). Another factor known as alkali-silica reactivity (ASR) formed inside the concrete approach slabs is known to induce expansion stresses in surrounding environment. These stresses can potentially lead to slab expansion and distress in the approach slabs, approach joints, and vertical uplift of the slabs and pavement preceding the slabs (Lenke, 2006).

Bakeer et al. (2005) studied the influence of approach slab age by investigating a number of approach slabs built in the 1960s through the 1990s. Based on the condition ratings, the newer pile- and soil-supported approach slabs were generally in better condition than the older ones.

Laguros et al. (1990) reported that the flexibility of the approach pavements has a considerable influence as well. They observed greater differential settlement in flexible pavements than rigid pavements during initial stages following construction (short-term performance) while both pavement types performed similarly over the long term.

2.2.7 Approach Slab Design

The purpose of the approach slab is to minimize effects of differential settlement between the bridge abutment and the embankment fill, to provide a smooth transition between the pavement and the bridge, to prevent voids that might occur under the slab and to provide a better seal against water percolation and erosion of the backfill material (Burke, 1987). However, a rough transition can occasionally develop with time in bridge approaches due to differential settlements between the abutment and roadway. This is attributed to the different support systems of the two structures connected by the approach slab. The approach slab and the roadway are typically constructed over an earth embankment or natural soil subgrade whereas the bridge abutment is usually supported on piles.

Insufficient length of approach slabs can create differential settlements at the bridge end due to high traffic induced excessive destruction in the approach slab (Briaud et al., 1997). Based on an extensive survey performed by Hoppe (1999) in 39 states, approach slabs lengths varied from 10 to 40 ft (3 to 12 m) and thicknesses ranged from 8 to 17 in. (203 to 432 mm). Some studies, based on the IRI ratings, report that 80 ft (24 m) long slabs performed the best, and no significant difference was found when compared to 100 ft (30.5 m) long slabs (Bakeer et al., 2005).

The rigidity of the approach slab is also a major contributing factor. Dunn et al. (1983) compared the performance of various approach slab pavements in Wisconsin and reported that 76% of the flexible approaches rated poor, 56% of the non-reinforced approaches rated fair, and 93% of the reinforced concrete approaches rated good. All these ratings are based on the performance of the approach slab in controlling the differential settlements.

2.2.8 Skewness of the Bridge

Skew angle also has a significant effect on the formation of approach settlements and the overall bridge performance. Skewed integral bridges tend to rotate under the influence of cyclic changes in earth pressures on the abutment (Hoppe and Gomez, 1996). According to Abendroth et al. (2007), design of skewed integral abutment bridges must account for the transverse horizontal earth pressure applied along the skew. Also, the change in position of the ends of an abutment is attributed to a combination of two effects: the temperature-dependent

volumetric expansion or contraction of concrete in the pile cap and abutment, and the rigid-body translation and rotation of the abutment due to the longitudinal expansion or contraction of the superstructure for a skewed integral abutment bridge. This study also recommended that when skewed integral abutments are used, they should be placed parallel to each other and ideally be of equal height (Abendroth et al., 2007).

Nassif (2002) conducted a finite element study to understand the influence of skewness of bridge approaches and transition slabs on their behavior. Researchers found the skew angle of the approach slab resulted in an uneven distribution of the vehicle axial load so that the wheels only one side of the axles actually had contact with the approach slab. Figure 2.7 shows that for the same loading conditions, the tensile axial stresses on skewed approach slabs are found to be 20 to 40% higher than the same on straight approach slabs. In addition, the pinned connection at the edge of the approach slabs that connects them with the bridge abutment prevented any displacement taking place along this edge, thus providing more strength to the elements of this region (Nassif, 2002).

Additionally, higher rates of settlements at the bridge exit were considered to be accountable to the effect of the skew angle of the approach slab as well as improper compaction conditions in hard-to-reach soil areas close to the abutments (Nassif, 2002).

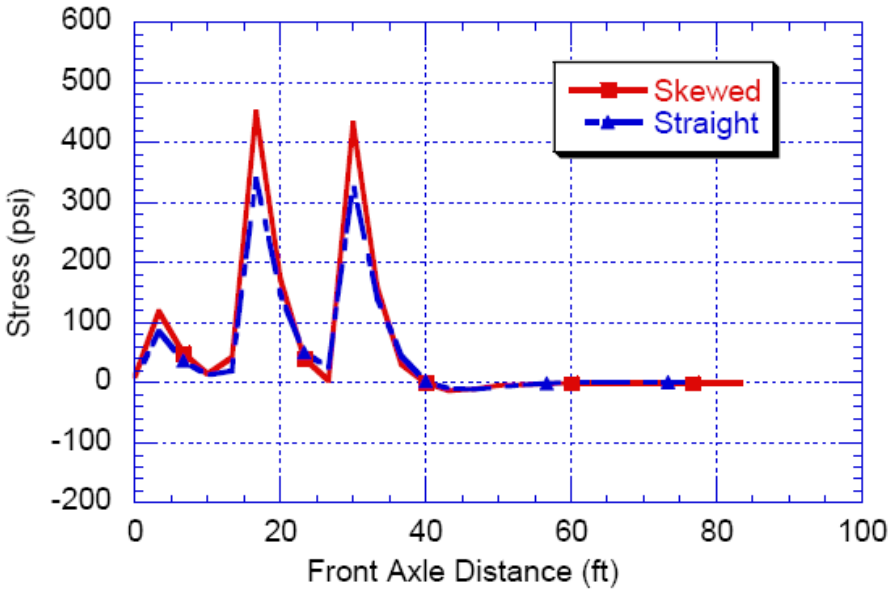

Figure 2.7. Variation of Tensile Axial Stress with Front Axle Distance for Skewed and Straight Approach Slabs (Nassif, 2002).

2.2.9 Seasonal Temperature Variations

Some of the factors that contribute to differential settlement between the bridge and the approach slab, especially for integral abutments, are seasonal temperature changes between summer and winter in the bridge deck (Schaefer and Koch, 1992; Arsoy et al., 1999; Horvath, 2005; White et al., 2005). This temperature change causes cyclical horizontal displacements on the abutment backfill soil, which can create soil displacement behind the abutment leading to void development under the approach slab (White et al., 2005). As a result, the infiltration of water under the slab and therefore erosion and loss of backfill material may accelerate.

Due to seasonal temperature changes, abutments move inward or outward with respect to the soil that they retain. During winter, the abutments move away (outward) from the retained earth due to contraction of the bridge structure while in summer they move toward (inward) the retained soil due to thermal expansion of the bridge structure (Arsoy et al., 1999; Horvath, 2005). At the end of each thermal cycle, abutments have a net displacement inward and outward from the soil that is usually retained (see Figure 2.8). This is attributed to the displacement of an active soil wedge, which moves downward and toward the abutment during winter but cannot fully recover due to inelastic behavior of the soil during the summer abutment movement. This phenomenon was noted in all types of embankment materials (Horvath, 2005). Besides, these horizontal displacements are observed to be greater at the top of the abutment and hence the problem is aggravated when the superstructure is mainly constructed with concrete (Horvath, 2005). Figure 2.9 shows how the expansion-contraction movements of the bridge with the seasonal temperature change will lead to the creation of voids below the approach slab.

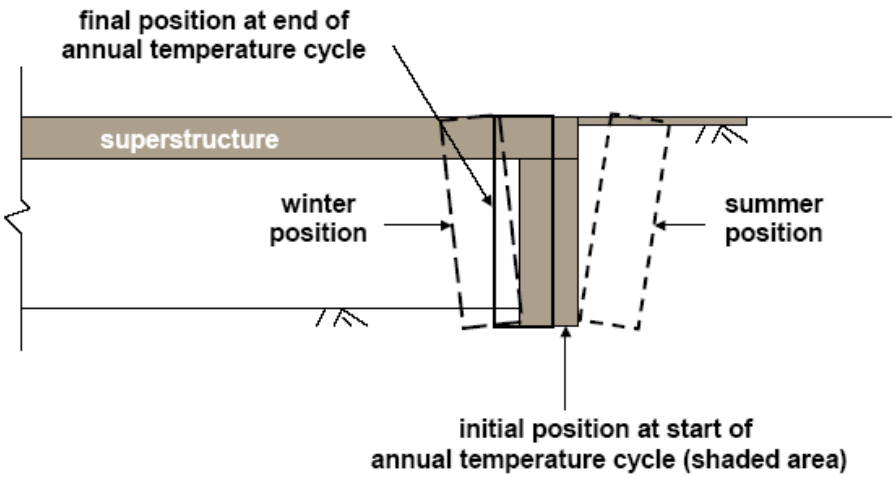

Figure 2.8. Thermally Induced IAB Abutment Displacements (Horvath, 2005).

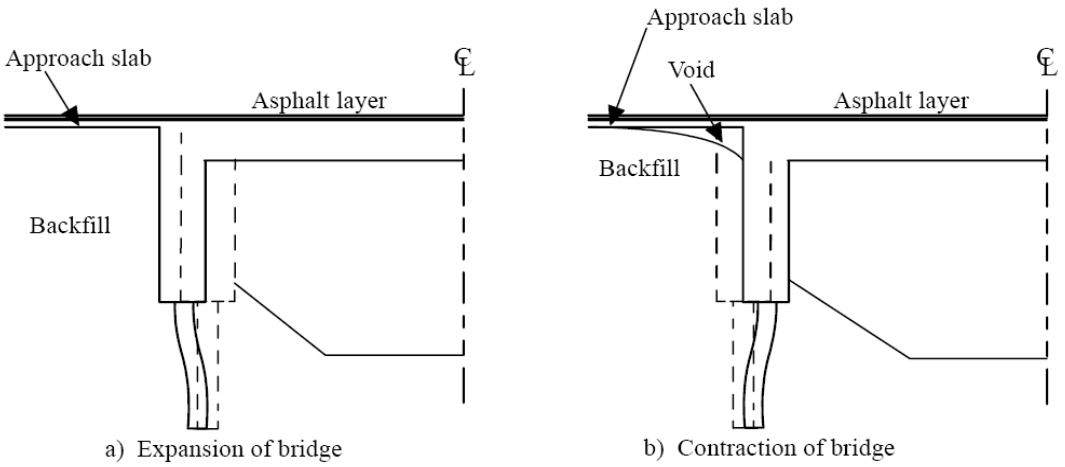

Figure 2.9. Movement of Bridge Structure (Arsoy et al., 1999).

The temperature effect on the bridge-abutment interaction also creates pavement growth due to friction between the pavement and its subbase (Burke, 1993). After the pavement expands, it does not contract to its original length because of this friction. This residual expansion accumulates after repeated temperature cycles resulting in pavement growth that can be rapid and incremental at pressure relief joints (Burke, 1993). The pressure generated will transmit to the bridge in terms of longitudinal compressive force and should be considered by engineers when designing the pressure relief joints.

James et al. (1991) documented a case of severe abutment damage for a bridge without pressure relief joints through a numerical study. This numerical stress analysis indicated that the

damage was caused by the longitudinal growth of continuous reinforced concrete pavement causing excessive longitudinal pressures on the abutments.

The cycle of climatic change, especially the temperature change, also can cause certain irreversible damage to the pavement or bridge approach slabs in terms of ice lenses due to frost action. Here ice lenses are derived from freezing and thawing of moisture in a material (in this case soil) and the structure that are in contact with each other (UFC, 2004). The existence of freezing temperature and presence of water on the pavement either from precipitation or from other sources such as ground water movement in liquid or vapor forms under the slabs can cause frost heave in pavements. This phenomenon causes the pavement rising because of ice crystal formation in frost-susceptible subgrade or subbase that can affect the durability of concrete. The frost induced heave is not a serious problem in pavements in dry weather areas like Texas.

As noted by the above sections, bump or differential settlements are induced by several factors either by individual mechanisms or by combination mechanisms. In the following sub-sections, different treatment or repair techniques adapted for new and existing bridges are detailed.

2.3 MITIGATION TECHNIQUES FOR APPROACH SETTLEMENTS OF NEW BRIDGES

This sub-section is a summary of various methods adopted for mitigating potential settlements expected in new bridges. These techniques are listed based on various groups of treatments such as improvement of foundation soil, improvement of backfill material, design of bridge foundation, design of approach slab, and effective drainage and erosion control methods.

2.3.1 Improvement of Embankment Foundation Soil

The behavior of foundation soil beneath the embankment fill is one of the most important factors in the better performance of bridges (Wahls, 1990). Generally, if the foundation soil is a granular material type, such as sand, gravel, and rock, which do not undergo long-term settlements, then the differential settlement between the bridge structure and the roadway embankment can be negligible. On the other hand, if the approach embankments are constructed on cohesive soils such as normal or underconsolidated clays, then those soils can undergo large settlements either from primary and/or secondary consolidation settlements. These settlements

will subsequently lead to the settlement of embankment structures and the formation of the bumps or approach settlement problems leading to poor performance of bridge approaches. Several attempts have been made by many researchers both from the U.S. and abroad to mitigate these unequal settlements arising from highly compressible embankment fills (Wahls, 1990; Dupont and Allen, 2002; White et al., 2005; Abu-Hejleh et al., 2006; Hsi, 2008).

When the soil/fill underneath the structure is not suitable for construction, the recommended approach is to enhance the properties of the foundation soil such that they undergo less compression due to loading (White et al., 2005). Successful ground improvement methods include preloading the foundation soil (Dupont and Allen, 2002), excavation and replacement of existing soft soil, reinforcement of soil to reduce time-dependent post construction settlements, and also lateral squeeze (White et al., 2005). The selection of a ground improvement technique for a particular project is mostly based on the type of soil and partly on the depth of the loose layer, degree of saturation, ground water table location, and permeability. If the soil is a granular material, then the ground improvement techniques such as surcharge (or) preloading, dynamic compaction, compaction piles, grouting, and gravel columns are preferred (Wahls, 1990; Abu-Hejleh et al., 2006); if the soil is cohesive in nature, excavation and re-compaction, preloading, installation of wick drains, dynamic compaction, stone columns, lime treatment columns and grouting are proposed (Wahls, 1990; Abu-Hejleh et al., 2006).

Based on the review of literature, stabilization techniques to improve the embankment foundation soil are grouped per the soil type. Table 2.1 summarizes these ground improvement techniques, not limited to one, for each foundation soil in a chronological order of their importance and the level of settlement problem.

Most of the combination techniques are chosen for a particular field situation. For example, preloading with the installation of wick drains will lead to faster consolidation settlement of weak soft foundation soils. These techniques are again divided into three subcategories such as mechanical, hydraulic, and reinforcement techniques based on the function of each stabilization technique (Table 2.2).

The following sections describe each ground improvement technique and available literature information with respect to approach settlement problems.

Table 2.1. Summary of Ground Improvement Methods Based on Soil Type.

Technique	Cohesionless soils	Cohesive soils
Excavation and Replacement	✗	✔
Preloading w or w/o Surcharge	✔	✔
Dynamic Compaction	✔	✔
Grouting	✔	✔
Wick Drains	✗	✔
Compaction Piles	✔	✗
Gravel Columns	✔	✗
Lime Treatment	✗	✔
Stone Columns	✗	✔
Soil Reinforcement	✔	✔
Geopier	✔	✔

Table 2.2. Summary of Ground Improvement Techniques Based on the Function.

Embankment on Soft Foundation Soil Improvement Techniques		
Mechanical	Hydraulic	Reinforcement
Excavation and replacement Preloading and surcharge Dynamic compaction	Sand drains Prefabricated drains Surcharge loading	***Columns*** Stone and Lime Columns Geopiers Concrete Injected Columns Deep Soil Mixing Columns
		Deep foundations In-situ: Compacted piles CFA piles Driven piles: Timber and Concrete piles
		Geosynthetics Geotextiles/Geogrids Geocells

2.3.1.1 Mechanical Modification Techniques

2.3.1.1.1 Excavation and Replacement

In this method, the undesirable top soil is excavated and replaced with a select fill from borrow sites. The removal and replacement concept is one of the options considered when the proposed foundation soils are prone to excessive consolidation (Luna et al., 2004; White et al., 2005; Wahls, 1990; Hoppe, 1999; Chini et al., 1992). Dupont and Allen (2002) reported that around 32 states in the U.S. replace the foundation soil near the bridge approach when they have low bearing stresses. The excavation was done in the range of 10 ft (3 m) to 30 ft (10 m) from the existing soil surface. The selected fill material from the borrow pit must be controlled carefully to avoid pocket entrapments during the compaction process.

Presently, the difficulties involved in this excavation and replacement method are due to the difficulty in maintaining uniform replacement and the expenses involved in the complete removal and land-filling of undesirable soil. Because of these reasons, this method becomes less favorable. Tadros and Benak (1989) discussed this technique in detail and reported that the excavation and replacement technique may be the most economical solution only if the compaction areas are underlain by a shallow bedrock or firm ground.

2.3.1.1.2 Preloading/Precompression

One of the effective methods reported in the literature to control foundation settlement is to precompress the foundation soil (Dupont and Allen, 2002). According to Bowles (1988), precompression is a relatively inexpensive and effective method to improve poor foundation soils. Bowles (1988) noted that this technique is used to accomplish two major goals; one is to eliminate settlements that would otherwise occur after the structure is built and the second is to improve the shear strength of the subsoil by increasing the density, reducing the void ratio, and decreasing the water content.

The precompression technique in embankment construction is a process in which the weight of embankment will be considered as a load inducing the consolidation settlement and completing the process before the beginning of actual pavement or roadway construction. In this method, the construction is delayed, even up to one year in most cases, so as to allow embankment settlement prior to roadway construction before the placement of the approach pavement (Cotton et al., 1987). Even though this method could be effective in reducing

foundation settlement and maintenance costs, many highway agencies do not implement this technique due to lengthy construction periods that could cause significant problems in construction schedules and increase in total project costs (Hsi, 2007). Hence, this technique is often combined with other ground improvement methods such as vertical drains and surcharge loading that will enhance the properties of subsoils from mechanical and hydraulic modifications, resulting in faster enhancements. Design of vertical drains deal with the hydraulic properties of the soil and hence these details are covered in modifications by hydraulic methods.

2.3.1.1.3 Surcharge Loads

A temporary surcharge load might also be applied on top of the embankment to accelerate the consolidation process (Bowles, 1988; Hsi, 2007). In order to achieve this, the applied surcharge load must be greater than the normal load, i.e., the weight of the embankment in this particular case. However, the desired extra load, in terms of extra height of embankment, has to be limited by its slope stability. In order to eliminate this limitation, sometimes a berm is constructed for this purpose. The cost of berm construction, excessive fill placement and its removal will result in an increased overall project cost and duration. These costs have to be weighed against the costs involved in avoiding construction delays (Bowels, 1988).

2.3.1.1.4 Dynamic Compaction

Dynamic compaction is another alternative to improve the foundation soil. This technique is best suitable for loose granular deposits in medium to soft clays. Heavy tamping and dynamic consolidation are also called dynamic compaction (Hausmann, 1990). In this technique, a heavy weight is repetitively dropped onto the ground surface from a great height (Lukas, 1986). During this process, densification of a saturated or nearly saturated soil are achieved due to sudden loading, involved shear deformation, temporary high pore pressure generation (possibly liquefaction) and subsequent consolidation (Lukas, 1986; 1995).

Generally the weight of the tamper mass ranges from 6 to 170 tons and the drop height is between 30 and 75 ft (Lukas, 1986). The use of a small mass falling from a lower height, usually 12 tons dropping from 36 ft, is typically employed during small scale tamping operations (Hausmann, 1990). The parameters such as degree of saturation, soil classification,

permeability, and thickness of the clay layer influence the suitability of a particular soil deposit for the dynamic compaction technique. Based on the grain size and the plasticity index (PI) properties of soils, Lukas (1986) characterized and grouped them into three different zones as shown in Figure 2.10.

This figure shows that the Zone I (pervious) soils are best suited for dynamic compaction. Zone II (semi-pervious) soils require longer duration to dissipate dynamic compaction induced excess pore water pressure to obtain the required level of improvement. Hence, soils in Zone II require multiple phases of dynamic compaction. It is observed that the soils grouped under Zone III are not suitable for dynamic compaction. The effective depth of dynamic compaction can be as deep as 40 ft (12 m) but usually ineffective for saturated impervious soils, such as peats and clayey soils (Wahls, 1990). This technique is not feasible when the area of improvement required is smaller such as for highway embankments of confined widths (Hausmann, 1990). The application of this technique in highway related projects is less when compared to the other applications, which include compacting sanitary landfills, rocky areas, dams, and air fields (Lukas, 1995). No documented cases where this method was used for mitigating settlements of fills underneath the slabs were found in the literature.

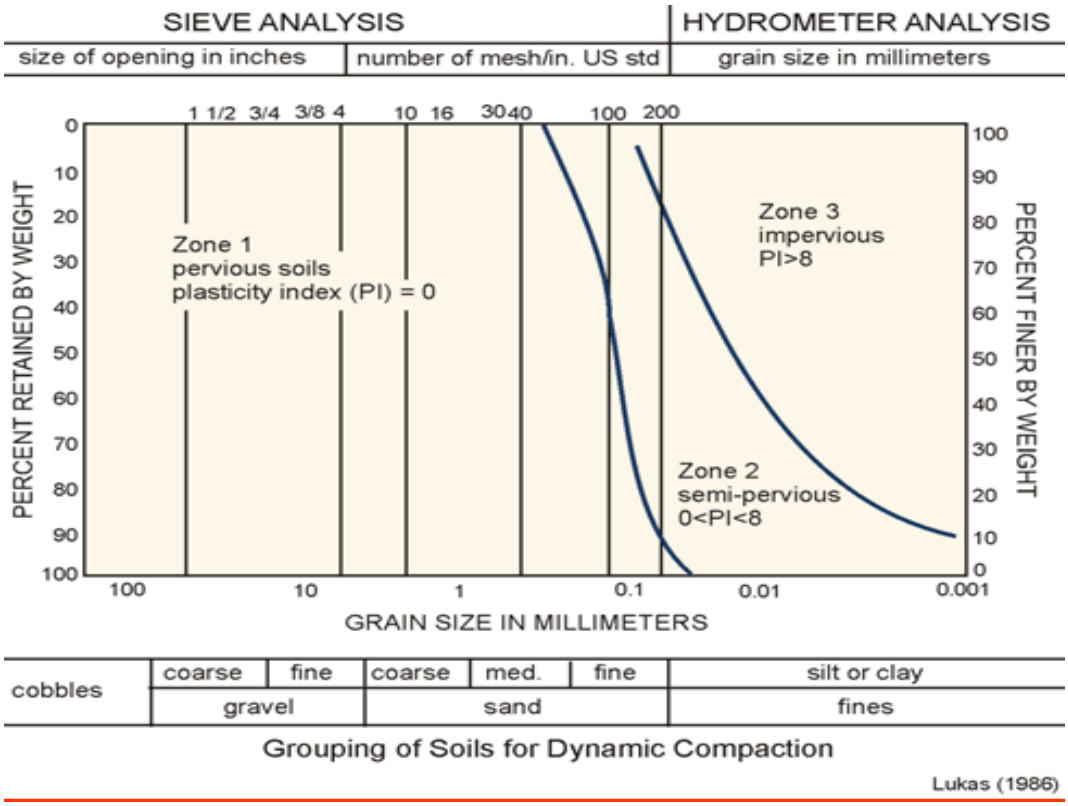

Zone 1: Best
Zone 3: Worst (consider alternate methods)
Zone 2: Must apply multiple phases to allow for pore pressure dissipation

Figure 2.10. Grouping of Soils for Dynamic Compaction (Lukas, 1986).

2.3.1.2 Hydraulic Modification Techniques

2.3.1.2.1 Vertical Drains

Vertical drains in the form of sand drains were successfully used to enhance the consolidation process by shortening the drainage path from the vertical to the radial direction (Nicholson and Jardine, 1982). Recently, the usage of sand drains has been replaced by prefabricated vertical drains, also called wick drains, accounting for their ease in installation and economy. Wick drains basically consist of a plastic core with a longitudinal channel wick functioning as a drain and a sleeve of paper or fabric material acting as a filter protecting the core. Configurations of different types of prefabricated vertical drains (PVDs) available in the market are shown by Bergado et al. (1996) as shown in the Figure 2.11. Typically PVDs are 3.94 in. (100 mm) wide and 0.24–0.32 in. (6-8 mm) thick and available in rolls (Rixner et al., 1986). The main purpose of prefabricated vertical drains is to shorten the drainage path and

release the excess pore water pressure in the soil and discharge water from deeper depths thereby assisting in a speedy consolidation process of soft soils. Generally, vertical drains are installed together with preloading to accelerate the consolidation process (Rixner et al., 1986; Bergado et al., 1996).

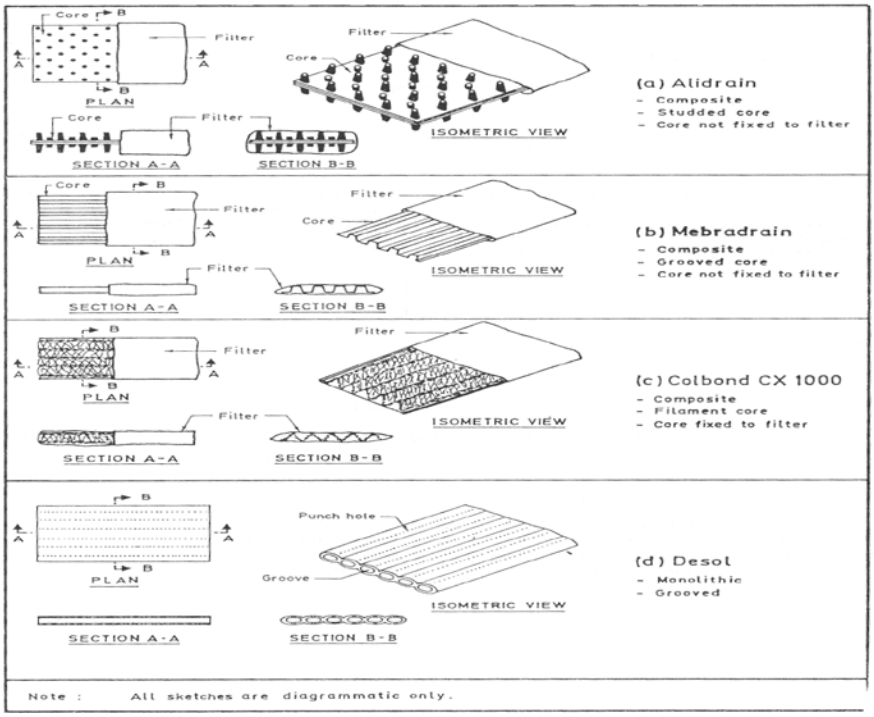

Figure 2.11. Configurations of Different Types of Prefabricated Vertical Drains (Bergado et al., 1996).

Based on classic one-dimensional consolidation theory by Terzaghi (1943), Barron (1948) developed a solution to the problem of consolidation of the soil specimen with a central sand drain using two-dimensional consolidation by accounting for radial drainage. Later, Hansbo (1979) modified Barron's equation for prefabricated vertical drain application. The discharge capacity, spacing, depth of installation, and width and thickness of the wick drains are prime factors controlling the consolidation process. These design factors again depend on the in-situ conditions of the project location (Hansbo, 1997a). These design procedures are described in detail by Hansbo (1979; 1997b; 2001).

The first prototype prefabricated vertical drains were pioneered by Kjellman in Sweden in 1937 (Jamiolkowski et al., 1983). The first application of vertical sand drains for settlement control was performed as an experiment in California in the early 1930s. Several researchers have reported the successful application and functioning of vertical sand and wick drains in

highway embankment constructions from all over the world (Atkinson and Eldred, 1981; Bergado et al., 1988; Indraratna et al., 1994; Bergado and Patawaran, 2000). Figure 2.12 shows a typical arrangement of vertical drains in a soft soil under embankment with surcharge load.

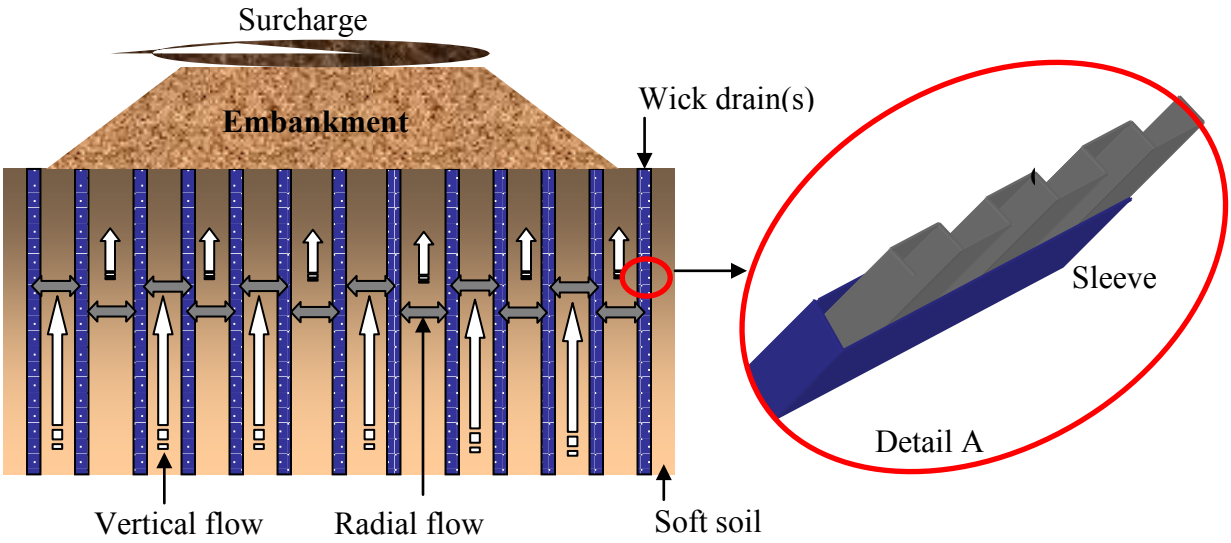

Figure 2.12. Preloading with Prefabricated Vertical Drains to Reduce Consolidation Settlements.

Hsi and Martin (2005) and Hsi (2007) described the successful use of wick drains along with reinforcing geotextile layers to mitigate unequal and differential settlements anticipated in highway approach embankments constructed over soft estuarine and marine clays in New South Wales, Australia. The proposed freeway connecting Yelgun and Chindera cities has 9 flyovers and 39 freeway bridges over creeks and waterways with most of them located on soft estuarine and marine clays. The involved risks due to the very soft nature of these soils including long-term time dependent consolidation settlements, short-term instability of the embankment, and increase in fill quantity due to excessive settlement of embankment fill led to the adoption of ground improvement techniques. They reported that installation of wick drains at a spacing of 3.3–9.8 ft (1–3 m) c/c on a grid pattern (Figure 2.13) allowed speedy construction of the embankment fills over these soft soils.

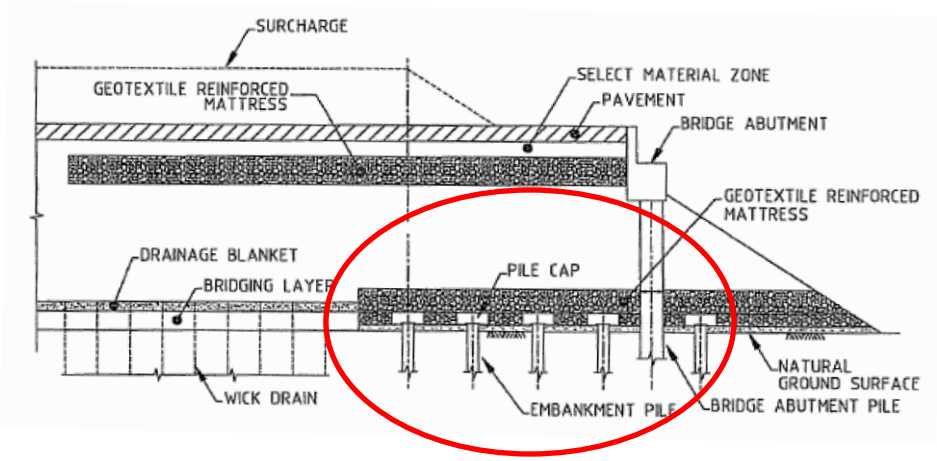

Figure 2.13. Schematic Arrangement of Approach Embankment Treatment with Wick Drains and Driven Piles (Hsi and Martin, 2005).

To increase the embankment stability against potential slip failure, which was anticipated due to the speedy construction operations on the soft soils, high strength geotextile reinforced mattresses were placed on the surface of the soft ground before placement of the embankment (Hsi and Martin, 2005). The embankment near the bridge abutment was supported on timber driven piles to reduce the differential settlements between the approach embankment and the pile supported bridge abutments. The details about the timber driven piles are discussed in the following section. The embankment section and the soft soil were instrumented with settlement plates to assess the risks during and after the construction.

Figure 2.14 presents the measured and predicted settlements in the soft foundation soil during and after the construction stages. In this figure, the long-term settlements were predicted based on the ratio ($c_\alpha/1+e_0$), where c_α is the secondary compression index and e_0 is the initial void ratio. The long-term differential and total settlements are predicted from back-calculated analysis of measured data from settlement plates also presented in the same figure. From this graph, note the reduced rate of long-term creep settlements after the removal of the surcharge and after the completion of construction (Hsi and Martin, 2005).

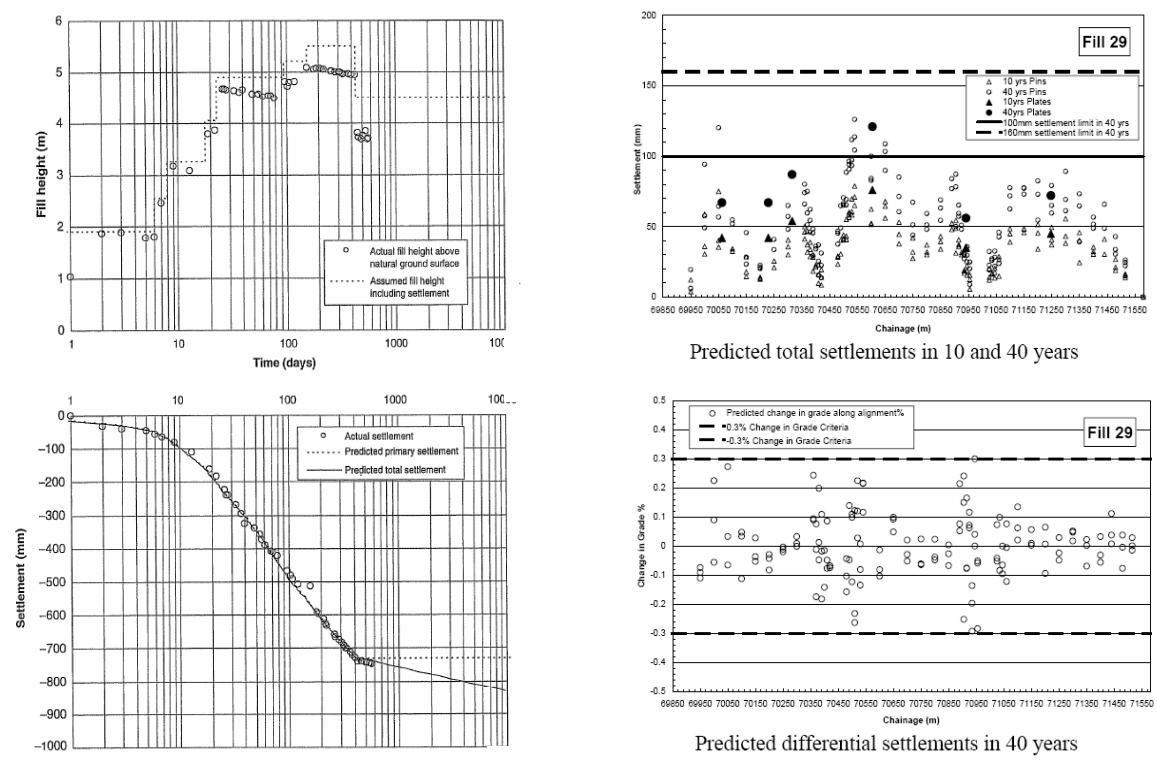

Figure 2.14. Measured and Predicted Settlements with Time (Hsi and Martin, 2005) (a) during Construction Stages and (b) after Construction Stages.

A wide variety of soil reinforcement techniques are available from which to choose. In all of these techniques, good reinforcement elements are inserted to improve the selected property of the native weak soil. These inclusions include stone, concrete, or geosynthetics. Based on the type of construction of these methods, they are grouped as column reinforcement, pile reinforcement and geosynthetic reinforcements. The following sections describe each technique in detail with the focus on controlling bridge approach settlements.

2.3.1.2.2 Column Reinforcement

a. Stone Columns

The stone columns technique is one of the classic solutions for soft ground improvement. This concept was first used in France in 1830 to improve a native soft soil (Barksdale and Bachus, 1983). The stone columns are a more common method to improve the load carrying capacities of weak foundation soils (Barksdale and Bachus, 1983; Michell and Huber, 1985; Cooper and Rose, 1999; Serridge and Synac, 2007) and provide long-term

stability to the embankments and control settlements beneath the highway embankments (Munoz and Mattox, 1977; Goughnour and Bayuk, 1979; Barksdale and Bachus, 1983; Serridge and Synac, 2007). The secondary function of the stone columns is to provide the shortest drainage path to the excess pore water allowing it to escape from highly impermeable soils (Hausmann, 1990). This technique is best suitable for soft to moderately firm cohesive soils and very loose silty sands. In the United States, a majority of the stone column projects are adopted for improving silty sands (Barksdale and Bachus, 1983).

Stone column construction involves the partial replacement of native weak unsuitable soil (usually 15–35%) with a compacted column of stone that usually penetrates the entire depth of the weak strata (Barksdale and Bachus, 1983). Two methods are generally adopted to construct the stone columns including vibro-replacement, a process in which a high pressure water jet is used by the probe to advance the hole (wet process), and vibro-displacement, a process in which air is used to advance the hole (dry process).

In both processes, stone is densified using a vibrating probe, also called vibroflot or poker, which is 12 to 18 in. (300 to 460 mm) in diameter. Once the desired depth is reached, stone is fed from the annular space between the probe and the hole to backfill the hole. The column is created in several lifts with each lift ranging from 1–4 ft (0.3–1.2 m) thick. In each lift, the vibrating probe is re-penetrated several times to densify the stone and push it into the surrounding soil. This procedure is repeated until the column reaches the surface of the native soil. Figure 2.15 shows the construction stages of stone columns.

Successful application of stone columns to improve the stability of highway embankments constructed over soft soils is found for Clark Fork, ID, in a report by Munoz and Mattox (1977) and for Hampton, VA, in a report by Goughnour and Bayuk (1979). Stone columns can also be used to support bridge approach fills to provide stability and to reduce the costly maintenance problem at the joint between the fill and the bridge. Based on an experience report circulated by a vibroflotation foundation company, Barksdale and Bachus (1983) have reported that stone columns were successfully used at Lake Okaoboji, Iowa, and Mobridge, South Dakota, for a bridge approach and an embankment structure built on soft materials.

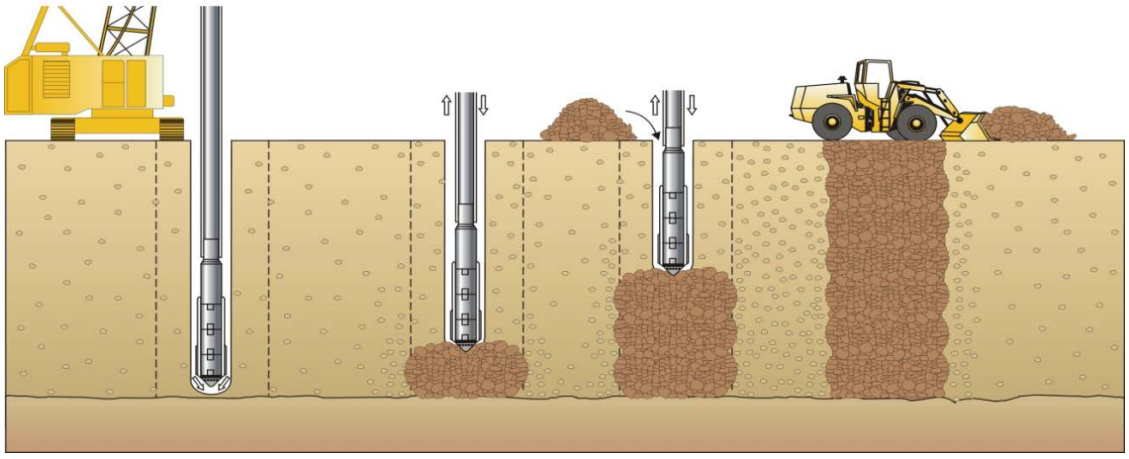

Figure 2.15. Construction Stages of Stone Columns.
http://www.haywardbaker.com/services/vibro_replacement.htm)

Serridge and Synac (2007) reported the successful use of stone columns along with vibro concrete columns in supporting highway embankment constructed over soft soil in South Manchester, UK. Figure 2.16 shows the schematic of the combination of ground improvement techniques used beneath the highway approach embankment. Prior to the actual construction, trial stone columns were constructed at a relatively low cost to verify their performance. Figure 2.17 depicts the performance of the stone columns in controlling settlements. Results from settlement plates show that the settlements occurring due to actual work were much smaller than the measured settlements in the trial sections.

The application or use of the stone columns technique is widely accepted and adopted in European countries (Barksdale and Bachus, 1983). In addition, McKenna et al. (1975) have reported a neutral performance of stone columns in soft alluvium supporting high embankment. They reported that the columns had no apparent effect on the performance of the embankment based on the comparison of instrumentation results obtained from both the piled and un-piled ground.

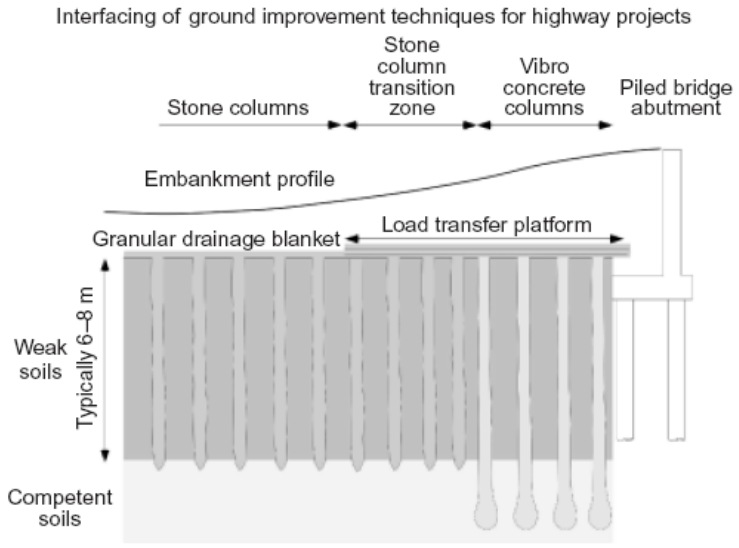

Figure 2.16. Interfacing of Ground Improvement Techniques beneath Embankment Approach to Piled Bridge Abutment (Serridge and Synac, 2007).

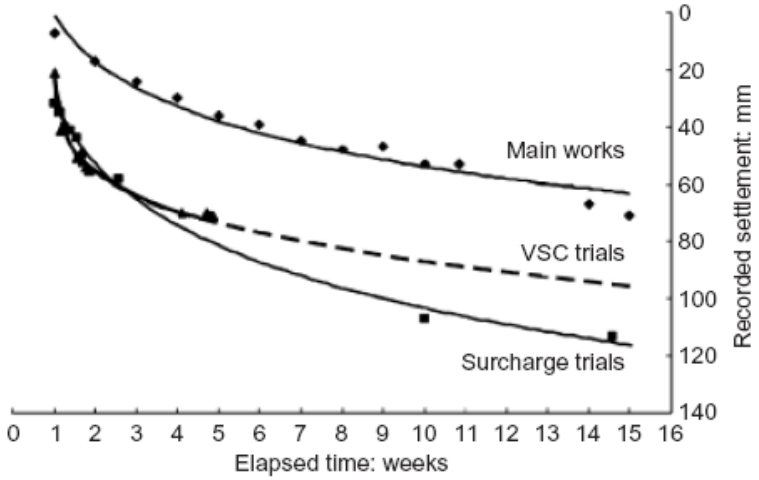

Figure 2.17. Settlement Monitoring Results for Both Surcharge Trials on Untreated and Soil Reinforced with Stone Columns (Serridge and Synac, 2007).

b. Compaction piles

A series of compaction piles are used to improve the foundation soil only when the deep deposits of loose granular soils, such as sand or gravel, are present and they can be densified by vibro-compaction or vibro-replacement methods (Hausmann, 1990). In these techniques, a probe is inserted into the soil until it reaches the required treatment depth (Hausmann, 1990). Then, the loosely deposited sands are vibrated in combination with air- or

water-jet at a design frequency. Some amount of granular backfill materials are added to compensate for the void spaces resulting from the compaction. Finally, the probe is removed and the compacted granular backfill column is left in-situ. Figure 2.18 depicts the sequential operations involved in the construction of compaction piles. Normally, the spacing of compaction piles is between 3 and 10 ft (1 and 3 m) and the depth of improvement can be achieved up to 50 ft (15 m) (Wahls, 1990). However, the vibro-compaction has its own limitation upon the grain size distribution of the granular fill material, which must contain fine material less than 20 percent (Baumann and Bauer, 1974) as shown in Figure 2.19.

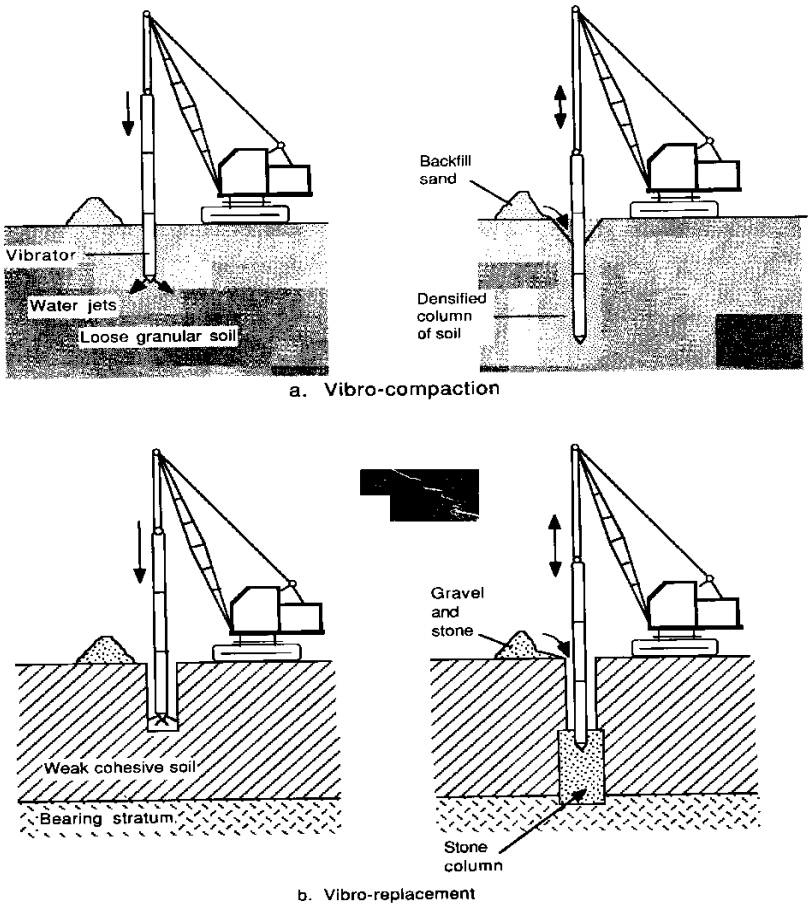

Figure 2.18. Sequential Operations Involved in the Construction of Compaction Piles (Hausmann, 1990).

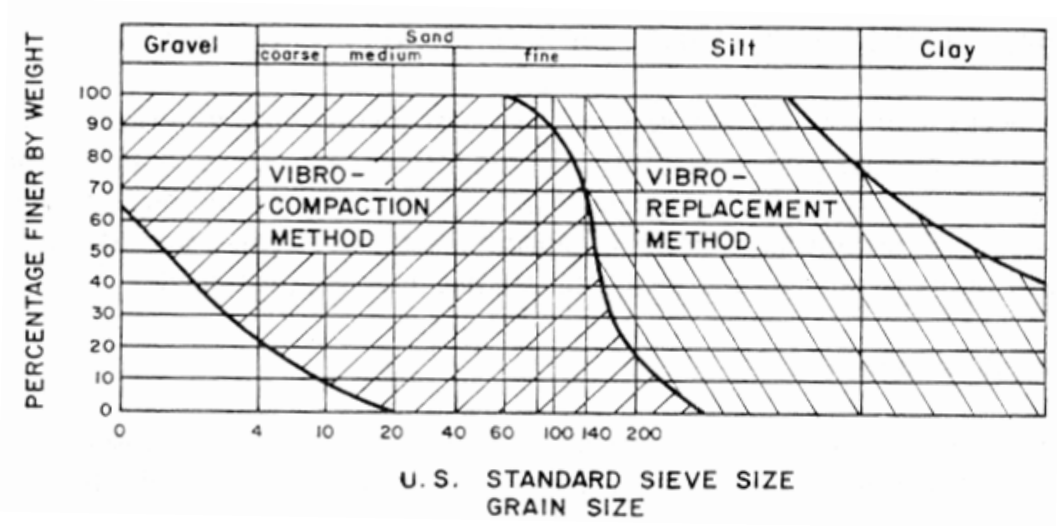

Figure 2.19. Range of Soils Suitable for Vibro-Compaction Methods (Baumann and Bauer, 1974).

Application of compaction piles to reduce the bridge approach settlements are not widely reported in the literature except in a few reported in Japan and Thailand. Sand compaction piles were used to support a road test embankment constructed at Ebetsu in Hokkaido, Japan (Aboshi and Suematsu, 1985). A combination of ground improvement techniques chosen in this project included sand compaction piles and lime/cement columns. The embankment was constructed using mechanically stabilized earth with grid reinforcement. Figure 2.20 shows a schematic of the ground improvement techniques adopted in this study. A control embankment was also constructed on native soft soil without any treatment. They reported that the combination of sand and lime/cement columns could support the embankment as high as 26.2 ft (8 m), while the control embankment of height 11.5 ft (3.5 m) was collapsed exhibiting high deformations on the subsoil and heavy cracks in the embankment section.

Similar studies were carried out by Bergado et al. (1988; 1990) on soft Bangkok clay and confirmed that the granular compaction piles along with mechanically stabilized earth would be an economical alternative to support bridge approach embankments and viaducts.

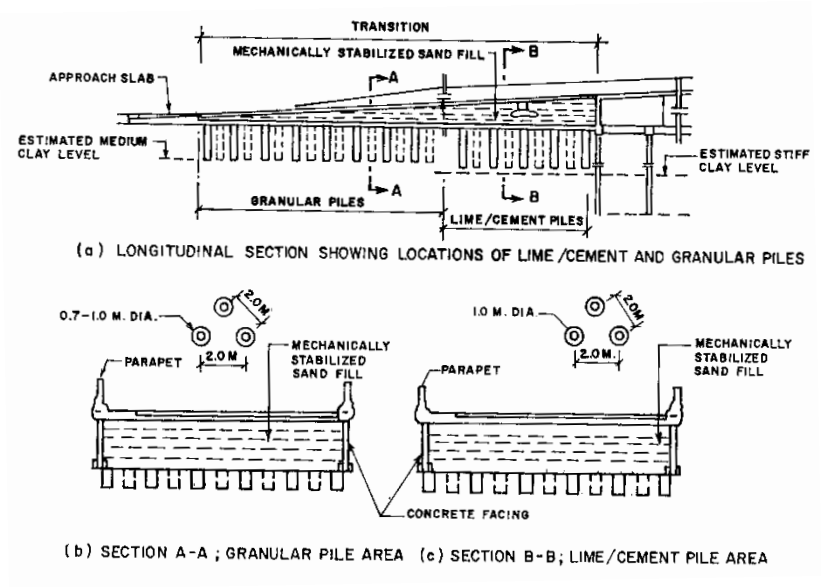

Figure 2.20. Schematic of Granular Compaction Piles with Mechanically Stabilized Earth to Support Bridge Approach Embankments (Bergado et al., 1996).

c. Driven Piles

To eliminate the impact of embankment settlement on the abutment piles, a nest of driven piles consisting of timber piles or precast concrete piles can be installed adjacent to the abutment under the embankment (Hsi, 2007). These driven piles are expected to transfer the embankment loads on to the stiffer layers beneath; as a result, negligible settlements can be expected on the embankment surface.

Hsi (2007) reported the use of timber and concrete piles installed on a 6.6 ft (2 m) c/c square grid near the pile supported bridge abutment to arrest the differential settlements between the abutment and the embankment constructed along the Yelgun-Chinderah freeway in New South Wales, Australia. A series of pile caps (3.3 ft [1 m] square each) overlain by a layer of geotextile reinforced rock mattress (2.5 ft [0.75 m] thick) was also placed over the piles to form an effective bridging layer to transfer the embankment loads on to the piles as shown in Figure 2.21. This method allowed for earlier construction of the abutment piles and hence earlier completion of the bridges to allow haulage and construction traffic through the alignment. The data obtained from the settlement plates and pins installed in the embankment section revealed that the total creep settlements were reduced considerably.

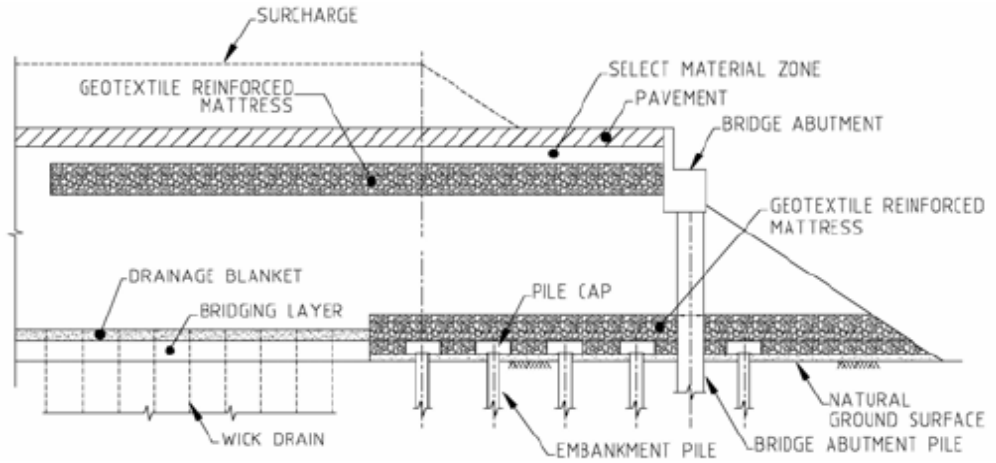

Figure 2.21. Schematic of Bridge Approach Embankment Supported on Driven Piles (Hsi, 2007).

d. Geosynthetic Reinforcement

Whenever highway embankments are constructed over soft soils, the embankment load is distributed over a large area. These soft soils often exhibit failure due to excessive settlements or due to insufficient bearing capacity (Liu et al., 2007). A variety of techniques are available to increase the stability of these structures as discussed above. The application of geosynthetics in supporting highway embankments is gaining popularity (Magnan, 1994). In conventional piled embankment construction, the spacing is very close between piles leading to higher construction costs. However, introducing a layer of geosynthetic reinforcement in the form of geotextile or geogrid at the base of the embankment would not only bring down the cost but also increase the stability of the embankment structure (Liu et al., 2007).

Maddison et al. (1996) reported that the combination of a geosynthetic layer at the base of the embankment constructed over highly compressible peats and clays along with a series of vibroconcrete columns has proven to be the most effective method to increase the stability of the embankment structure and reduce long-term settlements (Figure 2.22).

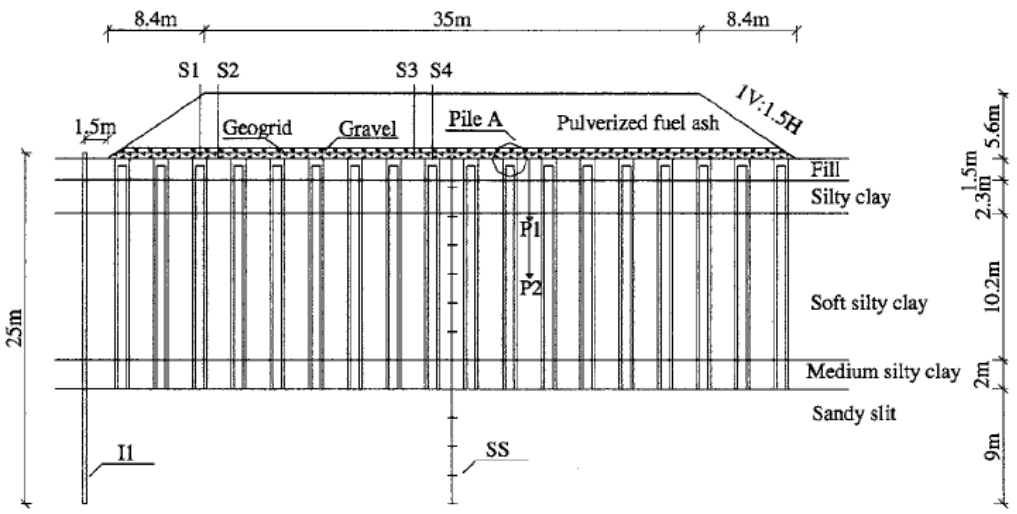

Figure 2.22. Cross Section of Embankment with Basal Geogrid and Columns (Liu et al., 2007).

A more recent development in geosynthetic reinforcement is to provide a confinement to the foundation soil using geocells (Bush et al., 1990; Rowe et al., 1995). A geocell is a three-dimensional, honey comb-like structure of cells interconnected at joints. These geocells provide lateral confinement to the soil against lateral spreading due to high structural loads and thereby increase the load carrying capacity of the foundation soil (Bush et al., 1990; Rowe et al., 1995; Krishnaswamy et al., 2000). The application of geocells as a foundation mattress for embankments constructed on soft soils has been studied by many researchers (Bush et al., 1990; Cowland and Wong, 1993; Rowe et al., 1995; Lin and Wong, 1999; Krishnaswamy et al., 2000).

Cowland and Wong (1993) reported a case study of the performance of a geocell mattress supported embankment on soft clay. A 33 ft (10 m) high embankment was constructed over soft ground comprised of a lagoon deposit overlain by alluvium supported by a geocell foundation in Hong Kong (Figure 2.23). The embankment was extensively instrumented with inclinometers, pneumatic piezometers, hydrostatic profile gauges, settlement plates, surface settlement markers, and lateral movement blocks to verify the design assumptions and also to control the speed of the staged construction. Typical instrumentation data are presented in Figure 2.24. Results revealed that the geocell mattress performed very well in most of the instrumented sections. The measured settlement of the embankment was less than 50% of the predicted settlement with the geocell foundation mattress. They reported measured excessive

settlements due to construction on soft lagoon deposits. Overall, they concluded that the geocell foundation mattress behaved as a much stiffer raft foundation supporting the embankment.

Jenner et al. (1988), making use of slip line theory, have proposed a methodology to calculate the increase in bearing capacity due to the provision of a geocell mattress at the base of the embankment resting on soft soil. Krishnaswamy et al. (2000) carried out a series of laboratory model tests on geocell mattress supported earth embankments constructed over a soft clay bed. Lin and Wong (1999) illustrated the use of mixed soil and cement columns along with geotextile mattress at the base of the embankment in reducing the differential approach settlements. These details are discussed in previous sections. In all these cases, geocell mattress, either backfilled with good granular construction material or locally available mixed soils, enhanced the load carrying capacity of the foundation soil and reduction in short-term and long-term settlements. Hence, geocell mattresses are an economical alternative for shallow to moderate soft soil deposits. However, field studies are lacking on this method and its potential in real field conditions.

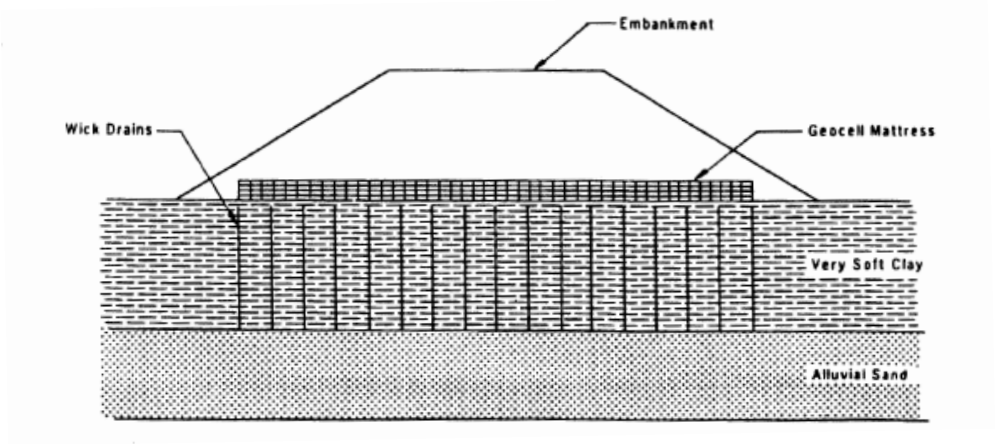

Figure 2.23. Geocell Foundation Mattress Supported Embankment (Cowland and Wong, 1993).

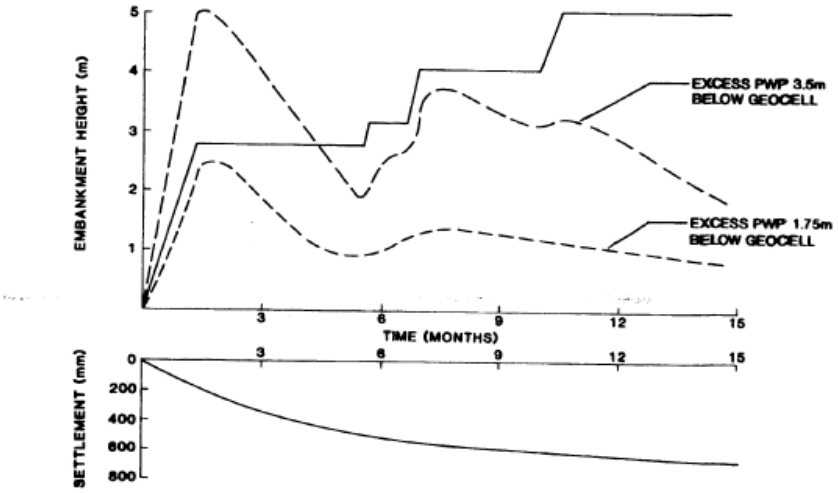

Figure 2.24. Typical Load/Settlement-Pore Pressure/Time Profiles for Embankment Section (Cowland and Wong, 1993).

2.3.2 New Foundation Technologies

2.3.2.1 Geopiers

Geopiers, sometimes also called as short aggregate piers, are constructed by drilling the soft ground and ramming selected aggregate into the cavity, formed due to drilling, in lifts using a beveled tamper (Lien and Fox, 2001). The basic concept in this technique is to push/tamp the aggregate vertically as well as laterally against the soft soil to improve the stiffness against compressibility between the piers. These short piers can also allow radial drainage due to their open-graded stone aggregate structure to accelerate the time dependent consolidation process and also to relieve excess pore water pressures generated in the soft soil (Lien and Fox, 2001).

The geopier soil reinforcement system has been adopted in transportation-related applications such as roadway embankments and retaining walls to mitigate settlement of these structures (Lien and Fox, 2001; White and Suleiman, 2004). The design and construction details of these short piers are well documented in the literature (Lawton and Fox, 1994; Minks et al., 2001; White and Suleiman, 2004). Figure 2.25 demonstrates the schematic of the geopier construction sequence. Figure 2.26 presents the typical geopier system supporting the highway embankment.

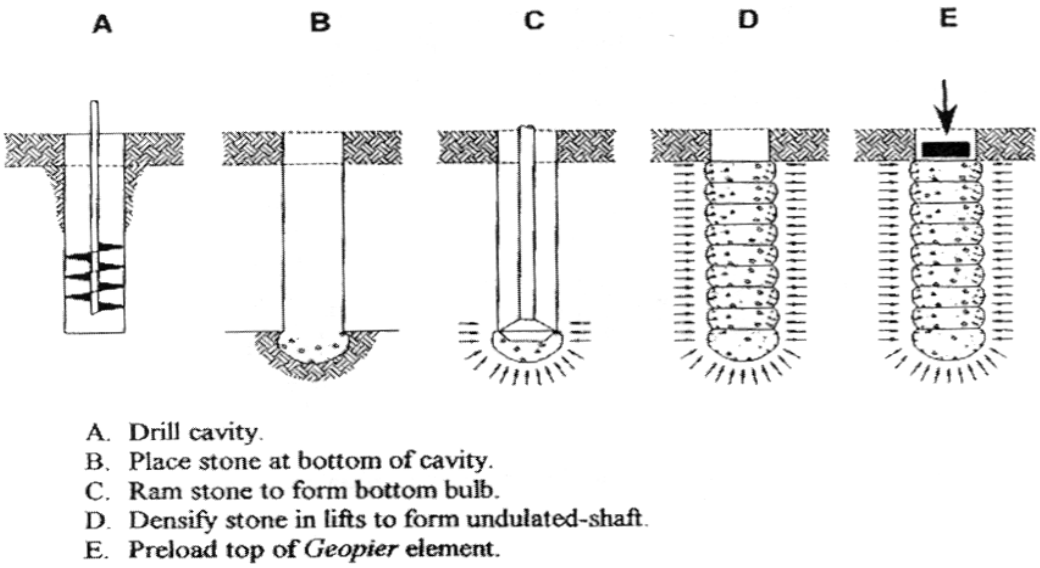

Figure 2.25. Geopier Construction Sequence (Lien and Fox, 2001).

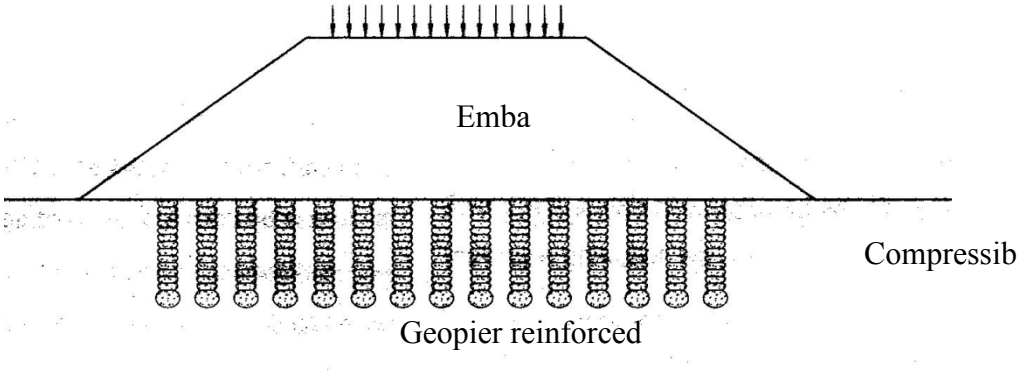

Figure 2.26. Typical Geopier System Supporting the Embankment (Lien and Fox, 2001).

White et al. (2002) demonstrated the performance of the geopier system over stone columns in supporting highway embankments in Des Moines, Iowa. The purpose of the reinforcement technique was to reduce the magnitude and increase the time rate of consolidation settlements and to facilitate rapid abutment construction. These two sections were instrumented with settlement plates to measure during- and post-construction settlements. Prior to the embankment construction, geotechnical measurements were made to characterize both the sections by performing standard penetration tests (SPTs), borehole shear tests (BSTs), and full scale load tests. The SPT tests performed through production columns revealed that average N-Values of 11 and 17 were obtained for stone columns and geopiers, respectively. Figure 2.27 compares the settlement readings with the increase in fill height obtained from

settlement plates from both the stone columns section and the geopier system. It is seen that the settlement of the matrix soil near the stone column is three times higher than the settlements observed in the matrix soil next to the geopier system.

White and Suleiman (2004) demonstrated the design procedures for short aggregate pier systems for a highway embankment construction. They observed two types of failure mechanisms, namely, bulging and plunging of the piers in their study on short aggregate piers. They recommend that the design of piers should be carried out based on the tip resistance to prevent bearing capacity problems.

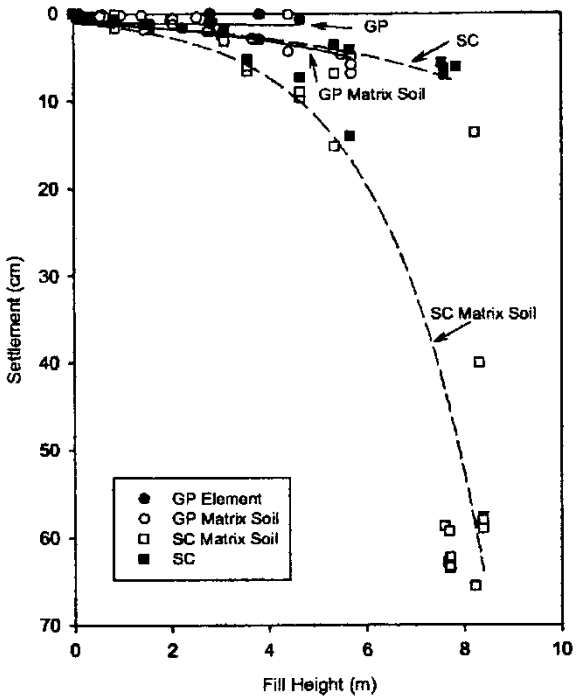

Figure 2.27. Comparison of Settlement with Fill Height for Both Stone Column and Geopier Systems (White et al., 2002).

2.3.2.2 Deep Soil Mixing (DSM)

Deep Soil Mixing (DSM) technology was pioneered in Japan in the late 1970s and has gained popularity in the United States over many years in the field of ground improvement (Barron et al., 2006). DSM is a process to improve soil by injecting grout through augers that mix in with the soil forming in-place soil-cement columns (Barron et al., 2006). Recently, the cement binder has been replaced with many other cementitious compounds such as lime, flyash, or a combination of any two compounds. Hence, in a broader sense, the DSM technique

is an in-situ mixing of stabilizers such as quicklime, cement, lime-cement, or ashes with soft and/or expansive soils to form deep columns to modify weak subgrade soils (Porbaha, 1998).

Figure 2.28 presents a typical DSM operation and resulting columns in the field. The DSM treated columns provide substantial improvements to soil properties such as strength and compressibility. The DSM columns have been used on several state highways to improve the stability of earth structures, to improve the bearing capacity of soils, to reduce the heave and settlement of embankments and roadways, to provide lateral support during excavations, to improve seismic stability of earthen embankments constructed over soft soils, and to reduce bridge approach settlements. This stabilization technique has been proven effective on soft clays, peats, mixed soils, and loose sandy soils (Rathmayer, 1996; Porbaha, 1998; Lin and Wong, 1999; Porbaha, 2000; Bruce, 2001; Burke, 2001).

The success of DSM-based ground treatment methods has led to improved processing and novel installation technologies with the use of different additives incorporated as either dry or wet forms to stabilize subsoils. Currently, there are more than 18 different terminologies used to identify different types of deep soil mixing methods (Porbaha, 1998, 2000). Irrespective of these terminologies, the stabilization mechanisms are similar and their enhancements to soil strength and compressibility properties are considerable. The development of new applications should take advantage of the unique characteristic of Deep Soil Mixing in which rapid stabilization is possible in a short period of time leading to accelerated construction in the field. Although the initial demand for DSM was to gain higher strength at lower cost, the recent complex construction dilemmas in expansive soils and other problematic soils have led to a greater need of evaluating this technology for expansive soil modification in field settings (Porbaha and Roblee, 2001).

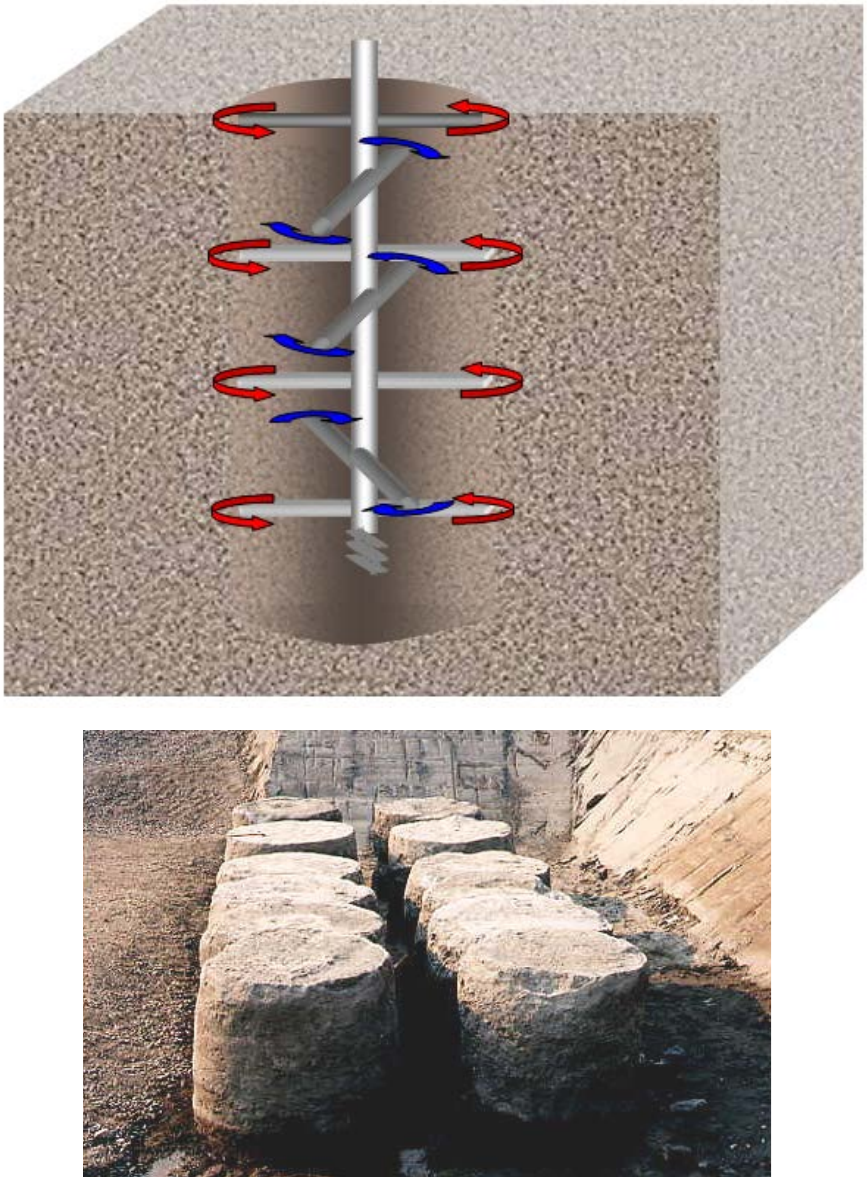

Figure 2.28. Deep Soil Mixing (DSM) Operation and Extruded DSM Columns.

This technology has been used by various state highway agencies such as Caltrans, Utah DOT, and Minnesota DOT in cooperation with the National Deep Mixing (NDM) Program, a research collaboration of the FHWA with 10 state DOTs. Several other case studies are reported both in and outside the U.S. for the use of DSM columns to reduce embankment settlements. Recently, TxDOT initiated Research Project 0-5179 to evaluate the DSM columns in mitigating the pavement roughness in expansive soils. The results from two instrumented sites demonstrate that the DSM is a promising technique to mitigate the pavement roughness.

Lin and Wong (1999) studied the deep cement mixing (DCM) technique to improve the strength of a 66 ft (20 m) thick layer of soft marine clay with high moisture content to reduce the total and differential settlements at bridge embankments constructed along Fu-Xia expressway in the southeast region of China. The bridge abutments were planned to be placed on deep pile foundations with little to no allowable settlements. The maximum settlement of the embankment fill on the soft marine clays was predicted as 11.8 in. (300 mm). To alleviate these differential settlements between the pile-supported abutments and the embankment fills, soil-cement DSM columns were selected to reinforce the embankment foundation soil.

Prior to the construction of the actual embankment(s) along the proposed Fu-Xia Expressway, trial embankment sections 1.7 mi (2.7 km) long were constructed to verify the efficiency of the selected ground improvement techniques such as prefabricated sand drains, plastic band drains, and deep cement mixing columns. They employed varying lengths of DCM columns with the longest columns placed near the bridge abutment and shorter columns away from the abutments as shown in Figure 2.29. This profile of DCM columns was adopted to increase the stiffness of the embankment toward the bridge abutments to result in gradual decrease in the settlements toward the bridge. A combination of band drains with a sand mat adjacent to the DCM treatment was to facilitate faster drainage of the pore water and to reduce the differential settlements between the DCM treated section and the rest of the untreated embankment sections.

The test embankment was heavily instrumented with inclinometers, settlement plates, multipoint settlement gauges, soil pressure cells, and piezometers to verify the performance of the DCM columns. Most of this instrumentation was done to the DCM columns and to the soft soil in between the columns except the inclinometer casings. Inclinometer casing was installed at the embankment toe. Figure 2.30 shows the complete instrumentation used in their study. The monitoring results indicated that the settlement and lateral movement of the soft clay treated by the DCM columns was reduced significantly. Use of the DCM columns of varying lengths having longer columns toward the pile supported abutments allowed the construction of the embankments to their full design height in a short period of time with acceptable post-construction total differential settlement at the bridge approaches.

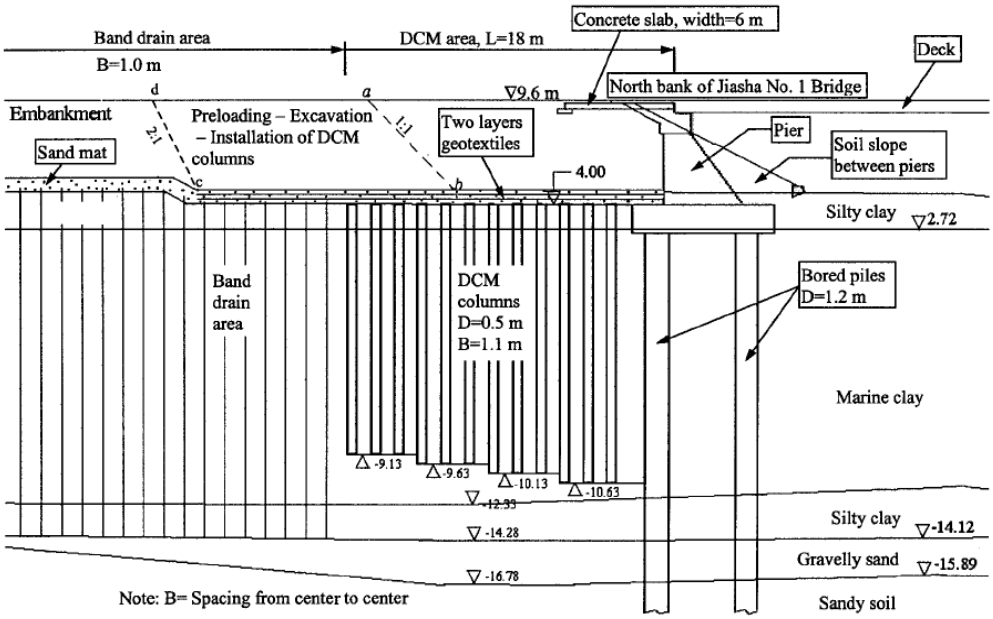

Figure 2.29. Schematic of DCM Columns with Varying Length to Support Highway Embankment over Soft Marine Clay (Lin and Wong, 1999).

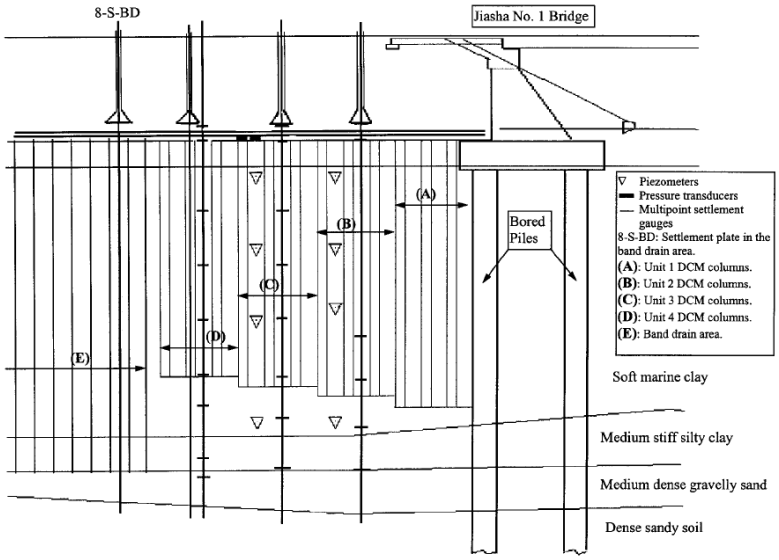

Figure 2.30. Instrumentation Details of DCM Treated Embankment (Lin and Wong, 1999).

A similar technique (soil-cement columns) was used as a remediation method by Shen et al. (2007) to mitigate differential settlement of approach embankments along the Saga airport approach road constructed on Ariake clay in Japan. The actual road project connected city of Saga with the Saga airport. After construction and open to traffic for two and a half years, the embankment fill adjacent to the bridge abutment settled 3.02 ft (0.92 m) although the

predicted residual settlement due to the traffic load was about 7.7–15.4 in. (0.2–0.4 m) over the 20 year design life. A detailed geotechnical investigation was carried out, which revealed these road sections were underlain by thick layers of the highly sensitive, soft Ariake clay.

Three remediation techniques were considered such as an asphalt concrete overlay, an approach cushion slab method, and a column approach (CA) method to mitigate these differential settlements between the approach embankment and the piled abutments. The first two conventional methods were selected based on Japanese pavement design guidelines. These two conventional methods were also adopted at two different sections of the road project to compare the cost and performance differences of the column approach method. In the CA technique, the road approach (transitional zone) was supported by a row of soil-cement columns with lengths reduced with the increased distance away from the rigid piled abutment structure to smoothen the settlement profile within the transition zone as shown in Figure 2.31.

A connecting slab was used to transfer the embankment loads to the CA system. The details of the design parameters of the CA method such as length of the soil-cement columns, spacing between columns, and details of the connecting slab are clearly described by Shen et al. (2007). They reported that the column approach method is proven to be economical and efficient in mitigating the differential settlements although the initial construction costs are higher than the conventional treatment methods discussed. Figure 2.32 shows that the CA method is economical when the differential settlements are more than around 11.8 in. (300 mm).

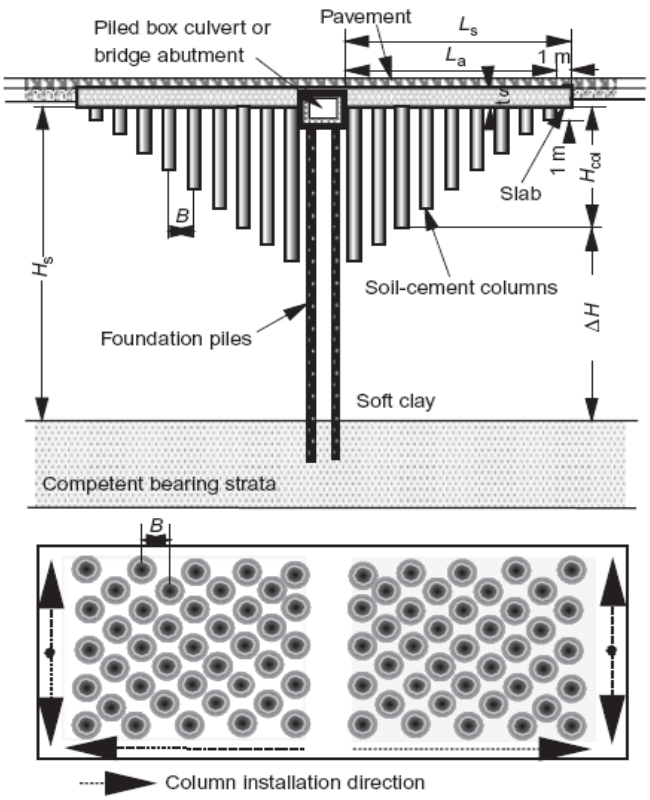

Figure 2.31. Section and Plan View of Soil-Cement Pile Supported Approach Embankment (Shen et al., 2007).

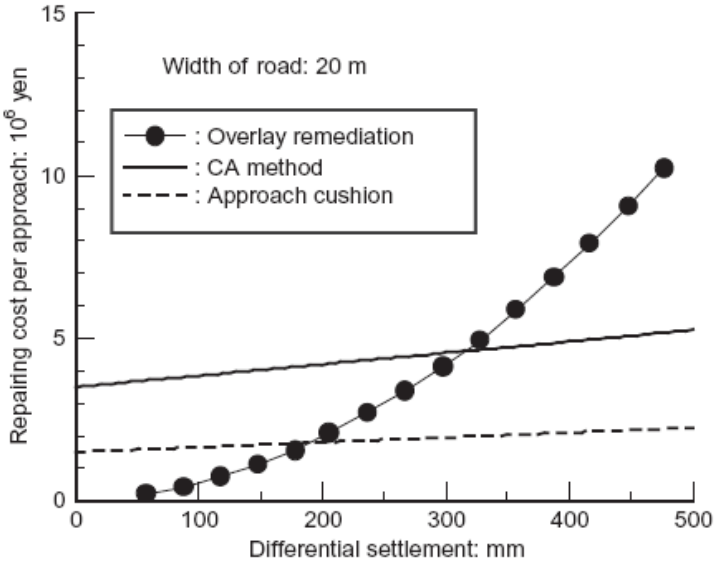

Figure 2.32. Maintenance Cost with Differential Settlements (Shen et al., 2007).

2.3.2.3 Concrete Injected Columns

Concrete injected columns (CICs) are an innovative technique where a soil displacement pile mechanism is used to create in-situ concrete columns without reinforcement (Hsi, 2007; 2008). CICs are installed by inserting a displacement tool (auger) into the soft soil and then rotating and pushing the tool. Upon reaching the final depth, concrete is pumped through the hollow stem of the tool during extraction as shown in Figure 2.33. Inserting reinforced casing into the CICs is optional and the depth to which the reinforcement casing can be installed is also limited (Hsi, 2008). Typically these columns are prepared at 19.7 in. (500 mm) diameter and the length of these columns can be extended to reach a stiff strata or shallow bed rock. This technique is widely used to reinforce the very soft to soft foundation soils (Hsi, 2007). CICs were recently adopted to control the excessive long-term settlements of approach embankments constructed on estuarine and marine soft clays along an upgrade to the Brunswick Heads – Yelgun Pacific Highway in Australia.

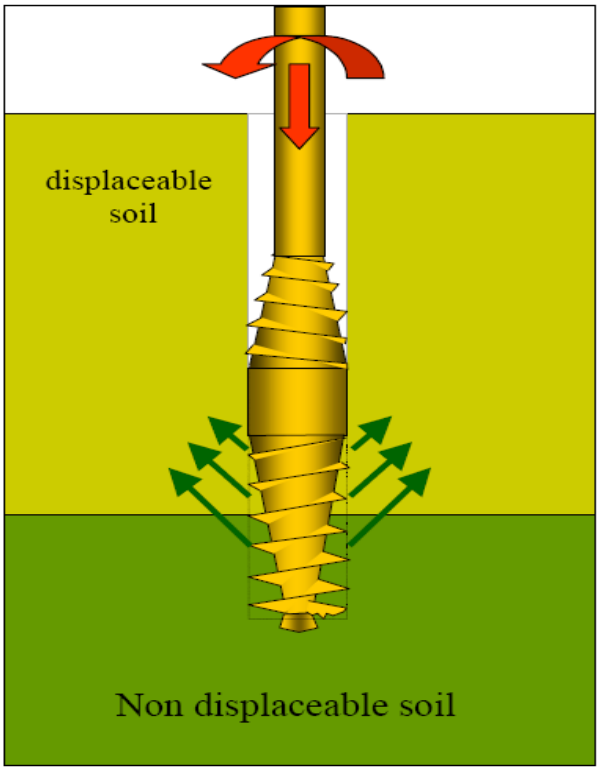

Figure 2.33. Installation of Concrete Injected Columns (Hsi, 2008).

Two geometric patterns (Zone 1 and 2) of CICs are installed in the soft foundation soil as shown in Figure 2.34. Zone 1 is for the support of the approach embankment, and Zone 2 is

to eliminate abrupt differential settlement between the closely spaced approach embankment section (Zone 1) and rest of the embankment. The spacing adopted for CICs in Zone 2 is around 6.6 ft (2 m) c/c and hence provided with a pile cap. These CICs were covered with a pair of geotextile blankets to uniformly distribute the embankment loads to the CICs. This combination of CICs with geotextiles provided a competent base for the embankment.

To assess the performance of the CICs, the embankment section was instrumented with inclinometers to measure the lateral movements of the embankment due to construction activity and further, settlement plates to measure the settlement of the embankment. Figure 2.35 presents the data obtained from the settlement plates. The data obtained from this instrumentation demonstrated that the settlements are well within the allowable limits stipulated for this project. These limits are that the pavement was required to achieve a maximum of 3.9 in. (100 mm) residual settlement and a change in grade of 0.3% in any direction over the 40 year design life. In addition, this technique allowed constructing the pile foundation for the abutment prior to preloading the embankment, which led to a reduction in total project costs.

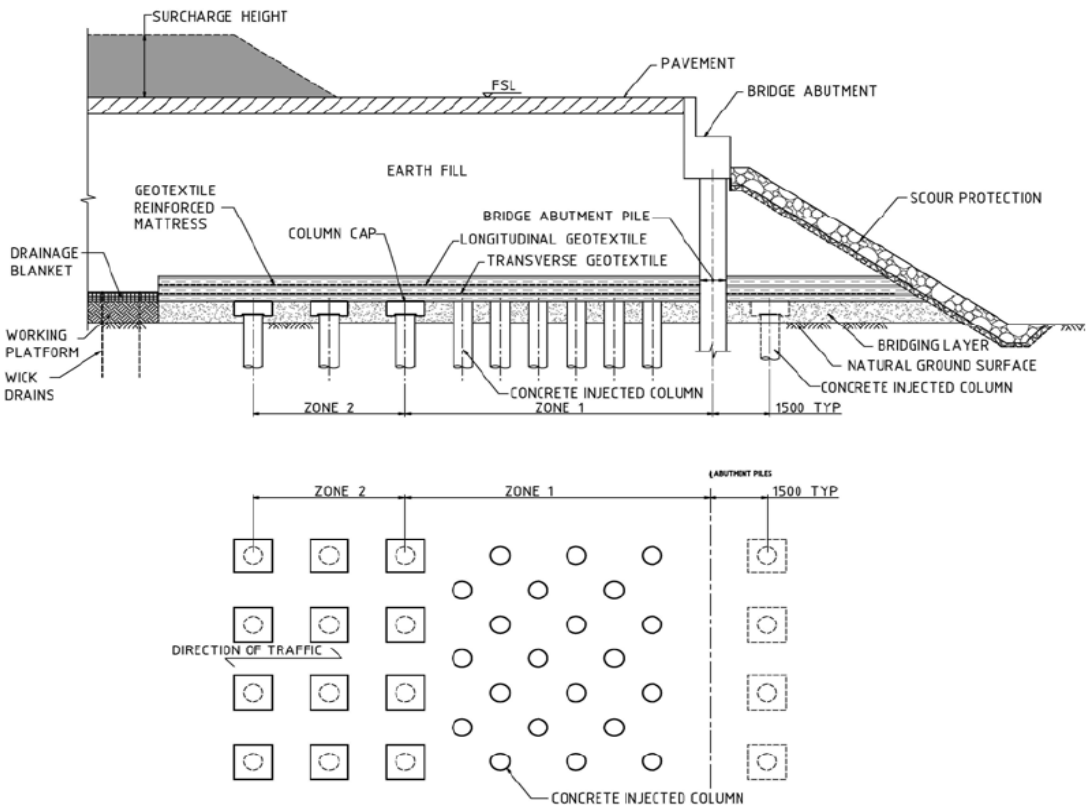

Figure 2.34. Bridge Approach Treatment with Concrete Injected Columns (Sectional and Plan View).

2.3.2.4 Continuous Flight Auger Cast Piles (CFA)

Continuous Flight Auger Cast Piles (CFA) are installed by rotating a continuous-flight hollow shaft auger into the soil to reach a specified depth. High strength cement grout, sand, or concrete is pumped under pressure through the hollow shaft as the auger is slowly withdrawn. If this process uses pressure grouting, these CFA piles are sometimes termed as Auger Pressure Grouted (APG) piles. The resulting grout column hardens and forms an auger cast pile (Neely, 1991; Brown et al., 2007). Reinforcing, when required, must be installed while the cement grout is still fluid, or in the case of full length single reinforcing bars, through the hollow shaft of the auger prior to the withdrawal and grouting process (Neely, 1991; Brown et al., 2007).

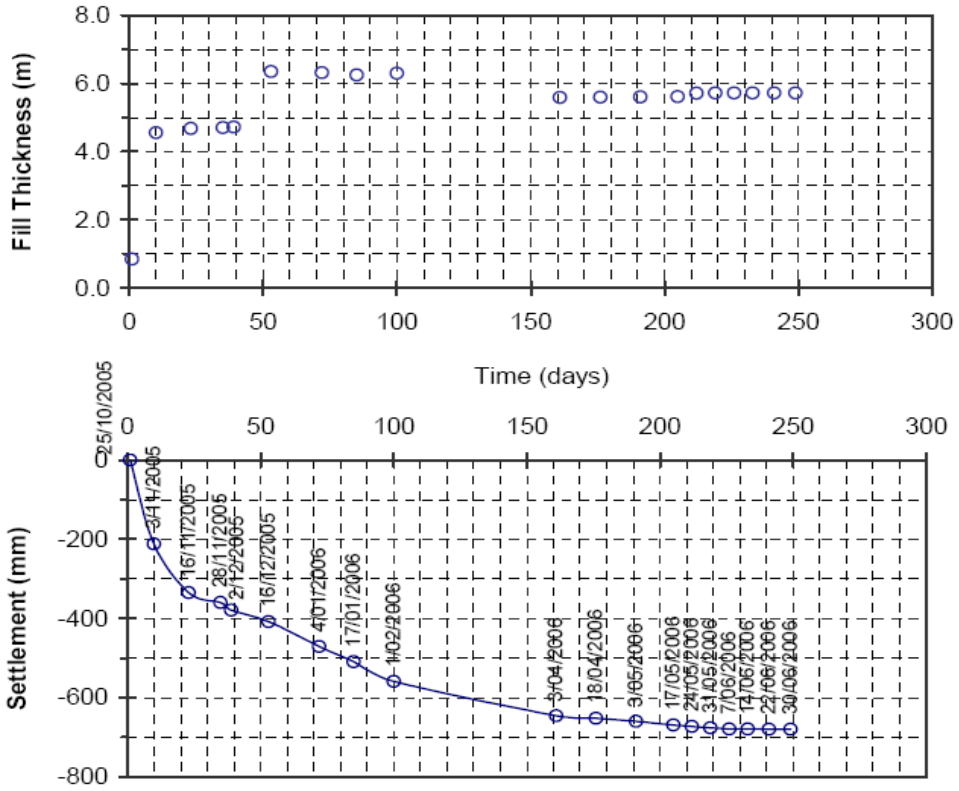

Figure 2.35. Settlement Profiles Obtained from Settlement Plates (Hsi, 2008).

Auger cast piles can be used as friction piles, end-bearing piles, anchor piles; auger cast vertical curtain wall or beam and lagging wall and sheet pile walls (Brown et al., 2007). The advantages of CFA piles over other pile types (driven piles) include less noise, no objectionable vibrations, no casing required, can be installed in limited headroom conditions, and soil samples can be obtained from each borehole (Brown et al., 2007). The typical dimensions reported are from 12 in. to 18 in. (305 mm to 457 mm). However, auger cast piles with diameters of 24, 30, and 36 in. (610, 760, and 910 mm) have been successfully utilized with tests being conducted as high as 600 kips (350 tons).

O'Neill (1994) and Brown et al. (2007) summarized the construction systems of augered piles and documented different methods available to estimate the axial capacity of CFA piles. Figure 2.36 shows the construction procedures for continuous auger cast piles and screw piles. Brown et al. (2007) summarized the advantages and disadvantages of CFA piles and driven piles. Although several advantages of CFA piles have been stated, the major two disadvantages of these piles must be noted. First, the available Quality Assurance (QA)

methods to assess the structural integrity and the pile bearing capacity of these piles are not reliable. Second, the disposal of associated soil spoils when the soils are contaminated. In addition, CFA piles were not considered by public transportation departments in the U.S. prior to the 1990s because of the lack of design methods. The use of CFA piles has been increased in the U.S. after recent developments in automated monitoring and recording devices to address quality control and quality assurance issues (EBA Engineering Inc., 1992; Brown et al., 2007).

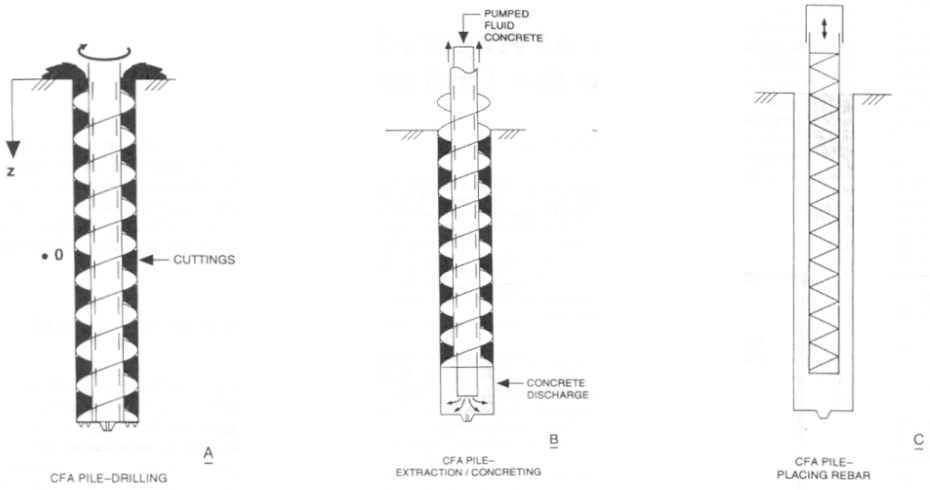

Figure 2.36. Construction Procedures for Continuous Auger Piles (O'Neill, 1994).

Since CFA piles behave somewhere between drilled shafts and driven piles, CFA piles have been designed using both approaches (Zelada and Stephenson, 2000; Brown et al., 2007). McVay et al. (1994) reported the successful use of auger cast piles in coastal shell-filled sands in Florida. They concluded that the equipment selection, drilling rate, grout's aggregate size, grout pumping, augur removal, and grout fluidity significantly affect the quality and the load carrying capacity of the augered piles. They summarized different empirical methods to estimate the capacities of auger cast piles, which include the Wright and Reese, Neely, and LPC (Laboratorie Des Ponts et Chausses) methods. McVay et al. (1994) compared the measured load-settlement data with predicted capacities from these methods. The Wright and Reese method gave reasonable predictions of capacities at 5% settlement of the pile diameter. They also concluded to use 5% of the pile's diameter for the failure criteria to be acceptable for typical augured cast piles in the 12 in. (305 mm) diameter range.

Vipulanandan et al. (2004) studied the feasibility of CFA piles as a bridge abutment foundation alternative to the driven pile system on a new bridge constructed by TxDOT near

Crosby, Texas. They noticed a few construction issues for the installation of the CFA piles including the difficulties involved in reinforcing the entire depth of piles due to excessive grout velocity and/or lack of timely workmanship by the contractor. They also reported that the load carrying mechanism of the CFA piles was entirely due to the mobilization of the side friction resistance of the pile based on the pile load test on the instrumented test piles. They also concluded that the cost involved in installing the CFA pile system was 8% less than that of the driven pile system for the same length of the foundations. In addition, the CFA piles are having a higher factor of safety against axial loading than the other foundations.

CFA piles to support bridge approach slabs are considered only when the foundation soil is highly compressible and the time required for the consolidation settlement is long, i.e., several years and when minimization of post-construction settlements and construction delays are required (Brown et al., 2007). Only a few studies are available in the literature where the CFA piles were used to support the embankment in order to mitigate settlements. Figure 2.37 shows the CFA pile supported railway embankment in Italy. Pile support was used to increase the stability of the embankment against excessive settlement anticipated due to extra fill on the existing embankment and load due to increased rail traffic. The CFA piles were capped using concrete filled cylinders and the fill overlain by the pile caps were reinforced with geotextiles. Performance details of these systems for settlement control are not yet documented.

Other details on the CFA piles including construction sequences, materials required, equipment specifications, and performance based design factors of these CFA piles are found in Brown et al. (2007).

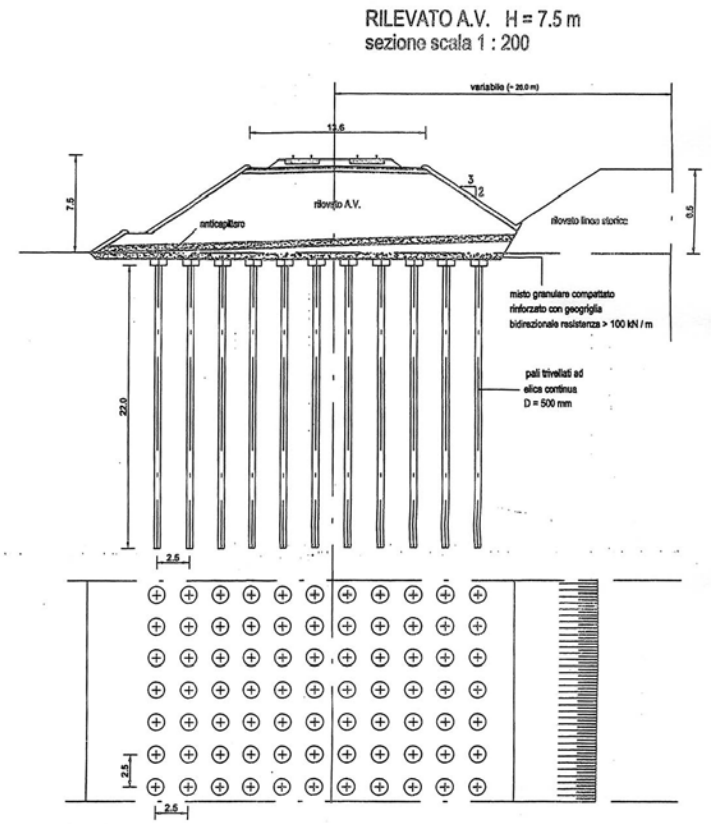

Figure 2.37. CFA Pile Supported Railway Embankment for Italian Railway Project (Brown et al., 2007).

2.3.3 Improvement of Approach Embankment/Backfill Material

The bridge approach embankment has two functions: first, to support the highway pavement system, and second, to connect the main road with the bridge deck. Most of the approach embankments are normally constructed by conventional compaction procedures using materials from nearby roadway excavation or a convenient borrow pit close to the bridge site. This implies that the serviceability of the embankment, in the aspects of slope stability, settlement, consolidation, or bearing capacity issues, depends on the geotechnical properties of the fill materials (Wahls, 1990). In addition, since the embankment must provide a good transition between the roadway and the bridge, the standards for design and construction considerations both in materials' quality requirements and compaction specifications must be specified in order to limit the settlement magnitude within a small acceptable degree (Wahls, 1990).

Generally, the materials for embankment construction should have these following properties (White et al., 2005):

- Being easily compacted.
- Not time-dependent.
- Not sensitive to moisture.
- Providing good drainage.
- Erosion resistance.
- Shear resistance.

Dupont and Allen (2002) cited that the most successful method to construct the approach embankments is to select high quality fill material with the majority of them being a coarse granular material with high internal frictional characteristics. Several research studies have been attempted to define methods to minimize the potential of settlement and lateral movement development in the approach embankments, and these studies are discussed in the following.

Hoppe (1999) studied the embankment material specifications from various DOTs. The results from his survey are presented in Tables 2.3 and 2.4. Table 2.3 shows that 49% of the state agencies use more rigorous material specifications for an approach fill than for a regular highway embankment fill. Furthermore, the study also shows that typical requirements for the backfill materials among the different states varied with one another. One common requirement followed by several states is to limit the percentage of fine particles in the fill material in order to reduce the material plasticity. As an example, the allowable percentage of material passing the No. 200 (75-micron) sieve varies from less than 4% to less than 20%. Another requirement commonly found is to enhance the fill drainage properties by a requisite of pervious granular material.

From the same study by Hoppe (1999), two other conclusions can be further drawn from Table 2.4. First, in many states, a 95% of the standard proctor test compaction condition is generally specified for the compaction of approach fill.

Table 2.3. Embankment Material Specifications (Hoppe, 1999).

State	Same/Different from Regular Embankment	% Passing 75 mm (No.200 sieve)	Miscellaneous
AL	Same		A-1 to A-7
AZ	Different		
CA		<4	Compacted pervious material
CT	Different	<5	Pervious material
DE	Different		Borrow type C
FL	Same		A-1, A-2-4 through A-2-7, A-4, A-5, A-6, A-7 (LL<50)
GA	Same		GA Class I, II or III
ID			A yielding material
IL	Different		Porous, granular
IN	Different	<8	
IO	Different		Granular; can use Geogrid
KS			Can use granular, flowable or light weight
KY		<10	Granular
LA			Granular
ME	Different	<20	Granular borrow
MA	Different	<10	Gravel borrow type B, M1.03.0
MI	Different	<7	Only top 0.9 m (3 ft) are different (granular material Class II)
MN		<10	Fairly clean granular
MO			Approved material
MS	Different		Sandy or loamy, non-plastic
MT	Different	<4	Pervious
NE			Granular
NV	Different		Granular
NH	Same	<12	
NJ	Different	<8	Porous fill (Soil Aggregate I-9)
NM	Same		
NY		<15	<30% Magnesium Sulfate loss
ND	Different		Graded mix of gravel and sand
OH	Same		Can use granular material
OK	Different		Granular just next to backwall
OR	Different		Better material
SC	Same		
SD	Varies		Different for integral; same for conventional
TX	Same		
VT	Same		Granular
VA	Same		Pervious backfill
WA			Gravel borrow
WI	Different	<15	Granular
WY	Different		Fabric reinforced

Table 2.4. Lift Thickness and Percent Compaction Requirements (Hoppe, 1999).

State	Lift Thickness, mm(in.)	% Compaction	Miscellaneous
AL	203(8)	95	
AZ	203(8)	100	
CA	203(8)	95	For top 0.76 m (2.5 ft)
CT	152(6)	100	Compacted lift indicated
DE	203(8)	95	
FL	203(8)	100	
GA		100	
ID	203(8)	95	
IL	203(8)	95	For top, remainder varies with embankment height
IN	203(8)	95	
IO	203(8)	None	One roller pass per inch thickness
KS	203(8)	90	
KY	152(6)	95	Compacted lift indicated; Moisture = +2% or -4% of optimum
LA	305(12)	95	
ME	203(8)		At or near optimum moisture
MD	152(6)	97	For top 0.30 m (1ft), remainder is 92%
MA	152(6)	95	
MI	230(9)	95	
MN	203(8)	95	
MO	203(8)	95	
MS	203(8)		
MT	152(6)	95	At or near optimum moisture
NE		95	
NV		95	
NH	305(12)	98	
NJ	305(12)	95	
NY	152(6)	95	Compacted lift indicated
ND	152(6)		
OH	152(6)		
OK	152(6)	95	
OR	203(8)	95	For top 0.91 m (3ft), remainder is 90%
SC	203(8)	95	
SD	203-305(8-12)	97	0.20 m (8 in.) for embankment, 0.30 m (12 in.) for bridge end backfill
TX	305(12)	None	
VT	203(8)	90	
VA	203(8)	95	±20% of optimum moisture
WA	102(4)	95	Top 0.61 m (2 ft), remainder is 0.20 m (8 in.)
WI	203(8)	95	Top 1.82 m (6 ft and within 60 m (200 ft) remainder is 90%
WY	305(12)		Use reinforced geotextiles layers

Second, the approach fill material is normally constructed at a lift thickness of 8 in. (203 mm). In Texas, a loose thickness of 12 in. (305 mm) compacted to 8 in. (203 mm) of fill is commonly used and the percent compaction is not always specified. Dupont and Allen (2002) also conducted another survey of 50 state highway agencies in the U.S. in order to identify the most common type of backfill material used in the embankments for bridge approaches. Their study shows that most of the state agencies: 38 states use granular material as the backfill, 3 states use sands, 6 states use flowable fill, while 17 states use compacted soil in the abutment area. The agencies identified more than one material type that was used as backfill material.

A few other research studies were conducted to study the limitations of the percent fine material used in the embankment fill. Wahls (1990) recommended that the fill materials should have a plasticity index (PI) less than 15 with percent fines not more than 5%. The FHWA (2000) recommended backfill materials with less than 15% passing the No. 200 sieve. Another recommendation of the backfill material by Seo (2003) specifies the use of a backfill material with a plasticity index (PI) less than 15 with less than 20% passing the No. 200 sieve and with a coefficient of uniformity greater than 3. This fill material is recommended to be used within 100 ft (30.5 m) of the abutment.

For the density requirements, Wahls (1990) suggested two required density values: one for roadway embankments and the other for bridge approaches. For embankment material, the recommended compaction density is 90 to 95% of maximum dry density from the AASHTO T-99 test method, while the density for the bridge approach fill material is recommended from 95 to 100% of maximum dry density from the AASHTO T-99 test method. Wahls (1990) also stated that well-graded materials with less than 5% passing the No. 200 sieve are easy to be compacted and such material can minimize post-construction compression of the backfill and can eliminate frost heave problems.

Seo (2003) suggested that the embankment and the backfill materials within the 100 ft (30.5 m) length from the abutment should be compacted to 95% density of the modified proctor test. White et al. (2005) also recommended the same compaction of 95% of the modified proctor density for the backfill. White et al. (2005) also used a Collapse Index (CI) as a parameter to identify an adequacy of the backfill material in their studies. The CI is an index that measures the change in soil volume as a function of placement water content. It was

found that materials placed at moisture contents in the bulking range from 3% to 7% with a CI value up to 6% meet the Iowa DOT specifications for granular backfills.

In the current TxDOT Bridge Design Manual (2001), the approach slab should be supported by the abutment backwall and the approach backfill. Therefore, the backfill materials become a very important aspect in an approach embankment construction. As a result, the placement of a Cement Stabilized Sand (CSS) "wedge" in the zone behind the abutment is currently practiced by TxDOT. The placement of the CSS wedge in the zone behind the abutment is to solve the problems experienced while compacting the fill material right behind the abutment. This placement also provides a resistance to the moisture gain and loss of material, which are commonly experienced under approach slabs. The use of CSS has become standard practice in several districts and has shown good results according to the TxDOT manual.

Apart from the embankment backfill material and construction specifications, the other alternatives, such as using flowable fills (low strength and flowable concrete mixes) as backfill around the abutment, wrapping layers of backfill material with geosynthetic or grouting, have also been employed to solve the problem of the excessive settlements induced by the embankment. The use of these construction materials and new techniques increases construction costs inevitably. However, the increased costs can be balanced by the benefits obtained by less settlement problems. For example, the use of a geosynthetic can prevent infiltration of backfill into the natural soil, resist lateral movements, and improve the quality of the embankment (Burke, 1987). Other benefits are explained while describing these new methods in the following sections.

2.3.3.1 Mechanically Stabilized Earth (MSE) Wall

Mechanically Stabilized Earth (MSE) wall have been rapidly developed and widely used since the 1970s (Wahls, 1990). The MSE method is a mitigation technique that involves the mechanical stabilization of soil with the assistance of tied-back walls. As shown in Figure 2.38, a footing of the bridge is directly supported by backfill; therefore, a reinforcement system in the upper layer of the embankment where the backfill is most affected by the transferred load from the superstructure must be carefully designed (Wahls, 1990). On the contrary, the facing element of the wall does not have to be designed for the loading since the

transferred load from the bridge in the MSE scheme does not act on the MSE wall (Wahls, 1990).

Based on a study conducted by Lenke (2006), the results of this research shows that the MSE walls tend to have lesser approach slab settlements than other types of bridge abutment systems due to these following reasons; first, the MSE walls will have excellent lateral constraints provided by the vertical wall system, and second, the tie back straps in the MSE system can provide additional stability to the embankment. These two reasons can minimize lateral loads in the embankment beneath the abutment. Consequently, the potentials of lateral settlements are reduced (Dupont and Allen, 2002).

Other advantages of the use of MSE walls are that they reduce the time-dependent post-construction foundation settlements of very soft clay as noted by White et al. (2005). Also, the MSE wall with the use of a geosynthetic reinforced backfill and a compressible material between the abutment and the backfill can tolerate a larger recoverable cyclic movement as noted by Wahls (1990) and Horvath (1991).

Regarding construction aspects, the MSE walls have recently become a preferred practice in many state agencies (Wahls, 1990). First, the MSE is considerably an economical alternative to deep foundation or treatment of soft soil foundations. Second, the MSE can be constructed economically and quickly when compared to conventional slopes and reinforced concrete retaining walls. Third, a compacted density in the MSE construction can be achieved easily by increasing lateral constraint. Finally, the MSE is also practical to build in urban areas where the right-of-way and work area are restricted (Wahls, 1990). Abu-Hejleh et al. (2006) cited that the use of an MSE wall for an abutment system should be considered as a viable alternative for all future bridges and it is reported as one of the practical embankment treatment systems to alleviate the bridge bump problem. Figure 2.38 shows an example of an MSE wall abutment.

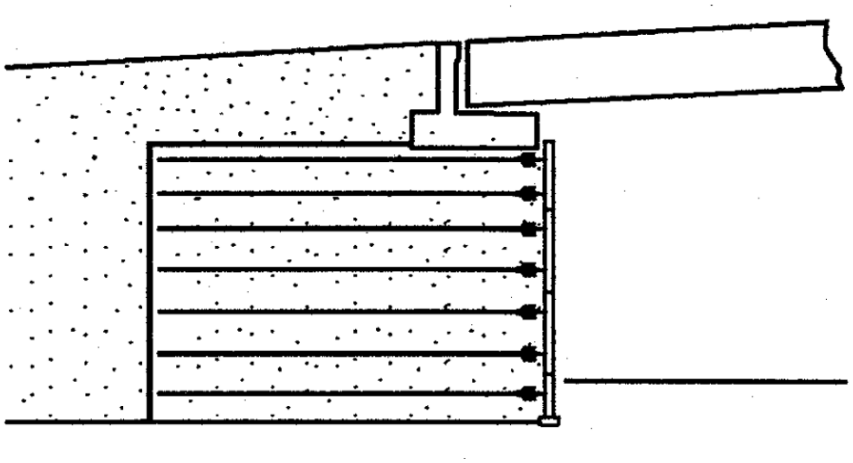

Figure 2.38. Typical Mechanically Stabilized Abutment (Wahls, 1990).

2.3.4 Geosynthetic Reinforced Soils (GRS)

Geosynthetic Reinforced Soil (GRS) is recommended as a method to achieve a backfill compaction at the optimal moisture content, especially for a coarse-grained backfill material (Abu-Hejleh et al., 2006). The GRS is a geosynthetic-reinforced soil structure constructed either vertically or horizontally in order to minimize the uneven settlements between the bridge and its approach. Figure 2.39 shows a schematic diagram of a GRS wall structure and a complete typical GRS system after construction. Abu-Hejleh et al. (2006) discovered that with the use of GRS, the monitored movements of the bridge structure were smaller than those anticipated in the design or allowed by performance requirements. In addition, they also stated that with the use of GRS systems, post-construction movements can be reduced substantially, thus the bump problem at the bridge transition is minimized.

Another advantage of geosynthetic-reinforced soil is that it increases backfill load carrying capacity and reduces erosion of the backfill material; both can help in the mitigation of approach bumps. Some states have also used layers of geosynthetic reinforcement soil in combination with shallow foundations to support the bridge abutment (Abu-Hejleh et al., 2000).

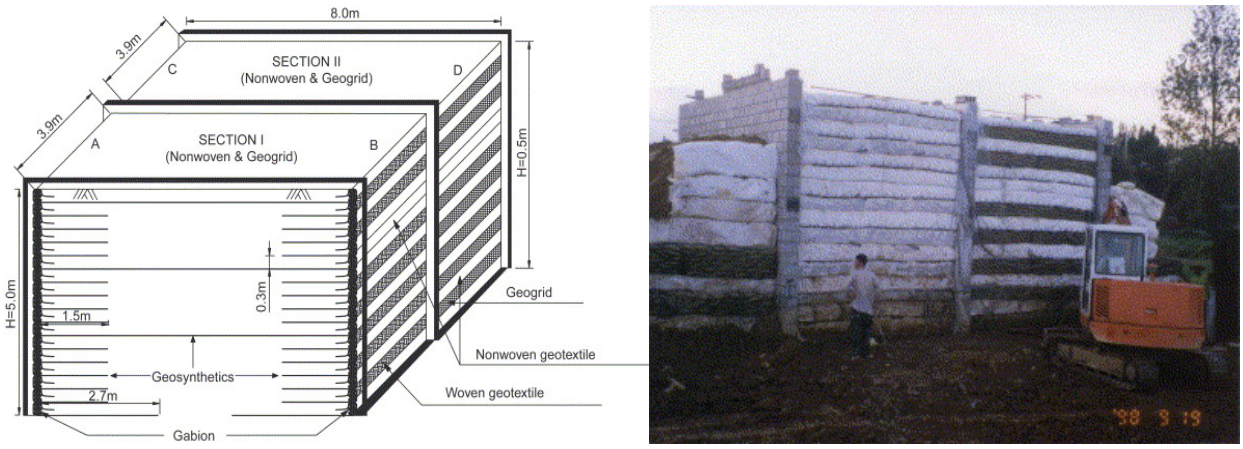

Figure 2.39. Schematic Diagram of a GRS Wall and GRS System after Construction (Won and Kim, 2007).

According to Wu et al. (2003), the GRS system becomes a more viable alternative than other conventional bridge abutments. It provides many advantages, such as being more ductile, more flexible (hence more tolerant to differential settlement), more adaptable to the use of low quality backfill, easier to construct, more economical, and less over-excavation required. Wu et al. also presented a case study where the GRS was used in a condition in which each footing bears several preloading cycles greater than their design load and sustained for several minutes. It was found that after the first few cycles of preloads, the observed settlement reduced to negligible amounts and subsequent service settlements were less than 0.5 in. The Wyoming Highway Department has used multiple layers of geosynthetic reinforcement within compacted granular material since the 1980s (Monley and Wu, 1993).

Edgar et al. (1989) stated that none of the 90 approach slabs placed on geosynthetic reinforced embankments required maintenance or repair after 5 years of service. Excellent performance of these systems was also reported by Abu-Hejleh et al. (2006) for both short- and long-term performance of the GRS approaches.

Wu et al. (2006) summarized the advantages of the GRS bridge abutments with flexible or rigid facing over conventional reinforced concrete abutments as follows:

- GRS abutment increases tolerance of foundation settlement to seismic loading.
- GRS abutments are remarkably more stable and have higher ductility.
- With a proper design and construction, bumps can be alleviated.
- GRS abutments are constructed more rapidly and less expensive.
- GRS abutments do not require embedment into the foundation soil for stability.

- The lateral earth pressure behind a GRS abutment wall is much smaller.
- GRS performs satisfactorily longer under in-service conditions.
- The load-carrying capacity by GRS is significantly greater.

The GRS bridge-supporting structures can be grouped into two types: rigid facing and flexible facing structures (Wu et al., 2006). Flexibility or rigidity of GRS walls is explained in relation to its deformation capability and its responses to temperature changes during different seasons (Wu et al., 2006). If the construction is done in cold dry seasons (fall/winter), the GRS walls presents a rigid response whereas construction of GRS walls during warm, wetting, and thawing seasons result in GRS walls with a flexible response, capable of undergoing relatively large deformations.

Rigid facing is typically a continuous reinforced concrete panel, either precast or cast-in-place. Rigid facings offers a significant degree of global bending resistance along the entire height of the facing panel, thus offering greater resistance to global flexural deformation caused by lateral earth pressure exerted on the facing. Figure 2.40 shows a typical cross section of a GRS system with rigid facing.

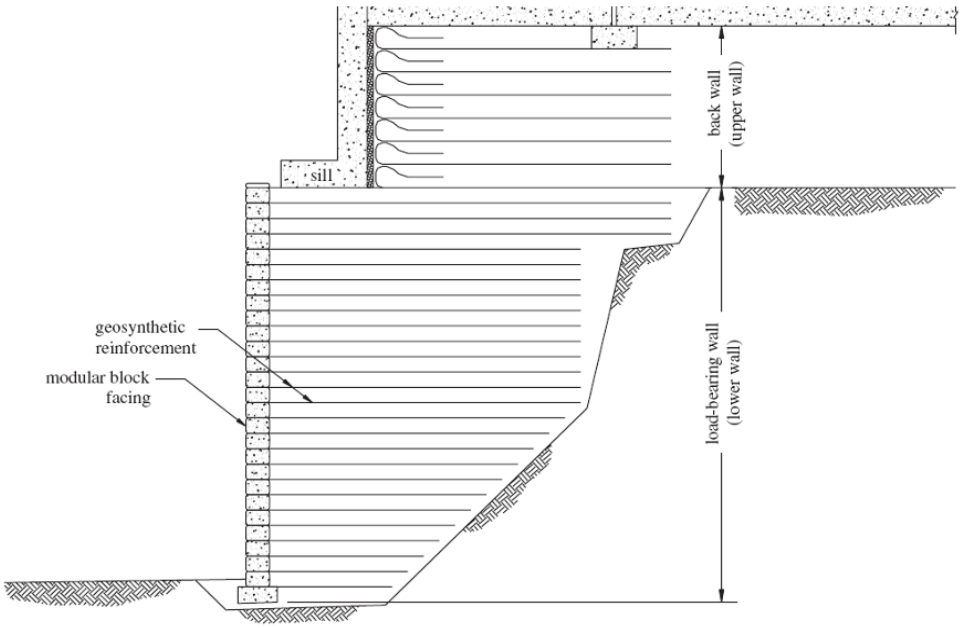

Figure 2.40. Typical GRS Bridge Abutment with a Segmental Concrete Block Facing.

Flexible facing is typically a form of wrapped geosynthetic sheets, dry-stacked concrete modular blocks, timbers, natural rocks, or gabions. These wall structures have shown great promise in terms of ductility, flexibility, constructability, and costs. The main advantages of

this system over the rigid facing are summarized in the following (Abu-Hejleh et al., 2003; Wu et al., 2006):

- Larger mobilization of the shear resistance of the backfill, thus taking more of the lateral earth pressure off the facing and connections.
- More flexible structure, hence more tolerant to differential settlement.
- More adaptable to low-quality backfill.

Guidelines of GRS walls are provided by the Colorado DOT for designing and constructing GRS bridge abutments (Abu-Hejleh et al., 2000), and a few of the assumptions used in this guideline are presented here:

- The foundation soil should be firm enough to limit post construction settlement.
- The desired settlement of the bridge abutment should be less than 1 in. (25 mm).
- The maximum tension line needed in the internal stability analysis should be assumed nonlinear.
- Ideally construction should be done in the warm and dry season.
- The backfill behind the abutment wall should be placed before the girders.

Overall, the GRS system walls have been used with success to alleviate approach settlement problems. However, very few state DOTs have implemented this in practice, probably due to the limited amount of familiarity of this method.

2.3.4.1 Lightweight Fill

Another concept to reduce the vertical loading or stress from the embankment as it exerts itself on the foundation subsoil is the use of lightweight material as an embankment fill material. The reduction of embankment weight or load increases the stabilities of the embankment and also reduces the compression on the underlying foundation soil. As a result, the settlement potential of the embankment will be decreased.

The lightweight fills such as lightweight aggregate, expanded polystyrene, lightweight concrete, or others can be used to achieve this benefit (Luna et al., 2004; Dupont and Allen, 2002; Mahmood, 1990). Based on the surveys conducted by Hoppe (1999) approximately 27% of responding DOTs have already experimented with the use of non-soil materials behind bridge abutments.

Horvath (2000) recommended the use of Geofoam as a light-weight compressible fill material (Figure 2.41). Other materials could be used as alternative lightweight backfill material; some of these alternative construction materials included shredded tires and expanded polystyrene. However, it must be kept in mind that the suitable fill material must not have only the lightweight property, but it must have other required properties, such as high strength, high stiffness, and low compressibility properties.

Hartlen (1985) listed some satisfactory requirements for the lightweight fill material as follows:

- Bulk density less than 63 pcf (1000 kg/m^3).
- High modulus of elasticity and high angle of internal friction.
- Good stability and resistance against crushing and chemical deterioration.
- Non-frost active.
- Non-corrosive to concrete and steel.
- Non-hazardous to the environment.

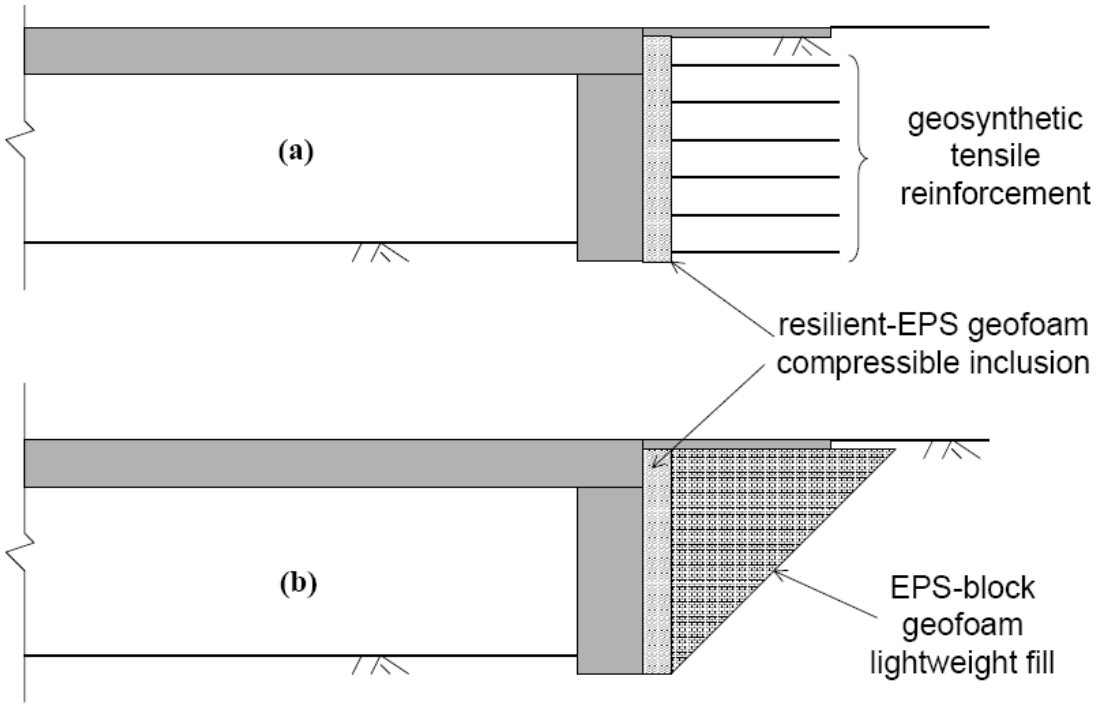

Figure 2.41. A Design Alternative by Using Geofoam as a Backfill (Horvath, 2000).

2.3.4.2 Flowable Fill (Flowfill)

Flowable fill is a low-strength mixing concrete used as a backfill behind the abutment wall to reduce the possibility of approach settlements near the surface resulting from the compression of the backfill itself (Abu-Hejleh et al., 2006). According to NCHRP (597), the fluidity of flowable fill makes it a rapid and efficient backfilling material. The low-strength mixing concrete works well to prevent erosion of the backfill and to improve constructability/compactability of the fill behind the walls and around corners. The self-leveling ability property allows the flowable fill material to fill voids without the need of any compaction (Folliard et al., 2008). Although this method is an expensive construction practice, it is still a practical alternative in certain field and construction scenarios where the use of such practice justifies the higher costs (Abu-Hejleh et al., 2006).

Snethen and Benson (1998) summarized that the use of flowable fill as an embankment material to reduce the potential for developing the bump at the end of the bridge. This seems to be a simple, reasonably cost effective, and less time-consuming method. This study also concluded that use of the flowable fill as an embankment material has resulted in the reduction of the lateral earth pressure and settlement of the approach embankment.

According to the Colorado DOT specifications, the maximum lift thickness for flowable fill material is 3 ft. (0.91 m) and a placement of additional layers is not permitted until the flowable fill has lost sufficient moisture to be walked on without indenting more than 2 in. (51 mm). CDOT specifications do not specify any need for vibration because the vibration may stiffen the flowfill by allowing the setting to occur faster in the field. CDOT specifications for the flowfill backfill are listed in Table 2.5 (Abu-Hejleh et al., 2006).

In a separate section, the use of flowable fills for remediation of approach slab settlements will be discussed.

Table 2.5. CDOT Material Requirements for Flowable Fill Backfill.

Ingredient	lb/cy
Cement	50
Water	325 (or as needed)
Coarse Aggregate (AASHTO No.57 OR 67)	1700
Fine Aggregate (AASHTO M6)	1845

2.3.4.3 Grouting

Edgar et al. (1989) reported that in a high-speed passageway, ground stabilization methods could be utilized to reduce maintenance requirements. In this study, the use of cement-treated backfill instead of conventional granular backfill material was chosen to reduce the hydro-collapse and increase soil strength. The grouting technique has been also recommended for mitigation of settlement of the embankment in the case of embankments underlain by organic peat layers that can be easily compressed and consolidated (Byle 1997, 2000). The pressure grouting method was also successful in preventing the loss of materials. However, the main objective of the grouting technique is to restrict the limited mobility displacement (LMD) of the material, as described by Byle (1997, 2000).

Figure 2.42 shows that the sleeve pipes can be installed in different angles of 50°, 30°, 20° from the horizontal surface (Sluz et al., 2003). The angle at which the sleeve port pipes installed in the soil is important and must be modified by monitoring the amount and the rate of settlement. Details including the settlement after mitigation and the type of grout used were not listed in the report.

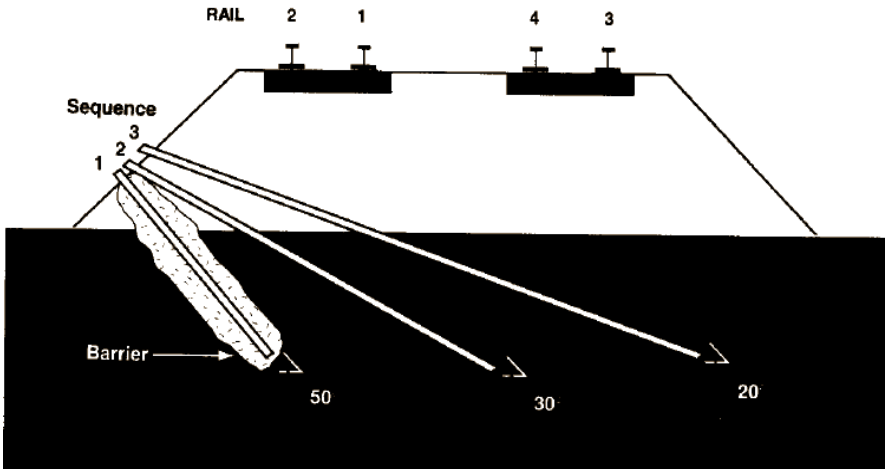

Figure 2.42. Sleeve Port Pipe Installation Plan (Sluz et al., 2003).

2.3.4.4 Other Recommendations

If possible, the slopes of soil embankments should be flattened, which tends to increase the stability and reduce the deformations of the embankment (Luna et al., 2004). Such practice will not be applicable due to limited right-of-way along many embankment sections especially in urban and metro areas. If the proposed embankment material is plastic clay with PI greater than 15–20, treatment of the soil or alternate borrow sources should be considered. The select

fill also needs to be extended to a certain distance from the abutment and the distance ranges between 50 and 100 ft (15.21 and 30.5 m) and is dependent on the type of embankment and material used as a backfill (Luna et al., 2004).

2.3.5 Design of Bridge Foundation Systems

The bridge foundation is considered as a major factor in bridge structure design. Bridges can be supported either by shallow or deep foundation systems (Wahls, 1990). In both cases, the foundations should be able to carry the loads from the above superstructures and the traffic volumes, but also to limit the horizontal and vertical movement of the abutment to acceptable levels (Wahls, 1990). The selection of a safe and economical foundation system requires consideration of structural loads, environmental factors, subsurface conditions, bedrock types and depths, performance criteria, construction methods, and economics (ODOT, 2005).

Spread footings, driven piles, and drilled shafts are generally used as bridge foundations. According to Wahls (1990), the spread footing has its advantage over the deep foundation in aspect of its inexpensive cost. However, the uncertainties in the performance prediction and the potential for scouring make shallow foundations an unattractive choice for a bridge foundation system. Moreover, since the compaction of backfill near the abutment is difficult to achieve, the possibilities of loads from the superstructure and traffic volume stressing the poorly compacted backfill and contributing to the settlement of bridge approaches can be high (Wahls 1990).

For those reasons the deep foundations, including driven piles or drilled shafts, are preferred to support the bridges. The deep pile foundations have been demonstrated to be the most efficient means of transferring heavy loads from superstructures to substructures and bearing materials without significant distress from excessive settlement (Abu-Hejleh et al., 2006). Hopkins (1985) cited that the settlement of the bridge abutment resting on pile foundations is usually negligible. However, due to the fact that the bridges supported by pile foundations do not usually settle as much as the approach embankments, the differential settlement between these two adjacent structures can lead to the bump problems at the bridge approach. Hopkins and Deen (1970) stated that the differential settlement between the abutment and the approach slab is usually high for pile support abutments.

The abutment with embedded pile caps can develop resistance to the movement of the bridge structures as the bridge superstructure expands and contracts with temperature variations, which is also claimed as a cause of high applied stresses on the pile foundations and a reduction of pile axial load capacity (Greimann et al. 1983). Greimann et al. (1986) performed a three-dimensional non-linear finite element analysis to study pile stresses and pile soil structure interaction of integral abutment bridges from thermal fluctuations. They found that the thermal expansion of the bridge reduces the vertical load carrying capacity of the piles. They reported that the vertical load carrying capacity for H piles in very stiff clays is reduced by approximately 50% for 2 in. (51 mm) of lateral displacement and approximately 20% for 1 in. (25.4 mm) lateral displacement.

Girton et al. (1991) measured the maximum pile stress at the Boone Bridge and the Maple River Bridge. They found that the maximum pile stresses were only 60% and 70% of the nominal yield stress at both sites, respectively. Lawver at al. (2000) reported that the maximum measured pile stresses were slightly above the nominal yield stress of the pile. Arsoy et al. (2002) investigated the performance of H-piles, pipe piles, and pre-stressed reinforced concrete piles subjected to cyclic lateral displacements. Based on that study, it was concluded that H-piles loaded on the weak axis were the best alternative to support the integral abutments. Figure 2.43 illustrates an example of bridge foundation construction using H-piles.

The use of precast, pre-stressed concrete (PC) piles in the foundation of bridge piers has been used as a valuable alternative for bridge construction for a long time (Abendroth et al., 2007). However, due to some concerns over pile flexibility at the abutment ends, the potential for concrete cracking induced by thermal expansions and seismic movements and the deterioration of the pre-stressing strands due to long-term exposure to moisture, PC piles in the integral abutment bridges have not been extensively used (Abendroth et al., 2007).

Figure 2.43. Example of Bridge Foundation Using Steel H-Piles.

According to a survey conducted in several states by Abendroth et al. (2007), the main reasons to avoid PC piles for bridge abutments are attributed to inadequate ductility (48%), insufficient research on the subject matter (52%), limited availability (33%), and high cost of the foundations (24%). In the last 10 years, the potential use of PC piles for integral abutments was reported in a few studies (Kamel et al., 1996; PCI, 2001; Burdette et al., 2004). However, the available literature presents different conclusions regarding the suitability of PC piles for this application (Abendroth et al., 2007).

The precast, pre-stressed concrete piles typically utilize both skin friction and end bearing conditions to carry the vertical loads. The results from the study by Abendroth et al. (2007) showed that with respect to construction costs, the usage of PC piles is more economical than the H-steel pipes in sandy and gravelly soils. Moreover, the study also showed that these precast, pre-stressed concrete piles usually experience less lateral displacement than the H-piles and lower longitudinal movements than the expected range. However, the study also evidenced pile cracking problems after excavation on the abutments. The cracking problems are attributed to moisture penetration, uncoated pre-stressing strands, and long-term corrosion problems (Abendroth et al., 2007). For these reasons, periodic inspection of the abutment piles is recommended to detect any additional concrete cracking or deterioration.

When piles are selected for a bridge foundation system, the ability of the foundation piles to carry the vertical loads even when the piles are subjected to temperature-induced displacements must be considered (Arsoy, 1999). The lateral displacements may reduce vertical-load carrying capacities of piles, resulting in pile failure if lateral loads are higher than the elastic buckling load (Greimann and Wolde-Tinsae, 1988). Another important factor is the

length of the pile, because it controls the allowable settlement of the structure. Bakeer et al. (2005) indicated that due to loading requirements and to minimize settlement, bridge piers and abutments needed to be supported on relatively long piles or piles with tips driven into stiff soil.

One negative effect that needs to be taken into account for the design of pile foundations is the consideration of negative skin friction or down-drag from compressible soils around the pile lengths. Figure 2.44 presents a schematic of the process that produces down-drag forces on piles. Down-drag is the sum of the negative shaft resistance along the length of the pile where the soil is moving downward relative to the pile, and this drag is always treated as a downward acting load (AASHTO, 2004).

Some of the successful methods to mitigate down-drag are listed below (Narsavage, 2007):

- Use larger H-pile sections to increase factored structural resistance for piles on rock.
- Use more piles and reduce the applied load for piles not driven to refusal on rock.
- Reduce soil settlement that occurs after pile driving by preloading and/or using wick drains.
- Reduce soil settlement by using lightweight embankment fill material.
- Use bituminous pile coating.

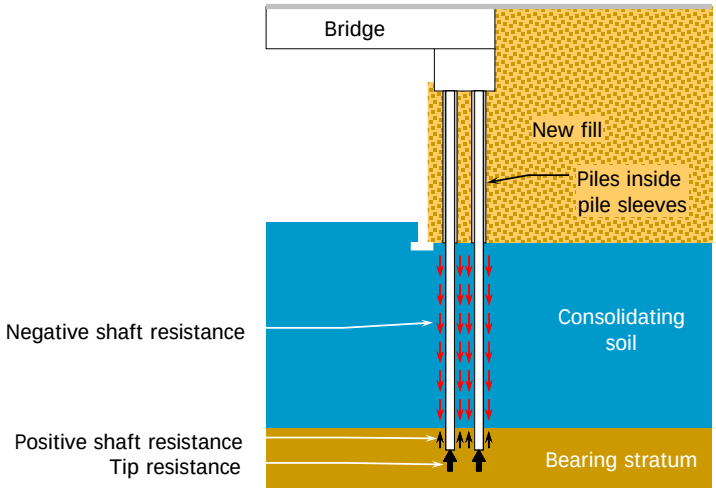

Figure 2.44. The Down-Drag in Piles.

In order to avoid the downward drag problems, the use of shallow foundations has been suggested (DiMillio, 1982). Generally, the shallow foundations are typically 50% to 60% less expensive and require less construction time than deep foundations (DiMillio, 1982). Some recent studies have demonstrated again the feasibility of implementing shallow foundations for

major bridges in the United States (Abu-Hejleh et al., 2003). For example, the Founders/Meadows bridge foundation was built on footings supported directly by a geosynthetic-reinforced soil system, eliminating the use of traditional deep foundations (piles and caissons) altogether. A typical section of the GRS system of this bridge foundation is detailed in Figure 2.45.

However, the shallow foundations have their own disadvantages. Grover (1978) compared the behavior of bridges supported by shallow and pile foundations in Ohio. The result of this study indicated that for the bridge constructed in the 1960s, 80% of the abutments supported by shallow spread footings experienced more than 2.5 in. (63.5 mm) of settlement and 10% of them experienced more than 4 in. (101.6 mm) of settlement. As a result, the Ohio DOT specifications asked for deep pile supported bridge abutments in the place of shallow foundation supported abutments (Grover, 1978).

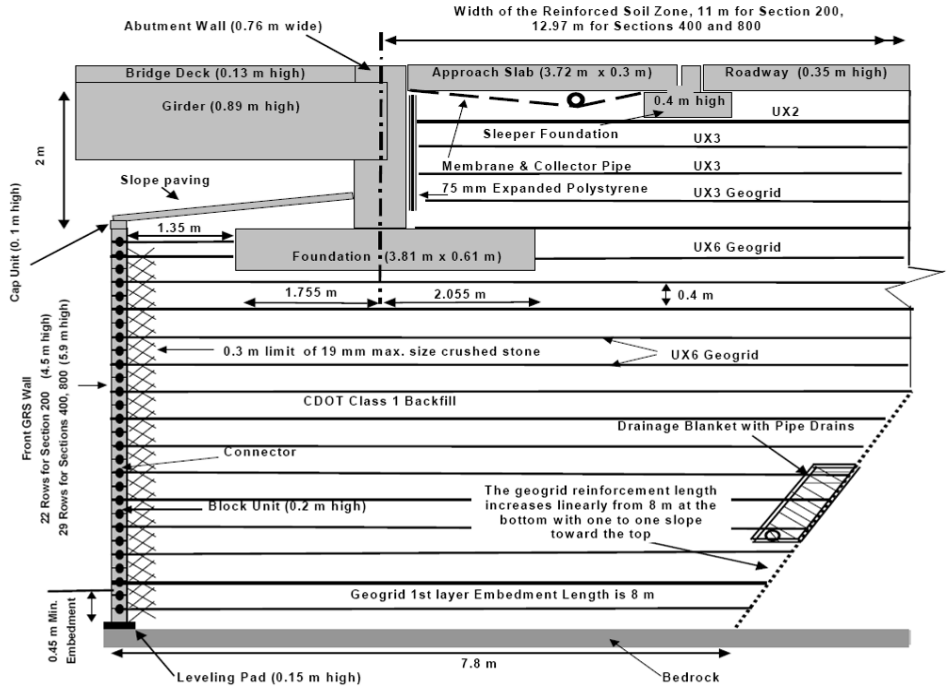

Figure 2.45. Typical Section through Front and Abutment GRS Walls (Abu-Hejleh et al., 2006).

According to the TxDOT Bridge Design Manual (2001), the spread footing was only an alternative used as bridge foundations in Texas in early bridge designs, although other options, such as timber and concrete piles, were already available. Since the late 1930s, the steel H-pile was introduced and then became widely used and a few caissons, pneumatic and open, were

used for larger stream crossings. A drilled shaft technology, which was developed in the late 1940s, and pre-stressed concrete pile foundations, have now become a dominant foundation in bridge construction in Texas.

2.3.5.1 Design of Bridge Abutments

The type of bridge abutment plays an important role (Mahmood, 1990). Generally, two types of abutments are used widely in the United States: a non-integral (or conventional) and an integral type (Greimann et al., 1987).

The non-integral or conventional type of bridge abutment (Figure 2.46) has bearing connections and expansion joints to provide the superstructure with a certain amount of lateral movement between the abutment and the bridge deck (Wahls, 1990). The lateral load caused by the lateral movement or the thermal strains in the deck will be lessened by both types of connections (White et al., 2005). However, increased traffic loads and frequent application of de-icing salts during winter could deteriorate the expansion joints and bearing connections, which can lead to costly maintenance problems (Horvath, 2000). These non-integral abutments are commonly used in many states including Texas.

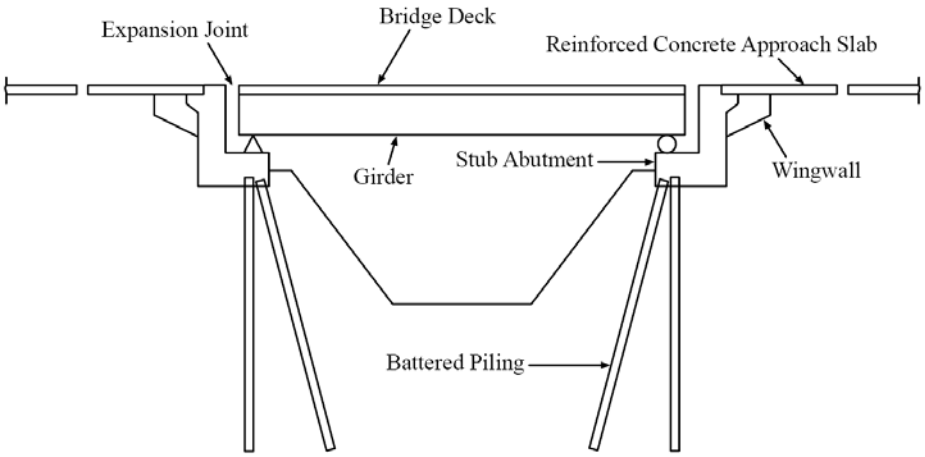

Figure 2.46. Simplified Cross Section of Non-Integral Abutment Bridge (Greimann et al., 1987; White et al., 2005).

The integral bridge abutment type (Figure 2.47) was developed in order to eliminate the use of bearing plates and to reduce potential maintenance problems (Horvath, 2000). The integral abutment is a stub abutment connected to the bridge superstructure tightly without any expansion joints (Wahls, 1990). The rigid connections need to handle thermal stresses from the

bridge deck and transfer them to the abutment. The advantages of this rigid connection are (Greimman et al., 1987; Hoppe and Gomez, 1996):

- Simple and reduced construction and maintenance costs.
- Minimum number of piles required to support the foundation.
- Improved seismic stability.

The use of integral bridge abutments has been increased since the 1960s because it avoids the use of the bearing plates and the potential maintenance problems associated with non-integral bridge abutments (Wahls, 1990; Horvath, 2000; Kunin and Alampalli, 2000). Pierce et al. (2001) stated that the bridge approaches with integral abutments tend to reduce the surface roughness. However, Wahls (1990) reported a problem related to cracking and bulking at the approach pavement due to a lateral cyclic movement of the abutment from thermal movement induced stresses at the bridge decks. Schaefer and Koch (1992) and Arsoy et al. (1999) also specified that the same lateral cyclic movements exerted on the backfill soils from daily temperature changes may form voids at the face of the abutment that contribute to the total approach settlement. The voids were observed within one year of the bridge construction indicating insufficient backfill moisture control/compaction followed by soil collapse upon saturation (White et al., 2005).

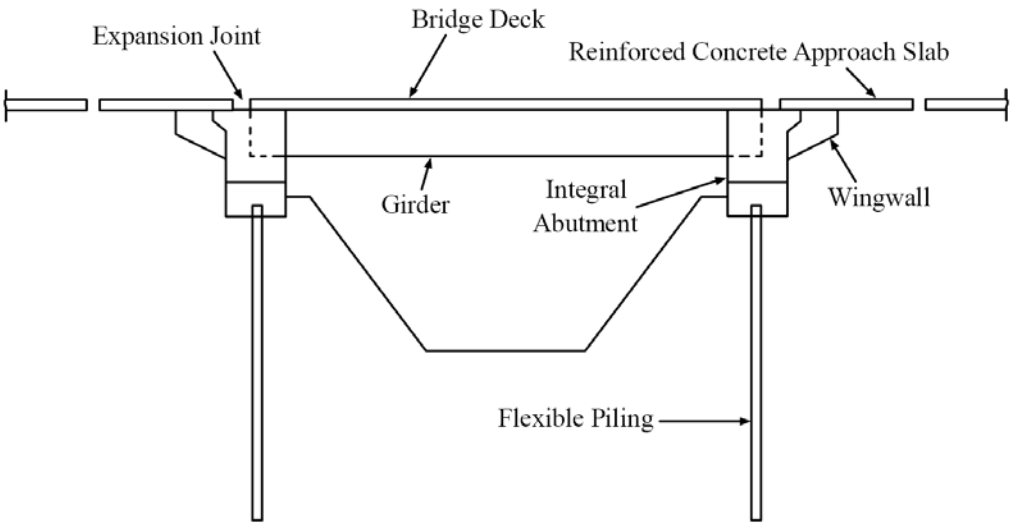

Figure 2.47. Simplified Cross Section of Integral Abutment Bridge (Greimann et al., 1987; White et al., 2005).

Lateral movement is a common occurrence of the integral bridges (Kunin and Alampalli, 2000; Arsoy et al., 2002; Arockiasamy et al., 2004). The bridge superstructures expand and contract by seasonal air temperature fluctuations according to concrete thermal strain characteristics. Because the bridge deck and abutment are integrally connected, both structures will laterally move together. The movement of the structures resulting from the temperature of the bridge deck seasonal changes can cause a cyclic loading subjected toward the approach backfill and the foundation. When the temperature rises, the bridge deck expands and the superstructure, including the bridge abutment, moves against the retained embankment soil. The lateral movement induces the stress in the soil and sometimes can reach the passive pressure limit (Schaefer and Koch, 1992). On the other hand, when the temperature lowers, the superstructure and the abutment move away from the soil and leave voids at the interface between the abutment and the backfill. The size of the voids can become bigger if the weather gets colder. The development of the voids can be a cause of soil erosion that increases the size of the void behind the abutment and below the approach slab as shown in Figure 2.48.

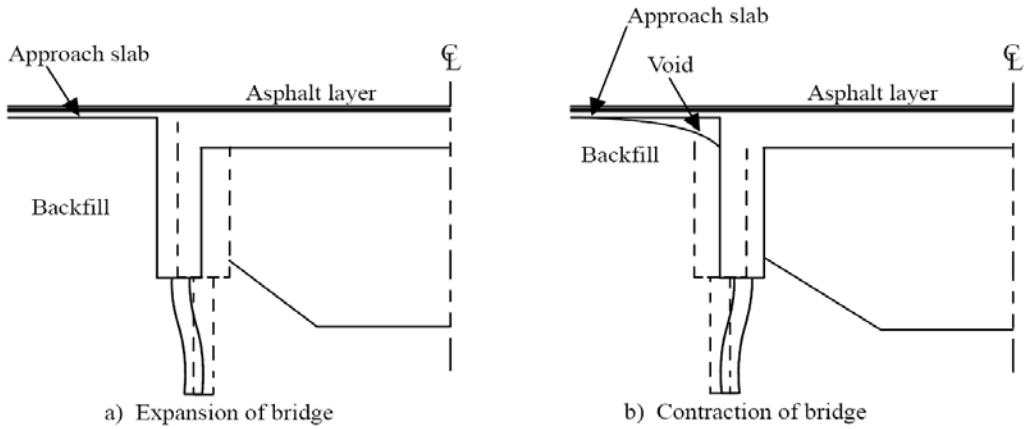

Figure 2.48. Movement of Bridge Structure with Temperature (Arsoy et al., 1999).

Wahls (1990) suggested that the performance of an integral abutment can be improved by installing compressible elastic materials between the abutment and the backfill. The material should have elastic properties that permit large recoverable cyclic movements and hydraulic properties that provide adequate drainage without erosion of fines from the backfill. Horvath (2000) advocated the use of geofoam as a compressible material. The successful use of compressible and collapsible materials behind the abutment was reported by the North Dakota DOT and Illinois DOT (Wahls, 1990; Kunin and Alampalli, 2000).

According to Mekkawy et al. (2005) and White et al. (2005), insufficient drainage is also another problem often found at the bridge abutments. Water that is collected on the bridge pavement can cause severe damage to the bridge approach. If collected water can flow into the underlying fill materials due to inefficient seals at the joints between the bridge approach slab and the abutments, the water can erode the backfill material resulting in voids development under the bridge abutments. Therefore, an efficient drainage system should be incorporated in the design of bridge approaches, such as drainage inlets at the end of a bridge deck to collect surface water before getting to the approach slab (Abu-Hejleh et al., 2006).

Furthermore, providing additional surface or internal drainage to keep water off the slopes is recommended for correcting the superficial erosion of embankments (Wahls, 1990). Keeping the water away from the soil is a simple significant factor in reducing the settlement of the soil. Construction costs added to incorporate a good drainage system are not high when compared to the expensive maintenance costs that might be experienced in the service life of a bridge (Dupont and Allen, 2002).

2.3.6 Design of Approach Slab

The bridge approach slab is a part of a bridge that rests on the abutment at one end and on the embankment or a sleeper slab on the other end (Wahls, 1990). The slabs are designed to provide a smooth transition between the bridge deck and the roadway pavement and to minimize the effect of differential settlements between the bridge abutment founded on shafts or piles and the embankment fill (White et al., 2005). There are two types of approach types used by highway agencies. Some agencies use a bituminous approach pavement because it can be maintained easily by overlay type rehabilitation. However, the use of bituminous approaches with Portland concrete roadways is still not highly preferred by the DOTs (Wahls, 1990).

Other agencies use a reinforced concrete slab because they believe the rigid approach slab is successful in preventing the bridge approach settlement (Wahls, 1990). In this case, one end of the slab is connected to the main structure by two methods; in the first alternative (Figure 2.49), the slab is connected directly to the bridge deck by extending the main reinforcement from the bridge deck to the approach slab. In the second alternative

(Figure 2.50), the approach slab is connected to the abutment by using a dowel/tie bar (White et al., 2005).

Based on a survey on over 131 bridges in Texas by James et al. (1991), they found that the bridges with a flexible pavement had a smoother transition than those with a rigid pavement. However, Pierce et al. (2001) reported that the approach slab with asphalt overlays tend to increase the surface roughness. According to the TxDOT Bridge Manual (2001), the use of approach slabs is only an option and districts have had success with and without their use. However, if the approach slab is constructed with the non-integral bridge system, the use of a dowel/tie bar must be implemented between the slab and the abutment (Hoppe, 1999).

James et al. (1991) stated that the roughness or IRI values of the approach slab are influenced by the longitudinal pavement movements resulting from temperature cycles. They also mentioned that the approach pavement settlement/roughness can be attributed to impact loads due to poor design and constructed expansion joints.

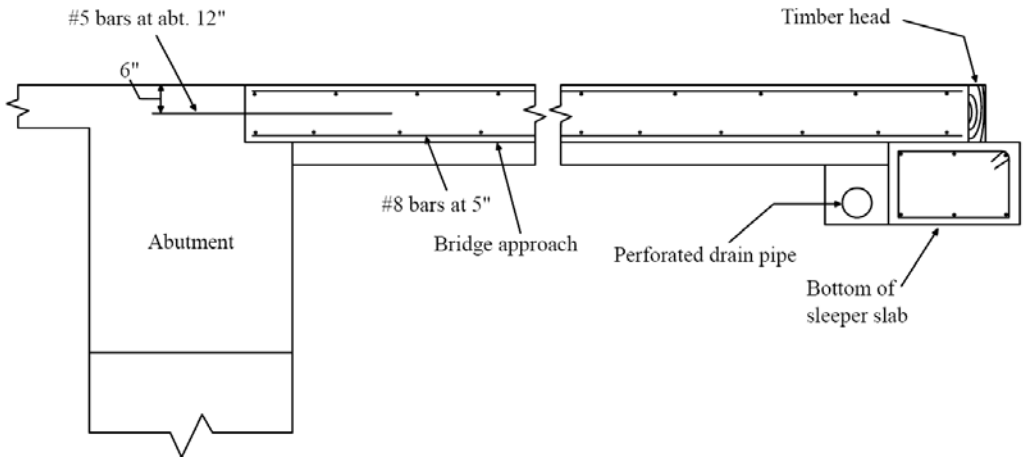

Figure 2.49. Bridge Approach Connected to Bridge Deck (Missouri DOT, 2003).

White et al. (2005) stated that the performance of the approach slabs depends on these following factors: approach slab dimensions, steel reinforcement, use of a sleeper slab, and type of connection between the approach slab and the bridge.

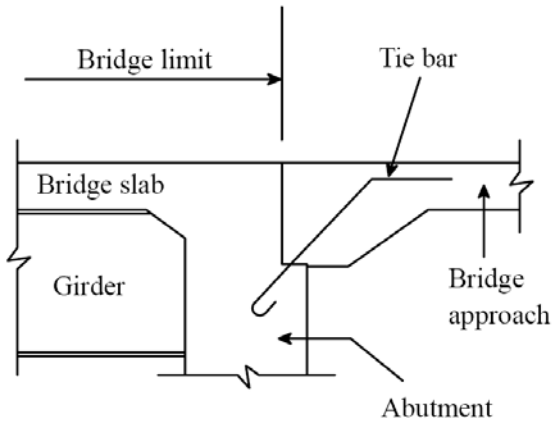

Figure 2.50. Bridge Approach Connected to Abutment (Ohio DOT, 2003).

2.3.6.1 Slab Dimensions

Most of the reinforced concrete approach slabs used in the U.S. have lengths varying from 20 to 40 ft (6 to 16 m) (Wahls, 1990). According to an extensive survey conducted by Hoppe (1999) of different state agencies, typical approach slab dimensions for the various states surveyed are collected and summarized in Table 2.6. From the table, it is seen that most approach slab dimensions vary between 15–30 ft (5–10 m) in length and 9–17 in. (23–43 cm) in thickness.

Table 2.6. Typical Approach Slab Dimensions Used by Various DOTs (Hoppe, 1999).

State	Length (ft)	Thickness (in.)	Width limited to:
AL	20	9	Pavement
AZ	15	N/A	N/A
CA	10-30	12	Curb-to-Curb
DE	18-30	N/A	N/A
FL	20	12	Curb-to-Curb
GA	20-30	10	Curb-to-Curb
IA	20	10-12	Pavement
ID	20	12	Length
IL	30	15	Curb-to-Curb
IN	20.5	N/A	N/A
KS	13	10	Curb-to-Curb
KY	25	N/A	Curb-to-Curb
LA	40	16	Curb-to-Curb
ME	15	8	Curb-to-Curb

MA	N/A	10	N/A
MN	20	12	Pavement
MS	20	N/A	Curb-to-Curb
MO	25	12	N/A
NV	24	12	Curb-to-Curb
NH	20	15	N/A
NJ	25	18	N/A
NM	15	N/A	Curb-to-Curb
NY	10-25	12	Curb-to-Curb
ND	20	14	Curb-to-Curb
OH	15-30	12-17	N/A
OK	30	13	Curb-to-Curb
OR	20-30	12-14	Curb-to-Curb
SD	20	9	N/A
TX	20	10	N/A
VT	20	N/A	N/A
VA	20-28	15	Pavement
WA	25	13	Pavement
WI	21	12	N/A
WY	25	13	Curb-to-Curb

N/A: Information is not available or not applicable

Some states consider the use of a short span slab and this is attributed to causing the bump problem (Lenke, 2006). As a result, some of these states moved toward the use of a slab longer than 40 ft (16 m) (LaDOTD, 2002). For example, the Illinois DOT prefers the design of a slab length of 100 ft (30 m), and the Louisiana DOT uses continuous slab lengths from 80 to 120 ft (24 to 36 m) (Wahls, 1990). In both cases, the bridge abutments are pile supported.

Other research summary studies by Briaud et al. (1997), Abu-Hejleh et al. (2006), Lenke (2006) suggest a criterion to calculate the slab length based on the maximum slope of the approach slab, which is defined as the change in elevation between the beginning of the approach slab (at the sleeper slab) and the bridge abutment divided by the length of the approach slab. The slope of the approach in their studies is defined as:

$$S = \frac{s_f - s_a}{L} \leq \frac{1}{200}$$

where S is the longitudinal slope of the approach slab, L is the length of the approach slab, and s_f and s_a are the settlements of the foundation (embankment and natural soil foundation) and the abutment, respectively. For example, if a settlement analysis indicates a differential settlement

between the abutment and the beginning of the approach slab ($s_f - s_a$) equal to 1.5 in. (38 mm), then the length of the approach slab must be greater than 300 in. (7620 mm) or 25 ft (7.62 m). From the equation, it is easily understood that when the same settlement happens at both ends of the slab, then a shorter approach slab will be needed.

One way of minimizing the bump is to lengthen the approach slab (Lenke, 2006). Seo (2003) suggested that the approach slabs should have a minimum length of 20 ft (6.0 m) and should be designed to support full traffic loading in a free span to account for any unexpected erosion beneath the slab.

Other aspects of approach slabs that are of interest to designers are the acceptable degree of the longitudinal slope. Several research reports recommended a maximum allowable change related slope of 1/200 (Wahls, 1990; Stark et al., 1995; Briaud et al., 1997; Seo, 2003). Long et al. (1998) also proposed a relative gradient of less than 1/200 to ensure rider comfort and a gradient of between 1/100 and 1/125 as a criterion for initiating remedial measures.

Wong and Small (1994) suggested that the slab with an angle can lessen the bump problem. They studied the effect of orientation of approach slabs on pavement deformation by varying the slopes of the approach slab at 0, 5, and 10 degrees with the horizontal and compared those results with no slab tests in a one-fourth scaled model as shown in the test setup in Figure 2.51. They concluded that the horizontal slab contributes little to remedy the bump problem. On the contrary, the slab with an angle sloped down beneath the pavement can alleviate the bump problem better than a horizontal one due to the fact that the deformations at the surface at the pavement above the slab are more gradual and the rate of change of the surface gradient is small.

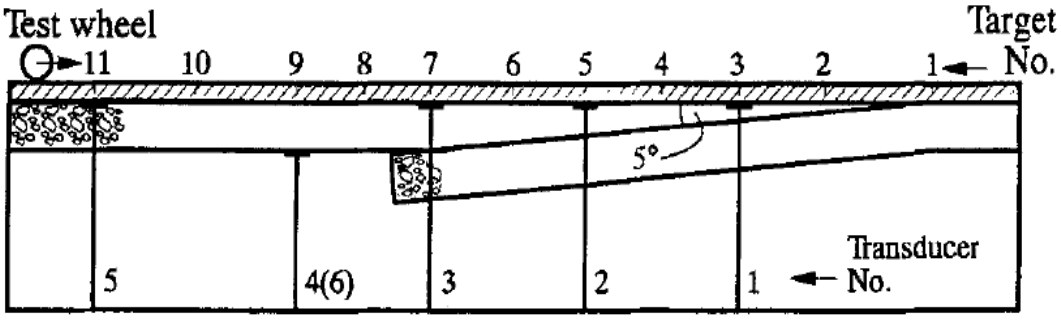

Figure 2.51. Test Setup for Subsoil Deformation (Wong and Small, 1994).

The slab thickness is another factor that needs to be considered for a slab design. Normally, the thickness of the rigid approach slab is uniform. Nassif (2002) conducted a numerical analysis on New Jersey's approach slabs. They concluded that the slab thickness is the most effective parameter in reducing the tensile stresses in the critical elements. From the same study, Nassif (2002) also suggested a constant thickness of the approach slab and embedded beam design to the New Jersey DOT for their use. Overall, the slab thickness can vary depending on the considerations of the length of the slab, other structures, and the foundation (Lenke, 2006). The thickness of the slab can be designed as a taper shape in different sections in order to provide more flexibility in areas near the abutment (Wahls, 1990).

Regarding the type of slabs, Cai et al. (2005) studied different types of approach slabs by performing 3D finite element analyses. They recommended the use of a ribbed slab type, as seen in Figure 2.52, over the flat slab type, especially for long approach spans. Since, the internal forces and deformation of the ribbed slab can be lessened due to its slab-on-beam behavior, the thickness of bridge decks or slabs can be reduced when compared with the flat slabs.

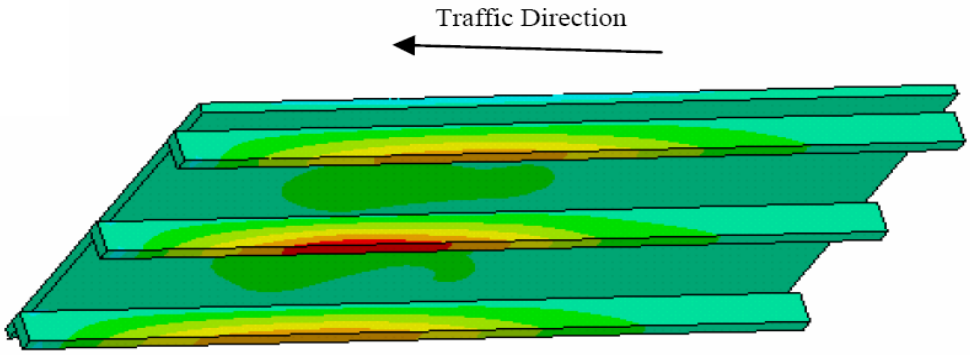

Figure 2.52. The Ribbed Slab as an Approach Slab (Cai et al., 2005).

In terms of the width of the approach slab, the curb-to-curb method is preferred (Briaud et al., 1997). By matching the width of the slab with the width of the bridge decking (between bridge guardrails, or barriers), a few advantages can be realized. These are better erosion control of the underlying embankment soils and effective drainage pouring water away from the bridge structure and approach slab system (White et al., 2005). Since these two factors contribute to the bump problem, use of such widths of approach slabs are often recommended (Briaud et al., 1997, White et al., 2005).

According to the TxDOT Bridge Manual (2001), the use of an approach slab is optional. However, when the use of an approach slab is utilized, the approach slab should have a thickness of 13 in. The slab must also be a lightly reinforced concrete slab that precedes the abutment at the beginning of the bridge and follows the abutment at the other end of the bridge.

This manual also cites that TxDOT discourages the use of approach slabs on wingwalls based on previous experience in Texas. Due to the difficulty in compaction of the backfill and the potential loss of backfill material, the approach slab becomes a slab supported on three sides (i.e., at the two wing walls and the abutment backwall). Without the bearing on the backfill, it leads to the development of a void underneath the slab, and consequently leads to bumps. For that reason, the standard approach slab and the wing walls designed to carry out the load are not reinforced. Hence, TxDOT suggests that the approach slab should be supported by the abutment backwall and the approach backfill only.

The appropriate backfill material is considered an essential component under the slab. TxDOT is currently supporting the placement of a cement stabilized sand (CSS) wedge in the zone behind the abutment (TxDOT, 2001). The use of CSS can solve the problem of difficult compaction behind the abutment. Furthermore, CSS wedges are resistant to the moisture gain and loss of material that are commonly occurring under the approach slabs. The use of CSS has become standard practice in several districts and has shown good results (TxDOT, 2001). The Fort Worth District in TxDOT uses a cement treated flexible base beneath the approach slab for the same purpose. The 3 ft (0.91 m) deep flex base is prepared by compacting four equal layers of 9 in. (0.23 m) thick, of Type 1 cement treated (2.4% by weight) base material as shown in Figure 2.53. However, approach slabs with the cement treated flexible base have also experienced the same settlement problems since the heavier flexible base has further consolidated the embankment fill and created a larger bump (Williammee, 2008).

An additional component to the approach slab, which is not widely applied, is the use of a sleeper slab. A sleeper slab is a concrete foundation slab placed transversally at the approach slab and opposite to the bridge end (Ha et al., 2002; Seo et al., 2002). Generally, one end of the rigid approach slab rests on the abutment or connects directly with the bridge deck while another end sits directly on the embankment or otherwise on a sleeper slab (Wahls,

1990). Figure 2.54 illustrates an example of a sleeper slab for an integral abutment system. The sleeper slab is a hidden slab placed under both the approach slab and the roadway pavement.

Dupont and Allen (2002) conducted a survey of the 50 state highways agencies in the U.S. Their study shows from 48 states agencies, which use approach slabs, that 31 states use sleeper slabs. Of the 31 states, 14 states said the sleeper was effective, 2 states said it was not, while 15 states were not sure.

The design purpose of the sleeper slab is to minimize the possibility of the differential settlement by allowing the approach slab to settle with the embankment, thus preventing the bump at the bridge (Dupont and Allen, 2002). However, the improper design of the sleeper slab geometry may lead to settlement problems as well (Lenke, 2006). In addition, when expansion joints are placed on top of the sleeper slabs, cracking and crushing of the approach slab concrete may occur due to the closure of the expansion joints and dragging of the approach slab (Abu-Hejleh et al., 2006).

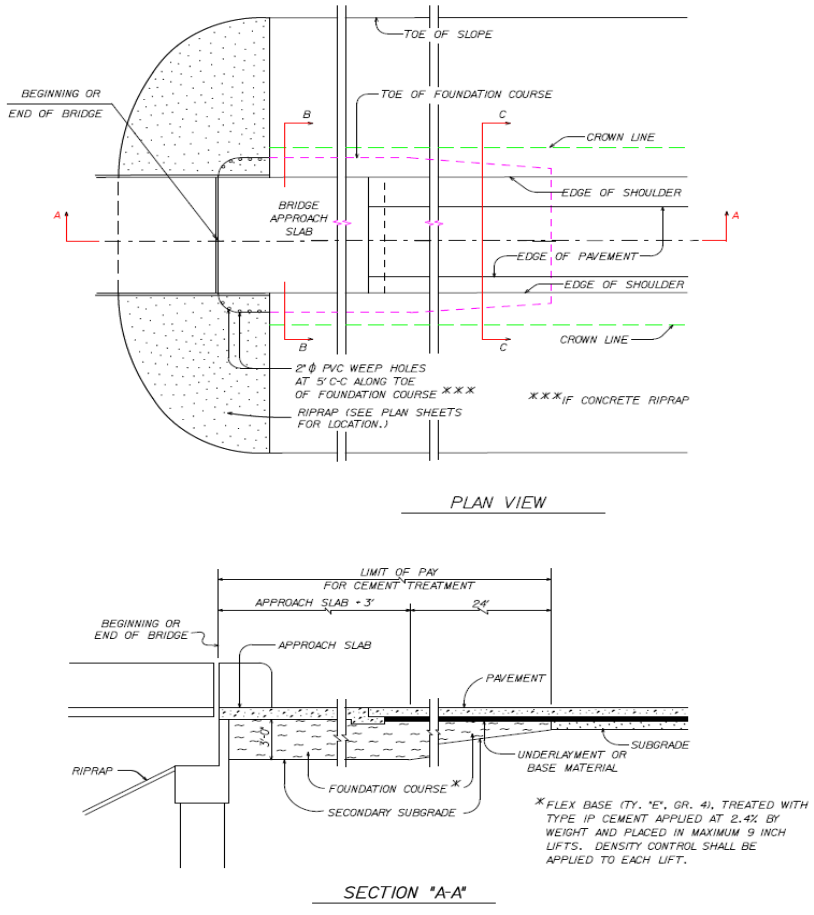

Figure 2.53. Schematic of Bridge Approach Slab Arrangement Adopted by the Fort Worth District of TXDOT, Texas.

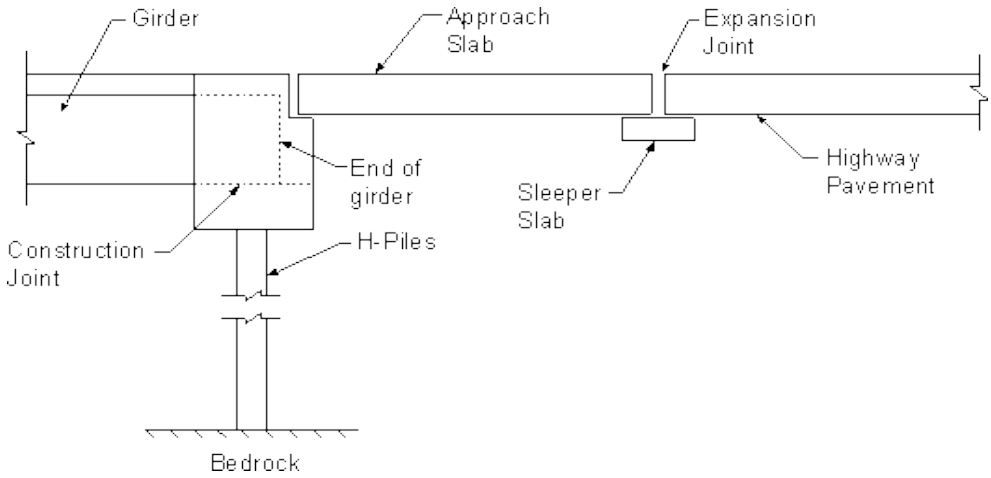

Figure 2.54. Schematic of an Integral Abutment System with a Sleeper Slab.

The minimum recommended length of the sleeper slab is 5 ft (1.5 m) (Seo, 2003). The width of the sleeper slab supporting the approach end of the approach slab should be 5 ft (1.5 m) to prevent the bearing failure within the backfill material under the slab (Seo et al., 2002; Lenke, 2006) while other researchers suggest the use of widths of 3 to 4 ft (0.9 to 1.2 m) (Cai et al., 2005; Abu-Hejleh et al., 2006).

Some studies have reported 16 in. (400 mm) thick sleeper slabs to prevent settlement or the creation of voids beneath the slab (Abu-Hejleh et al., 2000) while other studies recommend the use of thickness of 20 in. (500 mm) (Luna, 2004). Other design considerations of sleeper slabs include placement of drainage material beneath the entire slab and perforated pipes along the sleeper beam to evacuate water infiltrated from expansion joints placed on top of the slab (Luna, 2004; Abu-Hejleh et al., 2006).

Since the sleeper slab is typically supported on the backfill material used in the embankment, similar compaction efforts of the backfill material should be required underneath this slab. Compaction specifications require the maximum density of the fill to be at least 95% of the maximum dry density per AASHTO T-99 (Luna, 2004). Two new supporting systems for the sleeper slab are suggested by Abu-Hejleh et al. (2006). The first system consists of placing higher quality MSE backfill or flowfill under the sleeper slab rather than under the approach slab. The second supporting system consists of using driven piles to support the sleeper slab and using cheaper backfill material behind the abutments and expansion joint device typically placed on top of the sleeper slab. In some cases where the settlement problem would be significant and

continuous for extended periods, elimination of the approach and sleeper slabs altogether should be considered. As an alternative, full-depth asphalt approach slabs could be used with maintenance overlays as needed (Abu-Hejleh et al., 2006).

2.3.7 Effective Drainage and Erosion Control Methods

According to Mekkawy et al. (2005) and White et al. (2005), insufficient drainage is another problem often attributed to the settlements near the bridge abutments. Water collected on the bridge pavement can flow into the underlying fill materials due to ineffective seals at the joints between the bridge approach slab and the abutments and this infiltrated water can erode the backfill material. The material erosion can cause void development under the bridge abutments resulting in the eventual settlements of the bridge approach slabs. Hence, the design of bridge approaches has to be incorporated with an efficient drainage system, such as providing drainage inlets at the end of a bridge deck to collect surface water before getting to the approach slab (Abu-Hejleh et al., 2006).

Also, additional surface or internal drainage to keep water off the slopes is recommended for correcting the superficial erosion of embankments (Wahls, 1990). Keeping the water away from the soil is a simple and a significant factor in reducing the settlement of the soil. Construction costs added to incorporate a good drainage system are not high when compared to the expensive maintenance costs that they might experience during the service life of the bridge (Dupont and Allen, 2002). Hence, all efforts should be made to design the bridge embankments with effective seals and good drainage conditions in and around the bridge structures.

Some of the recommendations reported in the literature to improve drainage conditions include the use of a large diameter surface drain and gutter system in the shoulder of the approach slab and use of a geo-composite vertical drainage system around the embankments with both drainage systems having the potential to increase the drainage capacity (White et al., 2005). This study also recommended the use of porous backfill material or limiting the percentage of fine particles in the fill material to reduce material plasticity and enhance drainage properties.

Based on a survey conducted by Hoppe (1999), the allowable percentage of fine material passing the ASTM No. 200 sieve in the backfills varied from less than 4% to 20% by different state agencies. From the same study, typical provisions in state agencies include plastic

drainpipes, weep holes in the abutments, and the use of granular, free-draining fill. The use of geosynthetic materials, fabrics, and geo-composite drainage panels in the bridge systems was also reported. Other alternatives including the use of a thick layer of tire chips as an elastic zone behind the abutment with a high capacity of drainage was also successfully implemented (White et al., 2005).

Other recommendations including the grading off of the crest to direct runoff away from the back slope and the use of interceptor drains on the back slope are also cited (Wu et al., 2006). It is also recommended to perform periodic maintenance to minimize runoff infiltration and install a combination of granular drain materials, geotextiles, or a geo-composite drain along the back and the base of the fill (Wu et al., 2006).

When the MSE structures are used, the drainage systems are recommended to be constructed in many locations; for example, in the retained soil to intercept any seepage or trapped groundwater or behind and beneath the wall to interrupt water levels before intersect of the structure (NCHRP, 556). To reduce surface water infiltration into the retained fill and reinforced fill, an impermeable cap and adequate slopes to nearby surface drain pipes or paved ditches with outlets to storm sewers or to natural drains should be provided.

Internal drainage of the reinforced fill can be attained by the use of a free-draining granular material that is free of fines (less than 5% passing the No. 200 sieve). Arrangement should be provided for drainage to the base of the fill to prevent water exiting the wall face and causing erosion and/or face stains. The drains should have suitable outlets for discharge of seepage away from the reinforced soil structure (Elias et al., 2001). A suggested drainage system for MSE walls is depicted in Figure 2.55 (Abu-Hejleh et al., 2006).

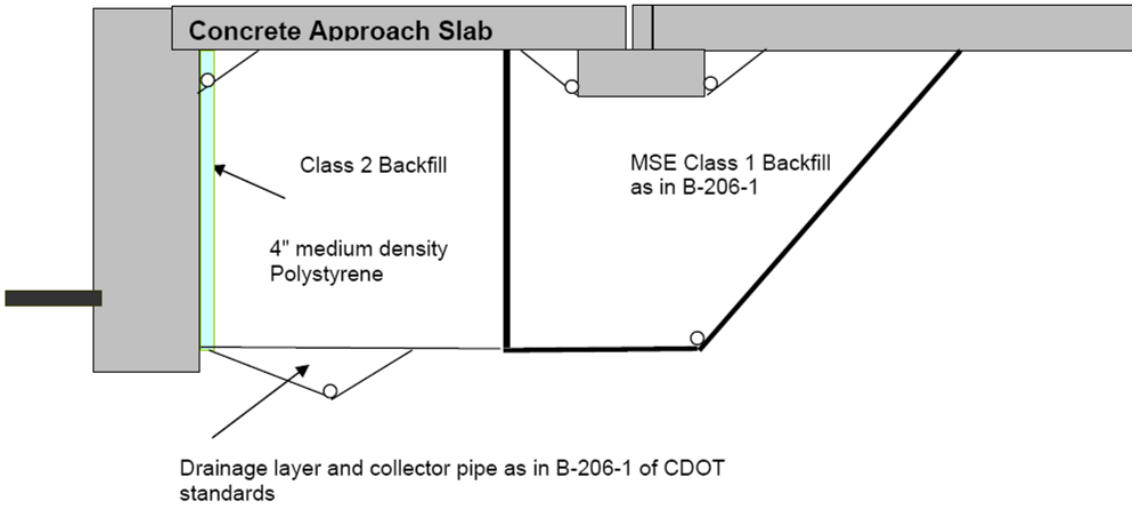

Figure 2.55. MSE Walls System under Sleeper Slab (Abu-Hejleh et al., 2006).

Gabions, which are sometimes used to ensure stability of the wall face during construction, have functioned also as a drainage layer after completion of construction and also as a buffer at the interface between the highly rigid concrete facing and the deformable backfill (Japan Railway Technical Research Institute, 1998).

Another approach to provide an adequate internal drainage system behind the abutment and wingwall is to construct a layer of filter material before placement of the backfill and then install a 6 in. (150 mm) diameter perforated pipe at the bottom to collect excess water (Abu-Hejleh et al., 2006). This water is then carried out by a non-perforated pipe directly through the wingwall (see Figure 2.56). This study also recommended placement of a drainage inlet in the approach slab, or end of deck, to collect the bridge surface water before reaching the expansion joints. In addition, it is also recommended that horizontal drainage measures should be installed from the side of the structure to remove the water from the interface zone between the embankment (often a granular soil layer) and the foundation soil (usually a cohesive soil layer) (Abu-Hejleh et al., 2006).

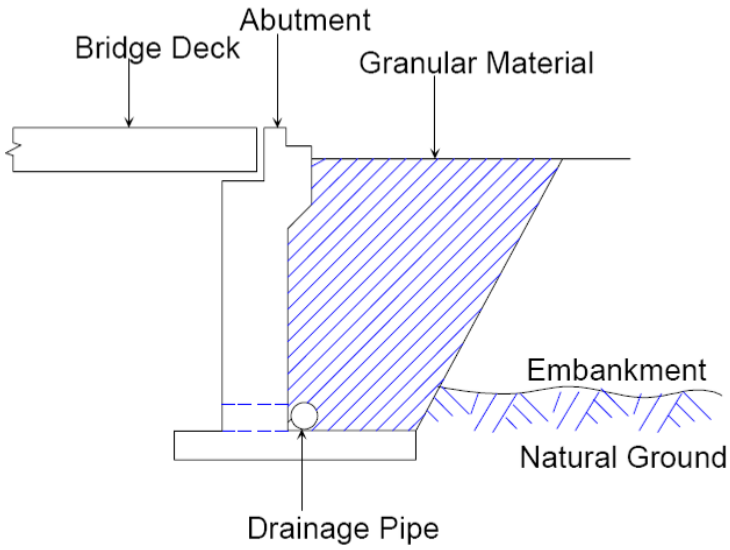

Figure 2.56. Drainage Layer of Granular Material and Collector Pipe.

Briaud et al. (1997) encouraged the use of a curb-to-curb design for erosion control and effective drainage of water away from the bridge structure and approach slab system. Figure 2.57a shows a poorly designed approach slab that will allow water into the backfill and embankment materials promoting erosion and weakening of these granular materials. On the contrary, Figure 2.57b shows a system that will prevent infiltration into the soils below the approach slab. Stewart (1985) suggested that the pavement should even be placed as a cantilever system over the wingwall to further mitigate infiltration below the approach slab.

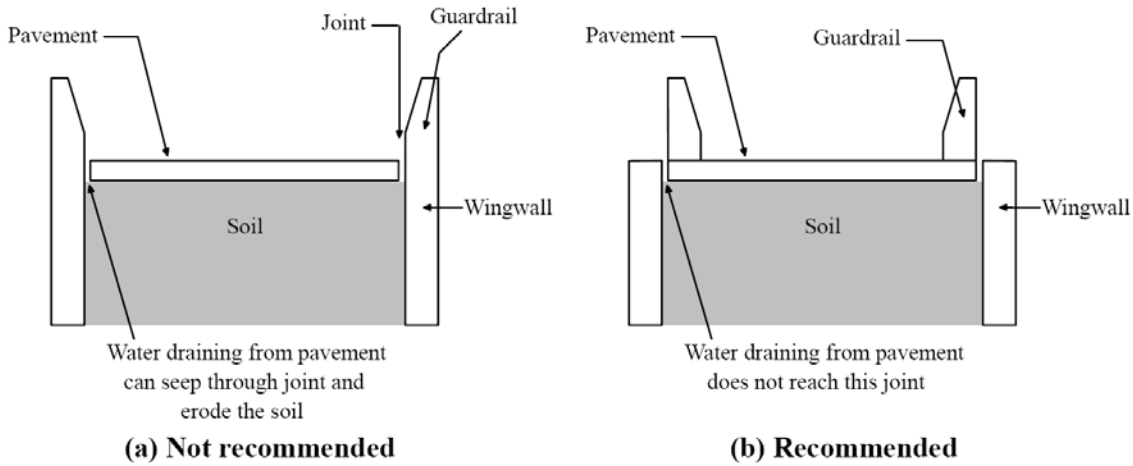

Figure 2.57. Approach Slab Joint Details at Pavement Edge (Briaud et al., 1997).

Figure 2.58 provides an excellent example of good drainage and erosion control on the embankment face underneath the bridge where rip-rap was effectively used to prevent scour on the

face that could cause erosion under the approach slab and bridge abutments (Lenke, 2006). In this research, the use of concrete slope protection on the embankment faces and sides and drainage channels were claimed to be successful in mitigating erosion problems and facilitating adequate drainage conditions (see Figure 2.59).

Figure 2.58. Riprap Used for Erosion Control (Lenke, 2006).

Figure 2.59. Concrete Slope Protection with Drainage Gutter and Drainage Channel (Lenke, 2006).

White et al. (2005) performed a review of several drainage designs implemented by various state agencies to compare different state-of-practices in the United States. The review

showed that three main variations of drainage systems were practiced in the U.S. These are: 1) porous backfill around a perforated drain pipe; 2) geotextiles wrapped around the porous fill; and 3) vertical geo-composite drainage system (Figures 2.60 to 2.62).

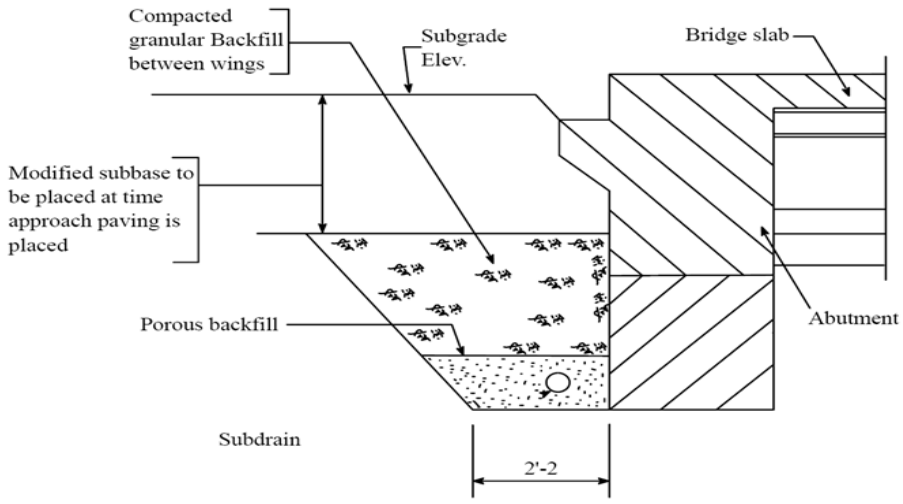

Figure 2.60. Schematic of Porous Fill Surrounding Subdrain (White et al., 2005).

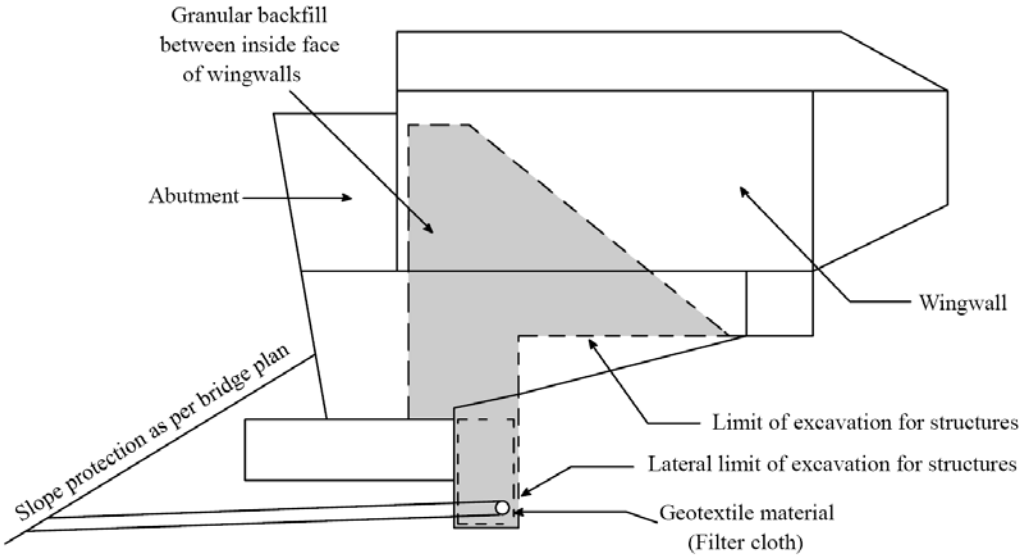

Figure 2.61. Schematic of Granular Backfill Wrapped with Geotextile Filter Material (White et al., 2005).

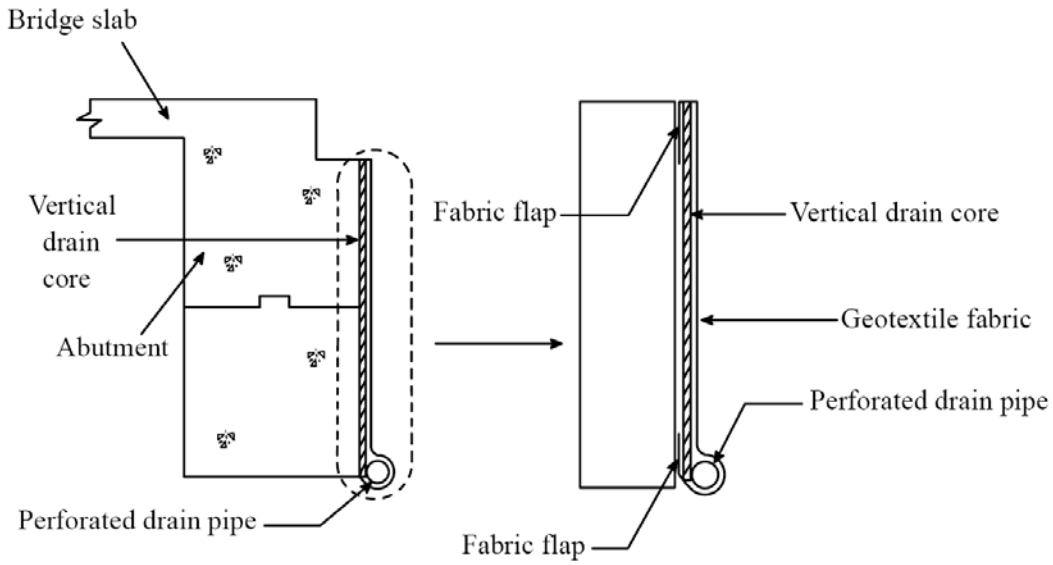

Figure 2.62. Schematic of Geocomposite Vertical Drain Wrapped with Filter Fabric (White et al., 2005).

From this study, it was reported that wrapping the porous fill with geotextiles has helped in reducing erosion and fines infiltration. Another interesting observation from Table 2.7 shows that approximately 14 out of 16 states reportedly have used a combination of two or more of these alternatives to increase the drainage efficiency. The Texas practice is predominantly using porous fills and geotextiles as drainage systems (White et al. 2005).

Mekkawy et al. (2005) and White et al. (2005) concluded from a series of large scale laboratory experiments that the porous backfill behind the abutment and/or geocomposite drainage systems would improve the drainage capacity and would reduce the erosion around the abutment, which will mitigate the differential settlements caused by the erosion and void formation of the backfill material.

2.4 MAINTENANCE MEASURES FOR DISTRESSED APPROACH SLABS

In the case of conventional bridges, much of the cost of maintenance is related to repair of damage at the joints because they require periodic cleaning and replacement (Briaud et al., 1997; Arsoy et al., 1999). Other times, pavement leveling at the ends of the bridge represents most of the maintenance costs. For longer bridges, the pavement leveling lengths are longer due to problems experienced by the temperature induced cyclic movements (Hoppe, 1999). However,

Arsoy et al. (1999) noted that the integral abutment bridges perform well with fewer maintenance problems than with the conventional bridges.

Table 2.7. Drainage Method Used by Various States (White et al., 2005).

State	Porous Fill	Geotextile	Geocomposite drainage system
Iowa	X	-	-
California	X	X	X
Colorado	-	X	X
Indiana	X	X	-
Louisiana	X	X	X
Missouri	-	X	X
Nebraska	-	X	X
New Jersey	X	X	X
New York	-	-	X
North Carolina	X	X	-
Oklahoma	X	X	-
Oregon	X	X	-
Tennessee	X	X	-
Texas	X	X	-
Washington	X	-	-
Wisconsin	X	X	-

Also, a periodic cleanout and maintenance schedule is required for all drainage structures on the bridge and bridge approach system to ensure proper removal of water away from the structure and to minimize runoff infiltration into underlying fill layers (Lenke, 2006). Most frequently, maintenance of drainage structures and joints is a low priority and must be improved in order to take full advantage of these design features (Lenke, 2006; Wu et al., 2006).

Lenke (2006) presented his study showing many cases of poor maintenance at the expansion joints between the bridge deck, approach slab, and approach pavement, and drainage systems resulting in many bridge replacement and rehabilitation costs. He suggested that to prevent stress buildup at the expansion joints between the bridge structure, the approach slab, and the pavement system, a good maintenance program for cleaning and replacement (when necessary) is required. Such stresses can not only cause damage to the deck and the abutment but can also cause distortions of the approach slab.

Lenke (2006) also identified another maintenance issue resulting from Alkali-Silica Reactivity (ASR) problems. The stresses caused by ASR expansion can lead to severe damage at

the joints connecting the bridge deck to the approach slab and the approach slab to the preceding concrete pavement. These ASR expansion stresses can cause spalling and resultant crack widening, which regularly requires joint filling with bituminous materials (Lenke, 2006).

White et al. (2005) also conducted a comprehensive study in a case of lack of maintenance of drainage structures, such as clogged or blocked drains, animal interaction, and deterioration of joint fillers, gutters, and channels. The study showed that due to the lack of maintenance, many problems occurred resulting in numerous and costly repair operations. White et al. (2005) also pointed out some potential causes of bridge approach settlement discovered during the maintenance activities. For example, they mentioned that the loose and improperly compacted backfill materials can cause poor performance at the approach slabs. Coring operations revealed that voids are highest near the bridge abutment and decrease with distance with void sizes ranging from 0.5 to 12 in. (10 to 300 mm). Snake cameras used at sub-drain outlets demonstrated that most of the investigated subdrains were not functioning properly. The subdrains were either dry with no evidence of water, blocked with soil fines and debris, or had collapsed. Some of these problems are attributed to erosion induced movements in the fill material from moisture infiltration. This signifies the need for constant maintenance of joints and drains so that infiltration into the soil layers will be low. Along with the maintenance, reconstruction or rehabilitation of distressed approach slabs are very necessary.

Several soil stabilization techniques were found in the literature to stabilize the fill under the approach slab. These techniques are intended to smooth the approaches by raising the sleeper slab and approaches especially if application of an asphalt overlay is not feasible (Abu-Hejleh et al., 2006). The most important techniques are pressure grouting under the slab, a slab- or mud-jacking technique, the urethane foam method, and compaction or high pressure grouting. Most of these techniques are often used as remedial measures after problems are detected. However, the same could be applied even in new bridge construction. A brief overview of these methods is presented below.

2.4.1 Replacement Method

Highly deteriorated approach slabs are mostly replaced with new approach slabs. This process is the most expensive and time consuming process as the construction process results in frequent lane closures, traffic congestion, etc. A new internal research project has been initiated

by the California Department of Transportation to examine different replacement alternatives for deteriorated approach slabs. In this project, prefabricated Fiber Reinforced Polymer (FRP) decks as well as FRP gridforms and rebars were investigated as replacement options. Full scale approach slabs were tested under simulated wheel loads. Performance of the approach slabs were also examined under simulated washout conditions. Figure 2.63 shows the test schematic.

Figure 2.63. Simulated Approach Slab Deflection due to Washout by UC Davis Research Team.
(http://cee.engr.ucdavis.edu/faculty/chai/Research/ApproachSlab/ApproachSlab.html)

2.4.2 Mud/Slab Jacking

Mud/slab jacking is a quick and economical technique of raising a settled slab section to a desired elevation by pressure injection of cement grout or mud-cement mixtures under the slabs (EM 1110-2-3506, 20 Jan 84). According to EM 1110-2-3506, slab jacking is used to improve the riding qualities of the surface of the pavement, prevent impact loading over the irregularities by fast-moving traffic, correct faulty drainage, prevent pumping at transverse joints, lift or level other structures, and prevent additional settlement.

In this method, the mud grout is prepared using topsoil that is free from roots, rocks, and debris mixed with cement and enough water to produce a thick grout. This grout is injected to fill the void spaces underneath the approach slab through holes made through the approach slabs (Bowders et al., 2002). The injection is performed in a systematic manner to avoid cracks on the

approach slab as shown in Figure 2.64. Precautionary measures need to be taken near to side retaining walls and abutment walls (Luna et al., 2004).

Even though this technique has been successfully adopted by several states including Kentucky, Missouri, Minnesota, North Dakota, Oklahoma, Oregon, and Texas for lifting the settled approach slabs, the mud/slab jacking can be quite expensive. Mud jacking may also cause drainage systems next to the abutment to become clogged and is sometimes difficult to control the placement of the material (Dupont and Allen, 2002). Other difficulties including limited spread of grout into voids, large access holes that must be filled and lack of sufficient procedural process can make this technique uneconomical (Soltesz, 2002). Abu al-Eis and LaBarca (2007) reported that the cost of this technique was between $40 and $60 per one square yard of pavement used based on two test sections constructed in Columbia and Dane Counties in Wisconsin.

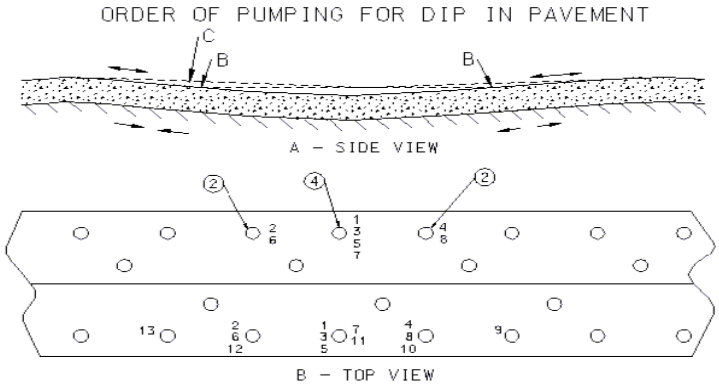

Figure 2.64. Mud-Jacking Injection Sequences (MoDOT, EPC).

2.4.3 Grouting

2.4.3.1 Pressure Grouting under the Slab

The presence of voids beneath the approach slab can lead to instability, cracking, sinking and pounding problems (Abu-Hejleh et al., 2006). In order to mitigate the problem, pressure grouting is commonly used for bridge approach maintenance practice as a preventive measure (White et al., 2005, 2007). Pressure grouting under the slab is used to fill the voids beneath the approach slab through injection of flowable grout without raising the slab (Abu-Hejleh et al., 2006).

White et al. (2007) noted that undersealing the approach slab by pressure grouting needs two grouting operations within the first year after completion of approach pavement

construction. The first grouting is done within the first 2–6 months while the second one is employed within 6 months after the first undersealing. The grout mix design consists of Type 1 Portland cement and Class C fly ash at a ratio of 1:3. Water is also added in the grouting material to achieve the specified fluidity (Buss, 1989). Moreover, in order to avoid lifting of the approach slab, grout injection pressures are kept to less than 35 kPa (White et al., 2007).

Abu-Hejleh et al. (2006) stated that the construction techniques for this method are to drill 1-7/8 in. holes through the concrete or asphalt approach slabs using a rectangular spacing as shown in Figure 2.65. The depth is determined by the ease of driving the stinger or outlet tube that is pounded into the hole (Abu-Hejleh et al., 2006). A fence post pounder is used to hammer the stinger and extension pieces into the soil (Abu-Hejleh et al., 2006). As the stinger is pounded down, the operator can determine if the soil is loose or soft and if there are voids under the slab.

Although grouting under the approach slab is commonly used for bridge approach settlement as a mitigation method, White et al. (2007) stated that the grouting is not a long-term solution for this problem. The grouting does not prevent further settlement or loss of backfill material due to erosion (White et al., 2005, 2007).

2.4.3.2 Compaction or High Pressure Grouting

Compaction grouting is a method for improving soil by densifying loose and liquefaction soils and resulting in an increase in the soil strength (Miller and Roykroft, 2004). The compaction grouting is a physical process involving pressure-displacement of soils with stiff, low-mobility sand-cement grout (Strauss et al., 2004).

According to the ASCE Grouting Committee (1980), the grout generally does not enter the soil pores but remains as a homogenous mass that gives controlled displacement to compact loose soils, gives controlled displacement for lifting of structures, or both. The Abu-Hejleh et al. (2006) also stated that apart from soil densification, the compaction grouting is also employed to lift and level the approach slab and adjacent roadways.

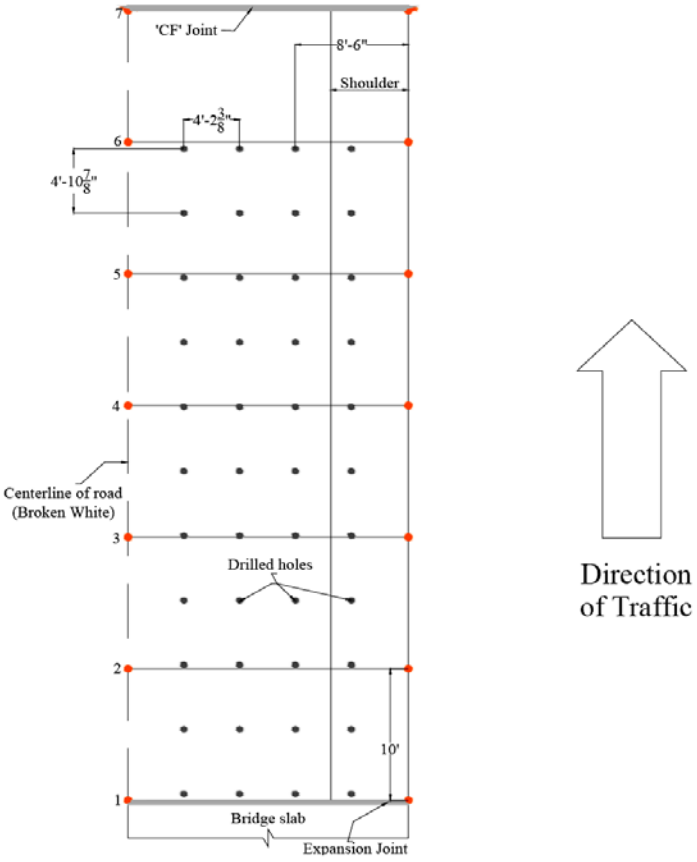

Figure 2.65. Location of Holes Drilled on an Approach Slab (White et al., 2005).

The compaction grouting can be used to stabilize both shallow and deep seated soft layers (Abu-Hejleh et al., 2006). Section 211 of the CDOT Standard Specifications describes that the grouting must be low slump and a low mobility grout with a high internal friction angle. When the technique is used in weak or loose soils, the grout typically forms a coherent "bulb" at the tip of the injection pipe; thus, the surrounding soil is compacted and/or densified (Miller and Roykroft, 2004). For relatively free draining soils including gravel, sands, and coarse silts, the method has proven to be effective (Abu-Hejleh et al., 2006).

2.4.3.3 Urethane Foam Injection Technique

The urethane foam injection technique was first developed in 1975 in Finland to lift and underseal concrete pavements and subsequently adopted in several states in lifting concrete pavements (Abu al-Eis and LaBarca, 2007). In this process, a resin manufactured from high density polyurethane is injected through grout holes (5/8 in. diameter) made through the approach slab to lift, it expands as a foam to fill the voids and to underseal the slab (Abu al-Eis

and LaBarca, 2007). The injected resin foam will gain 90% of its maximum compressive strength (minimum compressive strength is 40 psi) within 15 minutes. Once the voids are filled, the grout holes are filled with non-expansive grout material. Elevation levels are taken before and after the process to ensure the required lifting is achieved (Abu al-Eis and LaBarca, 2007).

As reported by Abu al-Eis and LaBarca (2007), the Louisiana Department of Transportation successfully adopted this technique for two different bridge approaches and observed that the international roughness index (IRI) values were reduced by 33% to 57% after monitoring for four years. This method involves the precise liquid injection of high-density polyurethane plastic through small (5/8 in.) holes drilled in the sagging concrete slab (Abu al-Eis and LaBarca, 2007). Once it is applied, the material foams and expands to lift and stabilize the slab while filling voids in the underlying soil and undersealing the existing concrete (http://www.stableconcrete.com/uretek.html). Based on the manufacturer provided information, this technology is simple and rapid. It can lead to a permanent solution and also can resist erosion and compression over a longer time period close to five plus years.

Brewer et al. (1994) first evaluated the urethane foam injection technique to raise bridge approach slabs in Oklahoma. They reported that three test slabs out of six were cracked during or after the injection and in one case, the PCC slab broke in half during the injection. The Michigan Department of Transportation reported that this technique provided a temporary increase in base stability and improvement in ride quality for one year (Opland and Barnhart, 1995). Soltesz (2002) noticed that the urethane foam treatment was successful even after two years when the injection holes were properly sealed. The Oregon Department of Transportation researchers reported that the urethane foam material was able to penetrate holes with diameters as small as 1/8 in., which was an added advantage of this technique to fill the minor pores of the subbase and lift the pavement slabs (Soltesz, 2002).

Abu al-Eis and LaBarca (2007) reported that the cost of this technique was between $6 to $7 per pound of foam used, which was calculated based on two test sections constructed in Columbia and Dane Counties in Wisconsin. They summarized the cost comparison of this technique with other slab lifting methods as shown in Table 2.8 and concluded that this technique is expensive when compared to other methods if calculated based on direct costs. They also reported that this technique is very fast and can open the lanes for traffic immediately after the treatment. The amount of urethane resin used in each project is also questionable as this

quantity is directly used in the cost analysis. Considering this fact, TxDOT amended its Special Specification 3043-001, which requires a Special Provision for determining the quantity of polymer resin used for "Raising and Undersealing Concrete Slabs." Regarding Special Specification 3043-001, the quantity of the resin utilized will be calculated by one of the following methods:

1. Payment will be made according to the actual quantity of polymer resin used in the work by weighing each holding tank with components by certified scales before and after each day's work.
2. Payment will be made according to the actual quantity of polymer resin used in the work by determining the weight of material placed by measuring the depth of polymer resin in the holding tanks before and after each day's work. A professional engineer and a site engineer must approve the calculation method, which is based on the certified measured volume of each tank and the unit weight of each component to determine the weight of resins used in the work.

Table 2.8. Cost Comparison for Four Slab Faulting Repair Methods.

Location	Method	Total Cost	Cost per yd^2	Days to Complete
I-30 ($80\ yd^2$)	URETEK Foam	$19,440	$243	0.75
	Slab Replacement	$34,000	$425	3
	HMA Overlay	$3,630	$45	1
	Mud-jacking	$3,000	$38	1
SH 114 ($53.4\ yd^2$)	URETEK Foam	$6,260	$117	0.5
	Slab Replacement	$22,670	$425	3
	HMA Overlay	$3,375	$63	1
	Mud-jacking	$3,000	$56	1

Several districts in Texas use this method as a remediation method and based on the present research contacts, these methods are deemed effective. Researchers visited two bridge approach slab repair projects recently completed in Hill County, Texas, and another completed several years ago on several highways in and around Houston, Texas. Both visits were made in late February 2008.

Figure 2.66 shows the schematic and photographic view of the bridge site with the void developed under the approach slab. The cause of the problem was identified as erosion of the granular backfill material under the approach slab.

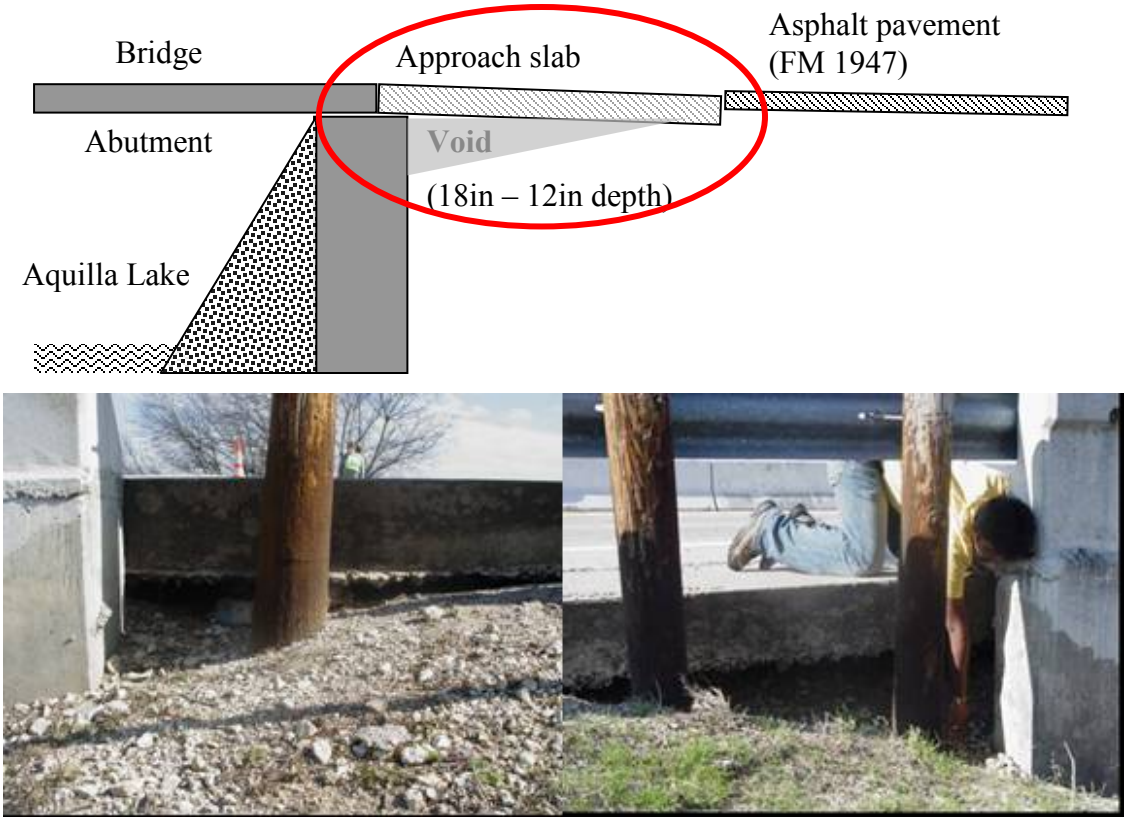

Figure 2.66. Schematic of the Approach Slab with Developed Void under the Bridge at FM 1947 Hill County, Texas.

Figure 2.67 depicts the position of the approach slab during and after the injection process. During and immediately after the injection process, researchers observed a few minor hairline cracks on the approach slab as shown in Figure 2.68. The minor cracks on the surface of the approach slab during this injection operation are relatively common and they will not lead to further distress of the approach slab. The post-performance of this method is very crucial to address the expansion of these hairline cracks and the movements of the repaired approach slabs. A simple field monitoring study including elevation surveys and visual inspection of these minor cracks would reveal the effectiveness of this technique.

Figure 2.67. Position of Approach Slab during and after the Urethane Foam Injection Process.

Figure 2.68. Hairline Crack Observed on the Approach Slab during the Urethane Foam Injection.

Per discussions with TxDOT engineers in Houston, the process was quite effective. Several Houston sites that were visited were repaired utilizing this injection method 10 years ago and they are still functioning adequately. The work reported in the Houston District was instrumental in the development of the TxDOT Special Specification for the use of the urethane foam injection method for lifting the distressed approach slabs.

2.4.3.4 Flowable Fill

Flowable fill or controlled low-strength material is defined by ACI Committee 229 as a self-compacting, cementitious material used primarily as a backfill in lieu of compacted fill. The flowable fill has other common names such as, unshrinkable fill, controlled density fill, flowable mortar, flowable fill, plastic soil-cement, and soil-cement slurry (Du et al., 2006). This controlled low-

strength filling material is made of cement, fly ash, water, sand, and typically an air-entraining admixture (NCHRP, 597). A significant requisite property of flowable fill is the self-leveling ability which allows it to flow; no compaction is needed to fill voids and hard-to-reach zones (Abu-Hejleh et al., 2006). Therefore, the flowable fill is commonly used in the backfill applications, utility bedding, void fill, and bridge approaches (Du et al., 2006).

A primary purpose of using flowable fill is as a backfill behind the abutment. CDOT has used the flowable fill backfill behind the abutment wall in an effort to reduce the approach settlements since 1992 (Abu-Hejleh et al., 2006). The other new applications for the flowable fill are for use as a subbase under the bridge approaches and a repair work of the approaches (Du et al., 2006). Historically, the application of using flowable fill as a subbase was first employed in Ohio by ODOT (Brewer, 1992).

In Iowa, the flowable fill is a favorable backfill used as a placement under the existing bridges, around or within box culverts or culvert pipes, and in open trenches (Smadi, 2001). Smadi also cited that the advantages of flowable mortar are not only due to its fluidity, but also due to its durability requiring less frequent maintenance. Moreover, the flowable mortar is also easily excavated. Therefore, the maintenance works, if required, can be done effortlessly (Smadi, 2001). Figure 2.69 shows details of flowable mortar used under a roadway pavement.

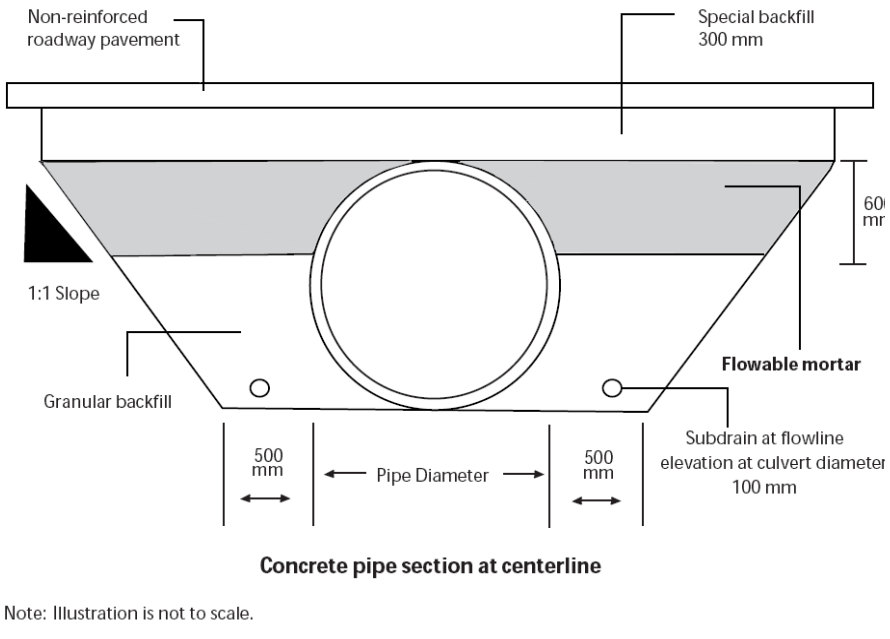

Figure 2.69. The Flowable Mortar Used under a Roadway Pavement (Smadi, 2001).

In Texas, the flowable fill was used for the first time for repairing severe settlements of bridge approaches at the intersection of IH 35 and O'Conner Drive in San Antonio in 2002 by TxDOT (NCHRP, 597; Du et al., 2006). For this practice, TxDOT used a specialized mixture using flowable fill, which consisted of sand, flyash, and water, but no cement (Williammee, 2008). The compressive strength of cored samples indicated that the long-term strength and rigidity of the flowable fill were strong enough to serve this purpose (NCHRP, 597). After the mixture proportions were adjusted to have adequate flowability for the application, the flowable fill has shown great success for repairing the approaches (Du et al., 2006; Williammee, 2008). Recently, the flowable fill was used in the Fort Worth District in place of a flexible base beneath the approach slab. The 3 ft (0.9 m) deep flex base is prepared with Type 1 cement (2.4% by weight) as a base material as shown in Figure 2.70.

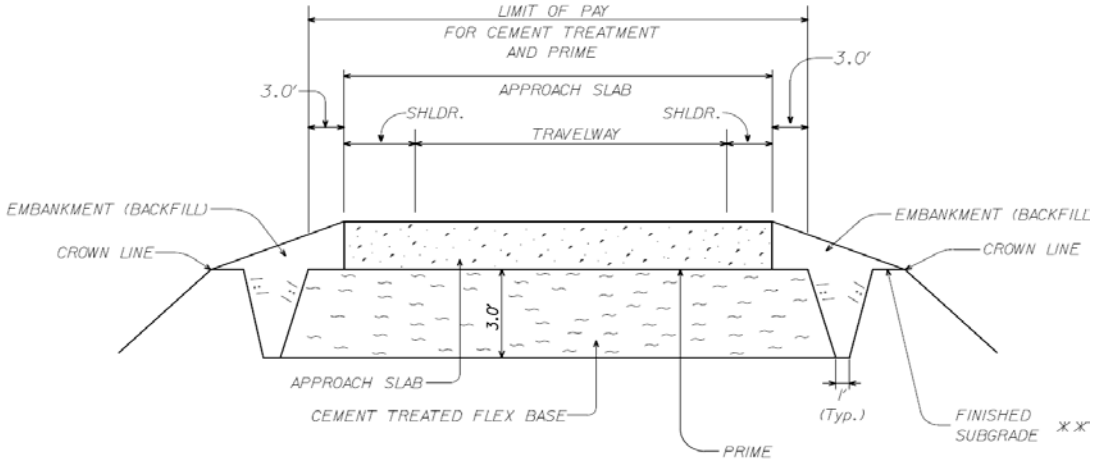

Figure 2.70. The Flowable Fill Used as a Base Material (Du, 2008).

2.4.4 Other Methods

Several other techniques are also available to mitigate the settlement problem caused in the approach slab area, and these techniques are discussed in the following.

2.4.4.1 Precambering

If the approach pavement settlement cannot be controlled economically, a pre-cambered roadway approach may be applied (Tadros and Benak, 1989). Hoppe (1999) recommended implementing pre-cambering of bridge approaches for up to a 1/125 longitudinal gradient. The

pre-cambering is used to accommodate the differential settlement that will inevitably occur between a structure constructed on deep foundations and adjoining earthworks.

Briaud et al. (1997) recommended pre-cambering with gradient values of less than 1/200 of the approach slab length to compensate for the anticipated post-construction settlements. The pre-cambered design utilizes a paving notch that supports a concrete slab. The notch must be effectively hinged, which allows the concrete slab to move radially (see Figure 2.71). The flexible pavement over the slab will absorb some movement below but not to a great extent (Briaud et al., 1997). The pre-cambered approach system also requires an accurate assessment of settlement potential (if possible). The pre-cambered approach design could be specified in situations where time is not available for more conventional settlement remediation, such as preloading, wick drains, and others (Luna, 2004).

Wong and Small (1994) conducted laboratory tests to investigate the effects of constructing approach slabs with an angle from the horizontal on reducing the bump at the end of the bridge. Horizontal slabs suffered a rapid change in surface deformation with the formation of obvious bumps while pre-cambering the slabs with angles of 5° to 10° provided a smoother transition.

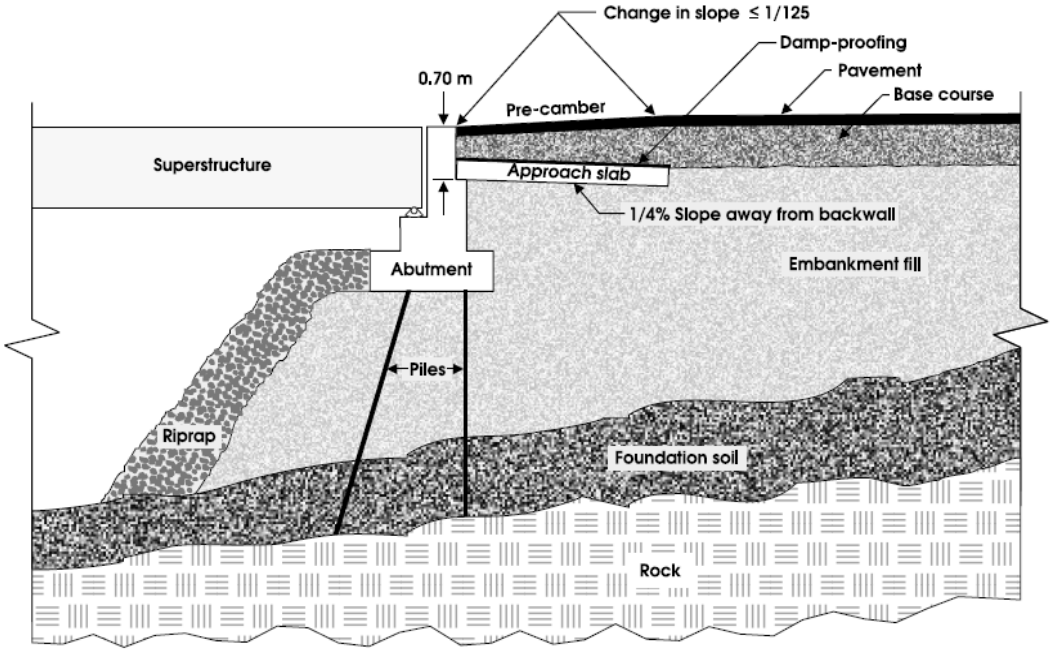

Figure 2.71. Pre-cambered Approach Design (Hoppe, 1999).

2.4.4.2 Lightweight Fill Materials

The lightweight materials such as Expanded Polystyrene (EPS) Geofoam and Expanded Clay Shale (ECS) can be used either as a construction embankment fill material for new bridge approach embankments or can be used as a fill material during the repair of distressed approach slabs. Description of this method was presented earlier in Section 2.4.3.

2.4.4.3 Expanded Polystyrene (EPS) Geofoam

Expanded Polystyrene (EPS) Geofoam is a lightweight material made of rigid foam plastic that has been used as fill material around the world for more than 30 years. This material is approximately 100 times lighter than conventional soils and at least 20 to 30 times lighter than any other lightweight fill alternative. The added advantages of EPS Geofoam including reduced loads on underlying subgrade, increased construction speed, and reduced lateral stresses on retaining structures has increased the adoptability of this material to many highway construction projects. More than 20 state DOTs including Minnesota, New York, Massachusetts, and Utah adopted the EPS Geofoam to mitigate the differential settlement at the bridge abutments, slope stability, alternate construction on fill for approach embankments and reported high success in terms of ease and speed in construction, and reduced total project costs.

Lightweight EPS Geofoam was used as an alternate fill material at Kaneohe Interchange in Oahu, Hawaii, while encountering a 20 ft (6 m) thick layer of very soft organic soil during construction. Researchers used 600,350 ft^3 (17,000 m^3) of EPS Geofoam to support a 69 ft (21 m) high embankment construction (Mimura and Kimura, 1995). They reported the efficiency of the material in reducing the pre- and post-construction settlements. Figure 2.72 shows the construction of the embankment with the EPS Geofoam.

Figure 2.72. Emergency Ramp and High Embankment Constructed Using the EPS Geofoam at Kaneohe Interchange in Oahu, Hawaii.

2.5 SUMMARY

This chapter presented a thorough synopsis of the literature review on settlement at the bridge approach. The definition of the settlement at the bridge approach problem was firstly presented followed with the magnitude of the bump tolerance. Afterward, major mechanisms causing the bump problem were introduced. The primary sources of the problem broadly divided into four categories as material properties of foundation and embankment, design criteria for bridge foundation, abutment and deck, construction supervision of the structures, and maintenance criteria. (Hopkins, 1969, 1985; Stewart, 1985; Greimann et al., 1987; Laguros et al., 1990; Kramer and Sajer, 1991; Ha et al., 2002; Jayawickrama et al., 2005; White et al., 2005, 2007).

Major focus of this chapter was given to several techniques used to mitigate the bump problem, which was presented into two main sections: the techniques for new bridge construction, and the measures for distressed approach slabs. The techniques for new bridge construction were divided into various groups such as improvement of foundation soil, improvement of backfill material, design of bridge foundation, design of approach slab, and effective drainage and erosion control methods. Several techniques fell into these groups as listed: for example, Excavation and Replacement, Preloading and Surcharge, Dynamic Compaction, Stone and Lime Columns, Geopiers, Concrete Injected Columns, Deep Soil Mixing Columns, Geotextiles/Geogrids, Geocells, etc.

Maintenance measures for distressed approach slabs are normally used as remedial measures after problems are detected. The most important techniques fell into this category as pressure grouting under the slab, slab-jacking or mud-jacking technique, the urethane foam method, and compaction or high pressure grouting. Many of these measures could be also applied for improvement of backfill material in new bridge construction.

CHAPTER 3

DISTRICT SURVEYS AND SELECTION OF SETTLEMENT MITIGATION METHODS

3.1 INTRODUCTION AND RESEARCH OBJECTIVE

The comprehensive literature review presented in Chapter 2 has resulted in the short listing of a few techniques that are proven to be viable to mitigate the settlements of the bridge approach slabs. A few techniques presented in the literature review are proven to be feasible to mitigate the problem but they still need to be evaluated in this research to address their potential for field use. This has been the main objective of this research and its focus is to evaluate methods that can be used to control approach slab settlements in the field. Therefore, in this chapter, an attempt is made to select two methods to mitigate settlements underneath the approach slabs.

The attempt to select two methods was accomplished by performing the following two tasks. In the first task, a survey questionnaire was distributed to all 25 districts to collect their practices with respect to this approach settlement problem. The results from the survey are valuable in understanding the problems existing in the field and the solutions used so far to minimize the bumps at the end of the bridges.

In the second task, a ranking analysis of viable techniques was attempted by using four criteria including 1) technique feasibility, 2) construction requirements, 3) cost considerations, and 4) overall performance. After each mitigation method was considered and analyzed according to the aforementioned criteria, the mitigation techniques were ranked and top two of the recommended methods considered for further research evaluation.

3.2 TXDOT DISTRICTS' SURVEY

As a part of this task, all 25 districts of the Texas Department of Transportation were contacted and then surveyed to learn about the problems existing in the field and the solutions used to minimize the bumps. The researchers distributed a survey questionnaire to all 25 districts with a total of 18 districts responding. In a few cases, responses from different engineers from the same district were received. All these results were tabulated and summarized in the following.

a) *Most districts have encountered bridge approach settlement/heaving problems.*

As shown in Figure 3.1, 17 out of 18 districts (94%) have encountered the bridge approach settlement. Among the 17 districts responses, 6 districts (33%) have experienced both settlement and heaving problems while 11 districts (61%) have only encountered the bridge approach settlement. The Odessa District reported that they have no problems either with bridge approach settlement or heaving.

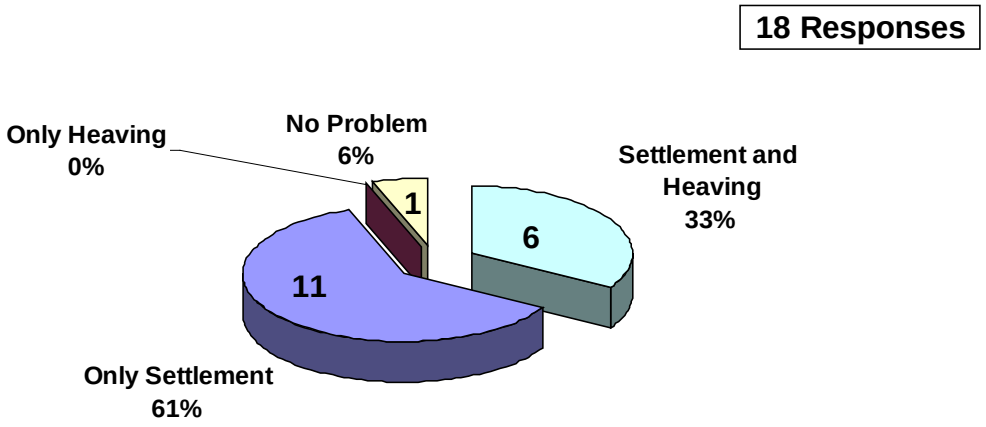

Figure 3.1. Number of districts that Encountered Bridge Approach Settlement/Heaving.

b) *Majority of the districts noted this problem from visual observations to identify the bump problem in the field.*

Figure 3.2 presents further responses from 17 districts that noted the bridge approach settlement/heaving. These responses related to the procedures followed for identifying the heave/settlement problem at the bridge approaches. All of the 17 districts noted this problem from visual observations. Some other forms of identification of this problem were through evaluation of rideability and from the receipt of public complaints as mentioned by 15 and 10 districts, respectively. Only two districts have reported that they have used rideability (International Roughness Index) measurements whereas three other districts have noted that they used other methods including notification from maintenance offices to identify the problem.

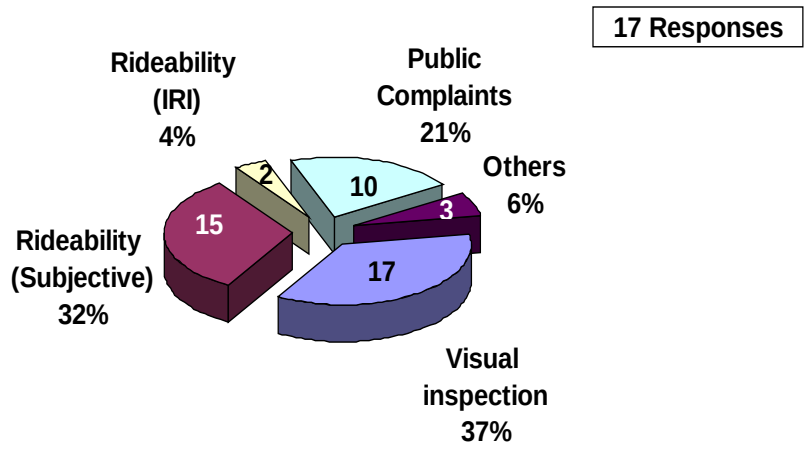

Figure 3.2. Procedure to Identify the Problem in the Field.

c) *Minority of districts conducted any forensic examinations on the distressed approaches to identify potential cause(s) of the problem.*

For the question related to whether a district has conducted any forensic examinations on the distressed approaches to identify potential cause(s) of the problem, most of districts (53%) reported in the negative (Figure 3.3).

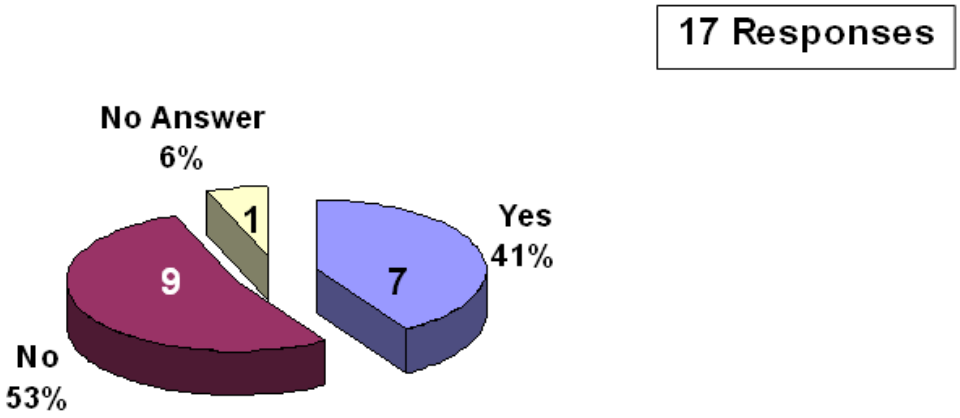

Figure 3.3. Number of districts that Conducted any Forensic Examinations on the Distressed Approaches to Identify Potential Cause(s) of the Problem.

d) *The compaction of the fill was considered as a major factor contributing to the approach settlements in the district.*

Figure 3.4 shows various factors that the districts attributed to the settlement or heaving problem. The districts were asked to select more than one response. As a result, the total

responses do not add up to 17. The following summarizes each of the factors and the number of responses received:

- Natural subgrade: 6 responses.
- Construction practices: 13 responses.
- Drainage and soil erosion: 12 responses.
- Void formation: 10 responses.
- Compaction of fill: 15 responses.
- Others: 3 responses mentioned poor design in old practices and sulfate problems.

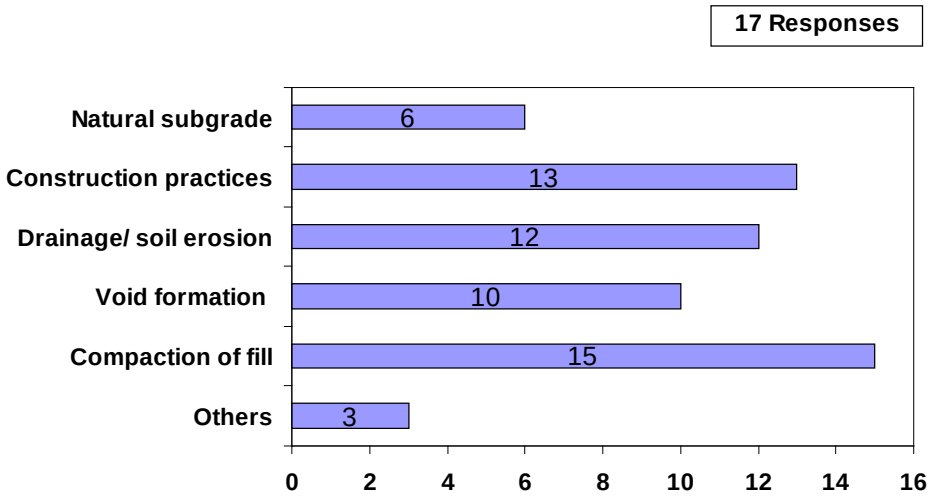

Figure 3.4. Factors Attributed to the Approach Settlement Problems.

e) *Geotechnical investigations on embankment fill and foundation subgrade material are normally performed by districts.*

Fifty-nine percent of the respondent districts noted that they typically perform geotechnical investigations on fill and foundation subgrades (Figure 3.5).

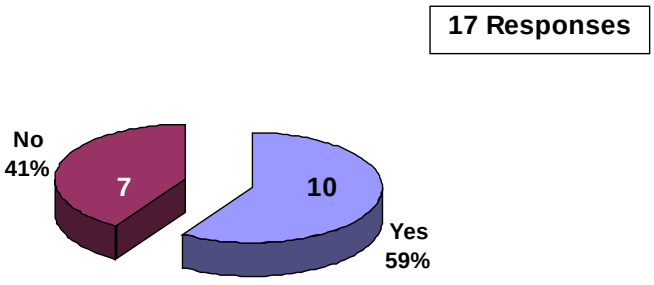

Figure 3.5. Number of districts that Perform a Geotechnical Investigation on Embankment Fill and Foundation Subgrade Material.

Figure 3.6 shows various plasticity index (PI) specifications listed by the districts that they followed in the selection of embankment fill material. As per Figure 3.6, the maximum PI of the fill material used by select districts was around 40 while most of them required it to be less than 25.

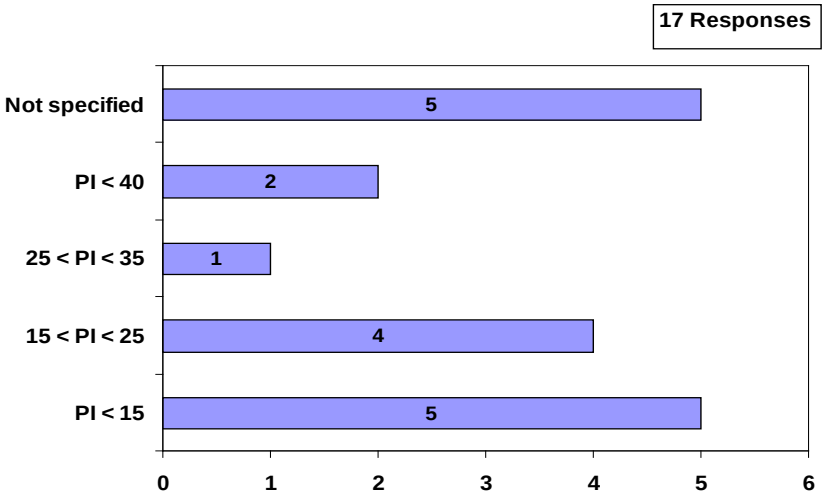

Figure 3.6. PI Value Required for Embankment Material.

f) *The Nuclear Gauge is normally used to perform Quality Assessment (QA) on compacted fill material*

Figure 3.7 presents districts' responses related to Quality Assessment (QA) studies performed on compacted fill material. Figure 3.7 results show that 15 out of the 17 districts (88%) noted that they have used the Nuclear Gauge for compaction Quality Assessment (QA) studies. Seven districts used sampling and laboratory testing, while only one district used the dynamic cone penetrometer (DCP) for the same purpose.

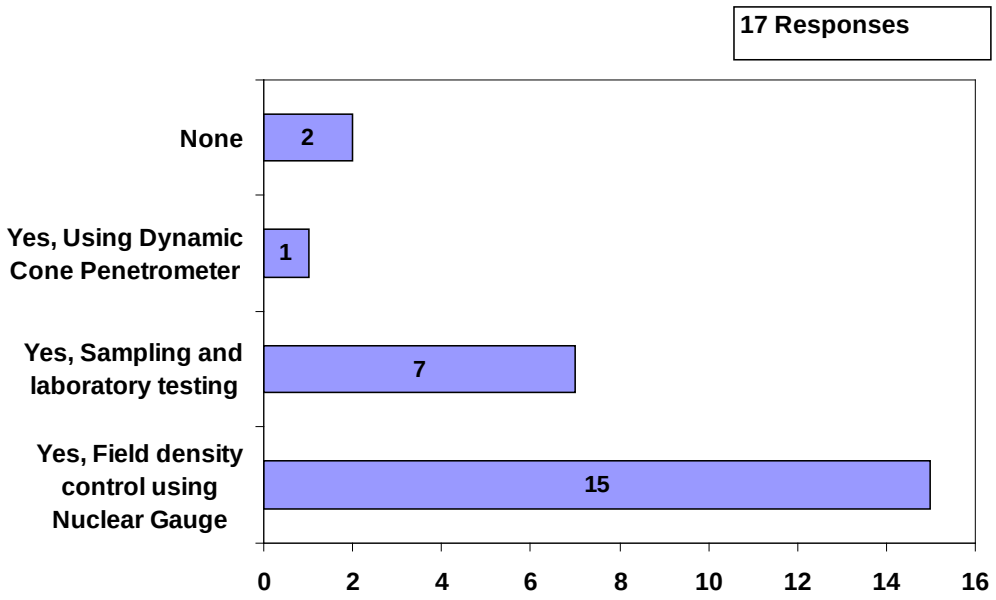

Figure 3.7. Number of districts Conducting Quality Assessment (QA) Studies on Compacted Fill Material.

Figure 3.8 lists various remediation methods used by the districts to repair the heave/settlement. Survey results revealed that the milling or level-up of the approach slab is a frequently used maintenance measure by the majority of the TxDOT districts (17 out of 18 respondents, 94%). With respect to its performance, only 3 districts noted that this method is working well, 8 districts as good, and 6 districts as fair. The use of the urethane foam injection process was the second choice by the districts as 10 districts (55%) have selected this as their remedial measure. With respect to its performance, 2 districts rated this technique as very well, well (2 districts), and good (2 districts), respectively, while 4 districts rated this method as fair. Other remedial measures include reconstruction of the approach slab, treatment of the subgrade, chemical treatment of the backfill, and the installation of effective drainage and reinforced backfill material. The performance rating of these methods is listed in the same figure. Two other districts responded that they have employed other methods such as pressure grouting and cement stabilized sand.

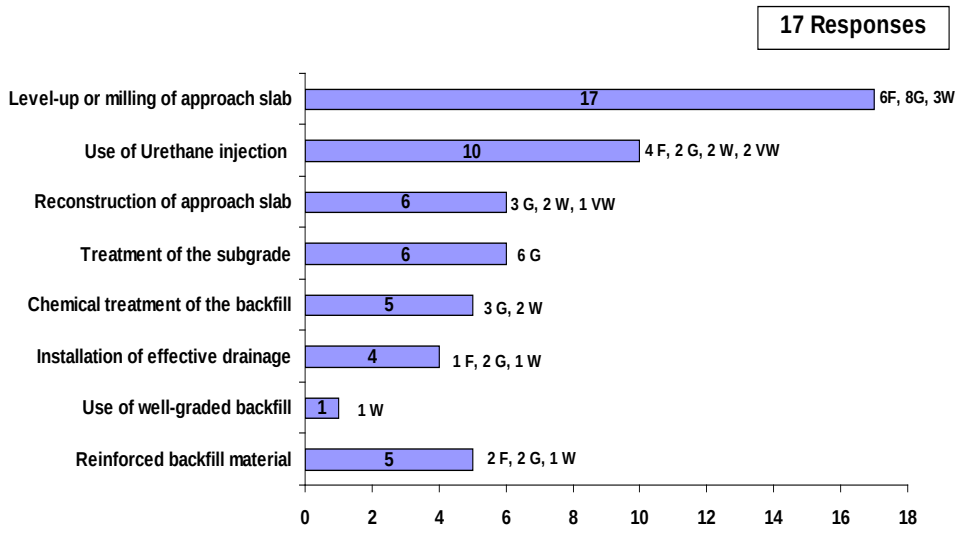

Figure 3.8. Remedial/Maintenance Measures Taken in Responded districts and Its Performance (Note: VW – Very Well; W – Well; G – Good; F – Fair).

Table 3.1 presents the information when controlling the PI value is the most recommended method by the districts in this survey. This was achieved either by using chemical treatment on the subgrade and/or backfill or by using density control compaction. Other recommendations include using rock embankment under the approach slab, select fill material, using two-sack concrete mix under the approach slabs and even quality control measures during embankment construction.

g) *Turf growth is typically implemented as a remedial method to control the erosion/slope failure problems.*

Figure 3.9 shows that 5 out of the 17 districts (30%) responding have employed turf growth and geosynthetics methods to control the erosion/slope failure problems while 5 other districts have implemented only geosynthetics to manage the problem. Six districts have done nothing, and some districts have chosen other methods such as, rock riprap, flatten the slope, flexible reinforcement, improve drainage, water intrusion, and erosion control. Nevertheless, none of 17 districts have chosen the baling method using straw bales to control the problem.

Table 3.1. Recommendations for Fill Material Used for Embankments.

District	Recommendations for fill material used for embankments
Abilene	PI ≤ 15, or lime treat to reduce PI≤ 15
Austin	1. Use rock embankment under the approach slabs to prevent settlement issues with success. 2. PI requirements to insure non-plastic materials.
Brownwood	1. Select fill for drainage behind abutment walls. 2. Cement or lime treat subgrade
Dallas	Graded backfill material with PI 10 to 25 with density controlled compaction
El Paso	2 sacks of concrete at approach slabs and backwall
Fort Worth	1. Test embankment for compliance with requirements at beginning of the bridge, end of the bridge, and at 25' intervals for a distance of 150' from each bridge end. 2. Embankments are supposed to be constructed to the final subgrade elevation prior to the excavation for abutment caps and approach slabs. 3. Additional density testing of roadway embankments near bridges
Houston	1. Lower the LL/PI 2. Good compaction 3. Cement stabilized backfill
Laredo	Item 132
Pharr	Cement stabilized backfill
Waco	Cement stabilized backfill

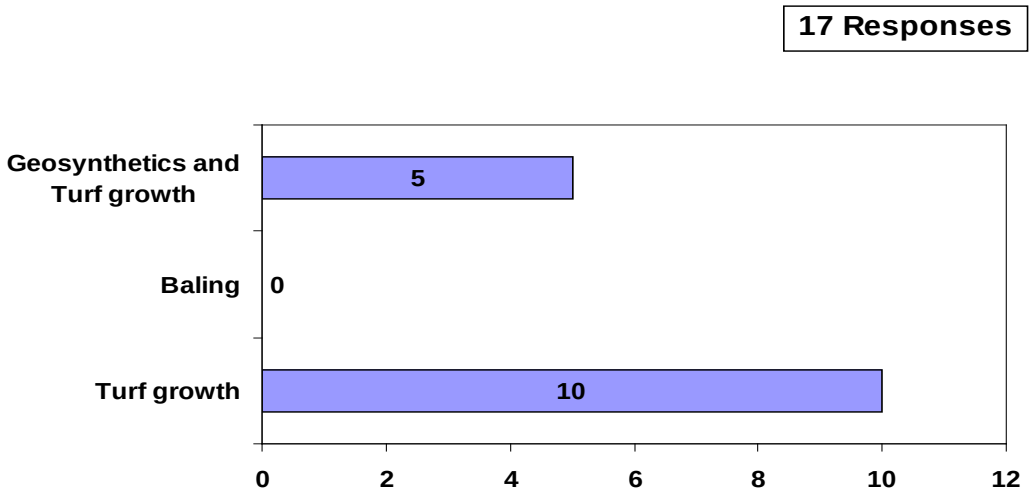

Figure 3.9. Methods to Control the Erosion/Slope Failure.

3.3 RANKING ANALYSIS OF MITIGATION TECHNIQUES

The non-parametric ranking analysis was performed in this task to rank the techniques presented from the literature review that is divided into two groups. One group focuses on novel methods used for foundation and fill improvement while another group deals with techniques normally used for approach slab maintenance. The first group focuses on novel methods used for foundation and fill improvement and these methods include Deep Soil Mixing (DSM), Continuous Flight Auger (CFA) piles, MSE wall, and other methods. The second group deals with techniques normally used for approach slab maintenance such as Hot Mix Asphalt (HMA) overlays, slab replacement, urethane foam injection, and others. Four criteria including 1) technique feasibility, 2) construction requirements, 3) cost considerations, and 4) overall performance were considered and for each criterion, a ranking was assigned to each method.

For technique feasibility, three levels of ranking (shown in parentheses) were considered and these were: 1) they have been already implemented and proven as well designed methods, 2) technique is effective but still under research, and 3) they are ineffective. Table 3.2 presents the ranks given for the methods listed in each group. All methods of the first group are novel and yet to be evaluated and hence they are assigned a rank of two. Ranks given in Group Two are also presented in the same table.

Two criteria were used in the case of construction requirements, and these are: 1) requiring mobilization of heavy equipment and 2) requiring quality control during construction. For cost considerations, the ranking was based on the costs of the construction for performing the field work. The last and third criterion for the ranking analysis is based on the overall performance of each method. This rank was based on the available literature. Table 3.2 presents all the ranks considered for each method.

In conclusion, after each mitigation method had been analyzed per the four criteria, the mitigation techniques were ranked. The results show that for the novel foundation and fill improvement methods, six of them showed potential for use and were recommended to be evaluated in this research while for the maintenance measures, the mud/slab jacking, grouting, and urethane foam injection has shown potential and were considered for further research evaluation.

Table 3.2. Ranking Analysis of Mitigation Techniques for Bridge Approach Settlement.

New or Maintenance Measure	Mitigation method	Technique Feasibility (a)			Construction Requirements (b)			Cost Considerations (c)			Overall Performance			Is this method recommended for present research?
		Ineffective	Effective but under research	Proven, well design method	Low	Medium	High	Low	Medium	High	Not proven	Ineffective	Effective	
Novel Methods for Foundation and Fill Improvement	MSE Walls/GRS		✔				✔			✔	✔			✘
	Geofoam		✔			✔			✔		✔			✔
	Lightweight Fill		✔			✔			✔		✔			✔
	Flowable fill		✔		✔			✔				✔		✔
	Deep Soil Mixing (DSM)		✔		✔				✔				✔	✔
	Continuous Flight Augercast piles (CFA)		✔				✔		✔			✔		✘
	Concrete Injection Columns (CIC)		✔			✔				✔	✔			✘
	Geopiers		✔			✔			✔			✔		✔
Maintenance Measures	HMA overlay			✔		✔		✔			✔			✘
	Mud/ Slab jacking		✔		✔			✔				✔		✔
	Slab replacement			✔		✔			✔			✔		✘
	Grouting			✔	✔				✔			✔		✔
	Urethane foam injection		✔		✔					✔			✔	✔

3.4 SUMMARY

This chapter presents the results of TxDOT's districts' survey and a ranking analysis. The ranking analysis was done concurrently with the districts' survey, which reveals each district's practices with respect to the approach settlement problem. The results from both the analysis and the survey are useful in this study. From the aspects of understanding of the bump problems encountered in each district and the techniques available to minimize the bump problem, five methods including Geofoam, Deep Soil Mixing, Geopiers, Lightweight Fill, and Flowable Fill are recommended as foundation and fill improvement methods to be evaluated in this research while the mud/slab jacking, grouting, and urethane foam injection are also recommended for maintenance measures evaluation.

Since the objective of the research was to investigate the methods that could be comprehensively evaluated from controlling approach slab settlements of new bridge construction, two methods, one for foundation treatment known as Deep Soil Mixing (DSM) and the other for embankment modification using lightweight Expanded Clay Shale (ECS) are considered for the present research evaluations. The next chapters describe these evaluation studies for settlement control of approach slabs.

CHAPTER 4

DESIGN STEPS FOR DEEP SOIL MIXING (DSM) AND LIGHT WEIGHT FILLS (LWF) FOR SETTLEMENT CONTROL OF EMBANKMENTS

4.1 INTRODUCTION

As discussed in Chapter 3, the soil-cement treatment using deep soil mixing or DSM was chosen as one of the viable techniques to improve the engineering properties of clayey soft soils beneath a bridge embankment. The chosen site on IH 30 in Arlington, Texas, was selected to evaluate the application of this technique in real field conditions. An embankment on the south side of the bridge was constructed over the DSM treated test section while the other side of the bridge was constructed on a local stiff soil with a conventional method (i.e., without the DSM treatment). This section was selected as the control section.

In this chapter, the subsections describe the procedure(s) developed for the design of the DSM columns.

4.2 PROCEDURE FOR DESIGN OF DSM COLUMNS

4.2.1 Theoretical Formulation

The design of DSM columns is based on the settlement prediction model for treated soils originally proposed by Rao et al. (1988). This model was used to predict the soil settlements that might occur in the DSM test section. The prediction of the settlement is based on the overburden pressures, thickness of soil layers, and the properties of soil in each layer. The equation used to predict the soil settlement is shown in the following:

$$\Delta h = \sum_{i=1}^{n} \frac{C_{s,i} h_i}{1 + e_{o,i}} \log \frac{p'_{i,i}}{p'_{p,i}} + \sum_{i=1}^{n} \frac{C_{c,i} h_i}{1 + e_{o,i}} \log \frac{p'_{f,i}}{p'_{p,i}} \qquad (4.1)$$

The settlement equation consists of two terms. When the overburden pressure is less than the pre-consolidation pressure, the first term of the equation is only used for the settlement prediction while the second term is disregarded. The second term is included as shown in the equation when the overburden pressure is greater than the pre-consolidation pressure. The $C_{s,i}$,

$C_{c,i}$, $e_{o,i}$, $p'_{f,i}$, $p'_{p,i}$, $p'_{i,i}$ and h_i are recompression index, consolidation index, initial void ratio, final effective stress (overburden ± any changes in total stress), preconsolidation stress, initial stress overburden, and thickness of each layer i, respectively (Figure 4.1).

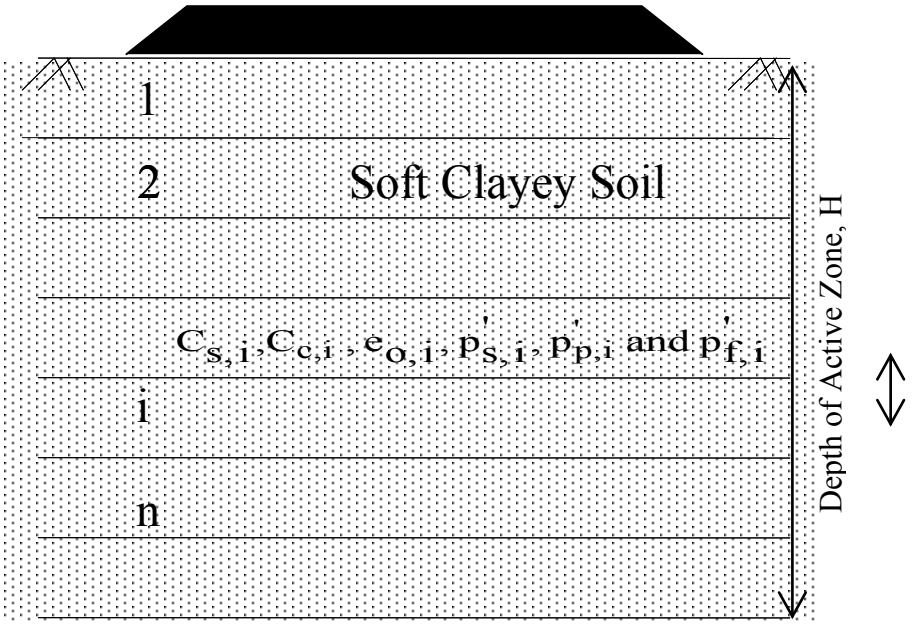

Figure 4.1. Schematic of Untreated Ground Depicting Layers for Settlement Prediction.

Most of the variable values, $C_{s,i}$, $C_{c,i}$, $e_{o,i}$, $p'_{p,i}$, are obtained from the 'constant volume' type Oedometer tests, which is discussed in Chapter 5. The final overburden stress, $p'_{f,i}$, is calculated accounting for the overburden stress as well as any net changes in total stresses from either traffic loading or surcharge loading as the weight of the embankment itself. It is assumed that the ground water level is far below the considered soil strata and will not affect the water content in the soil strata.

From Equation 4.1, the settlement in the DSM–soil composite section is predicted using the following equation.

$$\Delta h = \sum_{i=1}^{n} \frac{C_{r,i}^{comp} h_i}{1 + e_{o,i}^{comp}} \log \frac{p'_{i,i}}{p'_{p,i}} + \sum_{i=1}^{n} \frac{C_{c,i}^{comp} h_i}{1 + e_{o,i}^{comp}} \log \frac{p'_{f,i}}{p'_{p,i}} \qquad (4.2)$$

where the parameters $C_{r,i}^{comp}$, $C_{c,i}^{comp}$, and $e_{o,i}^{comp}$ are the composite properties of soil layer i in the treated ground (Figure 4.2). These parameters are estimated as shown below based on the treated and untreated soil properties determined from the laboratory studies.

$$C_{r,i}^{comp} = C_{r,i}^{col} \times a_r + C_{r,i}^{soil} \times (1 - a_r) \tag{4.3}$$

$$C_{rc,i}^{comp} = C_{r,i}^{col} \times a_r + C_{c,i}^{soil} \times (1 - a_r) \tag{4.4}$$

$$C_{c,i}^{comp} = C_{c,i}^{col} \times a_r + C_{c,i}^{soil} \times (1 - a_r) \tag{4.5}$$

$$e_{o,i}^{comp} = e_{o,i}^{col} \times a_r + e_{o,i}^{soil} \times (1 - a_r) \tag{4.6}$$

The symbols with 'soil' in the superscript indicate untreated soil properties and those with 'col' represent soil-cement column properties. The effect of the DSM treatment is taken into account for estimating the values of the composite parameters, which are then determined by estimating the weighted average of the treated and untreated soil properties as per their area ratio, α_r. The parameter α_r (area ratio) is defined as the ratio of the area of treated columns to the total area and used as the weighting factor.

Equation 4.2 is further simplified assuming that: (1) the initial void ratio ($\boldsymbol{e_{o,i}}$) and bulk unit weights for both the untreated and treated sections are the same and constant with the depth, and (2) the composite properties, C_i^{comp} is constant with depth. The settlement equation is typically used in three case scenarios per the magnitudes of the overburden and pre-consolidation pressures. These are presented in the following:

Case 1; When $p'_{f,i} \le p'^{soil}_{p,i} \le p'^{col}_{p,i}$

$$\Delta h_1 = \sum_{i=1}^{n} \frac{C_{r,i}^{comp} h_i}{1 + e_{o,i}} \log \frac{p'_{f,i}}{p'^{soil}_{i,i}} \tag{4.7}$$

Case 2; When $p'^{soil}_{p,i} \le p'_{f,i} \le p'^{col}_{p,i}$

$$\Delta h2 = \left\langle \sum_{i=1}^{n} \frac{C_{r,i}^{soil} h_i}{1 + e_{o,i}} \log \frac{p'^{soil}_{p,i}}{p'^{soil}_{i,i}} + \sum_{i=1}^{n} \frac{C_{c,i}^{soil} h_i}{1 + e_{o,i}} \log \frac{p'_{f,i}}{p'^{soil}_{p,i}} \right\rangle x(1 - a_r) +$$

$$(\sum_{i=1}^{n}\frac{C_{r,i}^{col}h_i}{1+e_{o,i}}\log\frac{p'_{f,i}}{p'^{col}_{i,i}})x(a_r) \qquad (4.8)$$

Case 3; When $p'^{soil}_{p,i} \le p'^{col}_{p,i} \le p'_{f,i}$

$$\Delta h_3 = \langle \sum_{i=1}^{n}\frac{C_{r,i}^{soil}h_i}{1+e_{o,i}}\log\frac{p'^{soil}_{p,i}}{p'^{soil}_{i,i}} + \sum_{i=1}^{n}\frac{C_{c,i}^{soil}h_i}{1+e_{o,i}}\log\frac{p'_{f,i}}{p'^{soil}_{p,i}} \rangle x(1-a_r) +$$

$$\langle \sum_{i=1}^{n}\frac{C_{r,i}^{col}h_i}{1+e_{o,i}}\log\frac{p'^{col}_{p,i}}{p'^{col}_{i,i}} + \sum_{i=1}^{n}\frac{C_{c,i}^{col}h_i}{1+e_{o,i}}\log\frac{p'_{f,i}}{p'^{col}_{p,i}} \rangle x(a_r) \qquad (4.9)$$

In the present design example of bridge embankment loading, the calculation for settlement happening in Cases 2 and 3 can be neglected since the overburden pressure due to a summation of traffic loading and embankment fill weight is not expected to be greater than the preconsolidation pressure of the underlying soil.

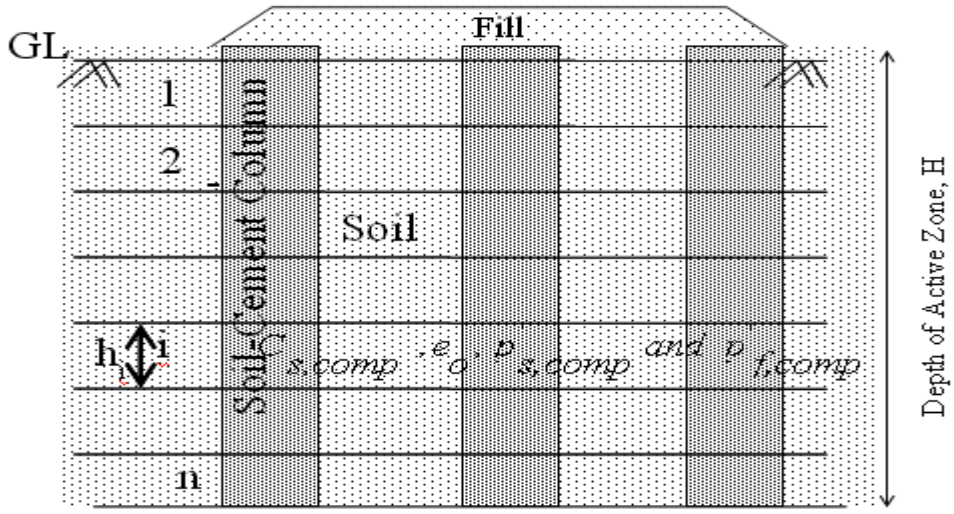

Figure 4.2. Schematic of Composite Ground Depicting Layers for Heave Prediction.

4.2.2 Design Steps

Based on the settlement prediction models in Equations 4.1 through 4.9, the design steps shown in the flow chart (Figure 4.4) are followed for determining the diameter, length, and

spacing of the DSM columns for mitigating the settlement distress caused from soft soil subgrades. The design steps involved are as follows:

1. Determine the compression index (C_c) and reconsolidation index (C_r), pre-consolidation pressure, initial overburden pressure, initial void ratio, and total unit weight of the untreated soil specimens retrieved from each soil layer at the site. Conduct consolidation tests on the soils from each layer per ASTM D2435-04 to estimate the compression indices and the preconsolidation pressures at the site.
2. Composite soil properties such as compression index, recompression index, preconsolidation pressure, initial void ratio, and bulk unit weight are determined as the weighted average of the individual properties of the soil layers from the surface to the maximum active depth.
3. Estimate the amount of settlement Δh_{unt} of the untreated ground by using Equation 4.1.
4. Establish the acceptable settlement, Δh_{tr}, for a given project. According to TxDOT bridge design, the permissible settlement for bridge approach slabs is 2.0 in. (50 mm). If the calculated settlement of the soil before treatment (estimated in Step 2) is less than the allowable settlements, then soil treatment is not needed. Otherwise, the next steps should be followed to design and establish the DSM treatments for the project site. Please note the costs incurred with the field treatments are inversely proportional to the magnitudes of the established permissible settlements; the lower the permissible settlement, the greater number of the DSM columns required. Consequently, the higher allowable settlements require lesser ground treatment costs. An acceptable settlement, Δh_{tr}, of 2 in. (50 mm) is needed in order to mitigate the bumps at the end of the bridge and provide a smoother ride.
5. Determine the properties for soil-cement columns by repeating the tests mentioned in Step 1 on soil specimens stabilized with different types and dosages of additives. In this research, only a cement additive is considered for soil treatments. The main objective of this step is to minimize the representative compression index values of the cement treated soil specimens. The criteria for selection of the binder and its dosage are to: 1) reduce the compressive index value of the treated soil (less than the same of untreated soil), and 2) increase the preconsolidation pressure of the treated soil when compared with the untreated soil.
6. Estimate the treated area ratio required for reducing the overall settlement of the treated soil to a permissible settlement value prescribed in Step 3. Based on the recompression and compression indices of the untreated soil measured in Step 1 and the permissible settlement

in Step 3, Figure 4.3 is used to estimate the area treatment ratio. This area treatment ratio is used in the following equations to estimate the column spacing. The figure presents various predicted settlement (which is equivalent to permissible settlement for the design exercise) versus area ratio plots for given recompression and compression index values. Equation 4.7 is used in the preparation of these figures. Please note that this equation for area ratio already accounts for composite consolidation properties of the treated and untreated soil. Binders and dosage rates that yield very low settlement consolidation characteristics (Step 3) are only considered here.

7. If the recompression and compression index of the untreated soil lies in between those used in the development of the design charts, then a linear interpolation method should be followed.
8. The diameter of the DSM column is either already known or pre-established based on the DSM rigs used by the DSM contractor in the field. If the diameter information is not known at the time of design, then the DSM columns can be designed for various diameter sizes. A DSM column size can be selected based on the overall costs of the DSM work for the project site. For example, a DSM contractor with a rig capable of making smaller diameter columns may charge a lesser amount for mobilization costs than a DSM provider with larger diameter rigs. Hence, the DSM column diameter is based on either locally available DSM rigs or other cost considerations.
9. The length of the DSM column is usually designed by considering the depth of the soft soil stratum. It is recommended that the bottom of the DSM columns be located on a hard, non-expansive stratum. The depth of soft soil stratum and elevations of each soil layer can be determined by bore logs taken on site.
10. Establish the configuration of the DSM columns in the field. In general, two configuration types—square and triangular— are used in practice. Figure 4.5 depicts the schematics of both configurations. Based on the area ratio, a_r derived in Step 5, and the diameter of the DSM columns, the optimum spacing of DSM columns can be determined by using either Figure 4.6 or Figure 4.7.
11. In the case of multi-shaft rigs, the treated area under the multiple shafts can be idealized as an equivalent circle and then the same spacing calculation can be followed per the above step.

12. Last, the final plans and section details shall be prepared using the above designed or established DSM column diameter, length, and spacing information. The spacing should be rounded to a lower bound value since this ensures that the overall design is more conservative; lower bound rounding of the spacing results in higher area ratios than determined from the design chart.

The plan and sectional views developed following the above design procedure for construction of a prototype test section are presented in the following section.

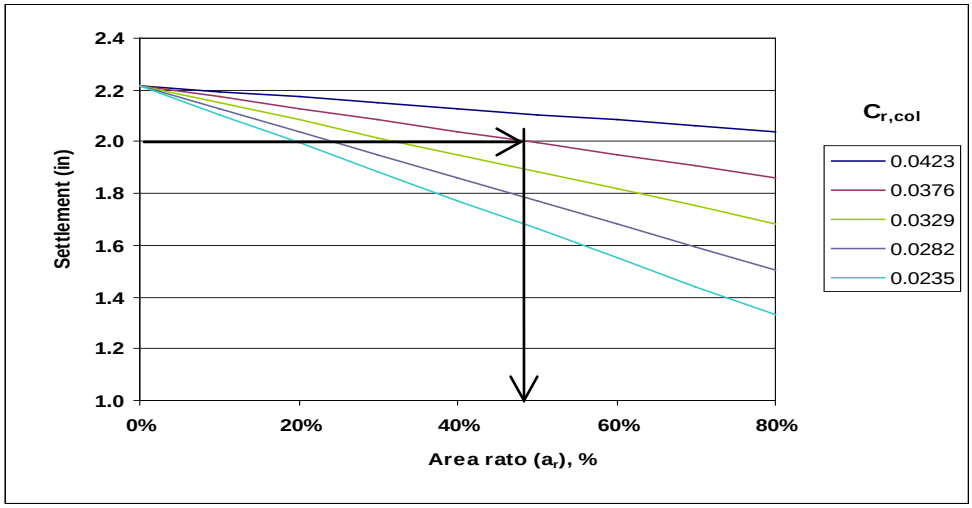

Figure 4.3. Design Charts for Estimating DSM Area Ratios for $C_{r,soil}$ 0.047 and $C_{r,coll}$ 50-90% of $C_{r,soil}$.

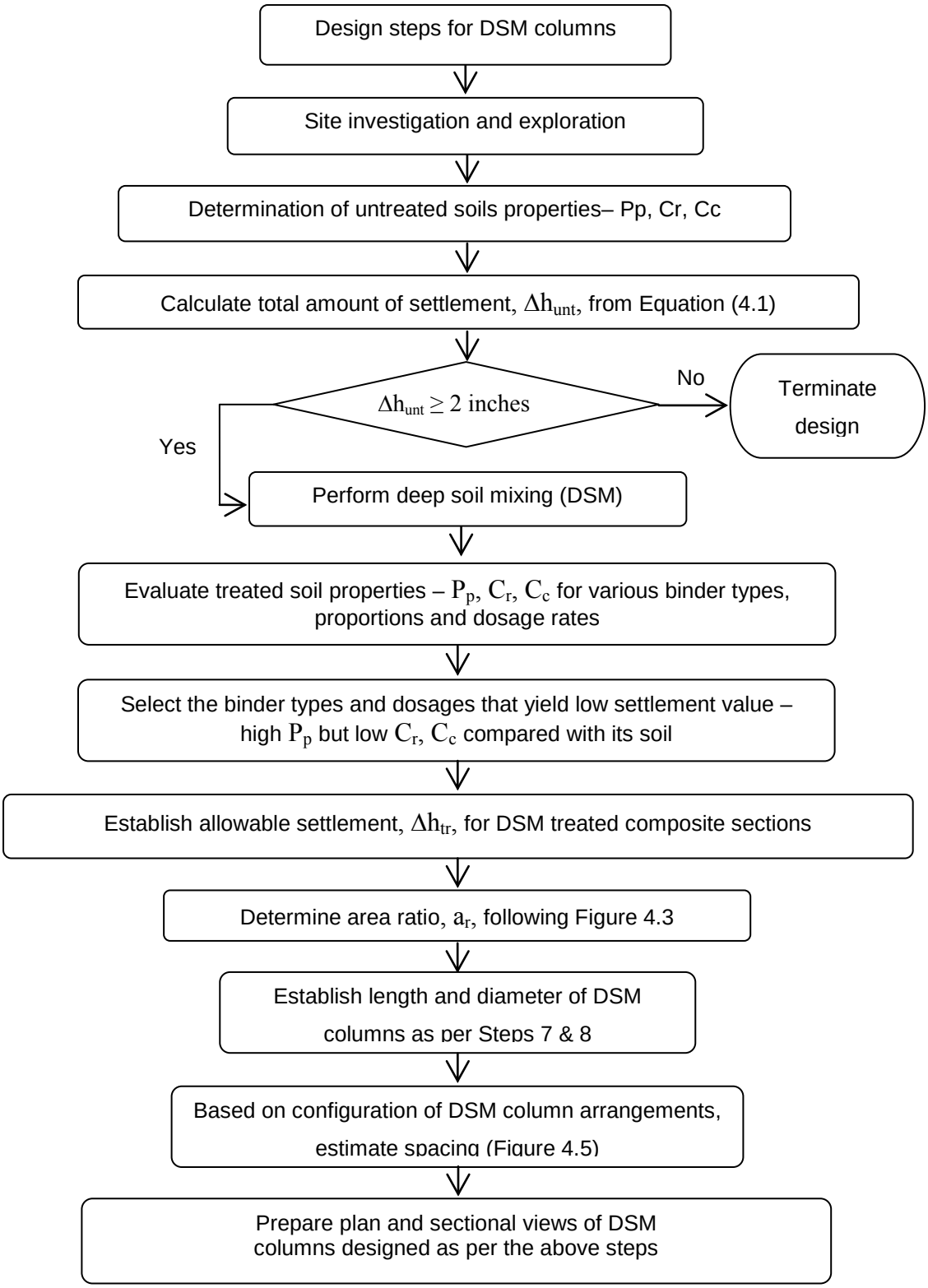

Figure 4.4. Design Flow Chart for DSM Treatment.

In the IH 30 project, a diameter of 4 ft (1.2 m) was used. Based on the survey results, there are three kinds of soil underlying the construction area. The top soil layer is clay with the thickness of 20 ft (6 m), the second layer beneath the clay stratum is sand with the thickness of 5 ft (1.5 m), and the last layer is hard shale. Therefore, according to the recommended criterion, the length of DSM columns was designed as 25 ft (7.5 m), and the bottom of the columns are resting on top of a hard shale layer.

4.2.3 Design Details of Materials for DSM Treated Test Sections

Below are the design details of the binder materials and water-binder ratio determined from the laboratory studies for construction of the DSM columns of IH 30 site.

1. Only cement is recommended for DSM construction.
2. A dosage rate of 160 kg/m^3 (10 pcf) is recommended.
3. A water-binder ratio of 4.0 or lower is recommended.

Based on these details, the total required quantities of binder and water for both test sections are estimated.

<u>SQUARE ARRANGEMENT:</u>

$$a_r = \frac{a_{col}}{a_{soil} + a_{col}}$$

$$= \frac{\text{area of column}}{\text{area of square}} = \frac{\left(\pi d_{col}^2 / 4\right)}{s_{c/c} \times s_{c/c}}$$

$$s_{c/c} = \sqrt{\frac{\pi}{4a_r}} d_{col} \qquad (4.10)$$

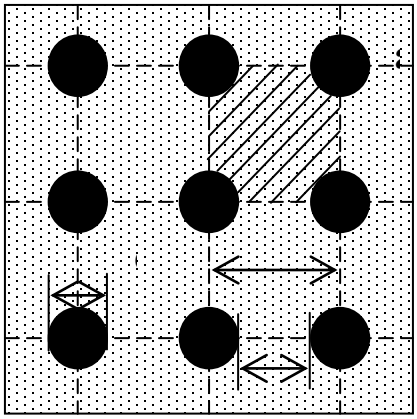

<u>TRIANGULAR ARRANGEMENT:</u>

$$a_r = \frac{1/2\, a_{col}}{a_{soil} + 1/2\, a_{col}}$$

$$= \frac{1/2 \text{ area of column}}{\text{area of equilateral } \Delta \text{le}}$$

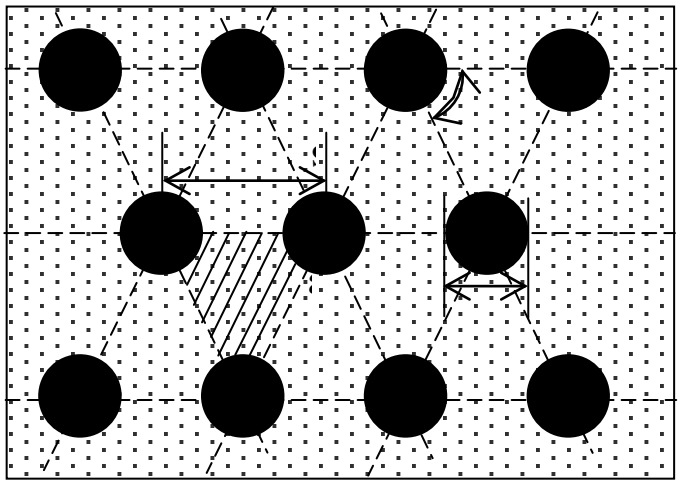

$$= \frac{\frac{1}{2}\left(\frac{\pi d_{col}^2}{4}\right)}{\frac{1}{2} \times s_{c/c} \times \frac{\sqrt{3}}{2} \times s_{c/c}}$$

$$s_{c/c} = \sqrt{\frac{\pi}{3.464 a_r}} d_{col} \qquad (4.11)$$

Figure 4.5. Configurations of DSM Columns and Corresponding Equations for Column Spacing.

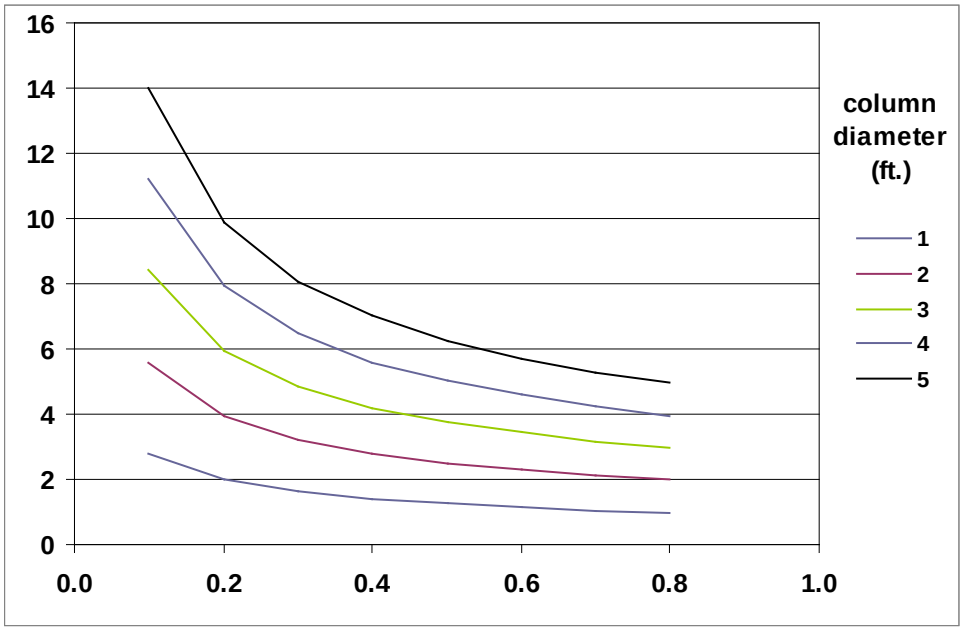

Figure 4.6. DSM Column Spacing Details for a Square Pattern.

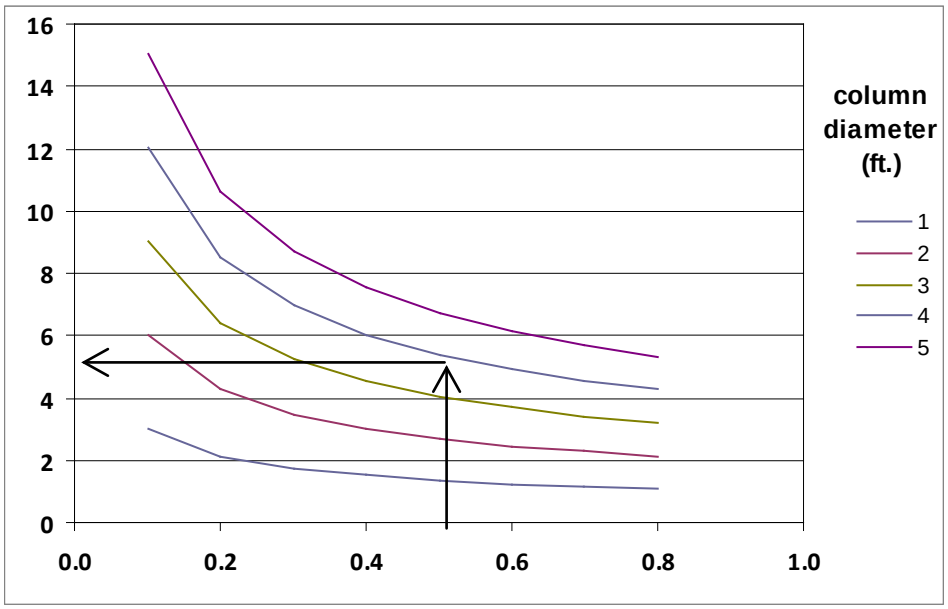

Figure 4.7 DSM Column Spacing Details for a Triangular Pattern.

4.2.3.1 Specifications of DSM Column Geometry and Arrangement

As shown in Figure 4.5, a triangular arrangement of the DSM columns is considered for the IH 30 site and for an area ratio of 0.50, the center-to-center distance of column spacing was 5.5 ft (1.65 m). The column dimensions, as aforementioned in Step 9, are 4 ft (1.20 m) in diameter and 25 ft (7.5 m) in length.

4.3 LIGHTWEIGHT FILL (LWF) EMBANKMENT DESIGN STEPS

Lightweight fill material has been used to control settlements of foundation layers for several years. Several materials, including EPS geofoam blocks, are being used with great success to mitigate settlements. Two issues related to the design and constructability should be addressed prior to using them in the field.

4.3.1 Design Issues

If the material used for the embankment is typically a native or modified material, then comprehensive material characterization studies are first needed. A few of these studies focus on shear strength properties, interface strength properties, and material compressibility properties. All these properties are needed when addressing the stability of a hypothetical embankment system with the lightweight fill material. Typical slope stability studies and also potential surface

erosion issues should be addressed. Also, the impacts of moisture saturation and contamination with petroleum hydrocarbons and their impact on strength and compressibility properties should also be measured and evaluated. If there are any issues due to the diffusion of chemicals, then protection measures are needed during the design phase.

4.3.2 Constructability Issues

In the case of certain lightweight aggregates, surficial slope stability issues should be checked. Also, the potential vegetation growth issues including the use of certain topsoils should be addressed. Use of specialized equipment, compaction methods, and quality control issues during construction should be identified when using a lightweight fill material. All these are addressed in the present research focusing on the expanded clay shale aggregates. Details of these are provided in the later chapters.

4.4 SUMMARY

This chapter presents the stepwise procedure developed for the design of the DSM columns for settlement control. These methods are followed to determine the column arrangement, size, and their spacings. Similarly, ECS design guidelines are closely followed for the construction of the ECS test sections. Construction details of these sections are presented in Chapter 6. The next chapter provides material characterization details.

CHAPTER 5

LABORATORY INVESTIGATIONS FOR NEW BRIDGES (DSM AND LWF)

5.1 INTRODUCTION

This chapter presents two laboratory investigations performed simultaneously which are presented in three sections: site selection and soil sampling, experimental test program, and discussion of laboratory results. The first section gives details of two actual construction sites used in this study. The second section describes the details of tests performed on the embankment fill and natural foundation soils. As discussed in the literature review, the factors responsible for the bump problem are not similar and vary from site to site. Therefore, the natural foundation soils and embankment materials from each site were tested to evaluate their compressibility properties.

Two methods, including deep soil mixing (DSM) and lightweight fills (LWF) methods, were the primary focus for the research investigations. A soil-binder mixture classified as the DSM treated soil was tested for its suitability as a foundation soil whereas an expanded clay shale (ECS) was used as the lightweight embankment fill material and it is characterized as an embankment material. In this chapter, the details of tests performed on the embankment fill and natural foundation soils along with the detailed test procedures that were followed, and the soil-binder mix design methods and specimen preparation procedures simulating the DSM technology are also provided. All the engineering tests performed were in compliance with the procedures outlined by TxDOT and the American Society of Testing Materials (ASTM) standards, whichever was applicable. The laboratory test results of the soils obtained from the test sites selected for this research are presented in the last section.

5.2 SITE SELECTION AND FIELD SOIL SAMPLING

Two new bridges in north Texas were chosen to study the selected mitigation techniques to control the approach slab settlements. The DSM treatment was used to improve the weak foundation soil underneath the embankment fills to connect to the new bridge crossing over IH 30 in North Arlington, Texas. The plan view of the site and the layout of the proposed DSM treatment zone are shown in Figure 5.1. The blue shaded area represents the weak soil zone

around the proposed bridge embankments. In this case, a 25 ft (7.5 m) height embankment was constructed on the DSM treated ground. The DSM treatment is shown in the hatched portion. Undisturbed and disturbed soil samples were collected from two soil borings along the center line of the bridge.

In another site in south Arlington, Texas, lightweight aggregate was used as a fill material to support an approach slab of a bridge along SH 360. In this site, the foundation soil was not treated with any stabilization methods. The layout of the bridge site of SH 360 is shown in Figure 5.2. Natural soil samples were collected from soil borings collected along the median of the proposed highways. The ECS aggregate material was obtained from a quarry 80 miles southeast of the project site and brought to the geotechnical laboratories at UT Arlington for analyses.

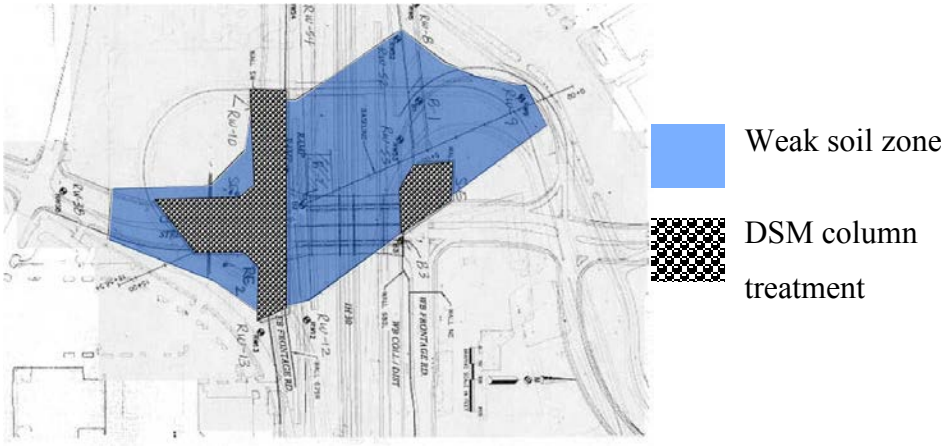

Figure 5.1. Details of Weak Soil and DSM Treatment, IH 30, Arlington, TX.

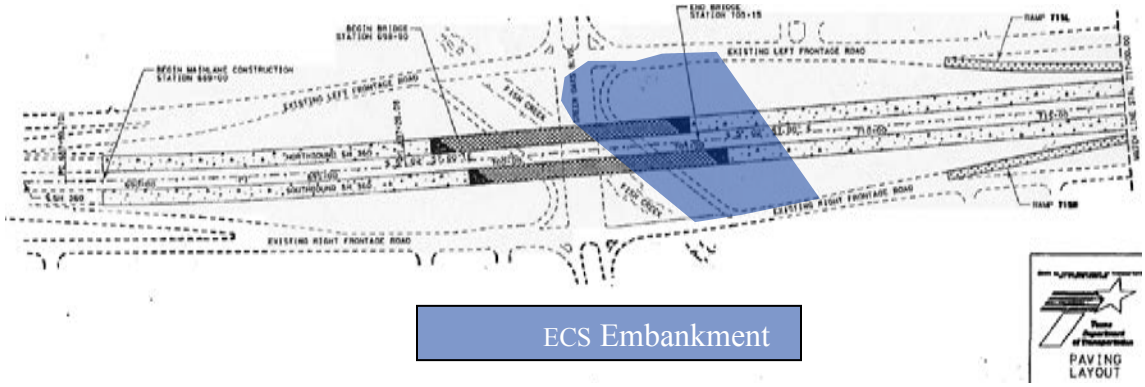

Figure 5.2. Details of ECS Bridge Site, SH 360, Arlington, TX.

For the IH 30 site, the DSM technique was employed to improve the weak subgrade foundation soil with a select fill placed on top to construct the embankments. Hence, properties of the embankment fill material, natural subgrade soil, and modified subgrade soil were determined. For the treated soil in the DSM columns, cement treated natural subgrade material with the same water-cement-soil content samples as constructed in the field were reproduced in a laboratory environment and subjected to geotechnical tests to determine their properties.

For the SH 360 site, the north bridge embankment was constructed with a select fill while the south embankment was constructed with ECS as the lightweight fill material. The engineering properties of the select and ECS embankment fill materials were investigated. The properties of both materials were needed for understanding the differences in the measured settlement magnitudes obtained at the bridge approaches on both ends of the bridges.

Another site in Houston (SH 6) was briefly studied as this site was constructed with geopiers to mitigate settlements. However, only minor details are included here as the geopiers were constructed a few years prior to the present research investigation.

To evaluate the physical and engineering properties of the representative soils, a series of laboratory tests were designed and conducted. To classify the soils, grain size analysis was carried out according to TxDOT Test Procedure Tex-110-E. The Atterberg Limit tests were performed according to Tex-104-E, Tex-105-E, and Tex-106-E. Compaction characteristics were determined in accordance with Tex-113-E. The test procedures stipulated in ASTM D-2435-96 were used to determine the compressibility characteristics of the soils. The linear shrinkage strain (Tex-107-E), free swell test (ASTM-D2166), and unconfined compression tests (ASTM-D2166) were also performed. The details of these tests are presented in the following sections.

5.3 EXPERIMENTAL PROGRAM

This section presents the details of the test procedures followed to conduct the index and engineering tests outlined in the previous section on the control soils. Table 5.1 summarizes the details of the experimental studies carried out on different samples.

Table 5.1. Summary of Tests Performed on Natural/Artificial Soils.

Test performed	SH 360, Arlington, TX		IH 30, Arlington, TX			
	Expanded Clay Shale (ECS)	Select Fill Embankment	Select Fill Embankment	Foundation Soil (Control Section, B2)	Foundation Soil (study section, B1)	Soil-Cement Moisture (DSM)
Grain Size Analysis	✔	✔	✔	✔	✔	
Atterberg Limit Test			✔	✔	✔	
Standard Compaction Test		✔	✔			
Linear Shrinkage Strains		✔	✔	✔	✔	✔
One-Dimensional Free Swell Tests		✔	✔	✔	✔	✔
One-Dimensional Consolidation Test	✔	✔	✔	✔	✔	✔
Direct Shear Test	✔					
Unconfined Compression Strength (UCS) Test		✔	✔	✔	✔	✔

5.3.1 Sample Preparation

The sample preparation used for determination of the Atterberg Limits was done according to the wet preparation portion described in the TxDOT Test Procedure Tex-101-E. In this procedure, the soil sample was first soaked in tap water for a period of 24 hours as shown in Figure 5.3a and then washed through a No. 10 sieve (2 mm). The portion of the sample passing the No. 10 sieve was again washed through a No. 200 (0.075 mm) sieve until at least 95% of the material passed through the sieve. The soil samples were transferred into a bowl with

a filter and allowed to dry until the water content was below the liquid limit. To enhance the process of drying, an electric fan was used as shown in Figure 5.3b.

5.3.2 Atterberg Limit Tests

Atterberg limit tests include the determination of the liquid limit (LL) and the plastic limit (PL) of a soil to determine the consistency properties of a soil. With the addition of water to a soil, the state of the soil changes from dry, then to a semisolid, to a plastic and finally to liquid state. The water content at the boundaries of these states are known as shrinkage (SL), plastic and liquid limits, respectively. The LL is a boundary having its water content at which the soil flows and the PL is determined as the water content at which the soil starts crumbling when rolled into a 1/8-in. (3.2 mm) diameter thread. The numerical difference between the LL and the PL value is known as the plasticity index (PI) as performed by TxDOT Test Procedure Tex-106-E and characterizes the plasticity nature of the soil.

(a) (b)

Figure 5.3. Sample Preparations by Wet Analysis for Soil Classification and Determination of Atterberg Limits (a) Soaking Stage and (b) Drying Stage.

Representative soil samples were prepared following the aforementioned procedure and are subjected to the Atterberg Limit tests to determine the LL and PL following TxDOT Test Procedures Tex-104-E and Tex-105-E, respectively. The water content of the samples during the tests was measured using the oven drying method.

5.3.3 Standard Proctor Compaction Test

To determine the compaction moisture content and dry unit weight relationships of the select fill used in the embankments, the standard Proctor compaction tests were performed to determine moisture content and dry unit weight relationships. These results were also used to prepare the specimens for unconfined compression strength tests and consolidation tests for the select fill specimens. Several samples of the same soil with different water contents were compacted in accordance with TxDOT Test Procedure Tex-114-E. After the wet density and actual water content of each compacted sample were measured, the dry density of the soil for each sample was calculated. The compaction curve was drawn by plotting the dry density and water content values of each soil sample. The optimum moisture content of the soil is the water content at which the soils are compacted to a maximum dry unit weight condition. Soils with a dense state exhibiting a high shear strength but low compressibility are best suited to support civil infrastructures such as roadway pavements.

According to TxDOT design guidelines, when the embankment is higher than 30 ft (9.0 m) the embankment fill is typically constructed at 98% of optimum moisture content of standard Proctor compaction condition. Following are the expressions for determining both wet unit weight and in-situ natural water content:

$$\text{Bulk unit weight, } \gamma_w \text{ (kg/m}^3 \text{ or pcf)} = \frac{W_b}{v} \tag{5.1}$$

$$\text{In situ natural water content, } w_n \text{ (\%)} = \frac{W_b - W_d}{W_d} \tag{5.2}$$

$$\text{Dry unit weight, } \gamma_d \text{ (kg/m}^3 \text{ or pcf)} = \frac{\gamma_w}{1 + w_n} \tag{5.3}$$

Where W_b = wet weight of soil

W_d = dry weight of soil

and v = volume of soil samples.

5.3.4 Determination of Linear Shrinkage Strains

As explained in TxDOT Test Procedure Tex-107-E, the soil specimens for the shrinkage test were mixed with sufficient water until the soil became a slurry at the LL state. The soil

slurry was then placed into a linear shrinkage mold of section dimensions, 5 in. long × 0.75 in. wide × 0.75 in. deep (127 mm long × 19 mm wide × 19 mm deep). The inner surfaces of the mold were greased sufficiently to reduce the friction between the specimen and inner surfaces upon subjecting the specimen to drying. Care was taken while placing the soil into the mold so that the entrapped air was removed. The surface was then leveled with the top of the mold using a spatula and the specimens were air dried at room temperature until a color change was observed. The mold was then transferred into an oven set at 230 ± 9°F (110±5°C) for 24 hours. The change in length was determined accurately using Vernier calipers and the linear shrinkage strain (Ls) was calculated in percentage as follows:

$$L_s = \frac{\Delta L}{L_0} \text{ x } 100\ \% \qquad (5.4)$$

where ΔL is the change in length, and L_0 is the original length of the specimen.

5.3.5 One-Dimensional Free Swell Tests

One-dimensional free swell strain tests were conducted in accordance with ASTM D-4546. Each soil specimen was kept in a conventional oedometer steel ring of size 2.5 in. (64 mm) in diameter and 1 in. (25 mm) in height. The inner face of the consolidation ring was lubricated to minimize the friction during free swell. Prior to the testing, the free swell specimens were kept in a humidity room for moisture equilibrium purposes. The samples were taken from the humidity room and weighed along with the oedometer ring prior to the testing. Porous stones and filter papers were placed on both the top and the bottom of the specimen to facilitate movement of water into the soil. The specimens were then transferred into a container and filled with water in order to soak the specimen under a no load condition. The amount of upward vertical movement (heave or swell) of the specimens was recorded at various time intervals by placing a dial gage on the top porous stone. Figure 5.4 shows a schematic sketch of the one-dimensional free swell test setup used in the study. The recording of readings was continued until no further movement was measured for at least one day. Soaked specimens were then carefully removed from the ring, weighed, oven dried, and weighed after drying in order to calculate the moisture content of the saturated specimen. The swelling of the expansive soil, measured as strain, is termed as the free swell index (FSI).

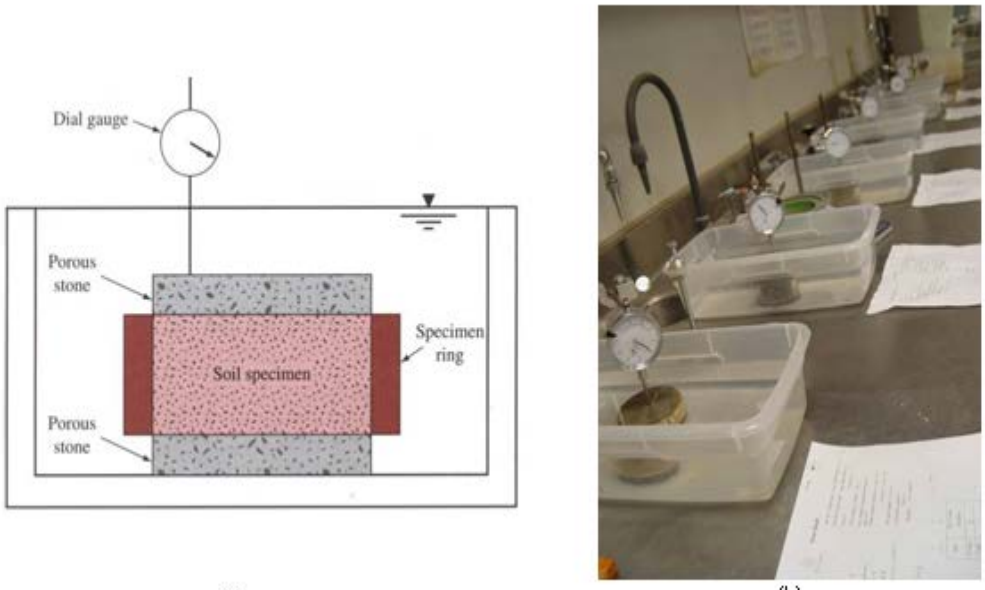

Figure 5.4. Free Swell Test (a) Schematic Sketch (Das, 2008) and (b) Test Setup.

5.3.6 Unconfined Compression Strength (UCS) Test

The UCS tests were performed on soil samples collected from different parts of the two sites to determine the strength properties of the soil samples. The unconfined compression test is a special form of a triaxial test in which the confining pressure is zero. The test can be conducted only on clayey soils that can withstand no lateral confinement. The test was performed per ASTM-D2166. In this test, a cylindrical specimen with dimensions of 1.3 in. (33 mm) in diameter and 2.8 in. (71 mm) in height was prepared. The specimen was first placed on a platform and then raised up until it came in contact with the top plate (Figure 5.5). Once the specimen reached this position, it was loaded at a constant strain rate of 2%, which is a typical value for testing clayey soils.

As the load approached the ultimate failure load, cracks began to appear on the surface of the specimen. Both deformation and corresponding axial loads on the specimen were recorded using a data acquisition system software and were used further to plot a stress-strain graph corresponding to the values of load and deformation. Stress is obtained by dividing the load by the cross sectional area of the sample whereas strain is obtained by dividing deformation by the original height of the specimen.

The data retrieved from the computer program contained load (Q) and deformation (δ), and the same was analyzed for maximum unconfined compressive strength (q_u) in psi or kPa. The following expressions show the computation of stress (σ) and strain (ε) corresponding to the load-deformation data.

$$\varepsilon = \delta/L \tag{5.5}$$

$$\sigma = Q/A_c \tag{5.6}$$

$$\text{and } q_u = \sigma_{max} \tag{5.7}$$

where δ = change in length, L = length of the specimen and A_c = corrected area of the cross-section of the specimen and is equal to A/(1- ε); A is the initial cross-sectional area.

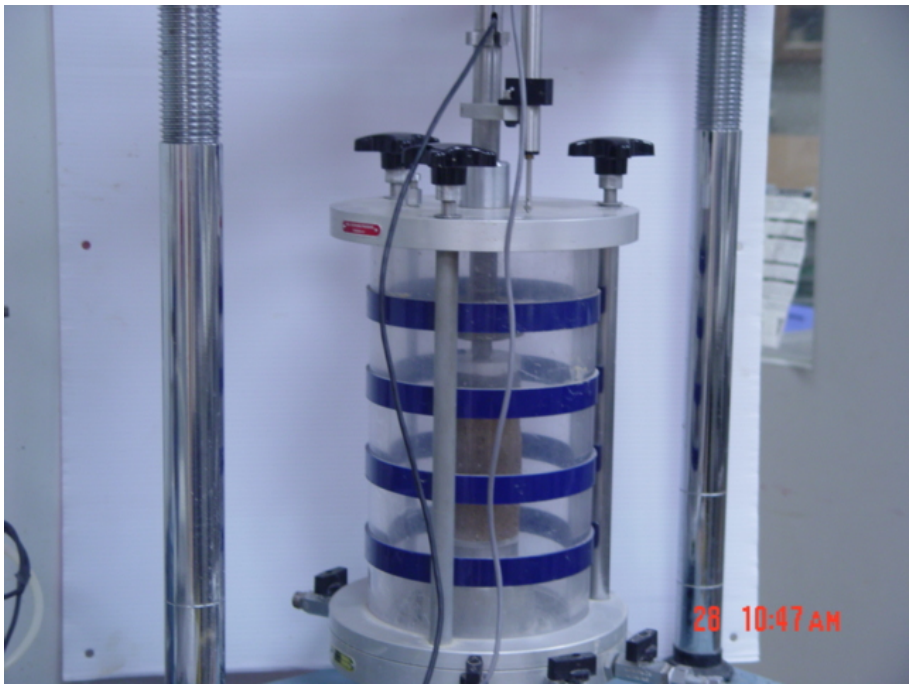

Figure 5.5 UCS Tests Performed in a Triaxial Test Setup.

5.3.7 One-Dimensional Consolidation Test

One-dimensional consolidation tests were performed in this study. The main objective of this test is to find the compressibility of saturated fine-grained soils, which is considered as a time-dependent phenomenon. In the tests, soil specimens were laterally restrained by a conventional oedometer steel ring of size 2.5 in. (64 mm) in diameter and 1 in. (25 mm) in height while axially loaded with total stress increments. Each load increments were maintained until excess pore water pressures were completely dissipated.

One-dimensional consolidation tests were conducted in accordance with ASTM D-2435-96. For the subgrade specimens, they were prepared at their natural in-situ densities obtained from the field using Shelby tube sampling methods while the soil embankment samples were prepared at a 98% of dry density from the standard compaction test in the laboratory. Porous stones and filter papers were placed on both the top and bottom of the specimen to facilitate water dissipation from the soil. Then, specimens were transferred into a container and filled with water in order to inundate the specimens. During the inundation period, normally 24 hours, the specimens were under a seating load of 100 psf (4800 kN/m^2) in order to be certain that the specimens became saturated with no swelling occurring prior to the loading. An automated consolidometer test setup (was used to perform this test). Figure 5.6 shows the consolidation test setup used in this research. The load increments were programmed and specimen deformations were automatically recorded by the test system until the end of the test. At the end, the specimens were then carefully removed from the ring, weighed, oven dried, and weighed after drying in order to calculate the moisture content of the saturated specimens. Then, the void ratios were calculated using the height of the solids method and plotted with the vertical stress to obtain the compression index of the specimens.

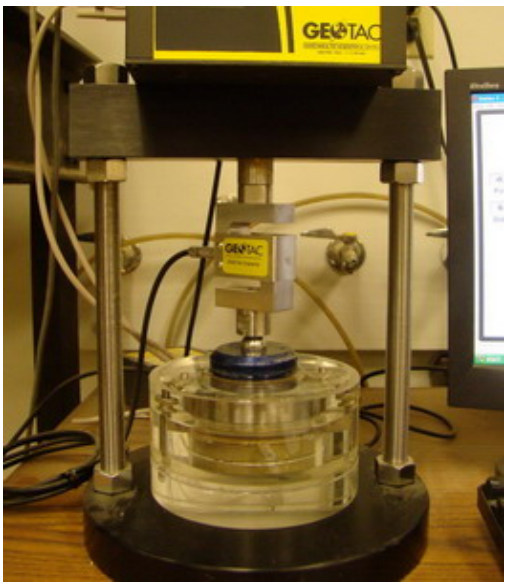

Figure 5.6. One-Dimensional Consolidation Test Setup.

5.3.8 Deep Soil Mixing Related Laboratory Studies

Deep soil mixing related studies were performed on soil samples collected from the IH 30 site. The binder used was a Type I Portland cement. The soil-cement binder mixes were prepared in the laboratory environment to simulate the mix designs that had been used in the field. These studies were carried out to understand the behavior of the weak foundation soil treated with DSM columns. The compressibility and strength properties of the soil-cement mixes were undertaken for this purpose. The following sections explain the procedures used to prepare the soil-binder mixes by quantifying the different material constituents of the matrix soil.

5.3.8.1 Preparation of Soil Samples

This section explains the steps involved in calculating the quantities of soil, cement, and water for the DSM columns followed by the test procedures used for preparing the natural soil and soil-cement specimens.

5.3.8.1.1 Soil Quantity

The in-situ soil properties, including bulk unit weight and water content, were estimated from samples obtained from the soil borings. The following expressions were used to determine the bulk unit weight and in-situ moisture content.

$$\text{Wet unit weight, } \gamma_b \text{ (kg/m}^3 \text{ or pcf)} = \frac{W_b}{v} \qquad (5.8)$$

$$\text{In-situ natural water content, } w_n \text{ (\%)} = \frac{W_b - W_d}{W_d} \qquad (5.9)$$

$$\text{Dry unit weight, } \gamma_d \text{ (kg/m}^3 \text{ or pcf)} = \frac{\gamma_b}{1 + w_n} \qquad (5.10)$$

where W_b,W_d, and v are wet weight, dry weight, and volume of soil samples, respectively.

The wet weights were obtained as soon as the samples were brought to the laboratory. The dry weights were obtained after placing the soil samples in an oven for 24 hrs. The weight of the dry soil mass required for preparing either an untreated or treated soil sample for one UCS, free swell specimen, or consolidation test are as follows.

Dry weight of soil for sample mix, $W_s = \gamma_d \times V \times N \times \eta$ (5.11)

where V is the volume of the specimen mold (shown in Table 5.2), N is the number of specimens and η is the extra mass to account for any loss of material during preparation, which can be in the range of 1.1 to 1.2.

Table 5.2. Details of Specimen Molds Used.

Mold	Dimensions, in. (cm)	Volume, in.^{3} (cm^3)
UCS	1.3 (3.30) × 2.8 (7.11)	3.65 (60.72)
Free Swell Strain and One-Dimensional Consolidation	2.5 (6.35) × 1 (2.54)	6.25 (80.44)
Linear Shrinkage Bar	4.0 (10.2) × 0.75(1.9) × 0.75 (1.9)	2.25 (36.82)

5.3.8.1.2 Cement Quantities

In the case of the DSM columns, the following are the expressions used for calculating the quantities of cement given the dosage or content in terms of lb/ft^3 (kg/m^3). The cement dosage (α in kg/m^3) is defined as the amount of the dry weight of the cement required for stabilizing 1 m^3 of in-situ soil, i.e., bulk volume. The amount of cement required to treat the soil quantity is as follows:

$$W_c = \alpha \times V \times N \times \eta \quad (5.12)$$

5.3.8.1.3 Water Quantity

The amount of water in the soil samples was calculated from the in-situ natural water content (w_n) for the untreated subgrade soil. For the embankment fill material, the water content in the soil samples was obtained from the compaction curve at 98% of maximum density from the standard Proctor tests.

Therefore, the weight of water for a sample mix is:

$$W_w = w_n \times \gamma_d \times V \times N \times \eta \quad (5.13)$$

In the case of the DSM columns, water must be added into the sample to create a slurry. The additional weight of water in accordance with the water-binder (w/b) ratio was calculated from:

$$\text{Weight of water from w/b ratio, } W_{w,\,slurry} = w/b \times W_b \quad (5.14)$$

This ratio typically varied from 0.8 to 1.3 in the study. Therefore:

Total amount of water for preparing soil-binder mix, $W_T = W_w + W_{w,\,slurry}$ (5.15)

5.3.8.2 Soil-Cement Mix Design - Example Calculations

This section explains the typical sample calculations carried out in the study to obtain the required amount of material for a soil-cement specimen for a consolidation test.

Previously measured in-situ bulk unit weight and moisture content values of the foundation soils were directly used in these calculations. The data obtained from the standard proctor tests were used to determine the molding water content, i.e., moisture content corresponds to 98% of maximum dry unit weight wherever necessitated.

A soil sample obtained from Sample Boring Number 1 was used in these calculations. The sample dimensions for the consolidation tests are 2.5 in. (6.35 cm) in diameter and 1 in. (2.54 cm) in height. The following shows the sample calculations:

Average in-situ bulk unit weight, γ_b:	112 pcf (1,800 kg/m^3)
Average in-situ water content, w_n (%):	19.59 %
Average dry unit weight, γ_d (from Eq. 5.3):	94.3 pcf (1,510 kg/m^3)
Dry weight of soil, W_s (from Eq. 5.11):	0.32lb (0.14517 kg)
Binder dosage, α or a_w:	9.99 pcf (160 kg/m^3)
Binder quantity, W_c (from Eq. 5.12)	0.028 lb (0.01287 kg)
Water-binder ratio (w/b):	1.0
Weight of water from w/b ratio for mixing, $W_{w,\,slurry}$ (using Eq. 5.14):	0.028 lb (0.01287 kg)
Weight of water from in-situ water content, W_w (from Eq. 5.13):	0.53lb (0.02420 kg)
Total water quantity for mixing (W_T) (from Eq. 5.15):	0.081lb (0.03707 kg)

Note: In these sample calculations, only one specimen is prepared from the soil-binder mix. In the estimation of the dry soil mass, an extra amount of soil (η) is kept aside to be added in case of any loss of material in the sample during the preparation process. In these calculations, the percentage of soil considered is 10% (i.e., $\eta = 1.1$).

5.4 DISCUSSION OF TEST RESULTS

5.4.1 Physical Properties of Subgrade Soils

5.4.1.1 Atterberg Limit Tests

Atterberg limit tests were performed on representative soil samples collected from each site. The soils were classified based on the Unified Soil Classification System (USCS), and the results for the soil samples collected from the IH 30 site are presented in Table 5.3.

From the results shown in Table 5.3, it is seen that all soil specimens obtained from Soil Boreholes 1 and 2 and the select fill are classified as low plasticity clays. The embankment was constructed using a local native soil and this fill material represents properties of a clayey soil.

Table 5.3. Physical Properties of Control Soils from the IH 30 Site.

Property	Test Designation		IH 30		
	TxDOT	ASTM	Bore Hole 1	Bore Hole 2	Select Fill
Liquid Limit (LL)	Tex-104-E	ASTM D4318	38	39	43
Plastic Limit (PL)	Tex-105-E	ASTM D4318	20	15	18
Plasticity Index (PI)	Tex-106-E	ASTM D4318	18	24	25
Specific gravity	Tex-108-E	ASTM D854	2.70	2.70	2.70
USCS classification	Tex-142-E	ASTM D2487	CL	CL	CL

The in-situ natural moisture content (w_n) and bulk unit weight (γ_b) for the subgrade soils from the IH 30 site were determined after the undisturbed specimens were brought from the construction site to the laboratory. The water content at Soil Boreholes 1 and 2 are 19.6% and

15.5%, respectively. The bulk unit weights of the representative samples are 115 pcf (1.85 g/cm^3) and 122 pcf (1.95 g/cm^3), respectively.

Figure 5.8 presents the grain size distribution curves for both the select and ECS fill materials. The normal fill or the control soil has a C_u = 18.9 and C_c = 0.61 along with a liquid limit = 29% and a plasticity index = 5. The select fill soil has been classified as silty sand (SM) according to the USCS. The ECS is a uniformly graded coarse grained material with little fines and has a coefficient of uniformity (C_u) = 2.8 and coefficient of curvature (C_c) = 2.6. ECS was classified with the letter symbol GP based on the USCS.

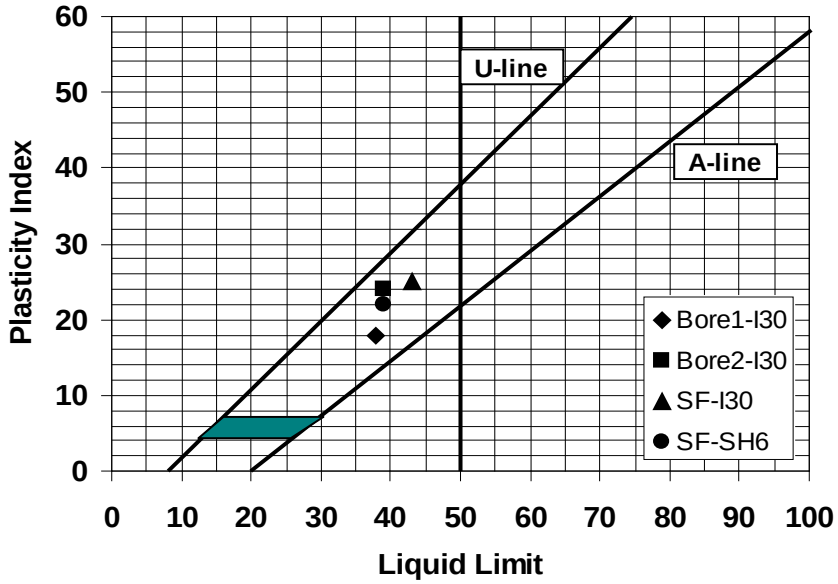

Figure 5.7. Casagrande's Plasticity Chart and Type of Soil Samples.

Compaction tests were performed to establish moisture-density relationships, especially for the select fill, of the embankment materials on both bridge sites. The optimum moisture content (OMC) of the soil is the water content at which the soil is compacted to a maximum dry density (MDD) condition. As shown in Figures 5.9 and 5.10, the select fill on the IH 30 site had a water content of 12% at the dry unit weight of 107 pcf (1.70 g/cm^3) while the select fill at the SH 360 site had a water content of 10.6% at the dry unit weight of 134 pcf (2.14 g/cm^3). These values of water content and dry density were used to further investigate the compressibility and strength properties of the select fill materials.

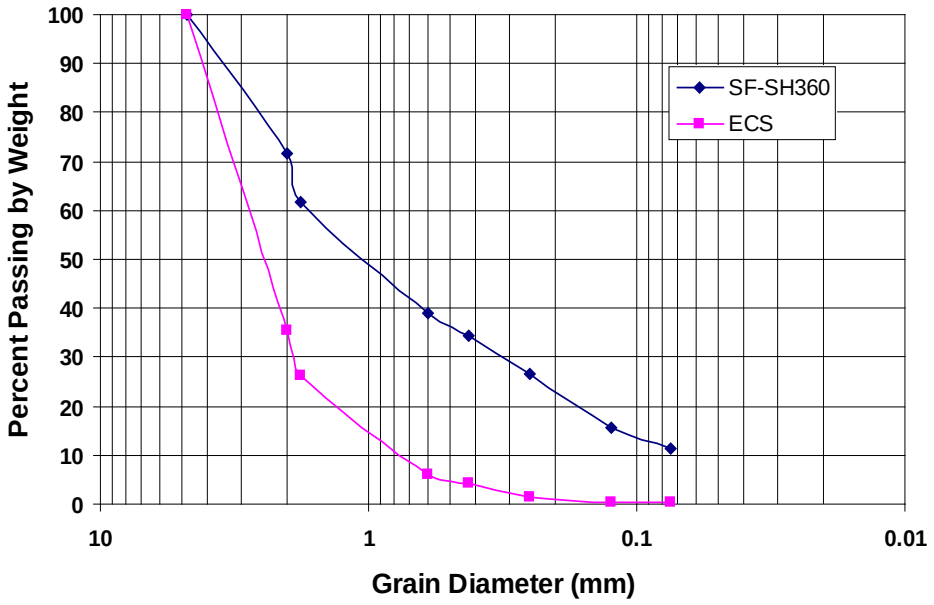

Figure 5.8. Grain Size Distribution Curves of Soil Samples from the SH 360 Site.

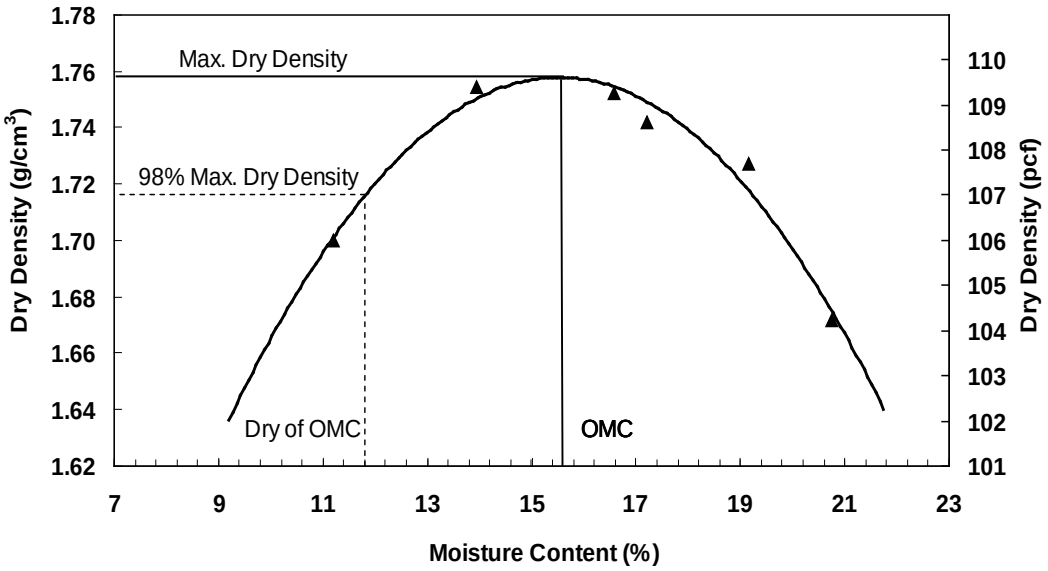

Figure 5.9. Standard Proctor Curve of the Select Fill from the IH 30 Site.

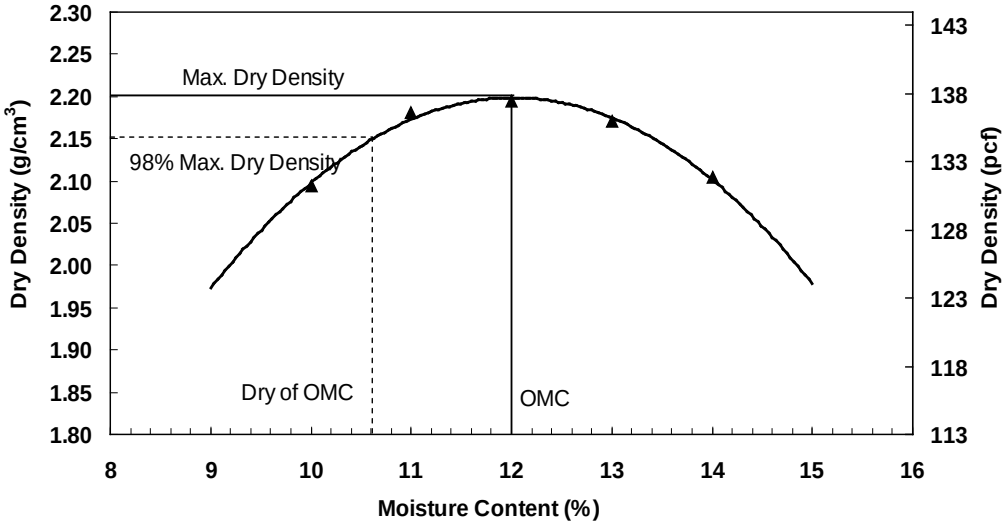

Figure 5.10. Standard Proctor Curve of the Select Fill from the SH 360 Site.

5.4.2 Engineering Properties of Soils

5.4.2.1 Swell and Shrink Properties

Swell properties are presented here to explain the swell potentials of fill material. This property is not related to settlements of the fills. Free swell (F_s) strains of the soil specimens from Boreholes 1 and 2 and the select fill from the IH 30 site are 4, 12, and 9%, respectively, while the swell strain value of the select fill from the SH 360 and SH 6 sites are 9 and 2.2%, respectively. The percent of free swell with time is reported in Figure 5.11 and these results indicate that the maximum swell was recorded in about 480 minutes under saturated conditions. The ECS and soil-cement samples showed low swell strain values. Contrary to the conventional hypothesis, the maximum swell strains recorded for the soil samples from Borehole 2 and the select fill from the IH 30 site are different although both soil specimens have the same PI value. Therefore, the swell properties do not correlate well with the PIs of the soils.

The shrinkage strains from the linear shrinkage bar tests (Tex-107-E) were performed on representative soil samples from the three bridge sites and the results are shown in Table 5.6. Opposite from the swell strain values, the shrinkage strain values are better correlated to the PI values of each soil. The soil samples from Borehole 1 (PI=18) from the IH 30 site has shrinkage strain values of 5.51 while the soil samples from Borehole 2 (PI=24) of the IH 30 site and select fill (PI=25) of the IH 30 site have shrinkage strain values of 11.81 and 14.76, respectively. The

same tendency is seen from the select fill soil from the SH 6 site of Houston has a PI = 22 and a linear shrinkage strain value of 12.67.

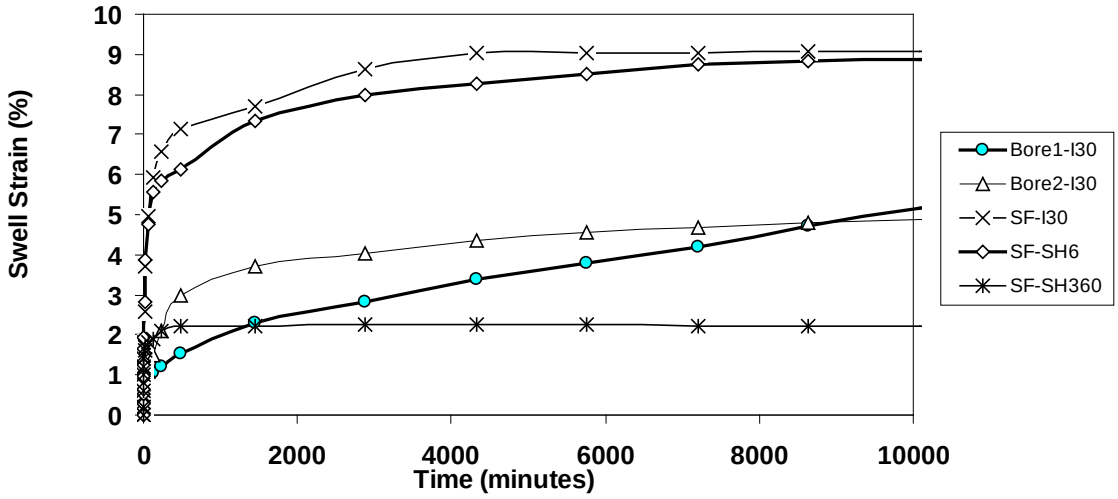

Figure 5.11. Free Swell Test Results from All Three Sites.

5.4.2.2 Compressibility Properties

After the one-dimensional free swell tests had been performed per ASTM D2435-96 and the void ratios had been obtained, the load increments and specimen deformations were plotted in a semi-log scale. The compression and recompression index of the soil specimens, C_c and C_r, respectively, were achieved by calculating the slope of the compression and recompression curves. The values of C_c and C_r of the soil specimens are shown in Table 5.4, and the consolidation curves are shown in Figures 5.12 and 5.13.

It is seen from Table 5.4 that the compression index of the subgrade soil from Borehole 1 has both compression (C_c) and recompression (C_r) indices more than the values from Borehole 2. However, both of the soil properties from Borehole 1 were improved after the soil had been modified with cement. From this treatment method, the C_c value decreased from 0.390 to 0.263 and the C_r value decreased from 0.046 to 0.035. Furthermore, the soil-cement mix also increased the pre-compression pressure (σ_r) of the specimens. From Figure 5.12, it is clearly seen that σ_r increased 3 times from 5,000 psf (240 kPa) to 15,000 psf (720 kPa) than the untreated soil. It leads to a conclusion that if the same amount of load acting upon the soil-cement and untreated soil is used, the soil-cement will have a lesser amount of settlement than a natural soil due to lower C_c and higher σ_r values. As shown in Table 5.4, the select fill specimens from the three sites

have low C_c and C_r values due to the reason that the soil was compacted to reach 98% of its highest density. For a granular material like ECS, both C_c and C_r values of this material are very low as expected.

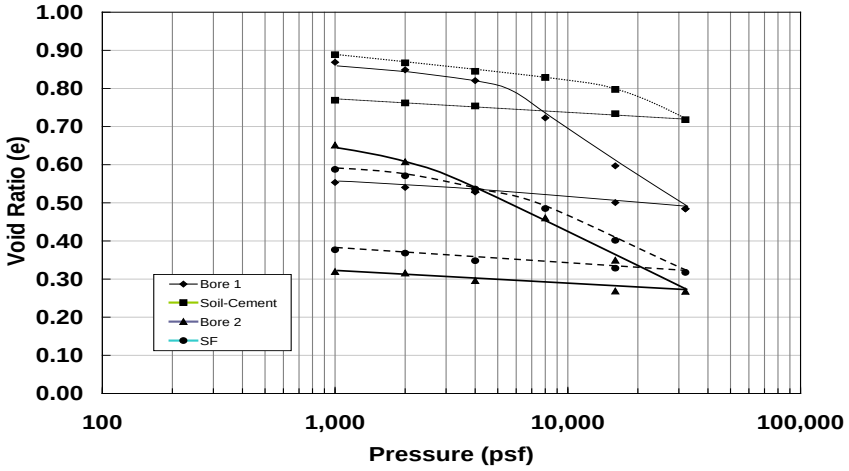

Figure 5.12. Consolidation Curves of the Soil Specimens from the IH 30 Site.

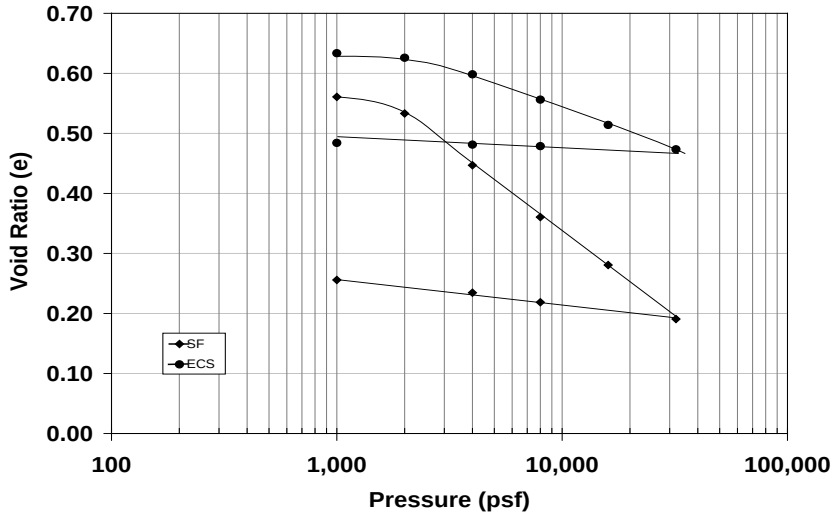

Figure 5.13. Consolidation Curves of the Local and ECS Soil Specimens from the SH 360 Site.

5.4.2.3 Strength and Stiffness Properties

The strength of the cohesive soils from the three sites was evaluated through unconfined compression strength (UCS) tests. These tests were performed in accordance with the procedure explained in Section 5.3.6. The unconfined compressive strength (q_u) is estimated from Equations (5.6) and (5.7) and the stress-strain curve shown in Figure 5.14. The average values of q_u are also shown in Table 5.6. The UCS values of the soil specimens from the IH 30

site, for Borehole 1 is 1.02 tsf (97.86 kPa) (range from 0.87 to 1.18 tsf [83.31 to 113 kPa]), for Borehole 2 is 0.80 tsf (76.61 kPa) (range from 0.63 to 0.96 tsf [60.33 to 91.13 kPa]), for the select fill is 1.02 tsf (97.68 kPa) (range from 1.43 to 1.64 tsf [136.94 to 157.05 kPa]), and for the soil-cement sample is 7.04 tsf (674.15 kPa) (range from 8.2 to 8.8 tsf [785.24 to 842.69 kPa]). The UCS values of the select fill specimens from the SH 360 site are 2.47 tsf (236.53 kPa) (range from 2.1 to 2.67 tsf [201.1 to 255.68 kPa]).

It is seen that ground improvement either by chemical or mechanical method can increase the unconfined compressive strength values. The untreated subgrade soils have a low value of unconfined compressive strength while the soil-cement specimen has a strength value of 7.04 tsf (674.15 kPa), which is almost 7 times higher than the strength value of the untreated soil.

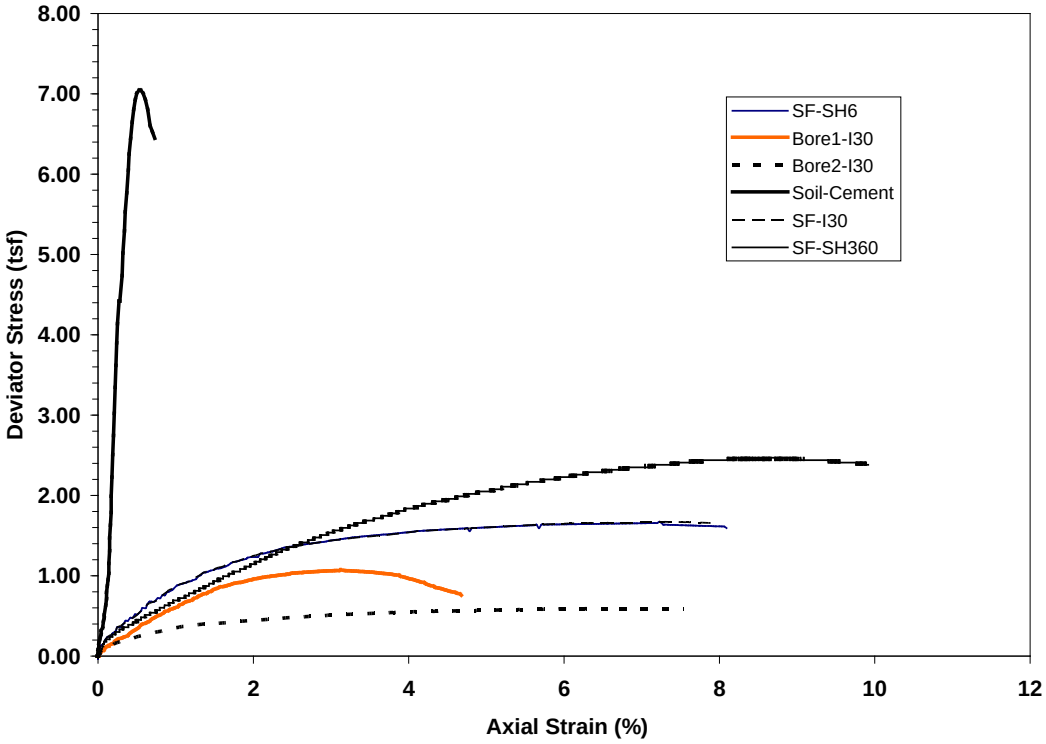

Figure 5.14. Stress-Strain Curves of the Soil Specimens from the UCS Tests.

Table 5.4. Engineering Properties of Soil Specimens from the IH 30 and SH 360 Sites.

Property	IH 30				SH 360	
	B1 (Treated Section)	B1 Soil-Cement	B2 (Control Section)	SF	ECS	SF
Swell Index (%)	13	2	4	9	0	2.2
Linear shrinkage strain (%)	5.51	1.57	11.81	14.76	n.a.	n.a.
Compression Index (C_c)	0.392	0.263	0.307	0.265	0.141	0.280
Recompression Index (C_r)	0.046	0.035	0.037	0.047	0.012	0.039
Unconfined Compressive Strength (tsf)	1.02	7.04	0.80	1.67	n.a.	2.47
c	n.a.	n.a.	n.a.	n.a.	74.5	n.a.
Φ	n.a.	n.a.	n.a.	n.a.	49	n.a.

Note: B1 – Borehole at treated section; B2 – Borehole at Control Section; SF – Select Fill Used; ECS – Expanded Clay Shale; n.a – not available

5.5 SUMMARY

This chapter presents a series of laboratory tests that were conducted on the natural, treated, and select fill materials obtained from two different bridge sites to evaluate their compressibility and strength characteristics. Limited physical soil information was only reported for soil sampled from another site, SH 6 of Houston where geopiers were used. For the natural soils, all soil samples obtained were classified as low plastic clays. Only the select fill used on the north side of the SH 360 site was classified as sandy silt (SM). The compressibility characteristics of the materials tested are found to be within permissible limits with the lowest value obtained for the ECS material used at the SH 360 site. Furthermore, the natural soil properties were improved using soil-cement treatment (DSM). The soil-cement treatment improved not only the compressibility characteristics of the foundation soils but also the strength

of the material. The results obtained from the laboratory work shown in this chapter are needed for the design of mitigation techniques and performance validation studies of the numerical analysis that are discussed in the following chapters.

CHAPTER 6

CONSTRUCTION AND INSTRUMENTATION OF TEST SECTIONS FOR NEW BRIDGES

6.1 INTRODUCTION

As discussed in Chapter 3, this research selected two methods as possible viable techniques to mitigate the settlements under the bridge approaches. The first technique focused on the DSM treated columns for improvement of cohesive soils underneath the highways pavement structures while the other technique focused on the use of ECS as a lightweight fill material for embankment fill to reduce the dead loads exerted on the fill and soft subgrade materials. To evaluate the application of these two techniques in real field conditions, DSM and ECS test sections supporting different approach slabs were constructed, instrumented, and monitored. In addition to the tests on the treated test sections, control section on untreated soils were also constructed and monitored at each site. Instruments used in the monitoring include horizontal inclinometers, vertical inclinometers, Sondex, and rod extensometers to monitor the settlements that were expected to transpire in the field. This chapter presents details of the field construction and monitoring of both methods in the field.

6.2 SITES DESCRIPTIONS

6.2.1 DSM Columns, IH 30, Arlington, Texas

As noted in Chapter 4, a new bridge was constructed on IH 30 in Arlington, Texas, on a soil strata stabilized with DSM columns to improve the weak foundation soils. Soil-cement columns of 4.0 ft (1.2 m) in diameter with a spacing of 5.5 ft (1.7 m) center-to-center spacing were constructed and the layout of the DSM treatment is shown as the dotted area in Figure 6.1. The blue shaded zone represents the weak soil zone in the bridge embankment area.

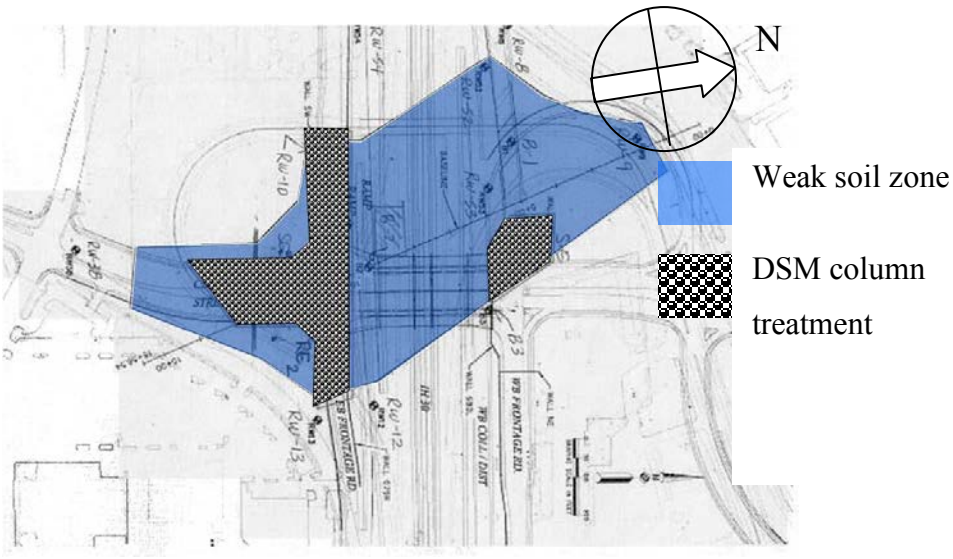

Figure 6.1. Details of the Weak Soil and DSM Treatment Areas, IH 30, Arlington, TX.

6.2.2 ECS Backfill Material, SH 360, Arlington, Texas

ECS was used as an embankment material for the approaches on the south end of two new bridge structures constructed as an extension of SH 360 (See Figure 6.2). The total quantity of the ECS used in this project was 26,242 yd^3 (20202 m^3). This site was used in this study as an example of a lightweight fill treatment for new bridge approach construction.

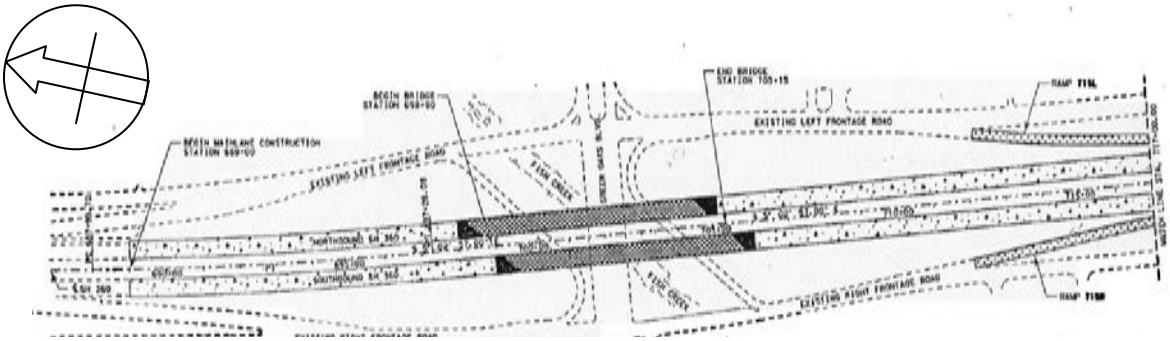

Figure 6.2. Details of ECS Bridge Site, SH 360, Arlington, TX.

6.2.3 Geopier, SH 6 over US 90A, Houston, Texas

The use of geopier columns is another mitigation method that was used to support the MSE walls and embankments of the SH 6 bridge constructed over US 90A in Houston, Texas. The geopier columns have a diameter of 30 in. (75 cm) and their lengths varied from 12 to 25 ft (3.5 to 7.5 m). Two locations of the geopier use, northbound entrance ramp and southbound exit

ramp, are shown in Figure 6.3. This site was not a major focus of this research as it was constructed and monitored a few years earlier than the initiation of this research project. Hence, no major conclusions are reported with respect to this technology and observations related to approach settlements are only mentioned in this report.

Figure 6.3. Details of Geopier Bridge Site, SH 6 and US 90A, Houston, TX.

The following sections provide detailed descriptions of both DSM and ECS fill materials used at the IH 30 and SH 360 sites, respectively.

6.3 DESIGN SPECIFICATIONS OF MATERIALS AND GEOMETRY DETAILS FOR DSM TREATED TEST SECTIONS

The following provides the specifications of materials used in construction of the DSM columns. The plan and sectional views showing geometrical specifications are also presented in the following sections.

6.3.1 Details of Binder Materials

The following describes the details of the materials used including the binder and water used for the construction of the DSM columns in the field:

1. Binder was composed of 100% Type I/II Portland cement.
2. Binder dosage rate of 10 pcf (160 kg/m^3) was used.
3. Water-binder, w/b, ratio of 4:1 was recommended for the field grout.

6.3.2 Specifications of Geogrid

Table 6.1 describes the specification details of the geogrid used during the construction of the DSM test sections. This was placed on top of the columns to support the upper layers of the pavement structure.

Table 6.1. Details the Geogrid.

Type	Biaxial Geogrid
Tensile Strength	1400 lb/ft (20 kN/m) (both in machine and cross-machine directions)
Material	Polypropylene

6.3.3 Specifications of DSM Column Geometry and Arrangement

According to the design of the DSM columns in Chapter 4, the DSM columns were constructed per a triangular arrangement with a center-to-center column spacing of 5.5 ft (1.65 m) and an area ratio (a_r) of 50%. The column dimensions were 4 ft (1.2 m) in diameter and 25 ft (7.5 m) in length or until the tip of the columns were seated on a hard shale layer. The sectional and plan views of the DSM treated sections are depicted in Figure 6.4. The perspective plan view of the DSM construction is shown in Figure 6.5.

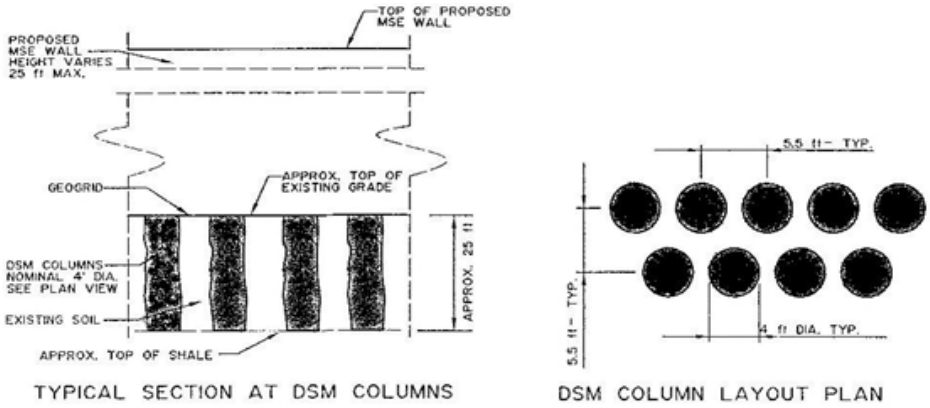

Figure 6.4. Sectional Details of the DSM Columns at the IH 30 Site.

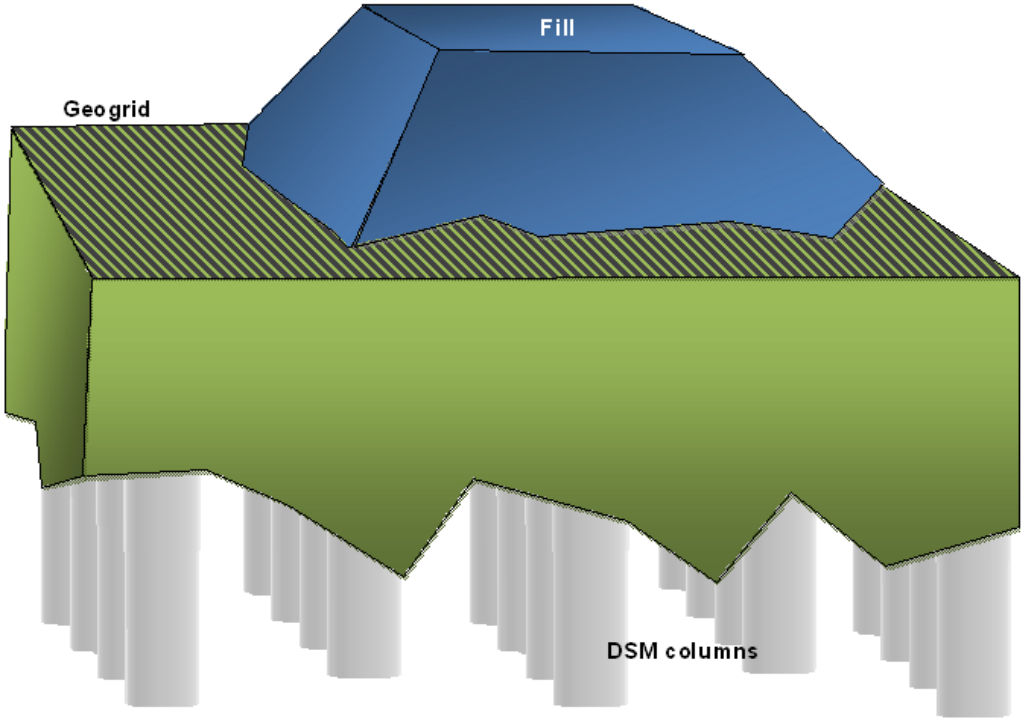

Figure 6.5. A Typical Perspective View of the DSM Treated-Geogrid-Reinforced Test Section.

6.4 CONSTRUCTION OF THE DSM COLUMNS

The construction procedure of the DSM column installation according to the DSM Work Plan Report (RECON, 2007) is presented in the following steps.

1. Following the design recommendation, a survey was done to establish the proper position of the DSM elements. In this step, the center points of each DSM column was surveyed and staked.
2. Before starting construction of the DSM columns, a hydraulic auger mounted on an excavator was used to remove soil from the ground surface at each of the DSM columns to create space to accommodate the soil-cement spoil collection.
3. After the pre-augering, the auger was positioned over each DSM column center mark and then a 4 ft (71 mm) diameter hole was bored to the required depth 25 ft (7.62 m) or until reaching the shale strata).
4. The cement binder slurry was prepared in a large mixing tank at the project site. The quantity of water was measured with a flow meter while the cement was measured

with a flow scale. A colloidal mixer was used to produce the grout. The cement and water was circulated and agitated. The finished grout was pumped to a holding tank.

5. During the DSM operation, the grout was pumped with high-pressure-progressive cavity pumps having a capacity of 100 gpm at a pressure of 100 psi. The grout was pumped from the holding tank through a hose to a grout swivel on top of the mixing tool shaft. The swivel allows the grout to flow through the shaft and exit through ports on the mixing tool while the tool is rotating. The grout flow rate was monitored at the pump with a flow meter and was regulated by bypassing a portion of the grout flow to the holding tank.
6. The hydraulic drill was mounted on a track crawler to systematically advance, rotate, and withdraw the 4 ft (71 mm) diameter mixing tools. Grout was injected through the bottom of the mixing tool during the initial penetration of the augers through the entire depth of each column and during removal.
7. The soil-cement element mixing was continued at adequate speed to mix soft and unmixed soil prior to final withdrawal of the mixing tool.

6.5 CONSTRUCTION OF THE ECS EMBANKMENT SECTIONS

The lightweight aggregate fill used in this study is termed as expanded clay shale or ECS. This material was used to construct the embankment fill for the new bridges on SH 360 in Arlington, Texas. The ECS was delivered to the project site in trucks identical to those used to haul natural fill materials. It was spread uniformly by tracked vehicles in layers not exceed 12 in. (305 mm) thick. Each layer was compacted using vibratory compaction equipment with 10 tons (20,000 lb) static weight. A minimum of three passes was required to ensure full compaction of this granular material. Although not used on this project, the best quality control method is to measure the settlement of the compacted layer to not be more than 10% of the layer thickness or 1.2 in. (30.5 mm). A total quantity of 26,242 yd^3 (20063 m^3) was used in the construction of the ECS embankment.

6.6 CONSTRUCTION OF THE GEOPIERS

The geopier system was used to support MSE walls and embankments of the SH 6 bridge constructed over US 90A in Houston, Texas, as shown in Figure 6.3. The research team was not involved during the design and construction of this site, which was done several years before the initiation of the present research; however, permission was granted to investigate the efficiency of the geopier system in providing sufficient support for the overlying approach slab structure.

In order to construct a geopier column, the weak subsurface soils are augered to create a borehole of 30 in. (762 mm) in diameter. Selected aggregate is poured into the borehole and then rammed from above with a beveled tamper to lift thicknesses, normally about 1 ft (305 mm). Successive layers of aggregate filling are performed until the element reaches its required height. The procedures to construct the geopier are shown in Figure 6.6. The ramming action causes the aggregate to compact vertically as well as to push laterally against the matrix soil. Consequently, very dense, high stiffness aggregate piers are formed resulting in a significantly increased composite stiffness of soil within the geopier-reinforced zone. In this project, geopiers were constructed using open-graded stone to afford radial drainage of the water in the soil to the piers. The geopiers act as vertical drains to allow radial drainage of excess pore pressure in the soil to increase the time rate of settlement.

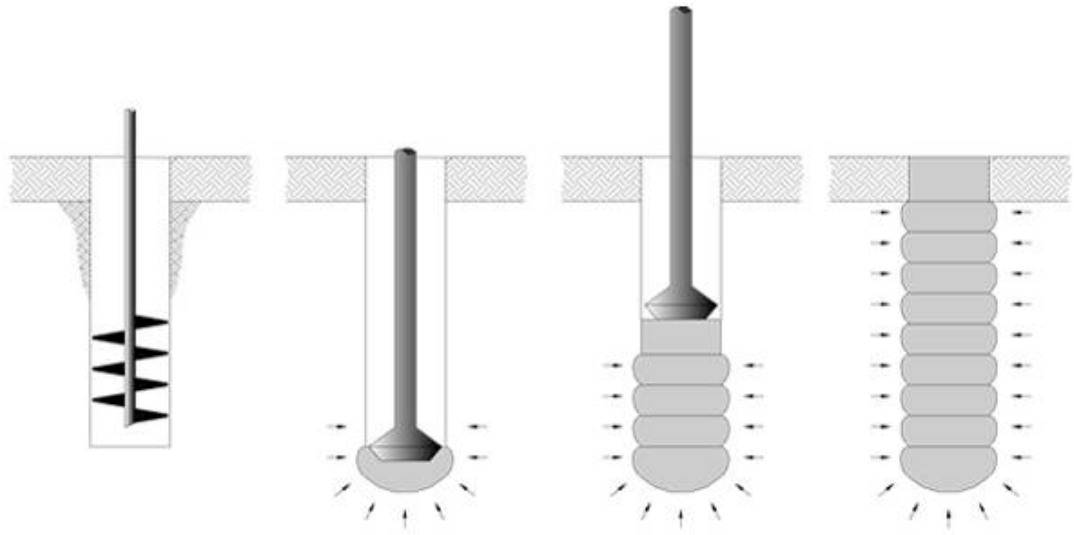

Figure 6.6. Rammed Aggregate Pier Construction Process.
(Source: http://sentezinsaat.com.tr/en/geopier-system.html)

6.7 INSTRUMENTATION DETAILS

In evaluating the field performance of the mitigation techniques in preventing the settlement problem, instrumentation plays an important role in collecting field data and understanding the performance of the structure with time. In this study, different types of instrumentation were installed in all three sites to observe the performance of the settlement mitigation techniques.

The performance evaluation of the mitigation techniques is achieved through regular data collection and analysis related to surface and underlying soil movements with time both in the vertical and horizontal directions. The instrumentation data collected at the IH 30 DSM site are shown in Figure 6.7 and this includes horizontal inclinometer, vertical inclinometer, rod extensometer, and Sondex. At the SH 360 ECS site, vertical inclinometers were installed as shown in Figure 6.8. For the SH 6 geopier site, the locations of previously installed Sondex systems and vertical inclinometers were used and the locations of the instrumentation are shown in Figure 6.9. Data collections were performed regularly (once every two weeks) at the IH 30 and SH 360 sites and once a year at the SH 6 site in Houston. The subsequent sections present the details of the instrumentation used and the installation procedures that were followed.

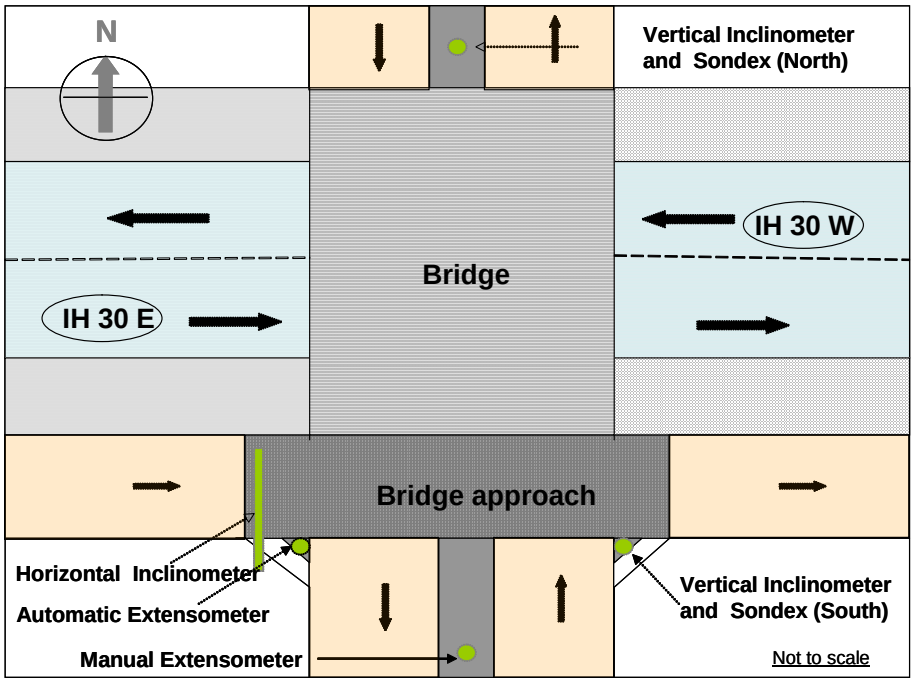

Figure 6.7. Instrumentation Details on the IH 30 Site, Arlington, Texas.

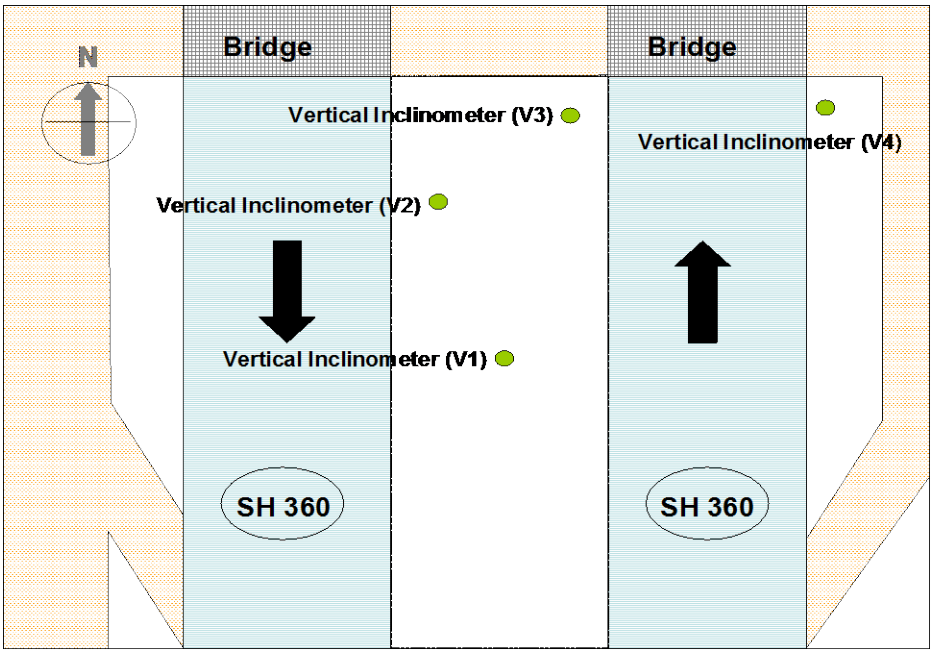

Figure 6.8. Instrumentation Details on the SH 360 Site, Arlington, Texas.

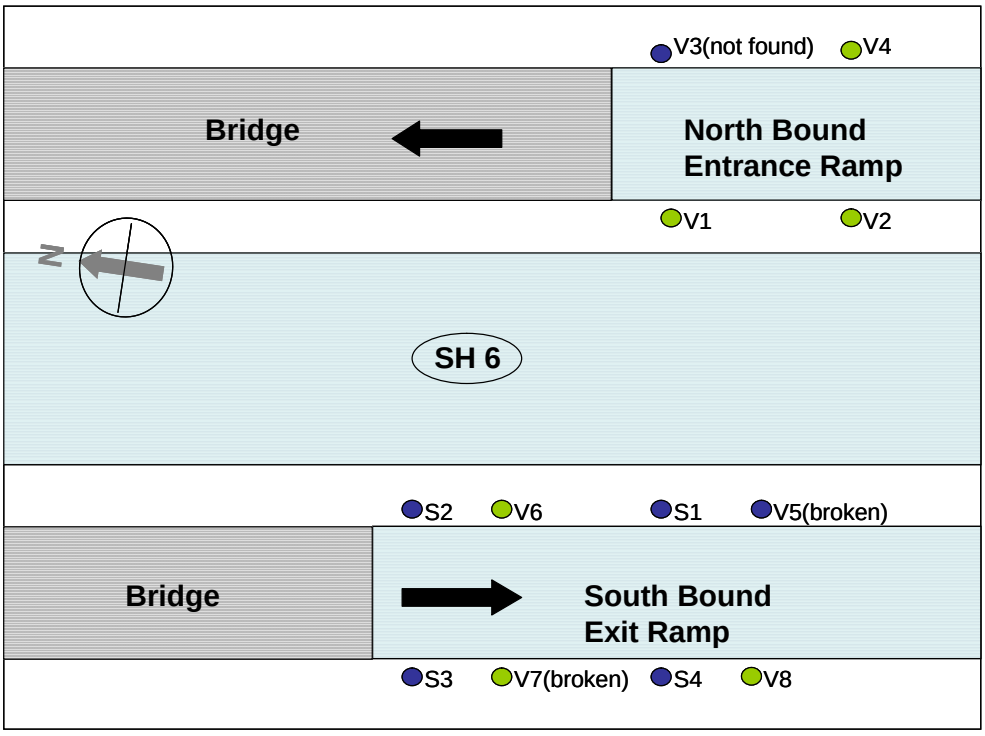

Figure 6.9. Instrumentation Details on the SH 6 Site, Houston, Texas.

6.7.1 Inclinometers

Inclinometers are defined as devices used for monitoring surface and subsurface deformations in a perpendicular direction to the axis of a flexible plastic casing by means of a probe passing through the casing (EM 1110-2-1908 – US Army Corps). The inclinometer casing is an ABS (acrylonitrile-butadiene-styrene) plastic pipe having four groves perpendicular with each other inside the casing as shown in Figure 6.10. The casings are available in various diameters: 1.9 in. (4.8 cm), 2.75 in. (7.0 cm), and 3.34 in. (8.5 cm). The small diameter casings (1.9 in.) are suitable for measuring small deformations and were not chosen for monitoring the soil movements in this study. The other two diameter casings are suitable for monitoring moderate to large deformations and were suitable for application and used in these construction projects (foundations, embankments, slopes, landslides, and retaining walls).

In this research, the 3.34 in. (8.5 cm) diameter pipe was selected to be a casing for the horizontal inclinometer probes while the 2.75 in. (7.0 cm) diameter casing was used for the vertical inclinometer probes. The casings used in this project have a length of 10 ft (3 m). Therefore, for the installations longer than 10 ft (3 m), the casings were assembled by joining them together as shown in Figure 6.11. Typical details of the casing are also depicted in Figure 6.11a. The following subsections present the principles involved, installation details, and subsequent monitoring procedures of both vertical and horizontal inclinometers.

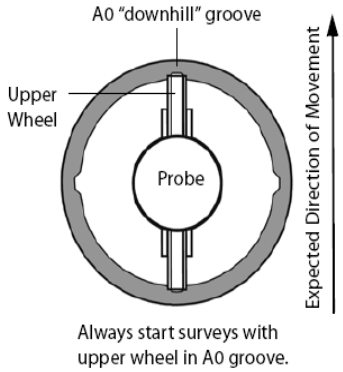

Figure 6.10. Details of inside Inclinometer Casing and a Probe (Slope Indicator, 1997).

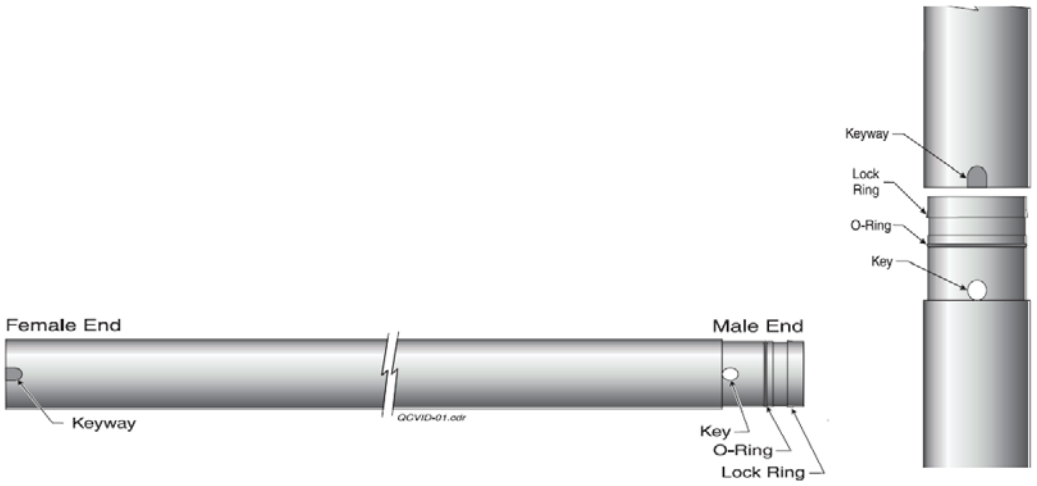

(a) (b)

Figure 6.11. (a) Details of Inclinometer Casing and (b) Assembling Procedure (Slope Indicator, 1997).

6.7.1.1 Vertical Inclinometers

An inclinometer probe is used to collect data that monitor the lateral deformations of engineering structures (foundations, embankments, landslides, slopes, retaining walls, etc.) by passing it through the inclinometer casing. The inclinometer probe uses its two force-balanced accelerometers inside the probe to measure the inclination of the axis of the casing pipe with respect to the vertical. The details of the probe and planes of measurement are shown in Figure 6.12. The two accelerometers help in measuring the lateral movements in both the A and B directions as shown in Figure 6.12b. The plane in which the deformations are measured along the wheels is the A-axis while the one perpendicular to the wheels is the B-axis. Therefore, it is necessary to align one set of grooves along the expected direction of movement during casing installation. The components included in the inclinometer unit are a flexible plastic guide casing, a portable probe, labeled control cable, data collection unit, and a pulley assembly.

The principle involved in measuring the lateral deformations using a vertical probe is as follows. The probe measures the angle of inclination of the inclinometer casing axis with respect to the vertical that is then converted into lateral movement using a sine function. From Figure 6.13, deviation, δ_i, at an interval i, is:

$$\delta_i = L \times \sin \theta_i \qquad (6.1)$$

In order to obtain the profile of the casing, the deviation at each interval is calculated by summing the values from the bottom of the casing until the next interval ($\Sigma\delta_i$) as shown in Figure 6.13.

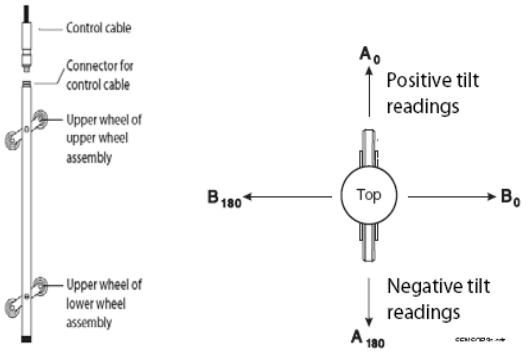

(a) (b)

Figure 6.12. Details of Inclinometer Probe (Slope Indicator, 1997); (a) Components and (b) Measurement Planes.

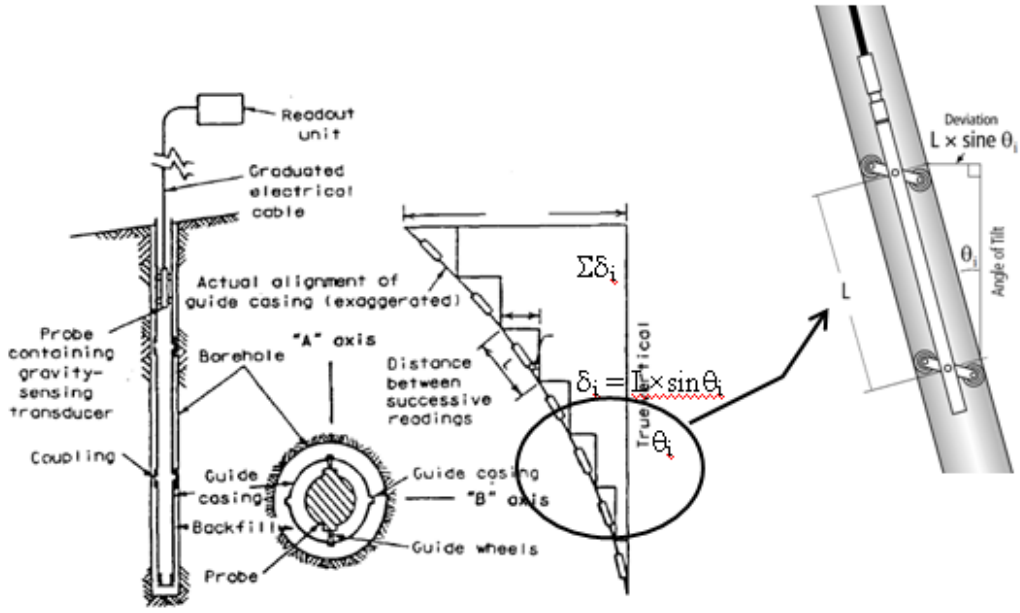

Figure 6.13. Principle in Inclinometers for Measuring Deformation (Dunnicliff, 1988).

In this study at the IH 30 site, two vertical inclinometers were installed in the DSM treated section while another inclinometer was installed in the control embankment section. Two locations near the side slopes of the treated embankments were selected to study and address

erosion performance issues of the treated area. The depth of inclinometers, from the surface of fill to the shale strata, varied from 52 to 54 ft (15.6 to 16.2 m).

The step by step procedure followed for installation of vertical inclinometers is as follows:

1. After the locations for each inclinometer were selected, boreholes were drilled using an auger as shown in Figure 6.14. While drilling, it is important to maintain the verticality of the boring stem throughout the monitoring depth.
2. Before inserting the first casing, the bottom of the casing was closed using a bottom cap as shown in Figure 6.15.
3. After the bottom of borehole reached the required depth, the inclinometer casing was inserted into the borehole (Figure 6.16). The casing was assembled during the casing installation with the pipe clamping technique (Figure 6.17). A bentonite-cement grout mix was used to fill the gap between the casings and borehole soil during this procedure (Figure 6.18). The grout mix was prepared at the site in a slurry form and delivered into the gap using a grout pipe or a hose. A well prepared grout mix should be free of lumps and thin enough to pump; at the same time, it should be able to set in reasonable time, but too much water will result in shrinking the grout leaving the upper portion ungrouted (Slope Indicator, 2000). Because of the low consistency of the grout mix, it was expected to maintain the continuity without any air pockets locked in along the full depth to allow proper movement of the inclinometer from the surrounding soil.
4. At the time of filling the gap with the grout mix, it was necessary to make sure the inclinometer casing was prevented from floating due to buoyancy forces. In this study, this was achieved by filling the casing with water as shown in Figure 6.19.

Figure 6.14. A Selected Location Was Bored to Install the Inclinometer Casing.

Figure 6.15. The Bottom of the Casing Was Plugged with a Bottom Cap.

Figure 6.16. The Casing Installation after Reaching the Required Drilling Depth.

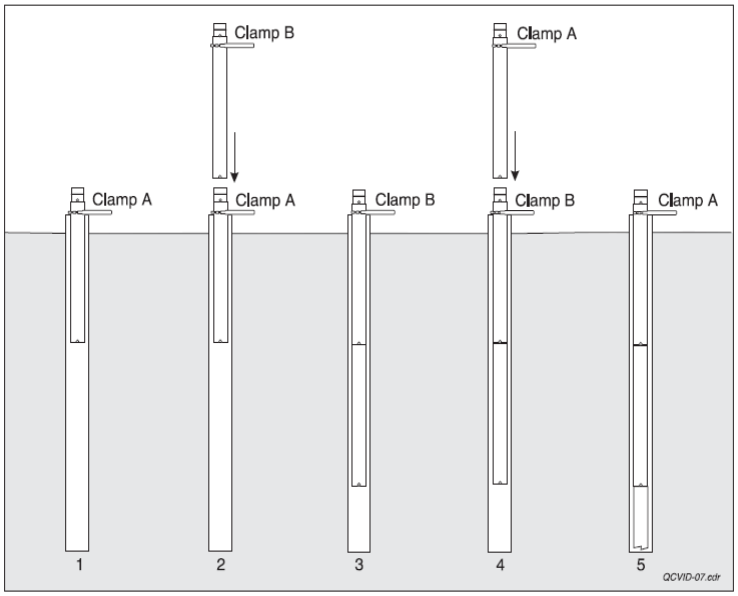

Figure 6.17. The Pipe Clamping Techniques Required for Casing Installation (Source: http://www.slopeindicator.com/pdf/manuals/qc-casing-installation-guide.pdf)

Figure 6.18. The Gap between the Casing and Borehole Wall Was Filled with Grout Mix.

Figure 6.19. Water Was Filled into the Casing to Avoid Floating due to Buoyancy.

5. The proportions of bentonite-cement grout mix were adjusted such that the 28-day strength was similar to the strength of the in-situ soils. The proportions of bentonite, cement, and water recommended for stiff and soft in-situ clayey soils can be found in Slope Indicator (2000). As soon as the installation of the casings and construction of the test section was completed, the initial profile of the casing was obtained by running the inclinometer probe through the casing. Readings were taken from bottom to top by initially lowering the probe to the bottom of the casing and then pulling it upwards to each interval. The details of monitoring and data collection procedures are presented in the next chapter.

6.7.1.2 Horizontal Inclinometer

Typical applications of horizontal inclinometers include measurement of settlement and/or heave under storage tanks, embankments, and dams, etc. In this study, horizontal inclinometers were used to monitor the vertical soil movements in the DSM treated composite test sections. This was achieved by passing a horizontal probe through the casing. Two inclinometer casings of 3.34 in. (8.5 cm) diameter were installed in the treated section on the south end of the bridge. They were placed under the bridge approach slab with traffic moving in the eastward direction. The casings had a total length of 80 ft (3.33 m) covering the highway pavement width, a pedestrian walkway, and a side slope.

The components of the horizontal inclinometer include the horizontal probe, graduated control cable, pull cable, and a data collection unit. The schematic of the horizontal inclinometer unit setup and details of the horizontal probe are shown in Figure 6.20. The wheels on one side of the probe are fixed and are always kept in the bottom groove of the casing during an inclinometer survey. The principle involved in measuring vertical movements is the same as that used for the vertical inclinometer probe. Unlike the vertical probe, the horizontal probe contains one force-balanced accelerometer and measures the deviation of the casing axis along the plane of wheels from the horizontal. The profile of the casing can be obtained by plotting the measurements at each interval along the length of the casing. Any change in the profile of the casing compared to the initial profile from subsequent surveys indicates the soils movement.

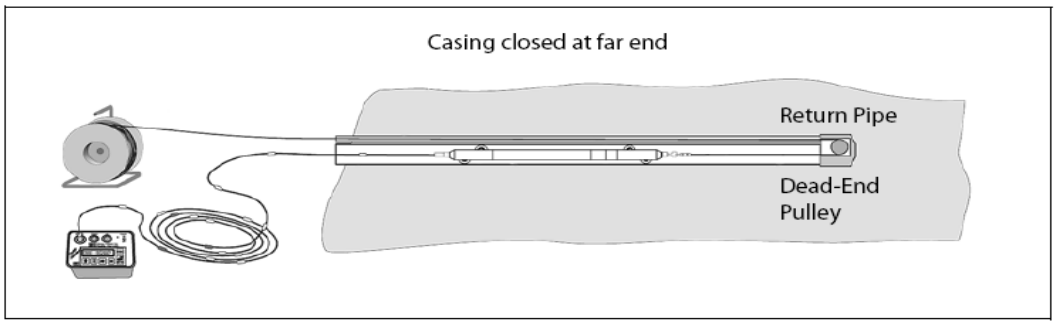

(a)

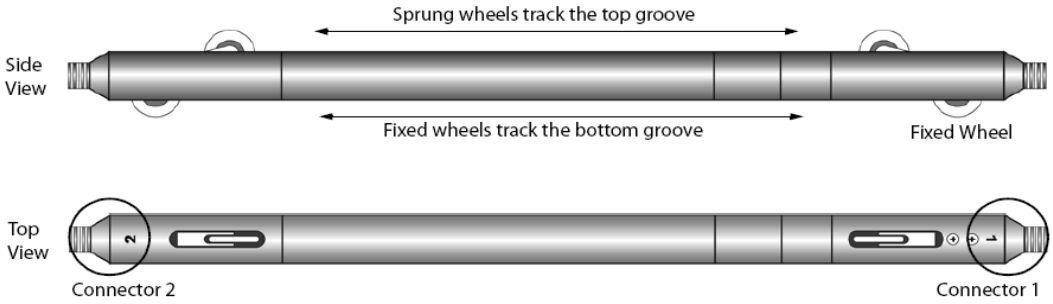

(b)

Figure 6.20. (a) Schematic of Horizontal Inclinometer Setup and (b) Horizontal Probe Slope Indicator (2004).

The following steps describe the procedure followed for installation of the horizontal inclinometers:

1. Trenches of 1.5ft × 2 ft (0.5m × 0.6 m) were excavated at selected locations along the width of the test sections as shown in Figure 6.21. Per the Slope Indicator manual (2005), a small gradient of 5% is maintained along the length of the casing for drainage purposes.
2. The trenches were cleaned and a layer of sand was uniformly placed for proper seating of the inclinometer casing.
3. The assembled casing sections were laid carefully into the trenches until the required length was reached. A stainless steel cable was simultaneously pulled through the casing. In this study, the casing closed at the far end as shown in Figure 6.20a.
4. At the time of assembling the casing, one set of grooves were aligned vertical to the ground surface to measure the soil movements.

5. To check the alignment of the grooves at the junction of two casing sections, the probe was run through the casing from the near end to the far end and back again to insure smooth operation of the probe after the trench is backfilled and overlaid with the rest of the pavement structure.

Figure 6.21. A Trench Was Excavated at the Selected Location.

6. Care was taken to avoid any debris and dirt from entering the casing during installation.
7. Finally, the trenches were backfilled and the casing ends were closed using caps. The ends should always be kept closed, except at the time of survey, to prevent any debris from entering the casing during the monitoring period.

6.7.2 Sondex Settlement System

The Sondex Settlement system was used along with the inclinometers to measure any settlement and heave associated with the excavation, construction, backfill, or tunneling operations of the embankment construction. The Sondex system is installed by placing corrugated pipes, which have stainless steel sensing rings attached around the outside circumference of the pipes, over the inclinometer casing as shown in Figure 6.22a. Figure 6.22b shows the components of the Sondex system including a Sondex data collection unit and the corrugated pipes. From the picture, the data collection unit consists of a reel with a built-in voltmeter, a measured cable, and a probe.

A depth measurement is taken by reading from the survey tape while the probe is being drawn through the center of the casing and a buzzer sounds when a metal ring is detected. The probe contains a reed switch that closes when a sensing ring is detected sounding a buzzer on the reel. The annular space between the borehole wall and the corrugated pipe is backfilled with soft grout, coupling the pipe to the surrounding ground, so that the corrugated pipe and rings move with settlement or heave. Settlement and heave are calculated by comparing the current depth to the initial value.

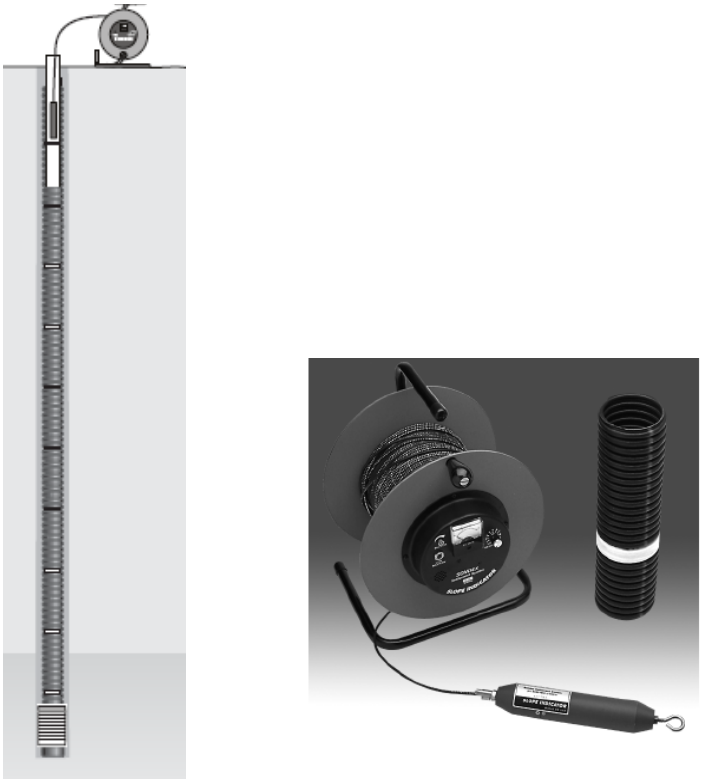

(a) (b)

Figure 6.22. (a) A Typical Sondex Installation (b) Sondex System Components (Slope Indicator, 2004).

Before the casing installation, corrugated pipes were placed on the vertical casing up to the design depths as shown in Figure 6.23. Each corrugated pipe was attached to the casing with mastic and vinyl tape, except for the bottom part corrugated that was riveted (Figure 6.24).

Figure 6.23. A Corrugated Pipe Was Placed on the Vertical Casing at Each Design Depth.

(a) (b)

Figure 6.24. A Corrugated Pipe Was Attached on the Casing with (a) Mastic Tape and (b) Rivet.

6.7.3 Rod Extensometer System

The rod extensometer is installed in boreholes to monitor the settlements in foundations, subsidence above tunnels, displacements of retaining structures, and deformations in underground openings. As shown in Figure 6.25, the main components of a rod extensometer are anchors, steel rods inside a protective pipe, and a reference head. The anchors in this project were installed with rods spanning the distance from the down-hole anchors to the reference head at the surface. The rods were placed inside the protective plastic pipe to prevent bonding between the rods and the grout backfill. Readings were obtained at the reference head by measuring the

distance between the top (near end) of the rod and a reference point at the surface either manually by a digital depth micrometer or automatically by vibrating wire (VW) sensors. A change in this distance indicates that movement has occurred. The resulting data can be used to determine the zone, rate, acceleration of movements, and to calculate strain. Anchors were selected to match the field conditions; in this study, a groutable anchor suitable for rock was selected.

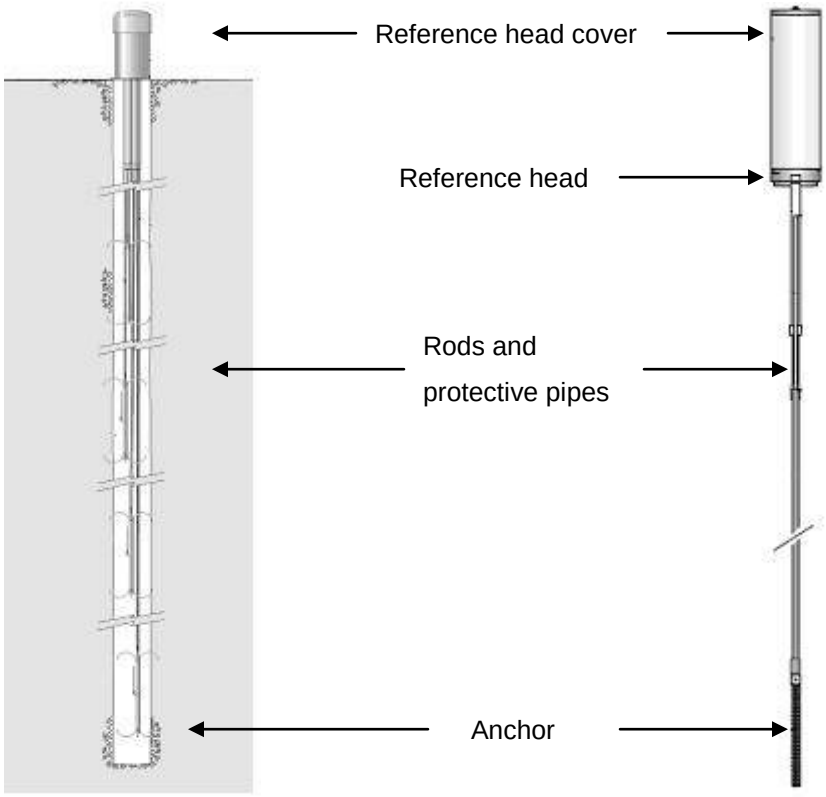

Figure 6.25. Main Components of Rod Extensometer System (Slope Indicator, 2004).

In this study, two rod extensometer systems were installed at the IH 30 site in the south embankment. A mechanical one was installed in the median while an electrical one was installed close to the approach slab as shown in Figure 6.7. To measure the soil movement occurring at different depths below the embankment surface, each of the extensometer system set of 4 steel rods and an anchor installed at depths of 10, 20, 40, and 50 ft, respectively, were installed. Since the deepest anchor was embedded in the shale layer and presumed to be stable, this anchor was used as a bottom reference in the settlement analysis. The settlement calculation must be done by subtracting each value of the other anchors from the change value for the deepest anchor. The

details of the calculation analysis can be found in the rod extensometer manual (Slope Indicator, 2004).

The step by step procedure to install the rod extensometer system is presented in the following:

1. After the locations of the rod extensometer were selected, boreholes were drilled using an auger until the auger tip reached 1 ft below the hard shale layer. In the meantime, the extensometer assembly was carried out near each borehole.
2. The rod assembly is shown in Figure 6.26 and the procedures are as follows:
    a. Cut 10 in. (254 mm) off the protective pipe.
    b. Screw the anchor adapter into the anchor.
    c. Fit the rod into the anchor adapter and then tighten the set screws.
    d. Slide the rubber sleeve over the anchor adapter.
    e. Screw the special pipe coupling onto the anchor adapter.
    f. Glue the protective pipe into the special pipe coupling.
3. After the rod assembly was finished, other rods and protective pipes were added until each rod reached the required design length. The connections were done as follows:
    a. Glue the coupling onto the protective pipe.
    b. Screw on the desired length of rod and tighten.
    c. Slide the protective pipe onto the rod and glue into the coupling.
    d. Continue until the correct rod length is obtained.
    e. Cut the last length of protective pipe so that it ends 17 in. (430 mm) below the top of the rod. Then slide the pipe onto the rod and glue it into the coupling.
4. When all the rods were built to their required depths, the 17-inch-top-part of the rods were installed. The procedures are depicted in Figure 6.27 and described as follows:
    a. Slide the telescoping joint onto the rod.
    b. Glue the coupling onto the protective pipe.
    c. Press the sensor adapter onto each rod and tighten both set screws.
    d. Pull the telescoping joint up over the sensor adapter.
5. Once the rod preparation was finished, all rods were connected with the reference head. The components of the reference head are shown in Figure 6.28. The reference head has two halves: a top and a bottom one. The center hole in the bottom half is

threaded to accept the all-thread rod while the hole in the top half has no threads. The procedures to assemble the reference head are shown in Figure 6.29 and described below.

a. Fit the bottom half of the reference head over the telescoping joints.
b. Fit the O-rings onto the telescoping joints.
c. Seat the O-rings in the reference head where the unused portions in the reference head are plugged.
d. Screw the all-thread rod into the bottom half of the reference head.
e. Fit the top half of the reference head onto the bottom half.
f. Place the steel reference plate onto the reference head, and then fasten it with the nut.

6. After the rods and the reference head were connected, the whole set of the instrument was placed into the borehole as shown in Figure 6.30.
7. Rope was used to hold up the assembly of rods and reference head in the required position (Figure 6.31). Then, a bentonite-cement grout mix was used to fill the gap between the casings and the borehole wall during this procedure. The grout mix was prepared at the site in a slurry form and delivered into the gap using a grout pipe or a hose. For the automatic reading system, the Vibrating Wire displacement sensors were installed in the last step after the grouting had finished. Instead of the procedure mentioned in Step 5, the installation of the automatic reading sensors were done following these procedures:
    a. Screw the sensor clamp into the reference head (Figure 6.32).
    b. Screw the sensor shaft into the adapter at the top of the rod (Figure 6.33).
    c. Connect the readout to the displacement sensor.
    d. Move the sensor up or down to achieve the desired initial reading.
    e. Tighten the set screws on the sensor clamps.

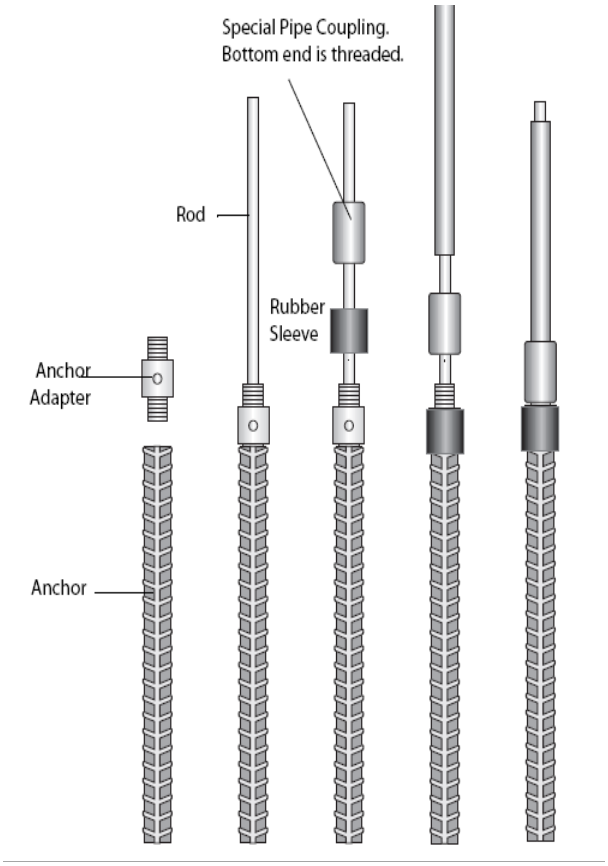

Figure 6.26. The Procedures in Rod Anchor Assembly (Slope Indicator, 2004).

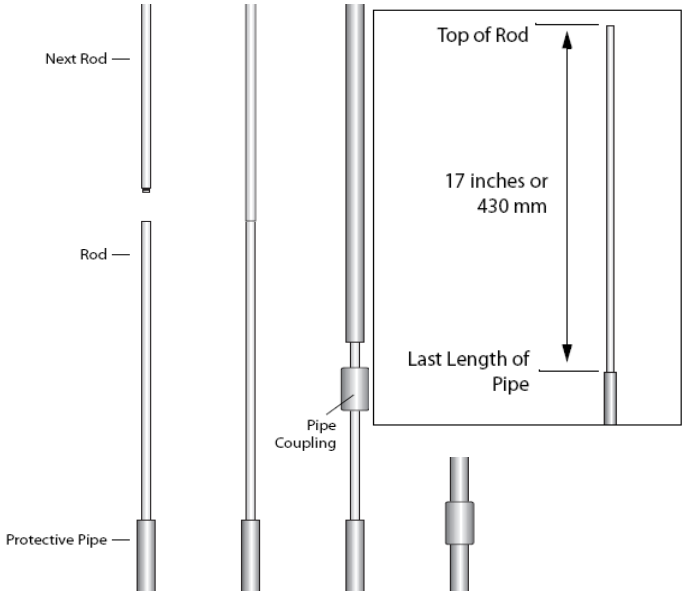

Figure 6.27. The Procedures in Adding Rods and Protective Pipes (Slope Indicator, 2004).

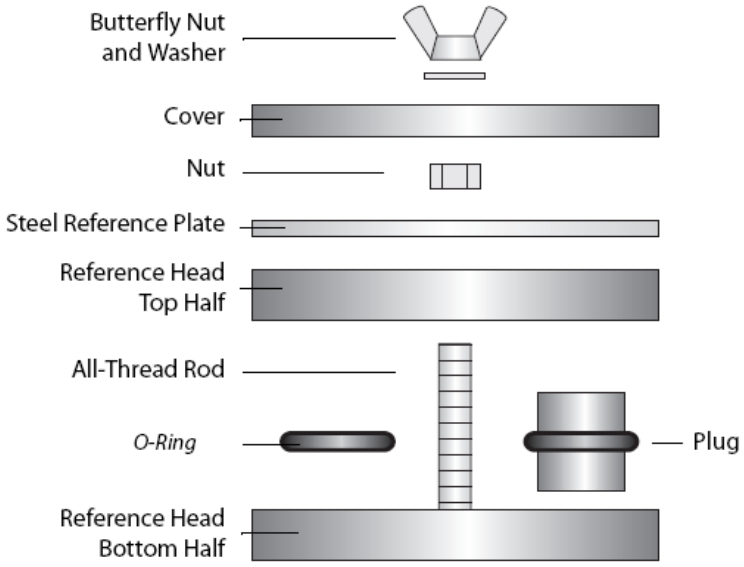

Figure 6.28. The Components of the Reference Head (Slope Indicator, 2004).

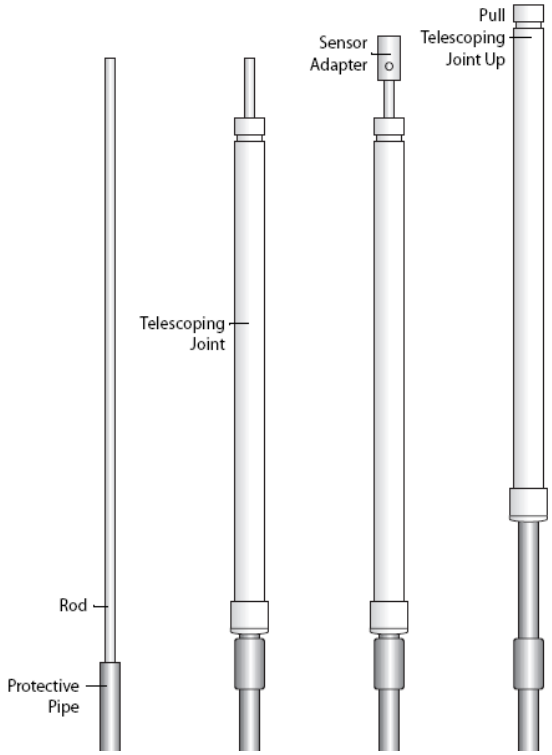

Figure 6.29. The Procedures in Installing the Top Part of the Rods (Slope Indicator, 2004).

Figure 6.30. Placement of the Assembled Rods and Reference Head into the Drilled Hole.

Figure 6.31. Set of Assembled Rods and Reference Head Held up by the Rope.

Figure 6.32. Placement of the VW Sensor Adapters into the Reference Head.

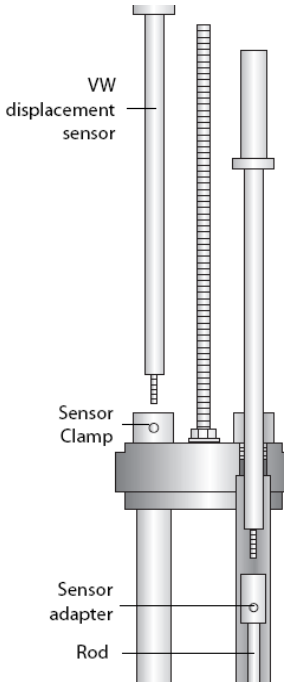

Figure 6.33. VW Sensors Connected into their Adapters (Slope Indicator, 2004).

At the ECS site, only vertical inclinometers were installed. For settlement monitoring at this site, total station elevation surveys were performed. After the instrumentation was completed, field instrumentation data were collected at regular time intervals. Data collection and analysis values are presented in later sections.

6.8 SUMMARY

This chapter presented the construction and instrumentation procedures used on two test sites supporting new bridge construction. In order to minimize the settlements, two different mitigation techniques were primarily used: one to control the settlements caused by the weak foundation layer and the other due to an embankment fill material. For the IH 30 site, the DSM column treatment was chosen to improve the strength of foundation subgrade whereas ECS was selected as the backfill of an embankment supporting the SH 360 pavements due to its lightweight property. The instrumentation used in the field to collect data and the specific details were also presented in this chapter.

CHAPTER 7

ANALYSIS OF MONITORING DATA FOR NEW BRIDGES

7.1 INTRODUCTION

As already discussed in previous chapters, two mitigation techniques were selected in this research to investigate their effectiveness in lessening the differential settlement on the bridge approach slabs. To evaluate the effectiveness of each technique, field instrumentations were performed on test sections. Field performance data were collected at regular time periods from November 2008 to September 2010. Collected data primarily included both lateral and vertical displacements of the approach slab. Data were collected from various sources including horizontal and vertical inclinometers, Sondex, rod extensometers, and elevation surveys that were used to extract the vertical movements experienced by the approach slab.

The data from the horizontal inclinometers and elevation surveys revealed the settlement movements close to the surface while data from the rod extensometers and Sondex provided ground movements at various embedded depths. The results were analyzed in this chapter to address the efficiency of both mitigation techniques.

7.2 PERFORMANCE EVALUATION OF DSM TREATED SECTION

7.2.1 DSM Treated Section

7.2.1.1 Vertical Soil Movements

DSM treatments were studied on the bridge sections built on the IH 30 site on the Center Street bridge overpass in Arlington, Texas. Instrumentation for settlement monitoring included elevation surveys for the vertical movements and horizontal inclinometers for vertical movements. Other instrumentation and their data collection are also mentioned. The following sections provide these settlement details.

7.2.1.1.1 Horizontal Inclinometer

At the IH 30 site in Arlington, two horizontal inclinometer casings were installed underneath the bridge approach slab placed on the DSM treated section located on the south side

of the bridge at two locations as shown in Figure 7.1. Figure 7.2 shows the horizontal inclinometer installation.

The data readings were collected regularly every two to three weeks to study and observe the settlement behaviors of the treated sections. A standard survey of the horizontal casing included two passes of the probe through the casing with the help of the pull-cable as shown in Figure 7.3. In the first pass, the labeled end of the probe was connected to the control cable (Figure 7.3a) and for the second pass the labeled end of the probe was connected to the pull-cable (Figure 7.3b). Figure 7.3 shows a schematic of a typical horizontal inclinometer survey (Slope Indicator, 2004). The data collected during the survey were stored using a data storage unit known as DataMate. Thereafter, the collected data were transferred from the DataMate to the computer with the associated software and the results were plotted and viewed with the DigiPro program.

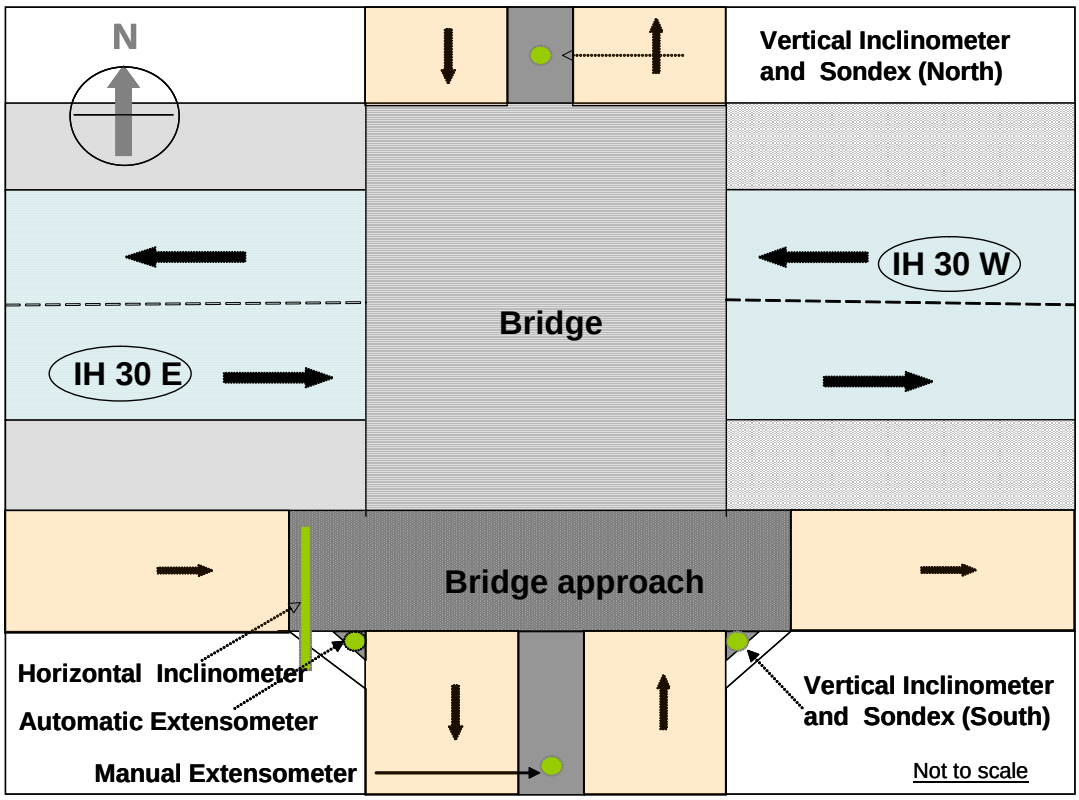

Figure 7.1. Instrumentation on the IH 30 DSM Site, Arlington, Texas.

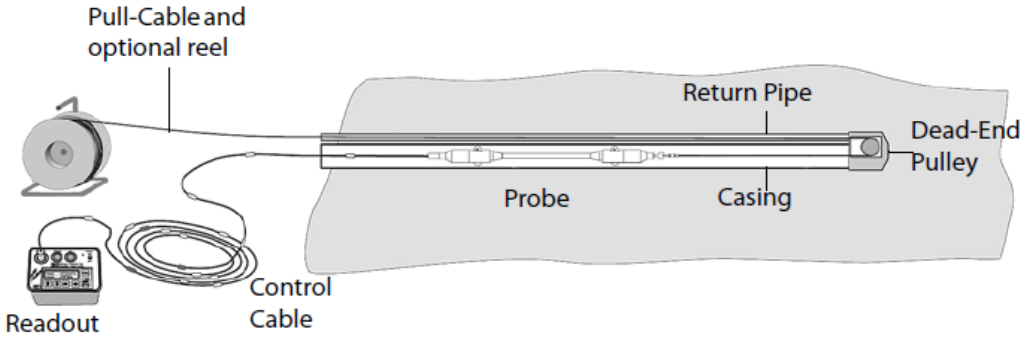

Figure 7.2. The Closed-End Installation of the Horizontal Inclinometer (Slope Indicator, 2004).

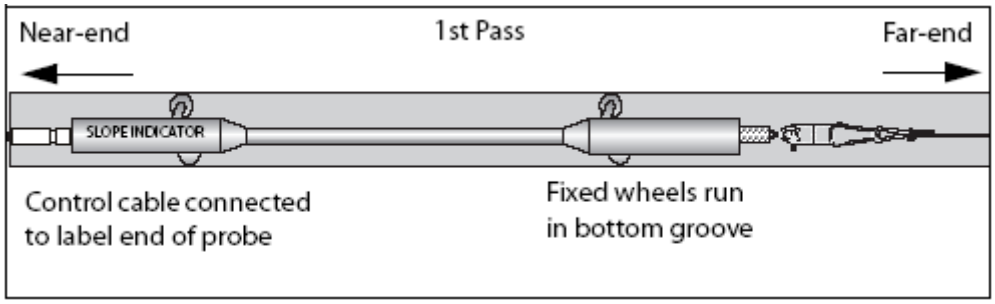

(a)

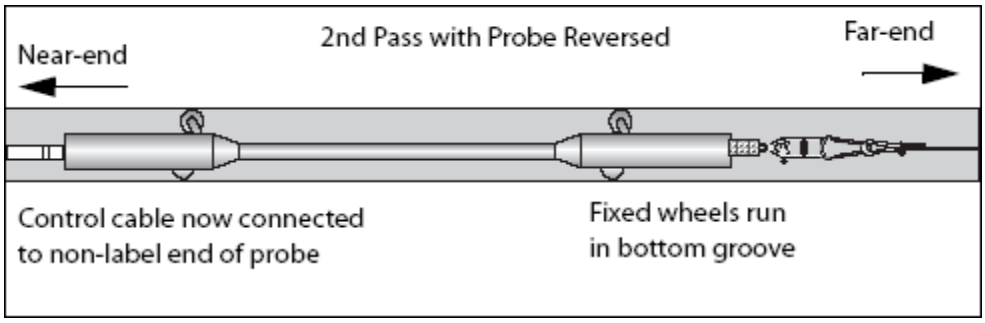

(b)

Figure 7.3. The Horizontal Inclinometer Readings Scheme (a) 1st Pass and (b) 2nd Pass (Slope Indicator, 2004).

As mentioned, two horizontal inclinometer casings were originally installed at this site. However, after the installation, one inclinometer located near the east end of the embankment was broken during the construction of the approach slab. Due to the difficulty and cost to repair this casing (Figure 7.4), it was abandoned for settlement monitoring.

The data readings of the other inclinometer casing on the west side were performed periodically every two to three weeks. The readings were obtained with an inclinometer probe and a data logger as shown in Figure 7.5.

Figure 7.4. The Location of the Broken Casing.

Figure 7.5. Inclinometer Data Collection Process.

The data are presented in the form of graphs plotted between the horizontal inclinometer displacements in inches versus the length of the probe in feet. Each plot normally shows the change of casing profile at that moment when compared with the initial one at the time of installation, which was used as a reference. Since the displacements occurred every fortnight, too much test data are available to show or to discuss; therefore, the displacements recorded on a monthly basis are used and plotted on the graphs. The horizontal inclinometer casing on this site has a total length of 78 ft (23.77 m); 32 ft (9.75 m) was laid beneath the fill slope and pedestrian sidewalk, 20 ft (6.1 m) was laid under the highway pavement, and 26 ft (7.92 m) was laid underneath the approach slab. However, the total length of the casing was reduced to 48 ft (14.63 m) in December 2009 when it was broken. The data collection was eventually terminated in April 2010 due to the loss of the cable that broke off due to probable rusting.

To clarify the plots of the cumulative displacements, the displacement data are presented separately into two graphs. Both graphs show the soil movement data happened over the two year monitoring period, but used a different date as their reference in the movement calculation (before and after the approach slab construction finished). Figure 7.6 shows cumulative displacements along a casing length of 78 ft (23.77 m) from July 2008 to December 2009 (during the construction of the approach slab), whereas Figure 7.7 presents the displacement data that occurred after the construction of the approach slab (used November 2008 data as a reference). The displacement data occurred after the casing were broken and are presented separately later.

From the profile of the inclinometer readings as shown in Figures 7.6, the following observations are noted:

- The inclinometer profiles before and after the approach slab construction had shown some major changes in the soil movements within the embankment sections.
- On November 8, 2008, in the first 8 ft (2.44 m), the straight line of the casing is noticeable. The reason is this part of the inclinometer pipe was damaged during the construction of the embankment and the approach slab. Since the broken part was located near the pipe end, the researcher was not able to repair the problem. A new 10 ft (3.05 m) section of casing was brought to replace the damaged one with the testing length reduced to 78 ft (23.77 m).
- The maximum displacement in the inclinometer casing occurred at a distance of 48 ft (14.63 m) from the open end and the displacement magnitude was 1.70 in.

(43.12 mm). This value is in respect to the initial position of the casing at the time of installation.

- In total, four humps with displacements greater than 1 in. (25.4 mm) along the inclinometer casing are noticed. These humps show that the casing profile had dramatically changed from the straight-line at the time of installation to the humps soon after the construction completion. The locations that have camel-hump curves are the points that significantly changed in the curvature between the right and left sides of the localized points. The bending at these convex or concave points also shows high strains occurring between the top and bottom parts of the casing inducing high stresses. Therefore, the humps along the casing can be considered as the weak points in the casing and adjacent subsoils that can result in the breaking of the casing.
- More settlements are noticed at distances from the opened end and up to 32 ft (9.75 m). This length of the casing was laid along the fill slope and the pedestrian sidewalk.

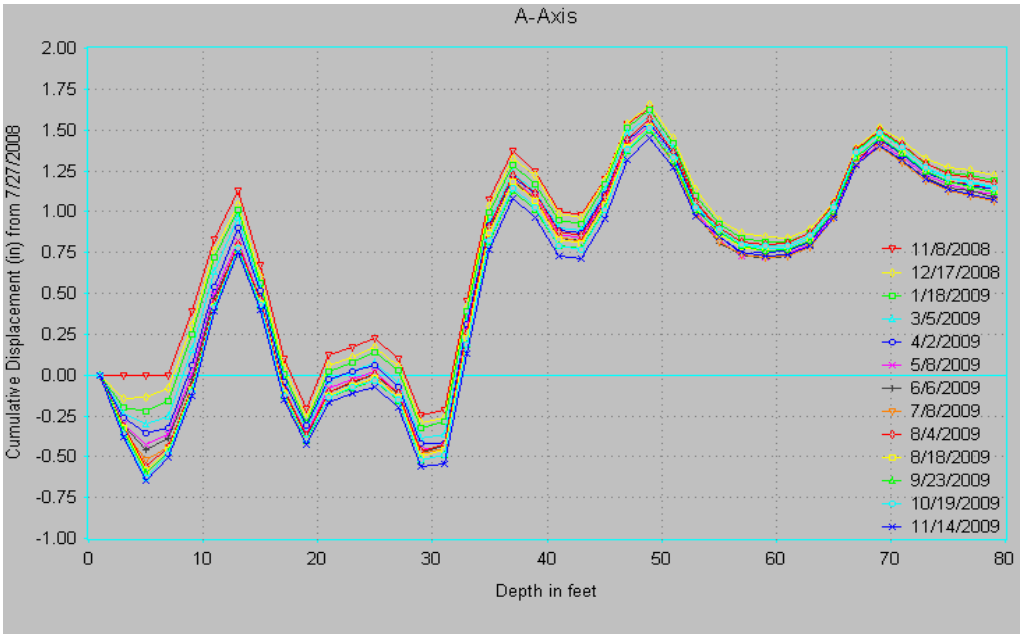

Figure 7.6. The Cumulative Displacements from 11/8/2008 to 11/14/2009 (Compared with a Casing Profile before the Construction of the Approach Slab Finished).

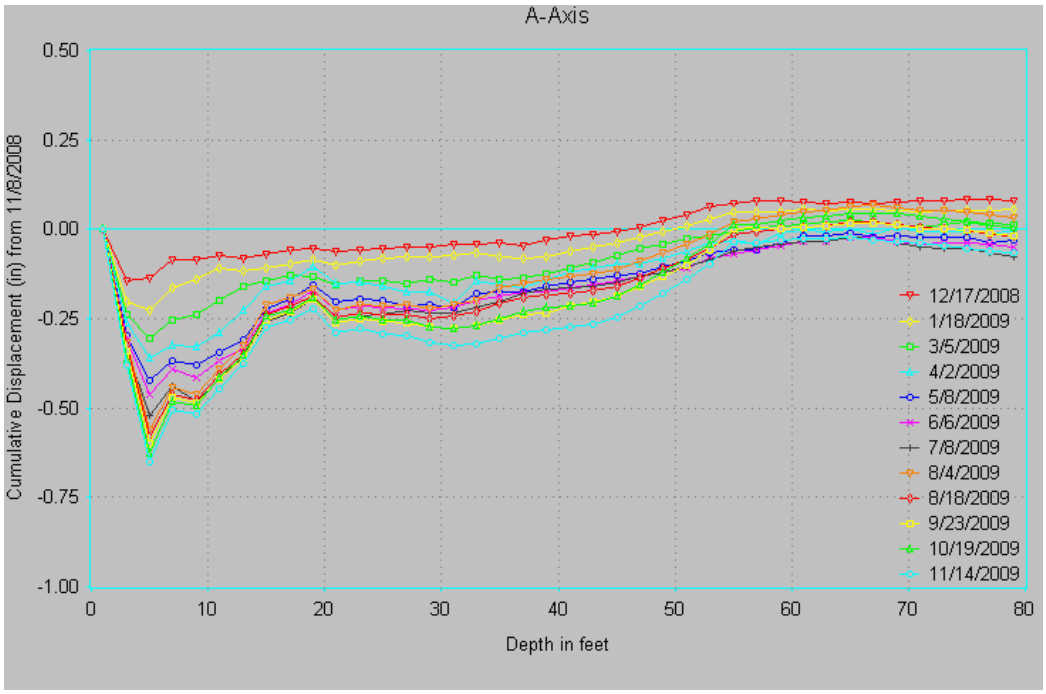

Figure 7.7. The Cumulative Displacements from 11/23/2008 to 4/14/2010 (Compared with a Casing Profile after the Construction of the Approach Slab Finished).

- Researchers observed during the site visits that the traffic on the approach slab is more concentrated on the right-turn pavement section; the casing profile and the data monitored show that the settlements that occurred in the approach slab section are lower than the other side. This reveals that the slab can mitigate the amount of the settlement induced from the traffic load.

From the profile of the inclinometer readings shown in Figure 7.7, the following observations can be noted:

- After the construction of the embankment and the approach slab, considerable movement of the casing is seen in the zone of the slope fill at distances between 0 and 20 ft (0 and 6 m). This trend happened only in the first six months and thereafter, lesser amounts of settlements were observed. Unlike the other section under the pedestrian and traffic pavement, the soil movements kept increasing as time increased.

Figures 7.8 and 7.9 present the soil movements after the breaking of the casing:

- From Figure 7.8, it is clearly seen that the casing was broken at the point where the highest hump was recorded.

- Most of the settlements occurred within the first 12 months whereas only small amounts of soil movements were recorded in the last four months before the readings were terminated.

From Figure 7.9, it is clearly seen that after the construction of the approach slab, the maximum amount of the settlement occurring under the highway pavement is 0.50 in. (12.7 mm) and the minimum settlement value is 0.25 in. (6.35 mm). Moreover, the highest value of the settlement is 0.75 in. (19.05 mm) and it happened in the slope fill area that has the lowest compaction effort.

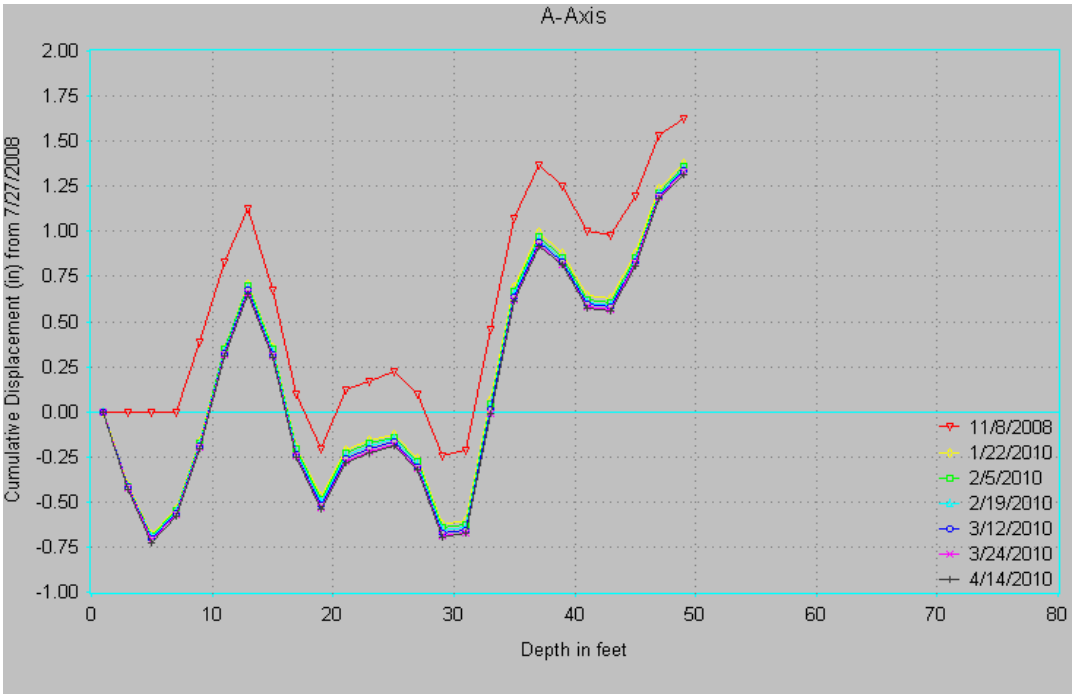

Figure 7.8. The Cumulative Displacements from 11/8/2008 to 4/14/2010 (Compared with a Casing Profile before the Construction of the Approach Slab Finished).

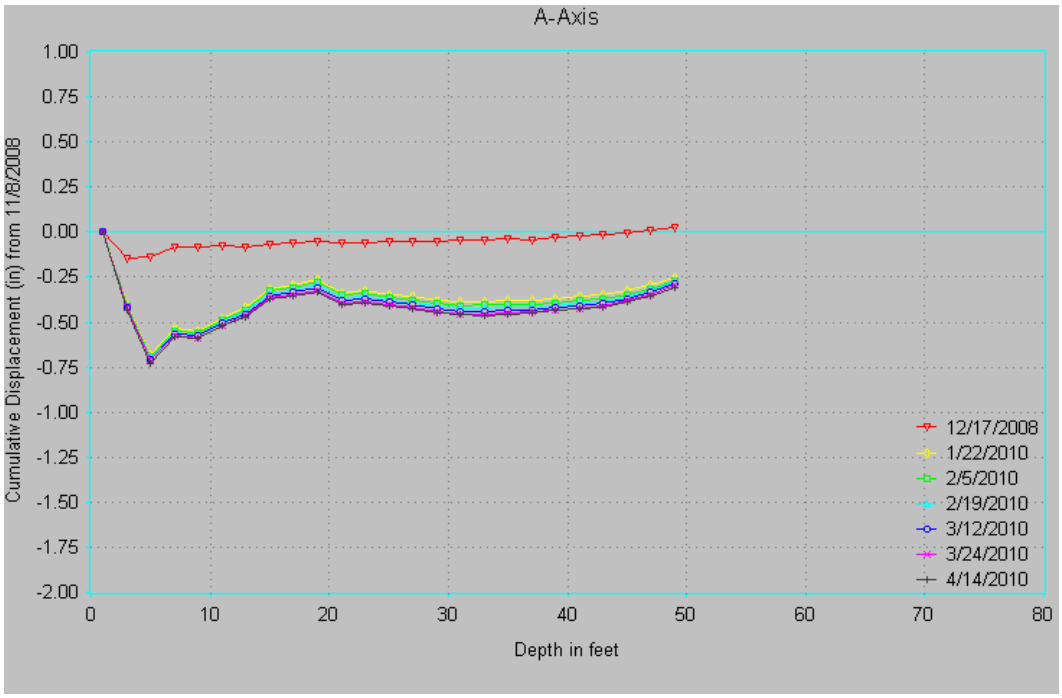

Figure 7.9. The Cumulative Displacements from 12/17/2008 to 4/14/2009 (Compared with a Casing Profile after the Construction of the Approach Slab Finished).

Elevation surveys were also performed at a location close to a highway pavement both in the treated and the untreated sections by using a Total Station (TS) device that has a resolution of 0.1 in. (0.25 cm). Generally, the data obtained from the surveys are the elevation data compared to a preset Benchmark (BM) value, which was fixed and located far from the area of the study to avoid any influencing circumstances affecting the BM elevation. The collected elevation data are presented in Table 7.1. To determine the vertical movements of the selected points, the elevation values at any date of survey must be subtracted by the value at the initial reading. For example, the movement in a treated section on March 20, 2009, is equal to 0.12 ft. (3.66 cm). The positive value shows that the selected point was settled.

Table 7.1. Elevation Survey Data on IH 30 Test Section Site.

Date	Elevation of the interested point		Soil settlements	
	(m)	(ft)		
24-Jun-08	9.29	29.74	0	0
13-Aug-08	9.28	29.70	0.04	12.19
2-Oct-08	9.27	29.67	0.07	21.34
25-Oct-08	9.27	29.66	0.08	24.38
23-Nov-08	9.27	29.65	0.09	27.43
30-Dec-08	9.26	29.63	0.11	33.53
13-Feb-09	9.26	29.63	0.11	33.53
6-Mar-09	9.26	29.62	0.12	36.58
20-Mar-09	9.26	29.62	0.12	36.58
6-Jun-09	9.25	29.61	0.13	39.62
8-Aug-09	9.25	29.60	0.14	42.67
21-Sep-09	9.25	29.60	0.14	42.67
8-Dec-09	9.25	29.60	0.14	42.67
8-Feb-10	9.25	29.59	0.15	45.72
14-Apr-10	9.25	29.59	0.15	45.72
13-Jun-10	9.25	29.59	0.15	45.72
22-Sep-10	9.24	29.58	0.16	48.77

7.2.1.1.2 Automatic Reading Rod Extensometer Surveys

As previously mentioned, one rod extensometer with automatic reading capabilities was installed at the site. The rod extensometer was installed to monitor settlements occurring in the embankment fill of the bridge and the natural subgrade foundation. As already discussed in the previous chapter, the main components of a rod extensometer are anchors, steel rods inside protective pipe, and a reference head. The anchors are installed down-hole with rods spanning the distance from the down-hole anchors to the reference head at the surface. Further details

about the rod extensometer installation are found on Slope Indicator's website (http://www.slopeindicator.com/instruments/ext-rod.html).

The frequency in the steel rods were obtained at the reference head by the VW readout and then stored in a data logger. Thereafter, the readings were downloaded to a notebook computer using VW Quattro Logger Manager Software and then these readings were converted to distance in length units by using calibration factors as shown in Equation 7.1.

$$\text{Readings}_{(\text{Engineering Unit})} = (A \times F^2) + (B \times F) + C \qquad (7.1)$$

where F is the sensor reading in Hz and A, B, and C are coefficients listed on the sensor calibration sheet. By using the VW Quattro Logger Manager Software, the readings obtained from the field were presented both in frequency and converted distance units. These readings were then used in a spreadsheet program to plot distance information as shown in Figures 7.10 and 7.11.

The readings were taken at the extensometer head level and used to calculate the changes in the distances between the reference elevation and each anchor. When the reference head is located on stable ground, movements of the anchor was calculated relative to the reference head. However, in this research, the reference head was not stable, and the deepest anchor was then used as the reference elevation. In this case, the data were calculated and inverted. The movements of each anchor were calculated relative to the bottom anchor. The calculation procedures are presented in the following:

- Construct a table of changes by subtracting the initial reading from the subsequent readings for each anchor. This shows movements relative to the reference head as shown in Figure 7.10.
- Since the reference anchor is the deepest anchor, the data must be inverted to show movements relative to the deepest anchor, which is done by subtracting the changes for each anchor from the changes at the deepest anchor as shown in Figure 7.11.
- From Figure 7.11, when using a bottom anchor as a reference, it is clearly seen that the soils at the 10 and 20 ft (3.0 to 6.0 m) depths from the top of the embankment settled. Moreover, it is seen that the rate of the settlements were high in the first four months (November 2008 to March 2009) and afterward gradually decreased. There

was an abrupt change of the direction of the movement that started in September 2009. This indicated the malfunction of the VW at the depth of 40 ft (12.2 m) and therefore the displacements data from this depth were not used for the settlement analysis.

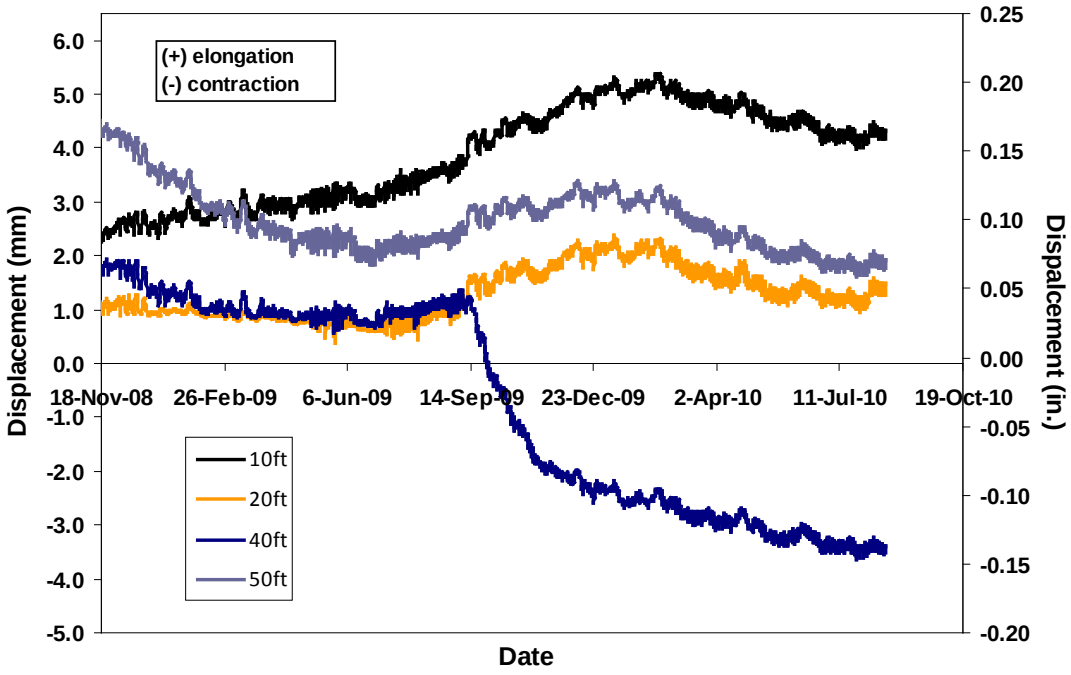

Figure 7.10. The Changes in Length of the Extensometer Rods.

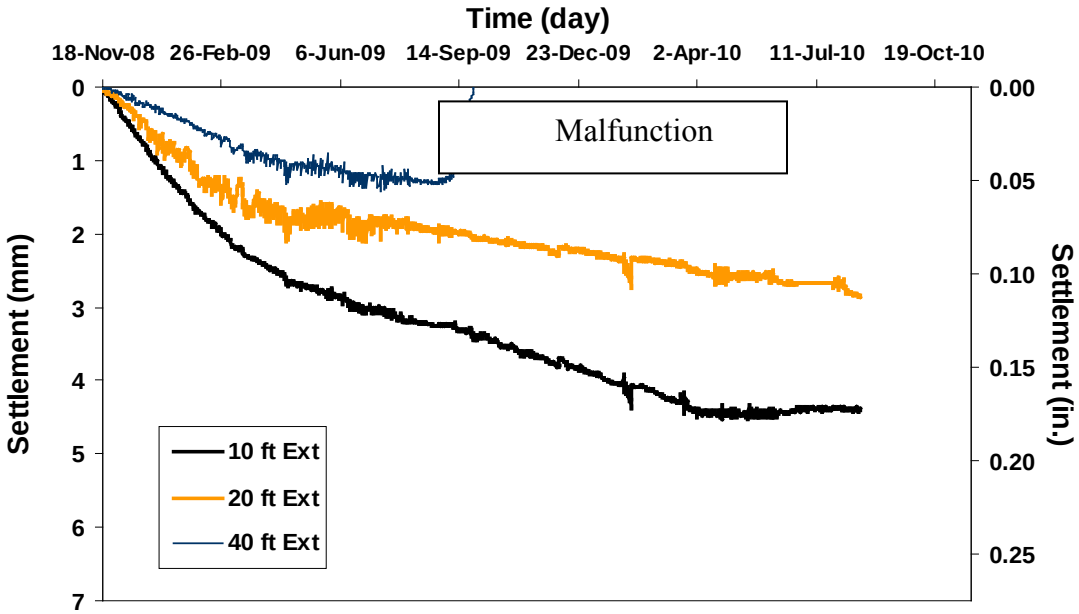

Figure 7.11. Soil Displacement from Extensometer.

7.2.1.1.3 Manual Rod Extensometer Surveys

Another rod extensometer of the manual type was installed on site at a different location of the same south embankment. Generally, the main components of both types of rod extensometer are the same with the exception that there are no VW sensors to detect displacements in the manual extensometer. Therefore, a digital depth micrometer was used to acquire the displacements that occurred at the head of each rod as shown in Figure 7.12.

As with the automatic extensometer, the observation readings were used to calculate changes in the distance between the reference elevation and each anchor by using the deepest anchor as the reference for calculation. The readings data were inverted and the movements relative to the deepest anchor were calculated by subtracting the changes for each anchor from the changes at the deepest anchor as shown in Figure 7.13.

Figure 7.13 shows a more comprehensive picture on how the soil settlements might have occurred in the embankment. The settlement occurred in the embankment and these values were increasing with time. Also, at the deeper depths, the higher settlement could be monitored. In addition, the plots from Figures 7.11 and 7.13 also reveal the time-settlement relation from the manual and automatic extensometers are similar. The automatic extensometer saves data collection time in the field.

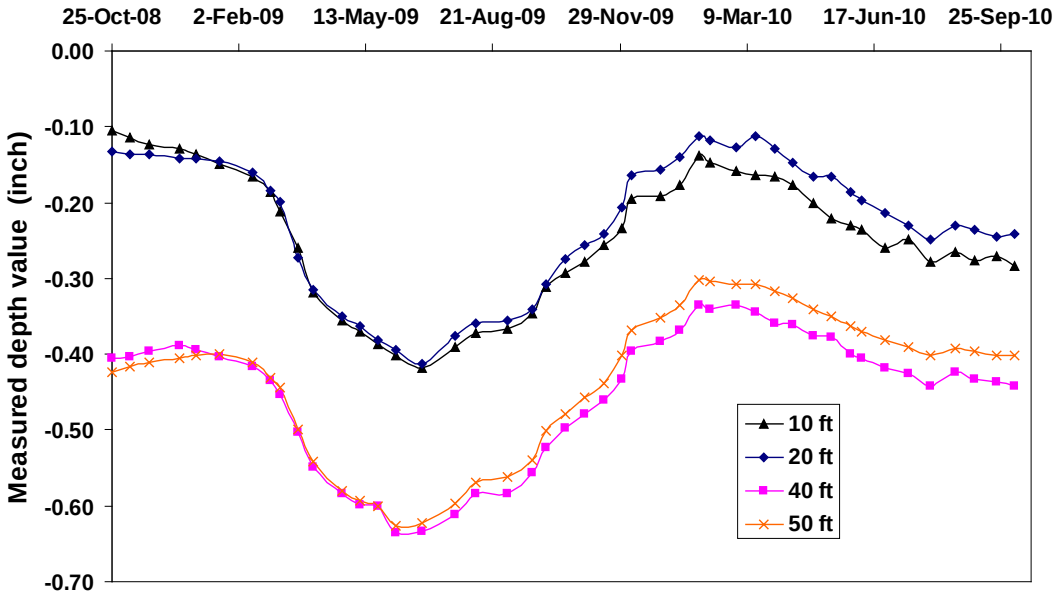

Figure 7.12. The Depth Values of the Rod Head Measured by Digital Gauge.

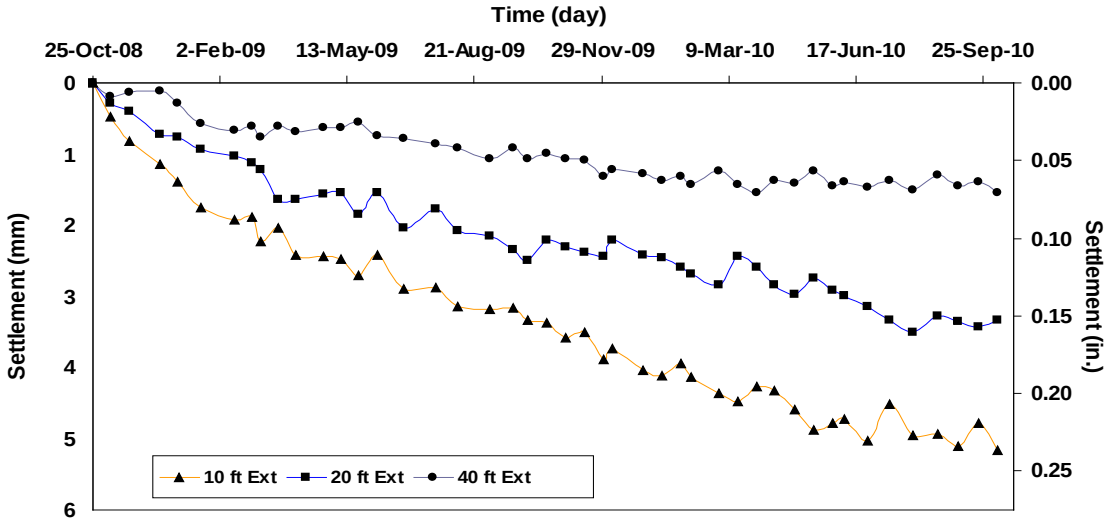

Figure 7.13. The Soil Displacement Having the Bottom Rod Anchor as a Reference.

The maximum settlements from the manual extensometer data at the depth of 10 ft, 20 ft, and 40 ft (3.0 m, 6.0 m, and 12.2 m) are about 0.20 in., 0.10 in., and 0.05 in. (5.1 mm, 2.54 mm, and 1.27 mm), respectively. These numbers have small differences from the settlements measured with the automatic extensometer and are practically negligible.

7.2.1.1.4 Sondex Readings

The Sondex devices were installed on the IH 30 DSM site with the vertical inclinometer casings. The readings were performed by lowering the probe through the center of the vertical casing. When the probe passed through the sensor rings, a buzzer sounded and the readings were collected on the tape as shown in Figure 7.14.

The Sondex was installed at the same time as the vertical inclinometer with its task to detect soil settlements larger than the capacity of the extensometer. The data obtained from the Sondex are normally fewer but more accurate compared with data obtained from the extensometer.

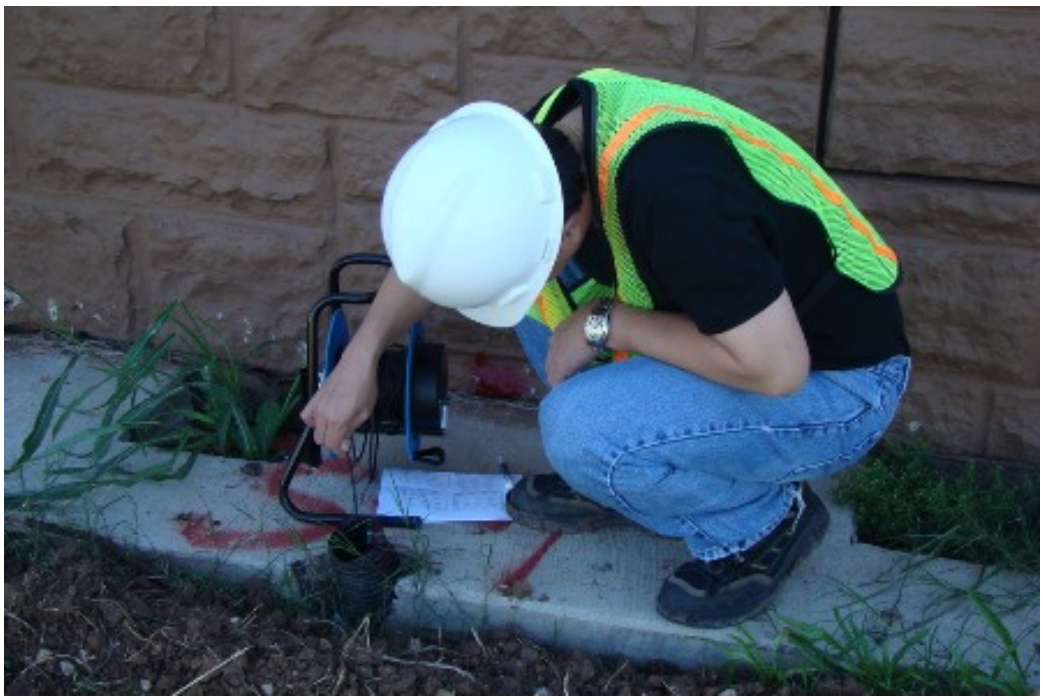

Figure 7.14. The Sondex Instrument and the Readings.

The bottom ring was fixed on the vertical casing by bolts with the rings above still able to move with the surrounding soil movements. Therefore, the bottom ring was chosen as a reference for the displacement calculation and the vertical movements were obtained similar to the steps performed in the extensometers. However, the data obtained from the Sondex are not as accurate as the rod extensometer due to two following reasons. First, the readings from the Sondex were performed by the movement of the probe through sensor rings inducing a magnetic field and the buzz around it. The schematic movement in inducing the magnetic field depends on the speed of the probe. If the movement speed is low, the magnetic field will not be induced and therefore the buzzing will not be sounded. However, if the movement is too rapid, then the readings on tape will be erroneous. Second, with the scale of the measuring tape in 0.01 ft (0.12 in., 0.305 cm) increments, the readings cannot be obtained as accurate as in the rod extensometers. Therefore, the readings of each depth must be performed three times to obtain the arithmetic average value to be representative of the depth. The plots of the average measured depth and time are shown in Figures 7.15 and 7.16. Figures 7.15a, b, c, and d show the average depth readings in the treated embankment at depths of 10 ft, 20 ft, 40 ft, and 50 ft (3 m, 6 m, 12 m, and 15.2 m), respectively.

From Figure 7.15, it is seen that the vertical movements occurred in the embankment on the treated DSM area within 0.8 in. (0.02 m). The results show that no large settlements could be detected in both of the embankments on the treated and on the untreated native material during the study period.

7.2.1.2 Lateral Soil Movements

To monitor the lateral movements occurring within the embankment, two vertical inclinometer casings were installed on the IH 30 site as shown in Figure 7.1 above. The lateral soil movement is not only an indication showing the instability of the slope but also a factor in structure deterioration. Therefore, both vertical inclinometer casings were installed at the locations closest to the approach slabs and also close to the slopes. This was to measure horizontal movements in the embankment and for monitoring the effect of the horizontal movements on the settlements of the approach slabs.

7.2.1.2.1 Vertical Inclinometer Surveys

On the IH 30 site, one vertical inclinometer was installed in a treated section in the south embankment of the bridge. The vertical inclinometers were used to monitor the soil movement in the horizontal direction. Normally, the readings were taken at the same intervals as for the horizontal inclinometer. To collect the readings from the vertical inclinometer, the orientation of the probe was critical since the orientation will state the direction of the casing movement. Therefore, the data readings were always performed by keeping the orientation of the probe A0 on the downhill direction as shown in Figure 7.16.

The inclinometer data were collected by sending the probe into the casing in the A– direction and the upper wheel of the probe was in the A0 groove as shown in Figure 7.17. The data at each depth interval were collected and stored using a Digitilt DataMate connected to the inclinometer probe. The readings were downloaded to a computer using a DataMate Manager (DMM) software. Plots, as shown in Figure 7.18, were developed using the DigiPro software.

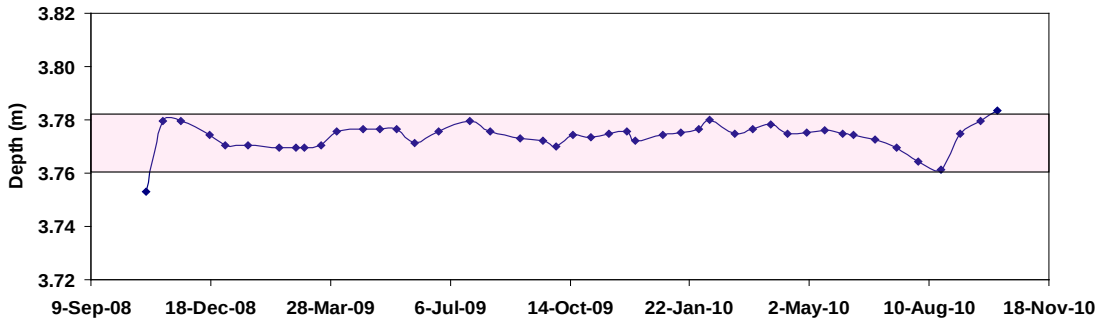

(a)

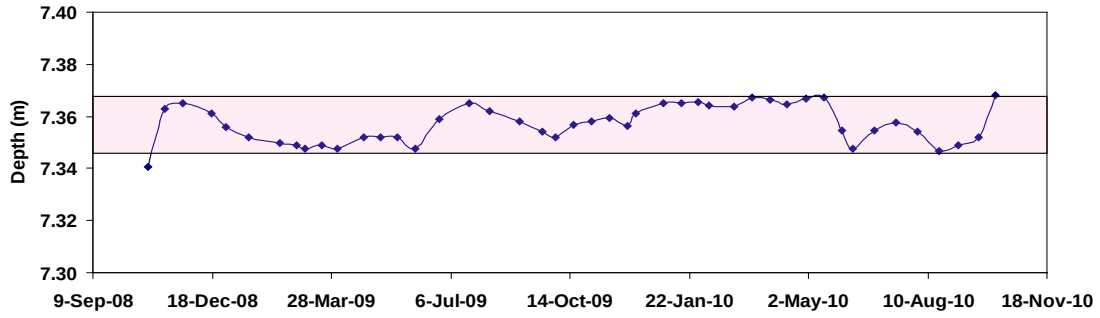

(b)

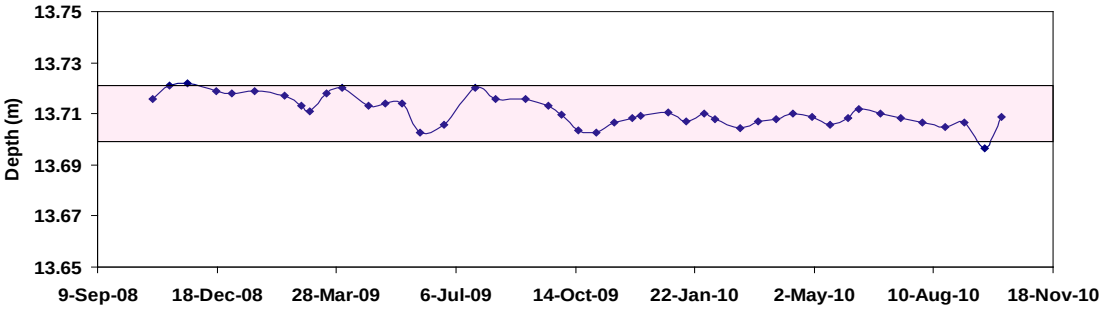

(c)

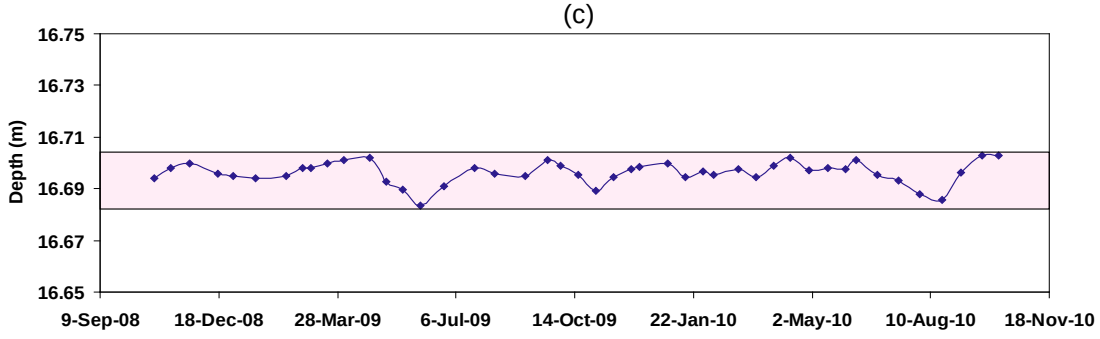

(d)

Figure 7.15. The Average Depth Readings in the Test Embankment at the Depths of (a) 10 ft (3 m), (b) 20 ft (6 m), (c) 40 ft (12.2 m), and (d) 50 ft (15.2 m).

Results from the vertical inclinometers showing the lateral movement of the soils in the test section at the IH 30 site is presented in Figure 7.18. In this figure, it is seen that the overall soil movements in the treated embankments are very small and less than 0.1 in. (2.54 mm) in both directions. These low movements in the lateral direction are attributed to high confinements of the soils surrounding the inclinometer casings. From Figure 7.18, it is seen that the soil movements in both directions are reversing direction through the period of the readings. This behavior can be attributed to the installation of the inclinometer casing in the treated soil sections close to the approach slab and away from the embankment slope. Moreover, the inclinometer is located at the corner of the highway intersection surrounded with traffic in all directions. Therefore, the traffic from all directions might be affecting the movement of the inclinometer.

Figure 7.16. The Vertical Inclinometer Reading.

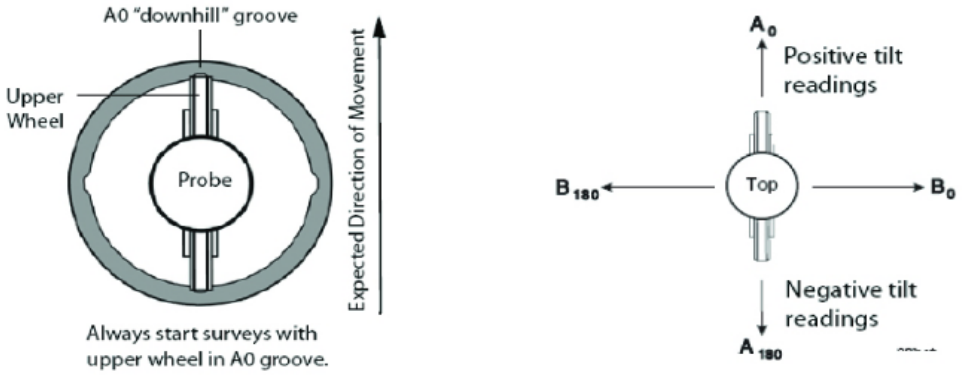

Figure 7.17. Orientation of Probe within Inclinometer Casing (Slope Indicator).

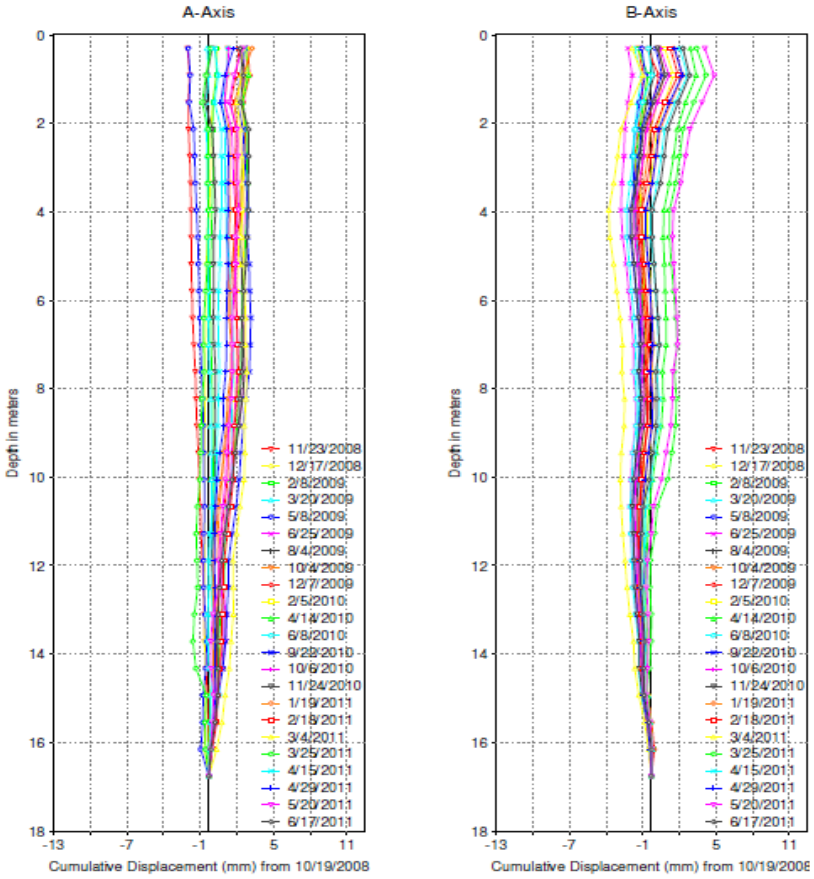

Figure 7.18. Lateral Soil Movements in the Test Section during 10/19/2008 to 6/17/2011.

7.2.2 Control Section

7.2.2.1 Vertical Soil Movements

In the control section, the Sondex readings and the elevation surveys were performed to obtain the vertical soil movement data. The elevation survey results are presented in Table 7.2

and show that the control embankment settled about 3.39 in. (86 mm) over 3 years. The vertical movements were also monitored by using Sondex and the collected data are plotted and presented in Figure 7.19. From the figure, it is seen that the depth readings of each sensor rings are varied during the period of the study. However, the depth reading variations within a range of 0.8–1.2 in. (0.02–0.03 m) are small and can lead to a conclusion that no large settlement can be detected in the control section.

Table 7.2. Elevation Survey Data on the IH 30 Control Section.

Date	Elevation of the interested point		Soil settlements	
	ft	m	ft	mm
24-Jun-08	32.07	10.02	0	0
13-Aug-08	32.03	10.01	0.04	12.19
2-Oct-08	31.99	10.00	0.08	24.38
25-Oct-08	31.95	9.98	0.12	36.58
23-Nov-08	31.91	9.97	0.16	48.77
30-Dec-08	31.89	9.97	0.18	54.86
13-Feb-09	31.88	9.96	0.19	57.91
6-Mar-09	31.87	9.96	0.20	60.96
20-Mar-09	31.86	9.96	0.21	64.01
6-Jun-09	31.84	9.95	0.23	70.10
8-Aug-09	31.84	9.95	0.23	70.10
21-Sep-09	31.83	9.95	0.24	73.15
8-Dec-09	31.82	9.94	0.25	76.20
8-Feb-10	31.81	9.94	0.26	79.25
14-Apr-10	31.81	9.94	0.26	79.25
13-Jun-10	31.80	9.94	0.27	82.30
22-Sep-10	31.79	9.93	0.28	85.34

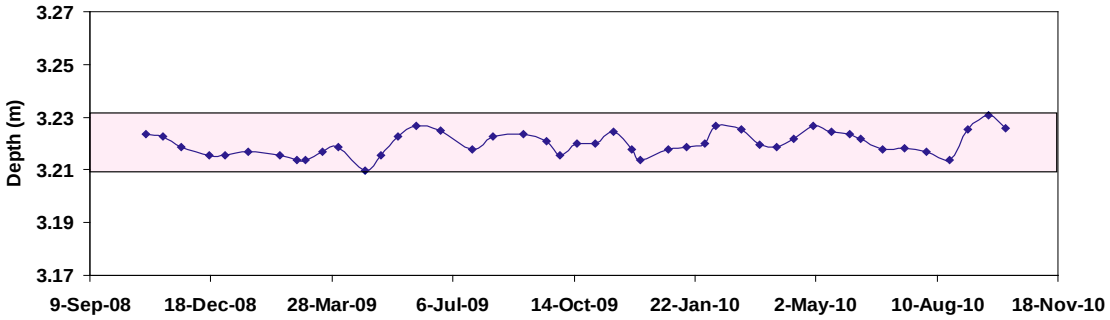
3.27
3.25
3.23
3.21
3.19
3.17
Depth (m)
9-Sep-08
18-Dec-08
28-Mar-09
6-Jul-09
14-Oct-09
22-Jan-10
2-May-10
10-Aug-10
18-Nov-10

(a)

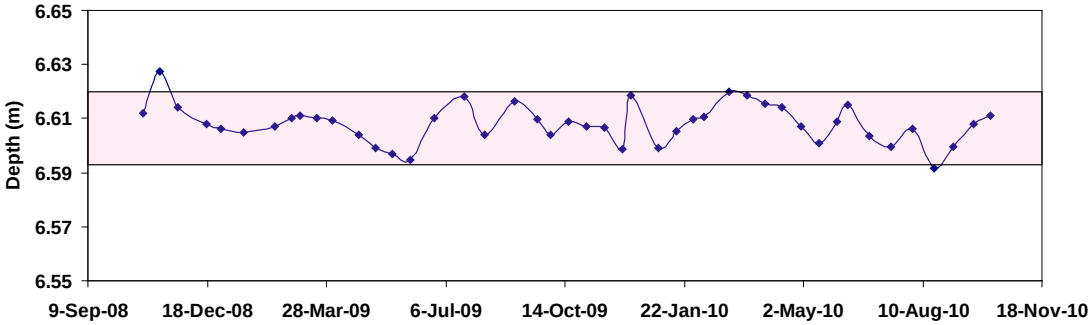
6.65
6.63
6.61
6.59
6.57
6.55
Depth (m)
9-Sep-08
18-Dec-08
28-Mar-09
6-Jul-09
14-Oct-09
22-Jan-10
2-May-10
10-Aug-10
18-Nov-10

(b)

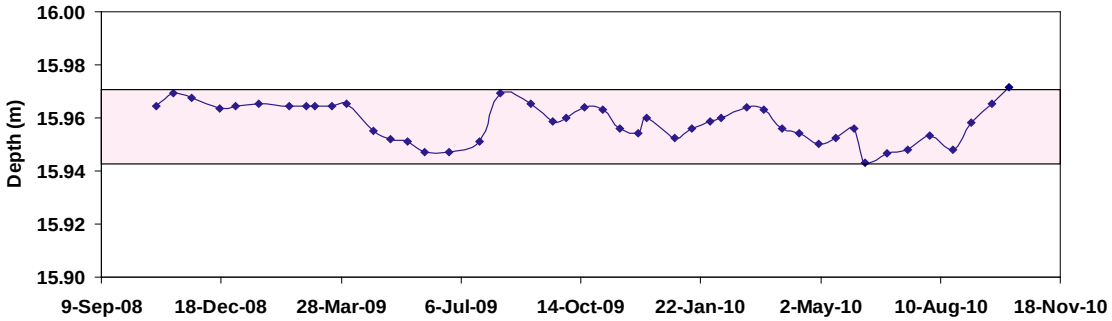
16.00
15.98
15.96
15.94
15.92
15.90
Depth (m)
9-Sep-08
18-Dec-08
28-Mar-09
6-Jul-09
14-Oct-09
22-Jan-10
2-May-10
10-Aug-10
18-Nov-10

(c)

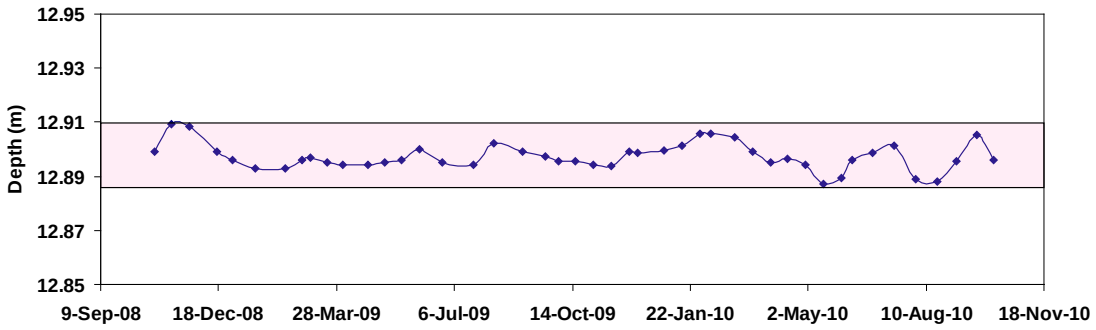

(d)

Figure 7.19. The Average Depth Readings in the Untreated Embankment at the Depths of (a) 10 ft (3 m), (b) 20 ft (6 m), (c) 40 ft (12.2 m), and (d) 50 ft (15.2 m).

7.2.2.2 Lateral Soil Movements

One vertical inclinometer was installed in the median of the control section, and the monitoring results are shown in Figure 7.20.

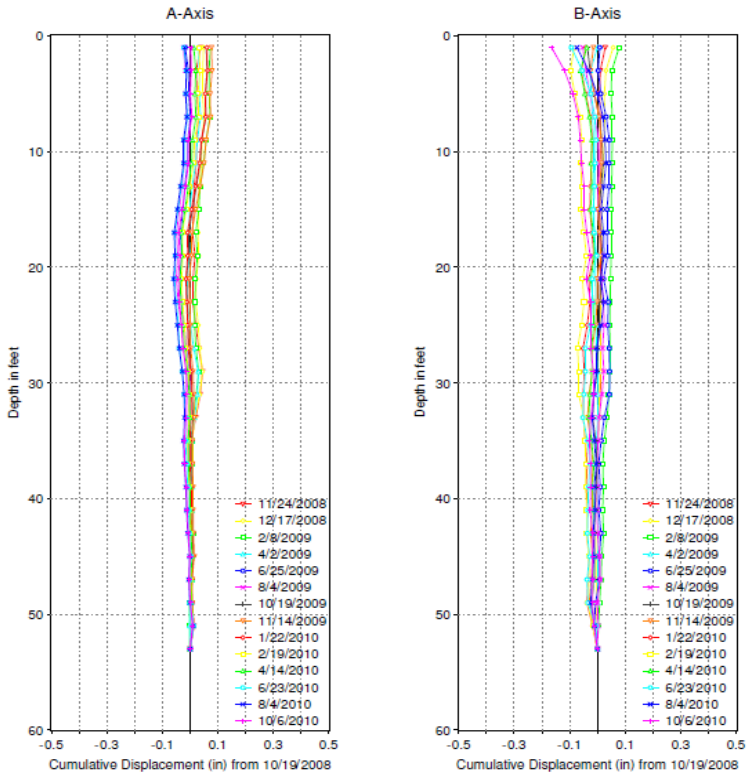

Figure 7.20. Lateral Soil Movements in the Control Embankment during 10/19/2008 to 8/4/2010.

Similar to the lateral movements monitored in the other test section, the swing-movements can also be noticed in the B-axis readings of the vertical inclinometer casing

installed in the control embankment as shown in Figure 7.19. Since the casing is located at the center in the highway median, the traffic from both directions in the B-axis could have equally affected the soil movement behavior. Therefore, the casing moved from one side to another with small displacements.

Although the casing still had sway-movements during the monitoring period, the displacement clearly moved toward the downward slope of the embankment. With the horizontal movement of 0.1 in. (2.54 mm) within 2 years, this amount of movement can be characterized as small and attributable to two factors. First, the casing was installed close to an approach slab in an area with a gradual slope of 4.0%, which is not too steep. Second, the embankment was well constructed and hence may have lesser soil movements. To summarize, the variations of the casing profiles with a very small movement less than 0.1 in. (2.54 mm) indicate that the lateral movements are not critical in the assessment of deep soil treatment methods in mitigating approach slab settlements.

7.2.3 Settlement Comparisons between the DSM Treated and Untreated Sections

In order to provide a clear idea about the differences of the soil displacements occurred over the treated and untreated sections, the data performed on both control and DSM sections at IH 30, DSM site is summarized and presented in Tables 7.3 to 7.6.

From Table 7.3, it is seen that the settlements occurred beneath the approach slab is equal to 0.25 in. The settlement from the horizontal inclinometer is less than the same value obtained from elevation surveys, since these two readings were started at different time periods. The settlement value from elevation survey (Table 7.4), which was initiated in June 2008, is less than the value from the horizontal inclinometer, which was started in November 2008. In addition, the data in Table 7.4 also reveal that the embankment in the control section experienced higher settlements than in the test or treated section.

Table 7.3. Measured Vertical Displacements in the Treated and Untreated Sections.

	DSM treated section	Untreated section
Horizontal Inclinometer (in.)	0.25	-
Elevation surveys (in.)	1.92	3.36

Table 7.4. Elevation Survey Data in the Treated Section and the Untreated Section.

Date	Soil settlements			
	DSM treated section		Untreated section	
	in	mm	in	mm
24-Jun-08	0.000	0.00	0.000	0.00
13-Aug-08	0.019	0.48	0.019	0.48
2-Oct-08	0.033	0.84	0.038	0.96
25-Oct-08	0.038	0.96	0.057	1.44
23-Nov-08	0.043	1.08	0.076	1.92
30-Dec-08	0.052	1.32	0.085	2.16
13-Feb-09	0.052	1.32	0.090	2.28
6-Mar-09	0.057	1.44	0.094	2.40
20-Mar-09	0.057	1.44	0.099	2.52
6-Jun-09	0.061	1.56	0.109	2.76
8-Aug-09	0.066	1.68	0.109	2.76
21-Sep-09	0.066	1.68	0.113	2.88
8-Dec-09	0.066	1.68	0.118	3.00
8-Feb-10	0.071	1.80	0.123	3.12
14-Apr-10	0.071	1.80	0.123	3.12
13-Jun-10	0.071	1.80	0.128	3.24
22-Sep-10	0.076	1.92	0.132	3.36

The lateral movements of the soil in both of the control and test embankments are presented in Table 7.5. Only small lateral displacements could be monitored from the vertical inclinometers. With movements monitored during the period of study, it can see that the lateral soil movements in the embankment are not critical in this study.

Table 7.5. Measured Lateral Displacements in Treated and Untreated Sections.

	DSM treated section	Untreated section
Lateral displacements	0.004in (+ 0.1mm)	0.004in (+ 0.1mm)

7.3 PERFORMANCE EVALUATION OF THE ECS FILL

7.3.1 ECS Test Section

7.3.1.1 Lateral Soil Movements

Four vertical inclinometer casings were installed in the test section in the south embankment of the bridges. The vertical inclinometers were used to monitor the soil movement in the horizontal direction in different locations as shown in Figure 7.20. Figure 7.21 shows that Inclinometers V1, V2, and V3 were installed in the median of the highway; Inclinometers V1 and V2 were located far from the slopes of the embankment while Inclinometer V3 was located near the front slope of the embankment. Inclinometer V4 was installed in the east side of the embankment slope. The orientation of the probe was placed in the north-south direction. As a result, the data readings were always performed by keeping the orientation of the probe A_0 to the north. The inclinometer readings at this site were collected once every fortnight.

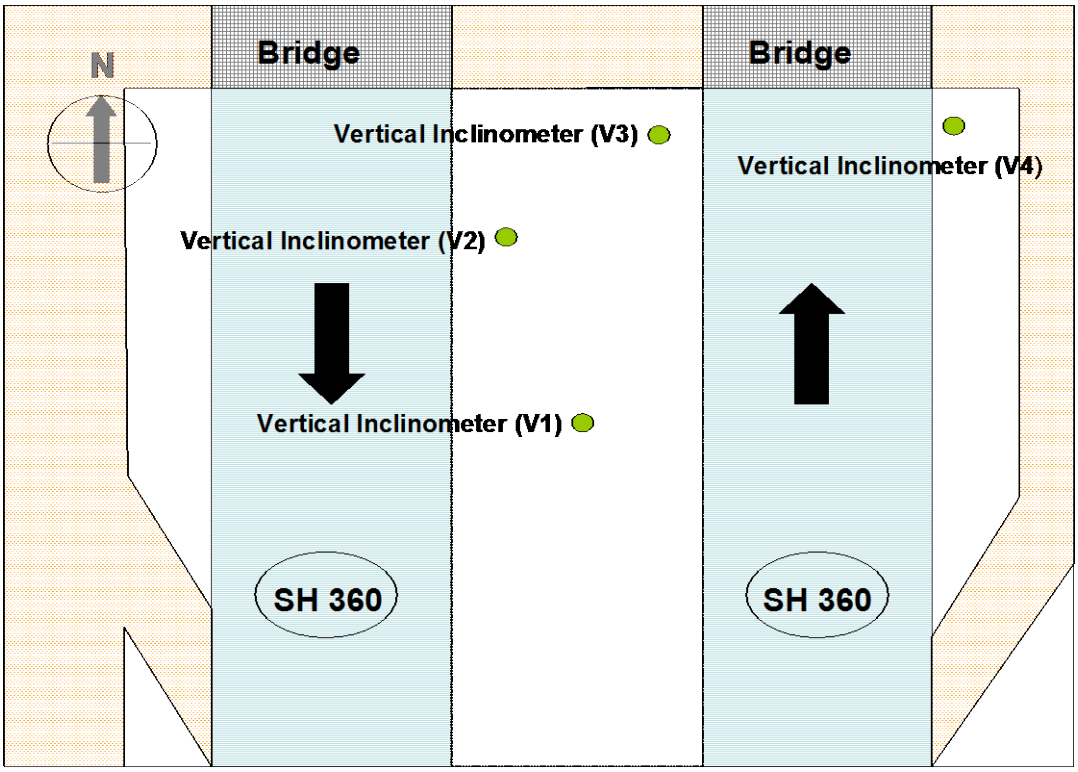

Figure 7.21. Inclinometer Placement on SH 360, Arlington, Texas.

Figures 7.22 and 7.23 present the lateral movement readings that occurred over the three year monitoring period. Figure 7.22a reveals the soil movements that occurred around Inclinometer V1. The lateral movements that happened both in the A-axis and B-axis were less than 0.1 in. (2.54 mm) and 0.5 in. (12.7 mm), respectively. The very small movements in the A-axis were due to the location of the installation far away from any slope resulting in small soil movements.

Figure 7.22b shows the soil movements that happened in Inclinometer V2. The scale of the soil displacements in both axes were almost the same at 0.5 in. (12.7 mm). Considering the movements in the A-axis, the direction of soil displacements are away from the slope while in the B-axis, the lateral displacement is in the opposite direction completely different from the displacement shown in Inclinometer V1. This possibly indicates a stronger influence from the traffic loading than the type of construction material that was used (ECS).

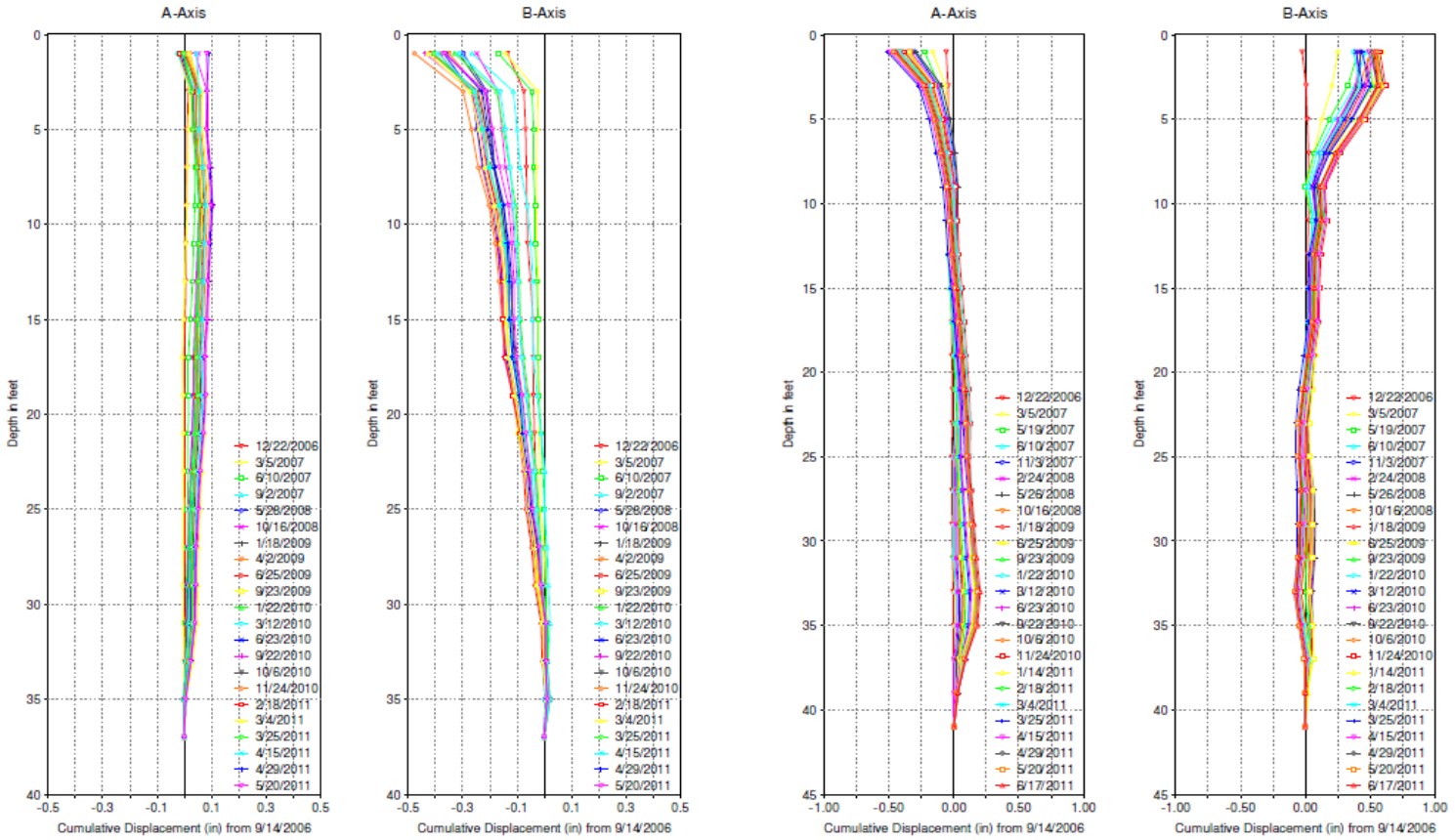

(a) (b)

Figure 7.22. Lateral Soil Movements during 8/31/2006 to 6/17/2011 in the Vertical Inclinometers (a) V1, (b) V2.

Figure 7.23a shows the soil displacement that occurred in Inclinometer V3. The lateral displacements have a magnitude about 0.75 in. (19.05 mm) in both directions. The graph also reveals that the soils around Inclinometer V3 moved away from the slope but toward the highway pavement. To explain these movement behaviors, it is also necessary to consider the soil displacements that occurred around Inclinometer V4, which was installed on the other side of the highway pavement and the outside embankment slope.

From Figure 7.23b, it is seen that Inclinometer V4 has lateral movements more than 2 in. (50.8 mm) in the A-axis and 5 in. (127 mm) in the B-axis. The 5 in. (127 mm) movements in the B-axis are not only shown in the plot but were also observed during site visits as shown in Figure 7.24. The magnitudes of these movements are more than the allowable horizontal movement of 1 in. (25.4 mm), a value typically used as a threshold value in foundation design practice. From Figure 7.23b, the movements in both directions occurred within the top 15 ft (4.56 m) from the surface, which is deemed as a rotation of the slope. In addition, the maximum displacement (2 in. [50.8 mm]) happened in the first year after construction especially during the winter and spring periods. Possible reasons for these movements could be heavy rainfall-induced soil erosion at the surface resulting in lateral movements of the slope.

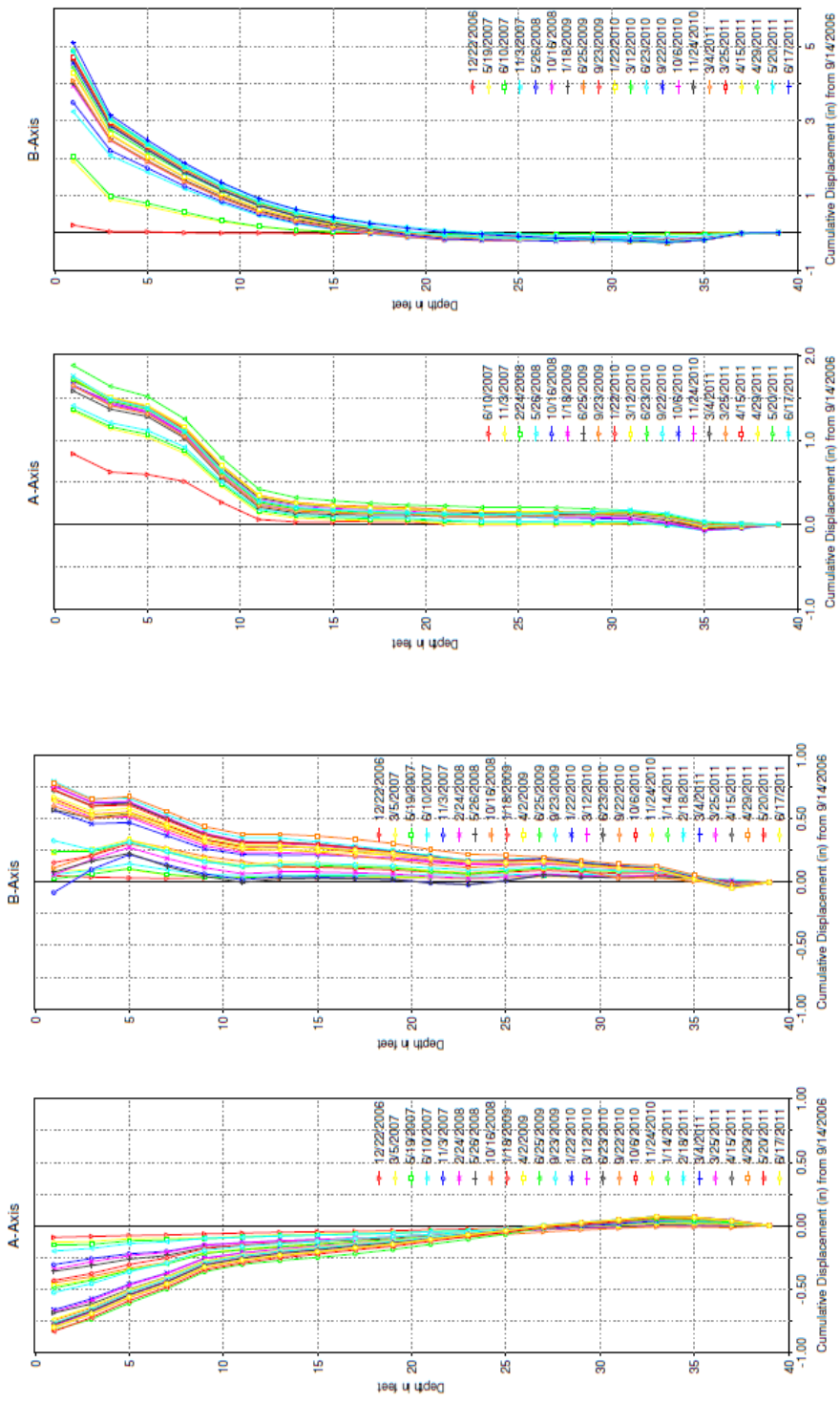

Figure 7.23. Lateral Soil Movements during 8/31/2006 to 6/17/2010 in the Vertical Inclinometers (a) V3, (b) V4.

Figure 7.24. Lateral Movement of the Platform around Inclinometer V4.

The amount of the lateral movements that occurred around Inclinometer V4 also induced the movements that occurred in Inclinometer V3. This phenomenon was observed at the surface of the highway pavement. As shown in Figures 7.25a and b, there is a gap that occurred close to the bridge between the highway pavement and the shoulder. However, no gap could be observed between the shoulder and the Inclinometer V3 platform shown in Figure 7.26. This means that the soils were moving from the median to the highway toward the outer slope. The median opening on the highway allowed more precipitation to collect and flow into the embankment inducing erosion that made the settlement problem become more severe. As seen in Figures 7.27a and b, there is an opening with a width of 1 in. (25.4 mm) and the settlement of the slope of 2 in. (50.8 mm) was observed next to the abutment.

(a) (b)

Figure 7.25. Opening Observed between the Highway Mainlanes Pavement and Its Shoulder.

Figure 7.26. Inclinometer V3 Platform close to the Highway Shoulder.

(a) (b)

Figure 7.27. Opening Observed close to the Abutment of the Bridge.

7.3.1.2 Vertical Movements

On the SH 360 ECS site, no horizontal inclinometer was installed to monitor the vertical soil movement; therefore, elevation surveys were performed to measure this displacement. The elevation survey data are presented in Table 7.6, which shows that the ECS embankment experienced a settlement of about 1.45 in. (37 mm).

Table 7.6. Elevation Survey Data on the SH 360 ECS Test Section.

Date	Elevation of the interested point, ft (m)	Soil settlements	
		ft	mm
16-Jul-06	1.41	0.00	0.00
14-Aug-06	1.39	0.02	6.10
18-Sep-06	1.37	0.04	12.19
14-Oct-06	1.36	0.05	15.24
17-Nov-06	1.35	0.06	18.29
10-Dec-06	1.35	0.06	18.29
15-Jan-07	1.34	0.07	21.34
17-Feb-07	1.34	0.07	21.34
20-Mar-07	1.34	0.07	21.34
13-Apr-07	1.33	0.08	24.38
20-May-07	1.33	0.08	24.38
3-Sep-07	1.33	0.08	24.38
16-Dec-07	1.32	0.09	27.43
18-Jun-08	1.32	0.09	27.43
19-Sep-08	1.31	0.10	30.48
17-Dec-08	1.31	0.10	30.48
18-Jan-09	1.31	0.10	30.48
20-Mar-09	1.31	0.10	30.48
2-Sep-09	1.30	0.11	33.53
6-Nov-09	1.30	0.11	33.53
8-Feb-10	1.30	0.11	33.53
5-Apr-10	1.30	0.11	33.53
14-Apr-10	1.30	0.11	33.53
8-Jun-10	1.29	0.12	36.58

7.3.2 Conventional Fill Section

7.3.2.1 Survey Elevation

In the conventional fill section (termed as control section) on the SH 360 site, elevation surveys were also performed to obtain the road profile by using a Total Station (TS). The collected elevation data are shown in Table 7.7 and are useful for comparing the settlements that happened between the control and the ECS test section as shown in the following section.

Table 7.7. Elevation Survey Data on the SH 360 Control Section Site.

Date	Elevation of the interested point, ft (m)	Soil settlements	
		ft	mm
16-Jul-06	-6.98 (-2.128)	0.00	0.00
14-Aug-06	-7.00 (-2.134)	0.02	6.10
18-Sep-06	-7.01 (-2.137)	0.03	9.14
14-Oct-06	-7.03 (-2.143)	0.05	15.24
17-Nov-06	-7.05 (-2.149)	0.07	21.34
10-Dec-06	-7.06 (-2.152)	0.08	24.38
15-Jan-07	-7.07 (-2.155)	0.09	27.43
17-Feb-07	-7.08 (-2.158)	0.10	30.48
20-Mar-07	-7.09 (-2.161)	0.11	33.53
13-Apr-07	-7.10 (-2.164)	0.12	36.58
20-May-07	-7.11 (-2.167)	0.13	39.62
3-Sep-07	-7.14 (-2.176)	0.16	48.77
16-Dec-07	-7.15 (-2.179)	0.17	51.82
18-Jun-08	-7.16 (-2.182)	0.18	54.86
19-Sep-08	-7.18 (-2.188)	0.20	60.96
17-Dec-08	-7.19 (-2.192)	0.21	64.01
18-Jan-09	-7.22 (-2.201)	0.24	73.15
20-Mar-09	-7.22 (-2.201)	0.24	73.15
2-Sep-09	-7.23 (-2.204)	0.25	76.20
6-Nov-09	-7.24 (-2.207)	0.26	79.25
8-Feb-10	-7.24 (-2.207)	0.26	79.25
5-Apr-10	-7.25 (-2.210)	0.27	82.30
14-Apr-10	-7.25 (-2.210)	0.27	82.30
8-Jun-10	-7.24 (-2.207)	0.28	85.34

7.3.3 Comparison of Data between the ECS Test Section and the Control Section

It is seen from Table 7.8 that during the study duration, settlement occurred in the control section more than in the test section. This is seen in the pavement near the bridge approach in the control section constructed with conventional fill overlaid with hot mix asphalt concrete (HMAC) pavement to mitigate the bump problem as shown in Figure 7.28. The HMAC was laid prior to completion of construction and opening of traffic on the roadway. This is an undesirable situation as it presents an image of unacceptable construction and/or inspection practices.

Table 7.8. Comparisons of Settlement Data on the Control and ECS Test Sections on SH 360.

Date	Soil settlements, in. (mm)	
	ECS Test Section	Control Section
16-Jul-06	0.00	0.00
14-Aug-06	0.24	0.24
18-Sep-06	0.48	0.36
14-Oct-06	0.60	0.60
17-Nov-06	0.72	0.84
10-Dec-06	0.72	0.96
15-Jan-07	0.84	1.08
17-Feb-07	0.84	1.20
20-Mar-07	0.84	1.32
13-Apr-07	0.96	1.44
20-May-07	0.96	1.56
3-Sep-07	0.96	1.92
16-Dec-07	1.08	2.04
18-Jun-08	1.08	2.16
19-Sep-08	1.20	2.40
17-Dec-08	1.20	2.52
18-Jan-09	1.20	2.88
20-Mar-09	1.20	2.88
2-Sep-09	1.32	3.00
6-Nov-09	1.32	3.12
8-Feb-10	1.32	3.12
5-Apr-10	1.32	3.24
14-Apr-10	1.32	3.24
8-Jun-10	1.44	3.36

Figure 7.28. Bridge Approach in the Control Section Overlaid by Hot Mix Asphaltic Concrete to Mitigate the Bump.

7.4 PERFORMANCE EVALUATION BASED ON GEOPIER REINFORCEMENT

On the SH 6 site, there were eight vertical inclinometers and four Sondex installed as shown in Figure 7.29. All of the instruments were installed in the treated sections both near the northbound entrance ramp and the southbound exit ramp. The Sondex was only installed in the exit ramp while eight vertical inclinometers were evenly spaced and installed in both ramps. On this site, the vertical inclinometers were used to monitor the soil movement in the horizontal direction in the different locations as shown in Figure 7.29, and the Sondex were used to monitor the soil movement in the vertical direction. To perform the readings in the vertical inclinometers, the orientations of the readings were performed in a direction outward of the ramp (A0 was on the farthest side to the ramp). Due to the instrumentation damages in certain casings, only readings in four inclinometers (V1, V2, V6, and V8) could be collected.

Figures 7.30 to 7.31 show only small scale lateral movements during two-year observation monitoring period (from 2008 to 2009). In most of the inclinometers, the magnitude of the lateral movements in both directions was less than 0.1 in. (2.54 mm) but in Inclinometer V2, the lateral movement was 0.3 in. (7.62 mm). However, with small amounts of movement

observed after the bridge construction in February 2008, the geopier could be a viable method to mitigate the soft soil movement underneath the embankments.

As a part of the research, an elevation survey was performed on February 20, 2009, to plot the profile grade and determine the IRI values on the ramps in the study area. The IRI results from each ramp of 117 inch/mile and 124 inch/mile (1.85 m/km and 1.96 m/km) reveal that the pavements were still in good condition; an IRI value of 250 inch/mile (3.9 m/km) indicates a very good ride quality. The numbers of the IRI values further confirm the engineer's decision to use the geopier technique at this site.

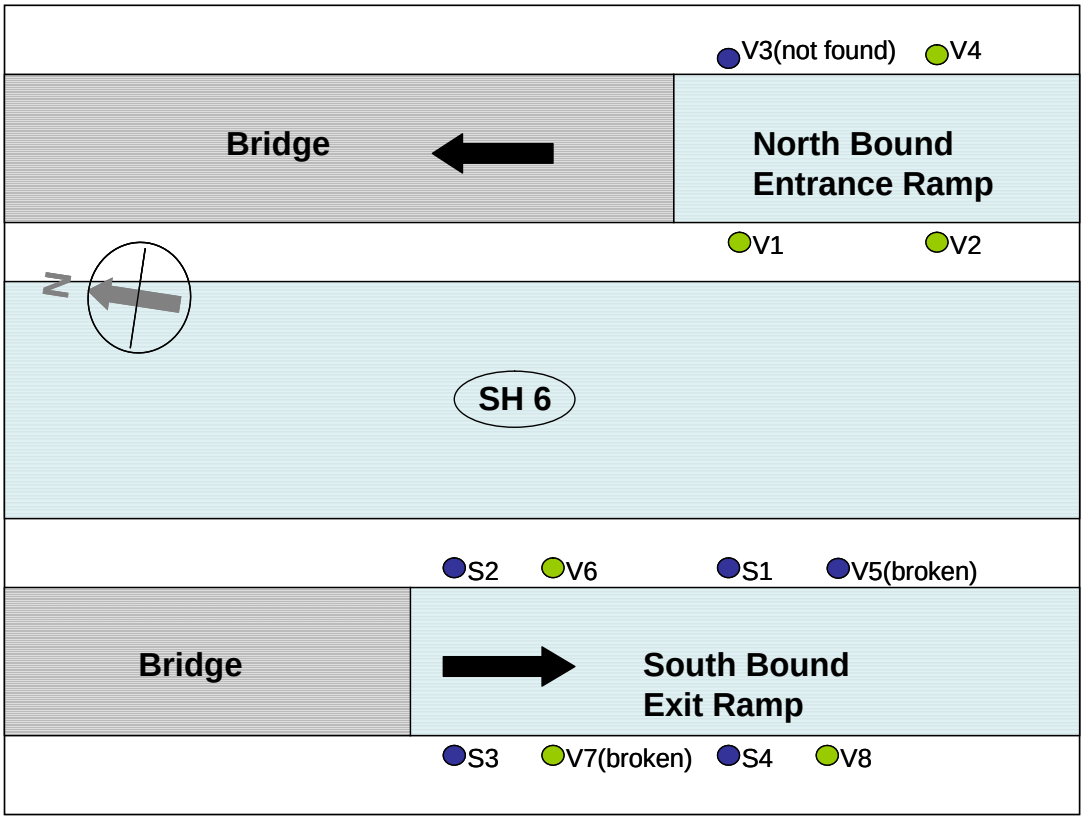

Figure 7.29. Instrumentation on SH 6 over US 90A, Houston, Texas.

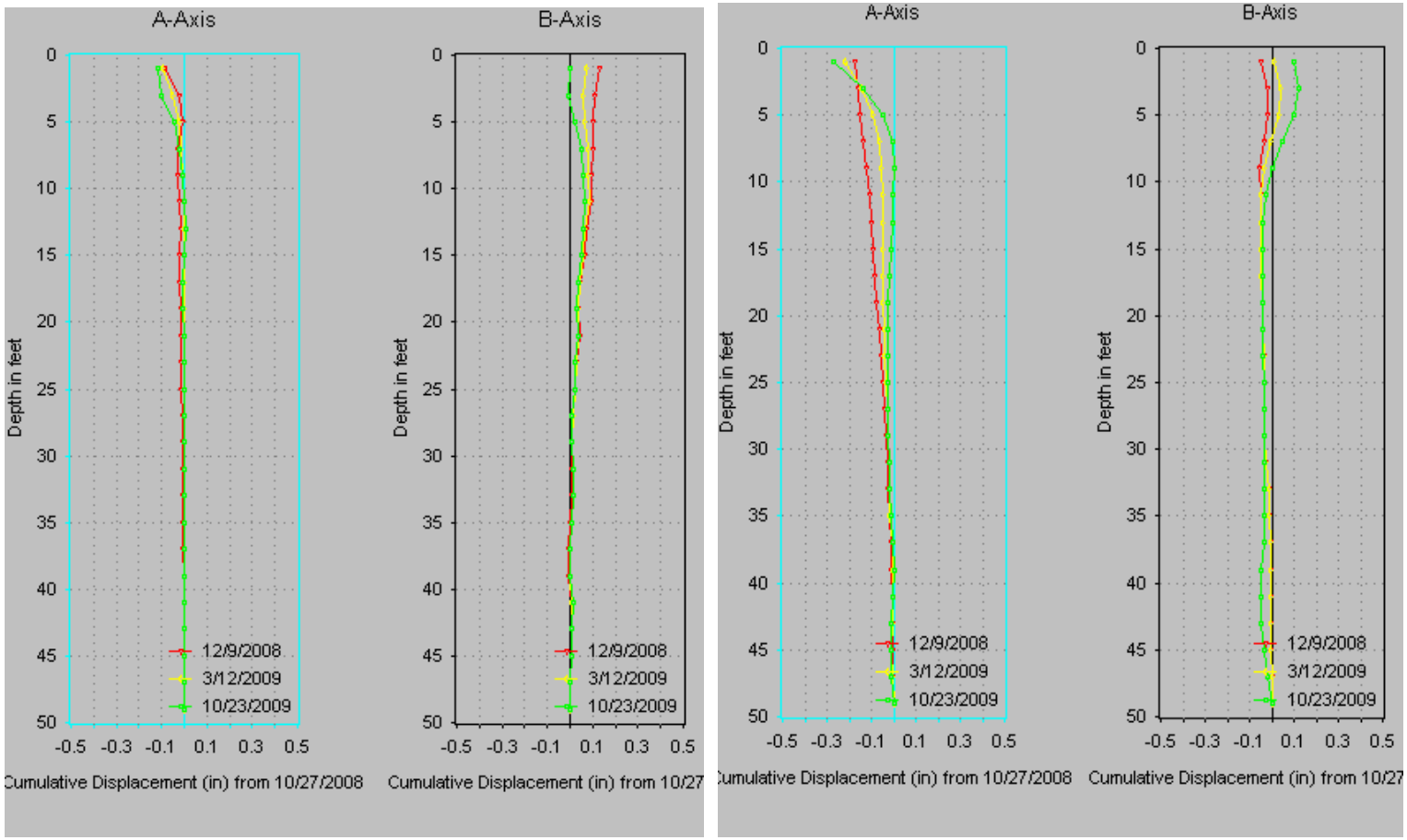

(a) (b)

Figure 7.30. Lateral Soil Movements during 10/27/2008 to 10/23/2009 in Vertical Inclinometers (a) V1, (b) V2.

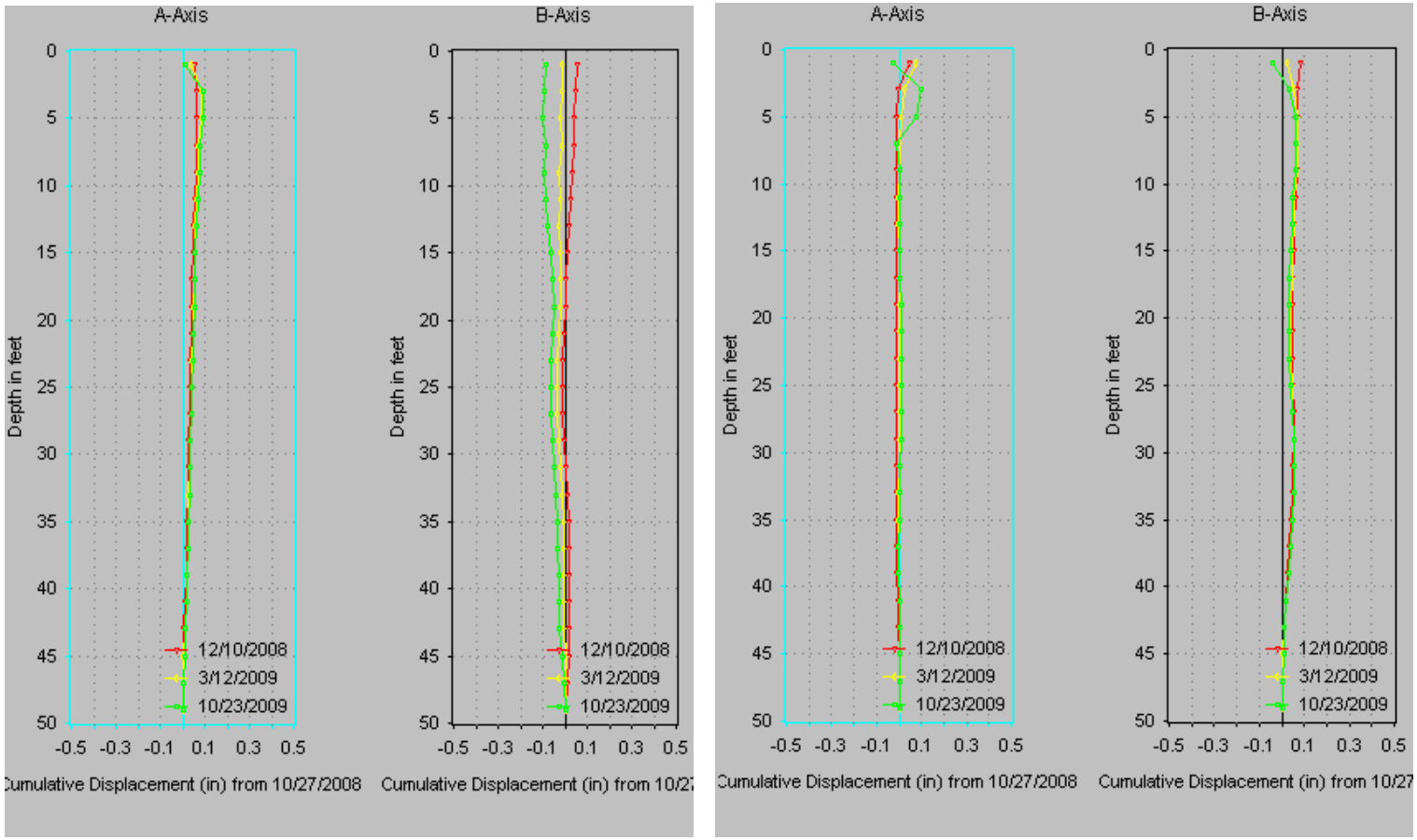

(a) (b)

Figure 7.31. Lateral Soil Movements during 10/27/2008 to 10/23/2009 in the Vertical Inclinometers (a) V6, (b) V8.

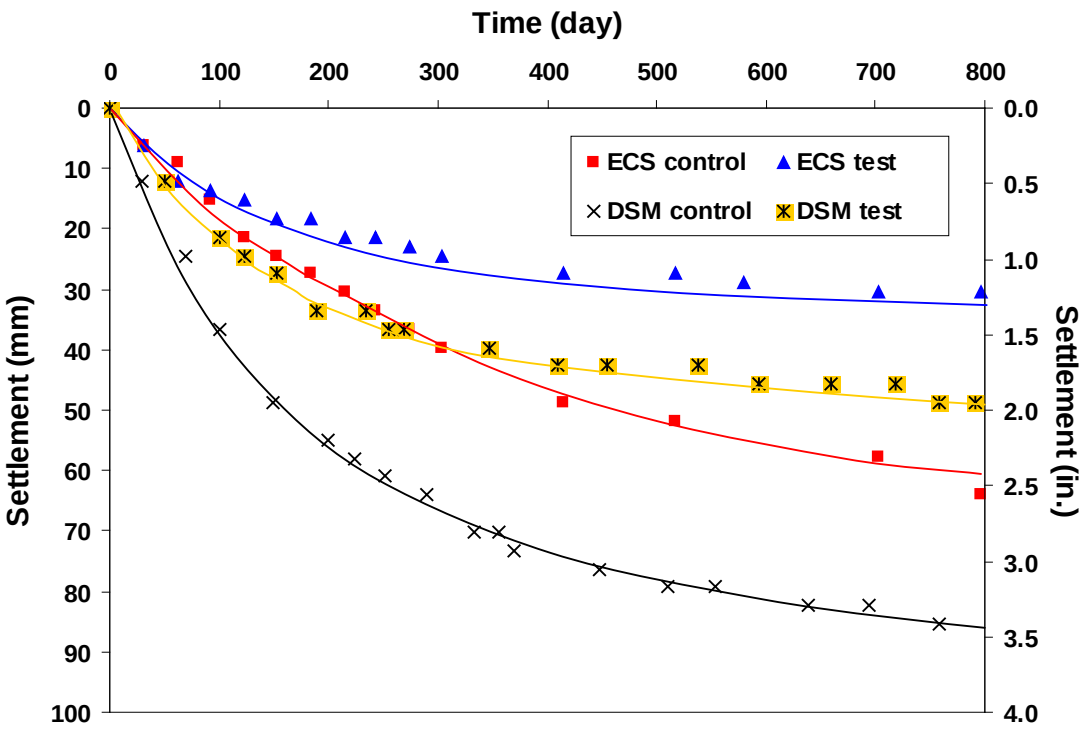

Figure 7.32. Monitored Settlement Values from DSM and ECS Sites.

7.5 PERFORMANCE COMPARISONS BETWEEN THE DSM AND ECS METHODS

The elevation survey data from the DSM (IH 30) and ECS (SH 360) sites were plotted to see the efficiency of each method in mitigating the embankment settlement. As shown in Figure 7.32, both the DSM and ECS products can be used to reduce the magnitude of the settlement. Within the same time duration, the embankment with the DSM support had a settlement of 2.0 in. (50 mm) while the embankment without the DSM support experienced a settlement of 3.5 in. (90 mm). The same trend was also found in the embankment constructed with the ECS that had a settlement of 1.25 in. (30 mm) while the embankment constructed without the ECS had the settlement value of 2.5 in. (60 mm). It is not practical to compare the amount of the settlement that occurred in the two different sites even though they were constructed on soft soil foundations. However, it is seen from these results that both mitigation techniques can be effectively employed to mitigate expected settlement that will occur at the bridge approaches.

7.6 SUMMARY

This chapter presents the collected data obtained in the field during the site visits on the DSM (IH 30, Arlington), ECS fill (SH 360, Arlington), and geopiers (SH 6, Houston) sites. Various types of instruments, horizontal inclinometer, vertical inclinometer, rod extensometer, and Sondex, were installed and used to monitor the soil movement in the horizontal and vertical directions at all three sites in the ontrol (untreated) and treated sections.

The data obtained in this chapter showed the efficiency of the mitigation methods used in the research by limiting the settlements induced by both embankment fill and foundation soils.

CHAPTER 8

NUMERICAL MODELING OF DSM AND LWF EMBANKMENT SECTIONS AND DEVELOPMENT OF DESIGN METHODS

8.1 INTRODUCTION

This chapter presents the results of numerical studies performed to understand the settlement behavior of the present embankments by using the commercially available geotechnical finite element software (Plaxis). The results of the laboratory testing presented in Chapter 5 were used as the input model parameters in the numerical analyses and the results from the finite element modeling (FEM) analyses were used to compare with the measured data obtained from the field to validate the models. The analyses were performed on the two test embankments described in Chapter 5. Once the modeling analyses were performed with satisfactory comparison results obtained, the modeling was extended to other embankment configurations using the same material properties by varying both the height and slope of the embankments. The area ratios of the DSM were varied in order to mitigate the settlements of the trial sections. The final outcome of these analyses led to the development of design charts for the DSM and the ECS sections.

8.2 FINITE ELEMENT MODELING

FEM analysis has been used as one of the numerical techniques for solving problems in the mechanics of continuous media (Bugrov, 1975). Nowadays, the FEM plays an important role in all branches of engineering for the analysis and design of the structures (Bathe, 2003). The analysis is typically performed by transforming the physical problem, an actual structure and structural components, into a mathematical model (Bathe, 2003). By using a series of algebraic equations, the numerical models can be solved and the quantities of the interested parameters, for example, stress, strain, and deformation at the points of interest, can be approximately obtained (Burde, 2004)

The FEM model consists of nodes and elements to form a finite element mesh of each structure. A typical two-dimensional mesh with six nodes is shown in Figure 8.1.

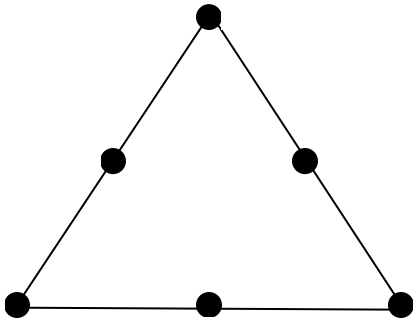

Figure 8.1. Six-Node Triangular Element (Plaxis Manual).

The nodes are not only the points where more than one or two elements connect to the others but also the points where the values of the primary variable of the interested parameter are calculated (Burde, 2004). In the FEM analysis, the values of the strain will be calculated and then interpolated for the entire structure. Later, a relationship between the stress-strain of a material behavior, usually termed as a constitutive law, is used to calculate the stress that has occurred in the mesh. Last, the force acting on each node obtained from the previous step will be calculated further to compute the nodal displacements by relating the nodal forces with stiffness equations.

For a one-dimensional (1D) consolidation, the phenomenon can be described by the following differential equation:

$$\frac{\partial p}{\partial t} = c_v \frac{\partial^2 p}{\partial z^2} \tag{8.1}$$

where

$$c_v = \frac{kE_{OED}}{\gamma_w}$$

$$E_{OED} = \frac{(1-v)E}{(1+v)(1-2v)}$$

$$Z = H - y$$

k is the permeability of the soil.

E is the Young's modulus.

υ is the Poisson's ratio.

γ_w is the unit weight of water.

E_{OED} is the oedometer modulus.

The analytical solution for Equation 8.1 in relation to p/p_0 as a function of time and position is presented by Verruijt (1983) and this equation is presented in the following:

$$\frac{p}{p_o}(z,t) = \frac{4}{\Pi}\sum_{j=1}^{\infty}\frac{(-1)^{j-1}}{2j-1}\cos\left[(2j-1)\frac{\Pi}{2}\frac{y}{H}\right]e^{\left[-(2j-1)^2\frac{\Pi^2}{4}\frac{c_v t}{H^2}\right]} \qquad (8.2)$$

Figure 8.2 presents the results of both numerical and analytical methods. The dotted lines are the results from the analytical method and the solid lines are the results from the numerical method. The results from both methods are close.

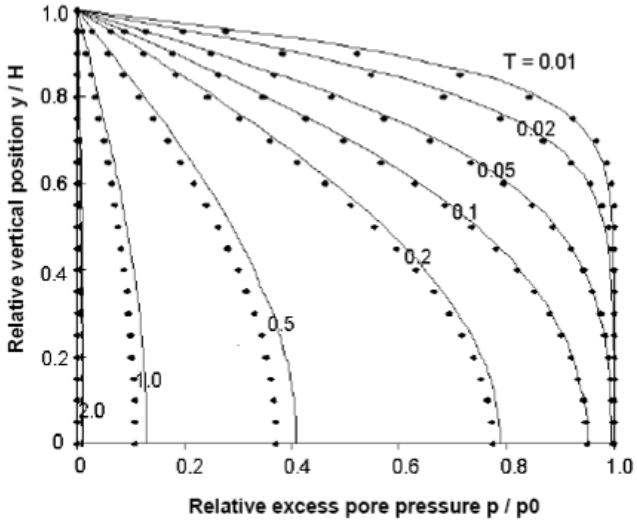

Figure 8.2. The Results of Excess Pore Pressure as a Function of Height from the Numerical and Analytical Methods (Plaxis Manual).

8.3 MODELING OF THE DSM AND CONTROL SECTIONS

8.3.1 Test Embankment Section

8.3.1.1 Geometry and Boundary Conditions of the DSM Columns Model

From the previous chapters, a cross-section and subsurface profile of the embankment passing through the installed rod extensometer is shown in Figure 8.3. The embankment has a total height of 19 ft (6 m) from an existing ground surface and has a side slope of 1V:4H. This section was used in the model to analyze the soil movements occurring within and underneath

the embankment. The embankment was constructed on soft clay with a thickness of 26 ft (8 m) underlain by 10 ft (3 m) of thick hard shale. The soil cement columns have a diameter of 4.0 ft (1.2 m) with a center-to-center spacing of 5.5 ft (1.67 m). However, in numerical analysis, instead of using the diameter of the DSM columns, the area-ratio (a_r) between the DSM and natural soil was used as described in Chapter 4. The area ratio (a_r) with the triangular arrangement using the 4 ft (1.2 m) diameter columns per Equation 8.3 is 0.50.

$$a_r = \frac{\frac{1}{2} a_{col}}{a_{soil} + \frac{1}{2} a_{col}} \tag{8.3}$$

$$a_r = \frac{\frac{1}{2}\pi \frac{(4)^2}{4}}{(\frac{1}{2} x 5.5 x 5.5 x \frac{\sqrt{3}}{2})} = 0.48 \approx 0.50$$

The columns were constructed with their bases placed on top of the hard shale layer. Therefore, the lengths of the columns used in this numerical analysis were equal to the thickness of the soft clay layer at 26 ft (8 m). The geometry of the embankment, modeled together with the boundary conditions, is shown in Figure 8.3.

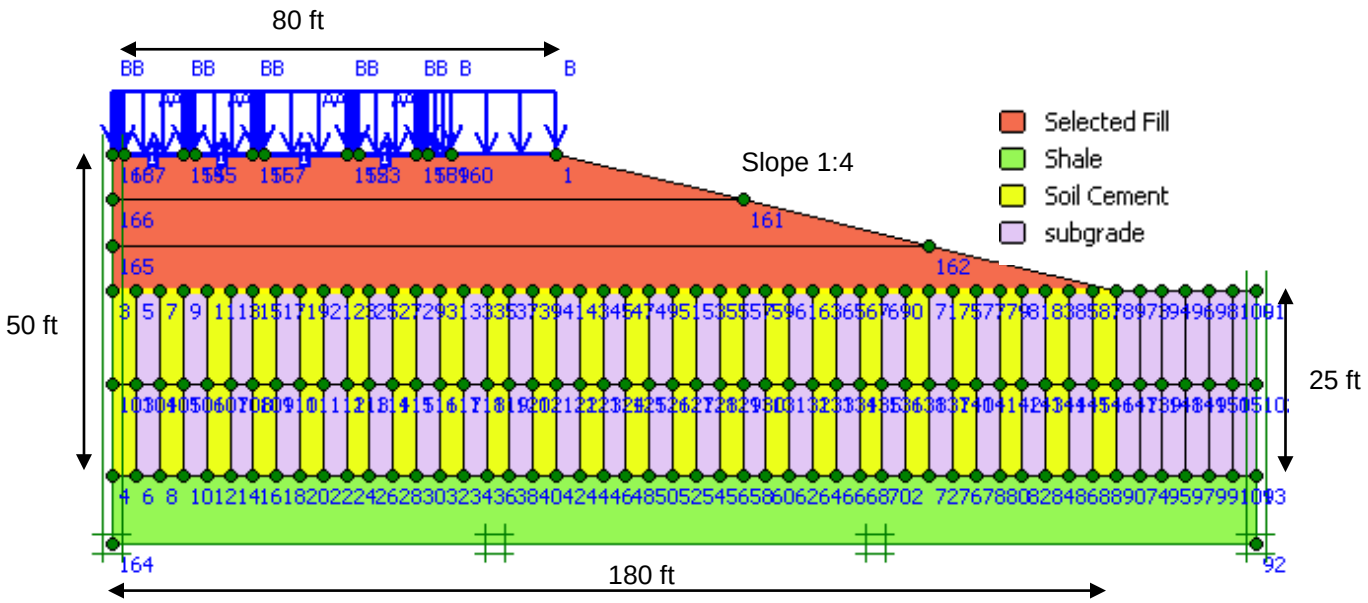

Figure 8.3. Geometry and Boundary Conditions of the DSM Columns Model.

8.3.1.2 Material Property Values in a Numerical Analysis

A soft soil model was used in this study to simulate a natural soft clayey soil while a stiffer soil was used to simulate the DSM treated foundation soils. Most of the deep-mixed and soft clay material strength and stiffness values comes from the unconfined compressive strength tests. The secant values from Young's modulus of elasticity were determined at 50% of the unconfined compressive strength E_u^{50}. The Poisson's ratio value used for the DSM section is equal to 0.25.

Since this research study focused on the long-term settlement behavior of the embankments supporting approach slabs, the short-term embankment settlements, during the construction stage, were disregarded in the analysis. The analysis was calculated by using a consolidation based model and carried out until the ultimate pore pressure state was reached or until the excess pore water pressure that developed during embankment loading was completely dissipated. The behavior of the reinforced concrete approach slab was assumed as a perfectly-plastic material. The displacement of the boundary at x=0, y=0 was restricted in all directions as well as the boundaries at the points of the base. The material properties used in the analysis are given in Table 8.1.

Table 8.1. Properties and Model Type of the Materials Used in the Model Analysis.

	Unit	Select Fill	Soft clay	DSM columns	Hard shale
Model type		Soft soil model	Soft soil model	Hardening Soil Model	Hardening Soil Model
Moist density, γ_m	pcf	107	110	110	119
Saturated density, γ_s	pcf	124	122	122	138
Elastic modulus, E^{50}_{ref}	psf	-	-	365,270	436,496
Poisson's Ratio	-	-	-	0.2	0.2
Cohesion, c	psf	830	540	3130	8830
Friction Angle, φ	°	5	5	40	10
Permeability, k	ft/min	2×10^{-6}	2×10^{-6}	2×10^{-6}	2×10^{-6}
Compression Index, C_c	-	0.265	0.39	0.263	0.02
Recompression Index, C_r	-	0.010	0.047	0.041	0.003
Over Consolidation Ratio, OCR	-	-	2.5	5.0	10.0
Initial void ratio, e_o	-	0.60	0.80	0.80	0.50

8.3.1.3 Discretization of the DSM Treated Section

The numerical analysis was performed using Plaxis software version 8.6. A two-dimensional, plain-strain model with 6-node triangular elements was used to model the soil layers and the DSM column mesh details as shown in Figure 8.4. The embankment in the model consisted of four types of material being select fill, shale, soil-cement, and natural subgrade soil. In Figure 8.4, geogrid is shown as a yellow line drawn between the embankment and its foundation. On the top left of the model, the approach slab is shown as a blue line having a length equal to the width of the slab in the field.

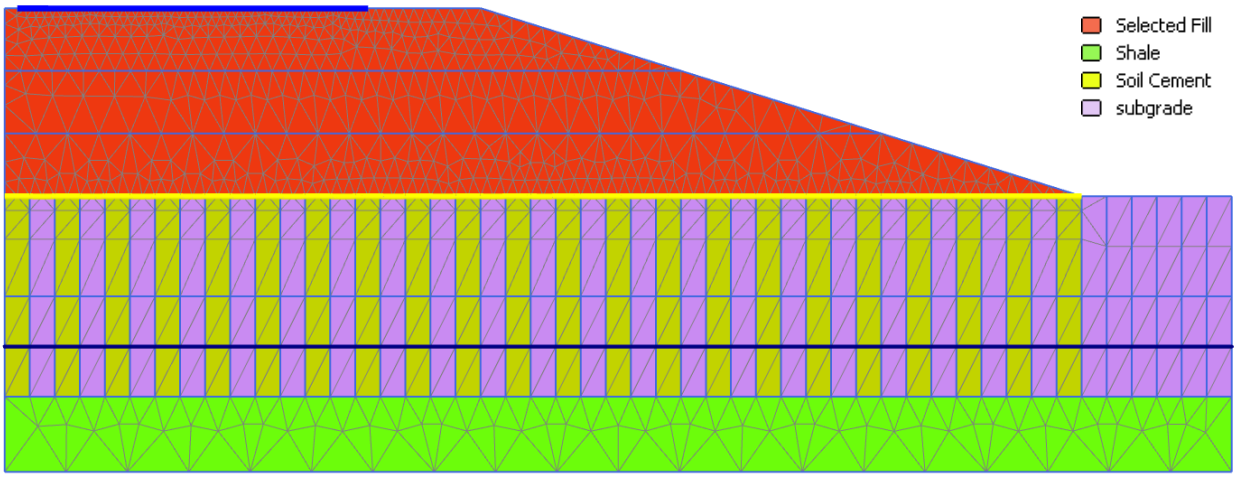

Figure 8.4. Finite Element Mesh of the DSM Treated Section.

8.3.1.4 Settlement Analysis

For the settlement analysis, a finite element modeling program was used in this research. The model consisted of a total height of the embankment of 20 ft (6 m) and was divided into three layers to simulate different phases during the embankment construction as shown in Figure 8.4.

Figure 8.5 presents the construction phases in the numerical analyses. The duration of the embankment construction for each layer was 25 days, and thereafter, the embankment was left to be consolidated for another 25 days in the second stage. In the initial stage, the soil self-weight was used as a parameter that induced soil stress. In the second stage, each layer in the embankment is modeled for consolidation. The embankment construction is simulated in that way until the whole embankment construction is completed. The simulation is done such that it replicates the compaction effort performed in real practice. After the completion of the last layer of the embankment, the whole embankment is compacted by applying a uniform load. The highway pavement is constructed after the compaction of the embankment and the calculation of the settlement was reset to zero. After the completion of the highway pavement construction, traffic load is applied. The model was analyzed by using a combined gravity load of the material and the traffic load equal to 11.6 psi (80 kN/m^2).

Identification	Phase no.	Start from	Calculation	Loading input	Time	Wa...	First	Last
Initial phase	0	0	N/A	N/A	0.00 ...	0	0	0
<Phase 1>	1	0	Plastic analysis	Staged construction	25.0...	1		
<Phase 2>	2	1	Consolidation ana...	Staged construction	25.0...	2		
<Phase 3>	3	2	Plastic analysis	Staged construction	25.0...	3		
<Phase 4>	4	3	Consolidation ana...	Staged construction	25.0...	4		
<Phase 5>	5	4	Plastic analysis	Staged construction	25.0...	5		
<Phase 7>	7	5	Consolidation ana...	Staged construction	25.0...	7		
<Phase 11>	11	7	Consolidation ana...	Staged construction	60.0...	11		
<Phase 10>	10	11	Consolidation ana...	Staged construction	70.0...	10		
<Phase 8>	8	10	Consolidation ana...	Staged construction	200....	8		
<Phase 12>	12	8	Consolidation ana...	Staged construction	1000...	8		
<Phase 9>	9	12	Consolidation ana...	Staged construction	2000...	9		
<Phase 6>	6	9	Consolidation ana...	Minimum pore pressure	1000...	9		

Figure 8.5. Calculation Phase in the Settlement Calculation.

To validate the results of the numerical analysis, five points were selected for studying the soil movements on top of and within the embankment system. Point A was selected to study vertical displacements occurring in a pavement with Point E used to obtain the displacement occurring at the edge of the approach slab. Points B, C, and D were located at the exact coordinates where the rod extensometers were anchored in the field and at the depths of 10, 20, and 40 ft (3, 6, and 12.2 m), respectively. In addition, another interesting location for analysis is at the edge of the approach slab and all these are seen in Figure 8.6.

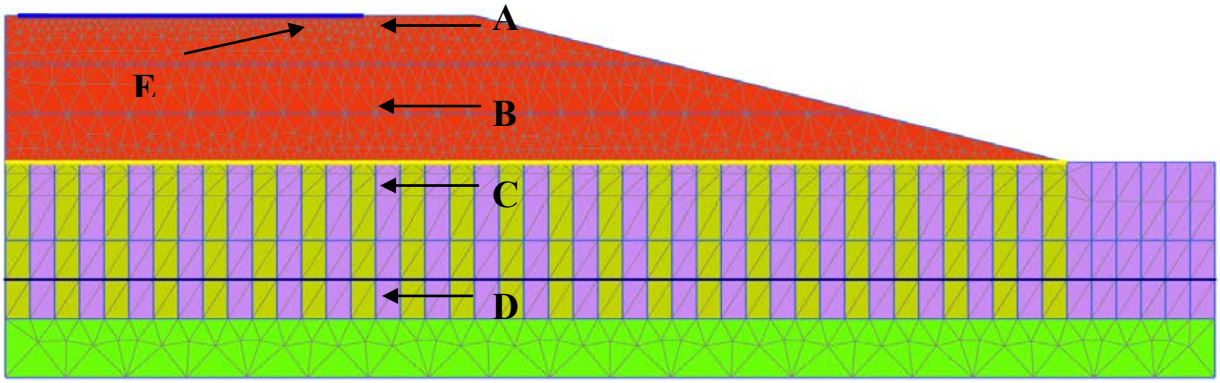

Figure 8.6. Observation Points in the Settlement Calculation.

8.3.1.5 Results of the FEM Model Analysis

The results from the FEM model analysis are presented in Figures 8.7 through 8.10. Figure 8.7 presents the deformed mesh after the construction of the approach slab with a magnification scale of 1:20. The maximum displacement in this analysis is equal to 3.5 in. (0.090 m) and this occurs in the right side of the slab. The elements from the DSM columns and

the natural subgrade soil are also deformed in the same area indicating that the settlement of the subgrade soil can affect the displacement of the approach slab above it.

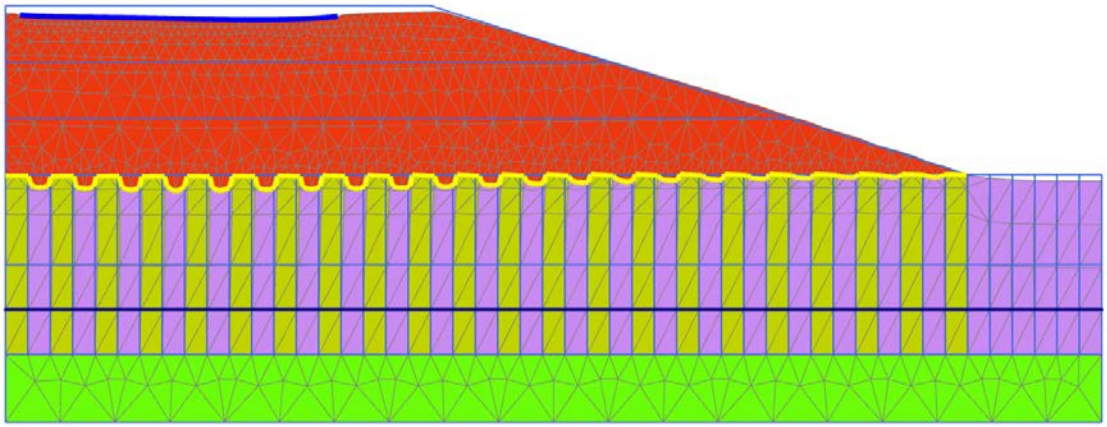

Figure 8.7. Deformed Mesh of the Model (Magnified 50 Times).

Figure 8.8 shows the total displacements occurring in the embankment. In this figure, the maximum total displacement occurs on the right side of the slab and the influence area starts from the top of the embankment down to a depth of 20 ft (6 m) below the surface of the natural subgrade soil. In addition, the affected area is mostly located under the embankment while the soft subgrade beyond the embankment is influenced very little.

Figure 8.9 shows the horizontal soil movements. The horizontal movements occur either under the embankment slope or beneath the approach slab but not within the zone of observation. Figure 8.10 presents the vertical soil displacements. The pattern of color shades from the results of the vertical movements is quite similar to the pattern from the results of total movements shown in Figure 8.8, which means that the vertical movement is the predominant factor in this study.

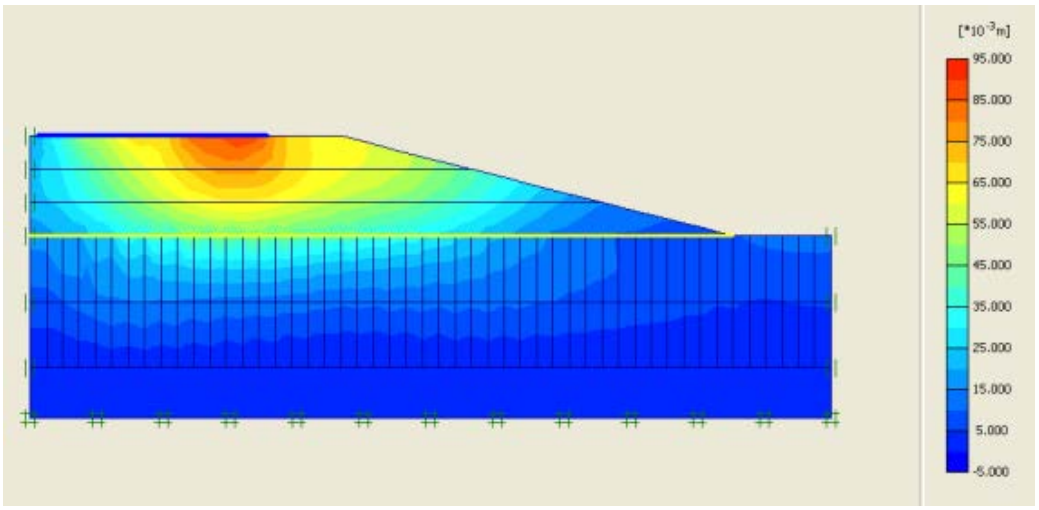

Figure 8.8. Total Displacements in the Embankment.

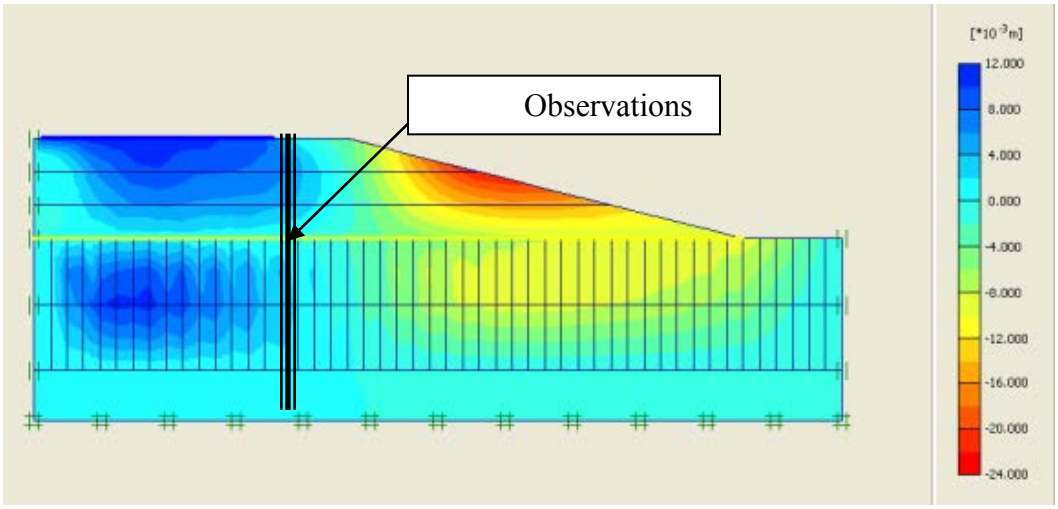

Figure 8.9. Horizontal Displacements of the Model.

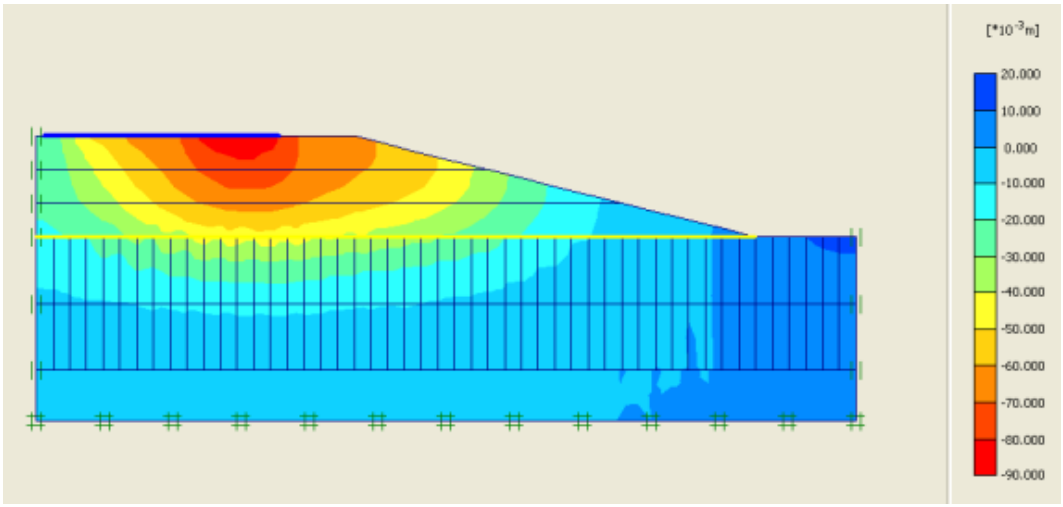

Figure 8.10. Vertical Displacements of the Model.

8.3.1.6 Validation

In this section, the results of the model analysis are compared with the data from the field studies. These comparisons were performed in order to validate the parameters used in the model analysis and to see whether or not they can be good representatives of the real soils. Figures 8.11 through 8.14 present the data comparisons, which were performed according to the directions of the soil movements. For example: 1) vertical displacements—used data obtained from the horizontal inclinometer, elevation surveys, rod extensometer, and Sondex field monitoring studies, and 2) lateral movements—used data monitored from the vertical inclinometer surveys. If the comparisons showed good agreement, then the validated model was planned to be used further for determining the ground improvement variables for a variety of embankment designs.

8.3.1.7 Comparisons in the Vertical Displacements

8.3.1.7.1 Data Comparisons with the Horizontal Inclinometer

The data obtained from the horizontal inclinometer are the vertical displacements that occurred beneath the approach slab and these are shown in Figure 8.11a. The total settlement of 1.38 in. (35 mm) occurred within the first 100 days after installation of the horizontal inclinometer, and thereafter, the settlement gradually increased to a maximum of 1.70 in. (43 mm) after completion of 500 days. Around that time, the inclinometer casing was broken and no more data were collected. The settlement trend is shown in Figure 8.11b where the rapid increase in the settlement is seen in the first 100 days before the settlement gradually increased to the maximum settlement value of 1.65 in. (42 mm).

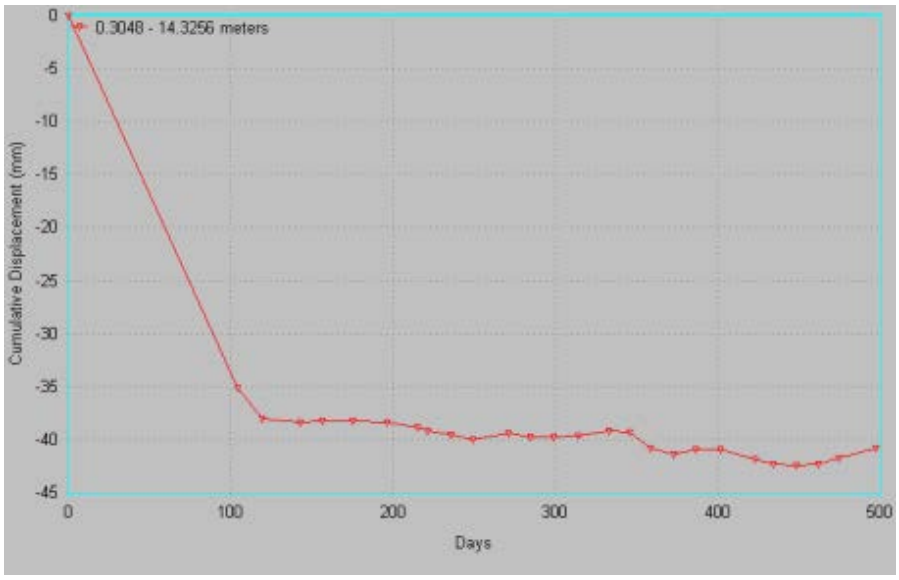

(a)

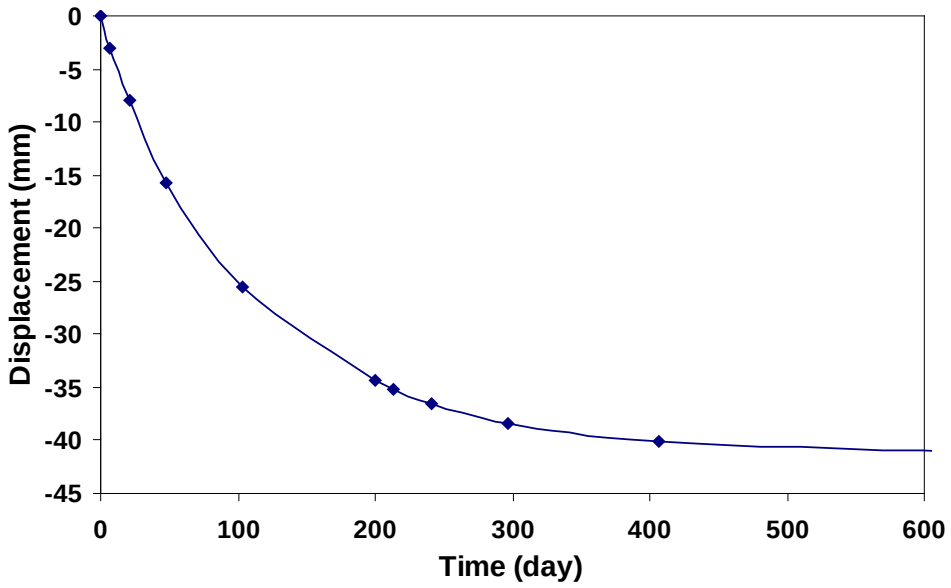

(b)

Figure 8.11. Vertical Displacements (a) from the Horizontal Inclinometer and (b) from the Numerical Analysis.

8.3.1.7.2 Data Comparisons with the Elevation Surveys

Another data comparison was performed by plotting the data from the elevation surveys presented in Table 7.1 of Chapter 7 with the results from the numerical analysis. The comparisons are shown in Figure 8.12. The time-settlements of the present comparison are in a

good agreement with each other. Even though the settlement values from the recent elevation surveys are slightly larger than the results from the model, the prediction on the whole is still in agreement with the measured data.

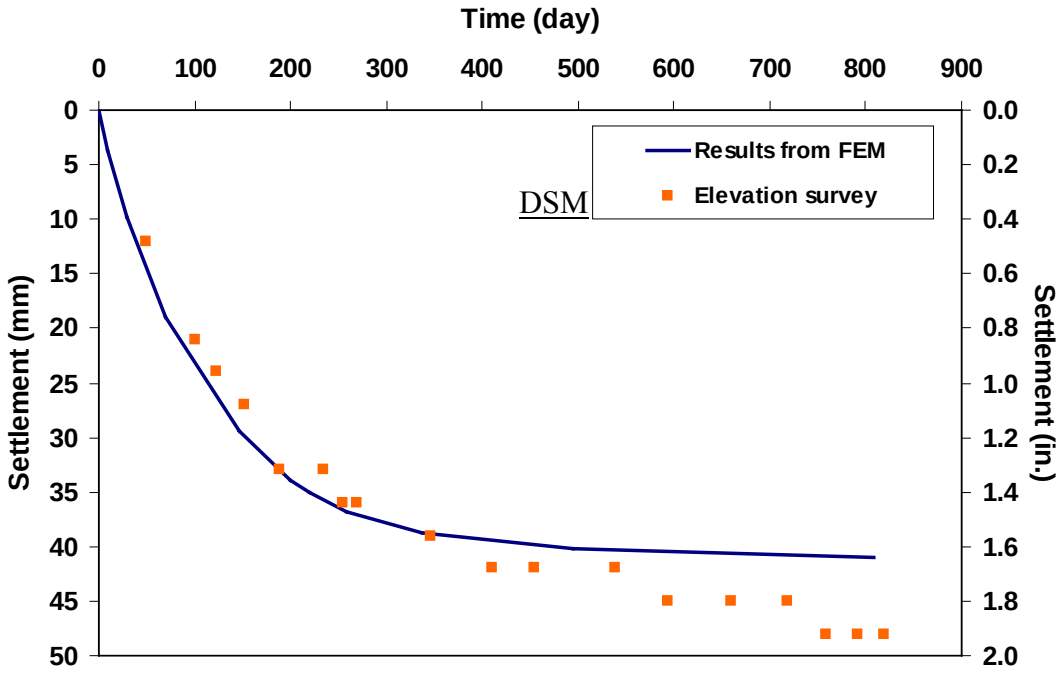

Figure 8.12. Comparison of Vertical Displacements in a Treated Section between Data Obtained from Elevation Surveys and Results from Numerical Analysis.

8.3.1.7.3 Data Comparisons with the Rod Extensometers

Data obtained from the automatic and the manual reading rod extensometers were plotted versus the results from the FEM numerical modeling and are shown in Figures 8.13 and 8.14, respectively. From both figures, the settlements of the soils at the different depths obtained from the FEM model have the same trends as the settlement values obtained from the field. The displacement values at the depth of 10 ft (3 m) are more than the measured values with a small difference of 0.04 in. (1 mm) between them. Overall, the settlement readings are in agreement with the numerical modeling results.

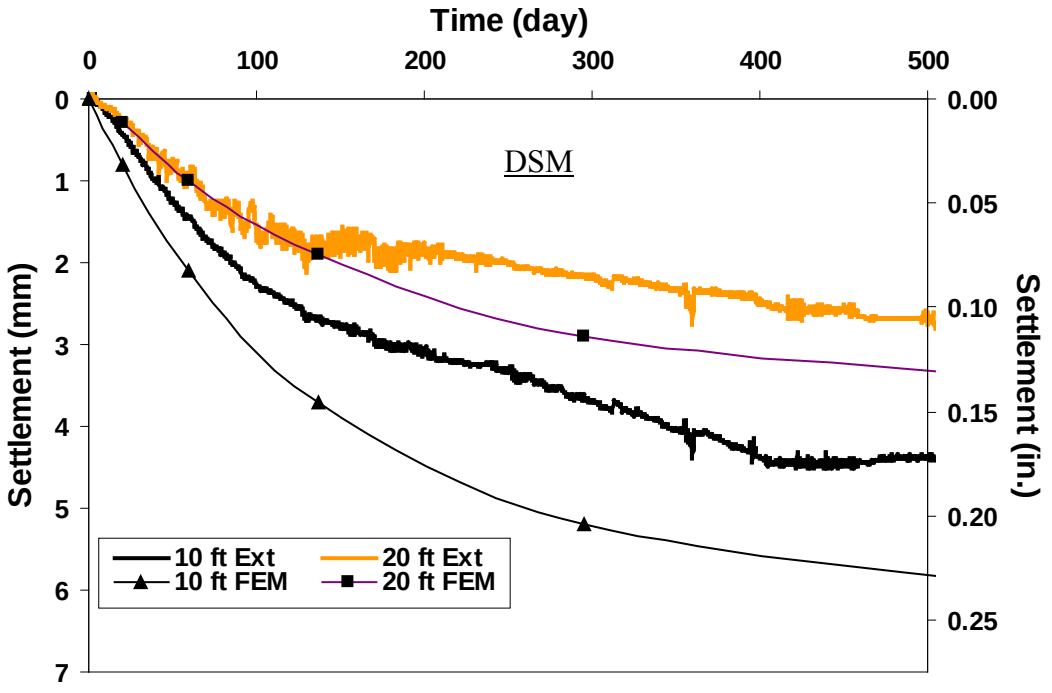

Figure 8.13. Comparison of the Vertical Displacement Values between the Data Obtained from the Automatic Extensometer and Results from the Numerical Analysis.

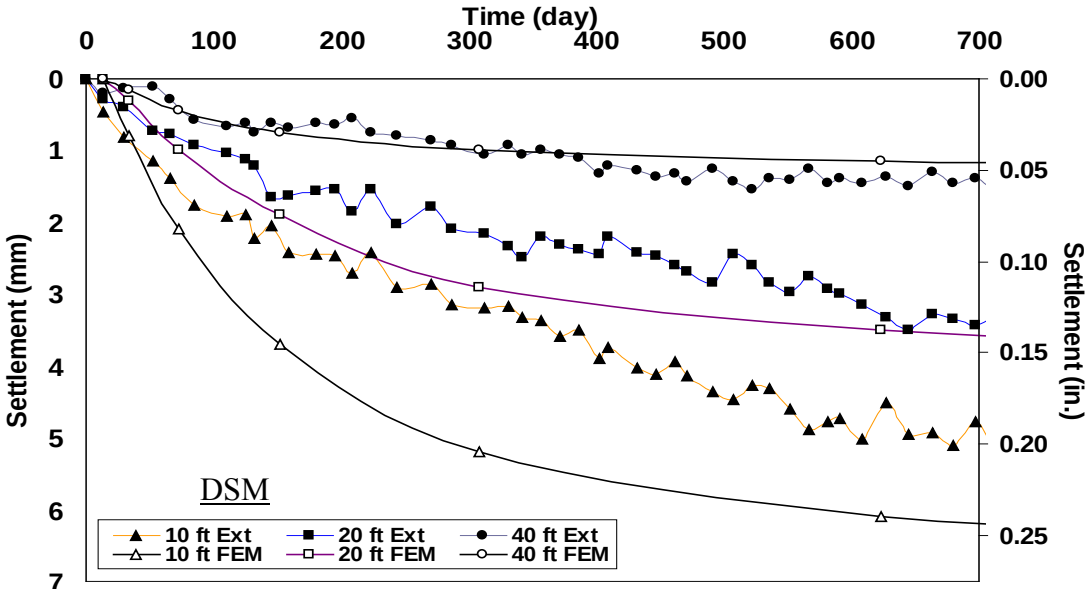

Figure 8.14. Comparison of the Vertical Displacement Values between the Data Obtained from the Manual Extensometer and Results from the Numerical Analysis.

8.3.1.8 Comparisons in the Horizontal Displacements

8.3.1.8.1 Data Comparisons with the Vertical Inclinometer

The lateral movements measured from the vertical inclinometer surveys were plotted and compared with the results of numerical analysis as shown in Figures 8.15a and b, respectively. As previously mentioned in Section 8.3.1.5, the numerical analysis yields only small values of lateral soil movements in the area where the vertical inclinometers were installed. However, when the maximum value of 0.36 in. (9.28 mm) is compared with the lateral displacement in the direction of the B-axis obtained from the field, the FEM analysis give results close to the data from the field. Although it is concluded from the previous chapter that the lateral movements are considered insignificant in the study of the DSM site, the results of the numerical analysis still prove that the soil parameters and other configurations used in the study have provided results that are in a good agreement with the performance of the test section and soils in the field.

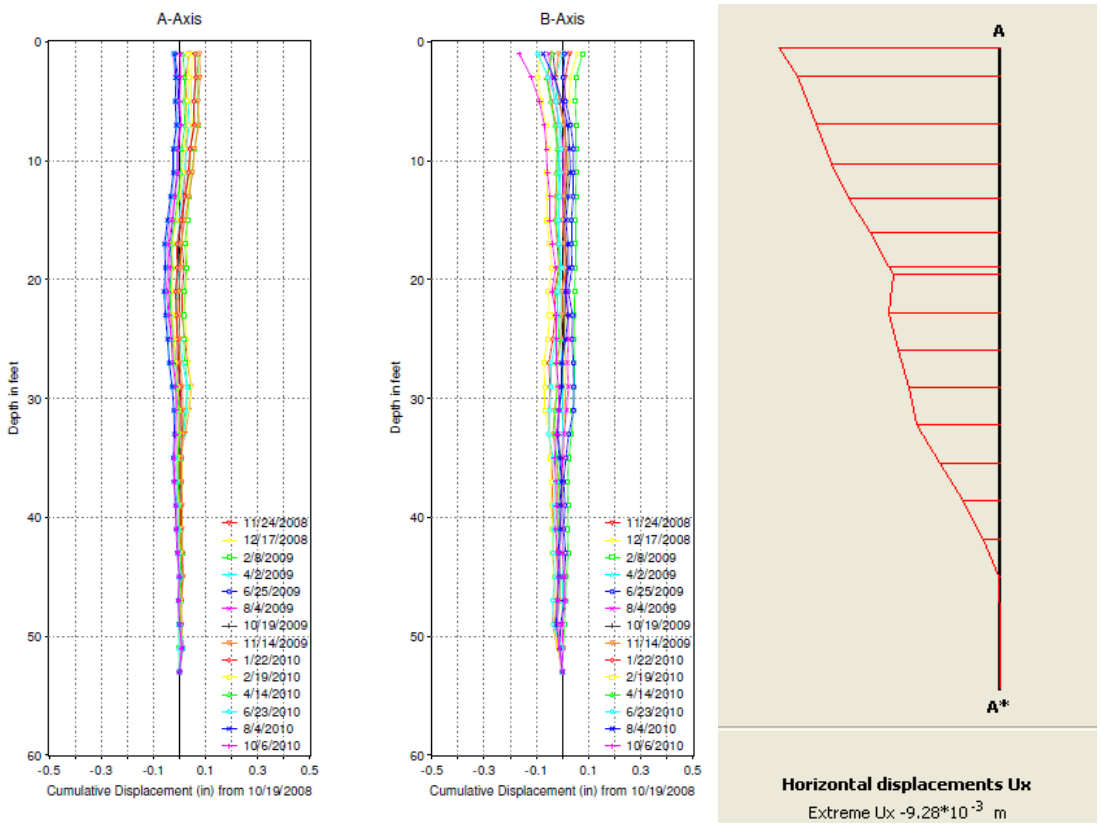

(a) (b)

Figure 8.15. Lateral Soil Movements (a) from the Vertical Inclinometer and (b) from the Results of the Numerical Analysis at the Location of the Inclinometer.

8.3.2 Control Embankment Section

To comprehend how the DSM columns lessen the settlement in the embankment, numerical analyses were also performed on the control embankment and then compared with the values from the treated section analyses. The control section is the embankment located on the north end of the Center Street bridge over IH 30. This embankment was constructed over the natural subgrade without any soil treatment or any support by DSM columns. Therefore, this control embankment section is labeled as an untreated section. In the untreated section, there was only one vertical inclinometer casing and one Sondex installed in the median of the four-lane divided street.

8.3.2.1 Geometry, Boundary Conditions, and Discretization of the Control Section

The geometry and boundary conditions used in the untreated section are similar to the ones used in the treated section. Both sections have a four-lane with a raised median and curb and gutter pavement section. Therefore, the embankment section is symmetric around a vertical line on the left side shown in Figure 8.16. Since the control section is the embankment without any support from the DSM columns, the numerical analyses on the control section were performed by removing the DSM elements and their input parameters from the modeling and then replacing the DSM elements with the soft subgrade and its properties as shown in Figure 8.16. Apart from changing the number of the elements and nodes, and boundary conditions are the same as used in the treated section analyses.

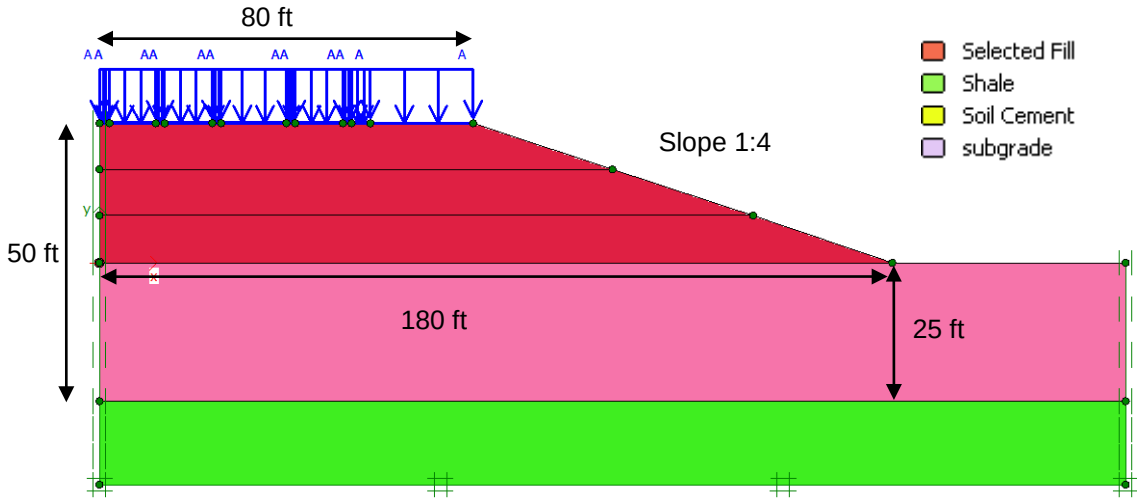

Figure 8.16. Geometry and Boundary Conditions of the Untreated Section in a Model.

8.3.2.2 Settlement Analyses

In the settlement analyses, the embankment section with a total height of 20 ft (6 m) is divided into three layers identical to the DSM treated section. The duration of the construction phases, including the calculation model, load multiplier factor, and traffic load in the treated section analysis was used here. The difference between this analysis and the treated section was the location of Points A, B, C, and D as shown in Figure 8.17.

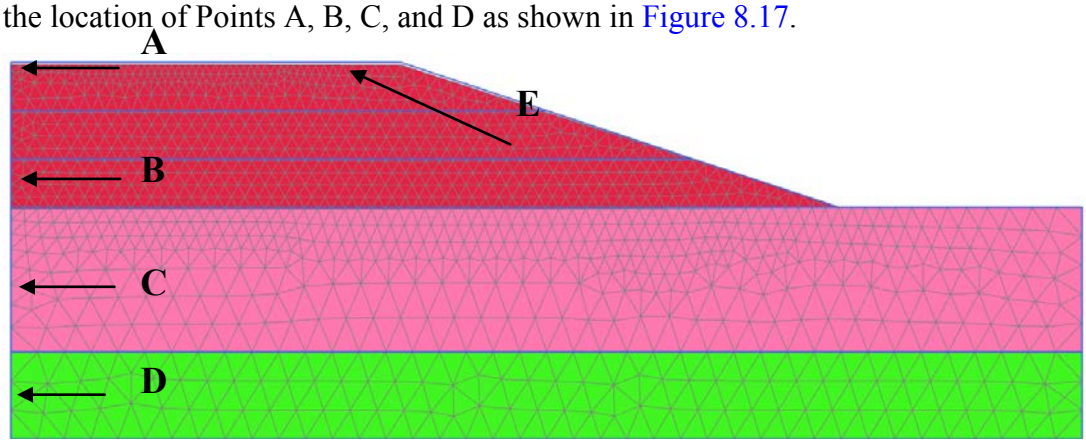

Figure 8.17. Observation Points in the Settlement Calculation.

Point A is a location in the control section where the elevation survey was performed. Points B, C, and D are the locations where the Sondex sensor rings were located and these points were selected such that they could be used for the settlement comparisons between the treated and the untreated sections.

8.3.2.3 Results of the Numerical Analysis

Figures 8.18 through 8.21 show the results from the numerical analysis. In Figure 8.18 the highest settlement recorded is 11 in. (0.28 m), occurring near the slope of the embankment. Additionally, the subgrade layer, especially in the area under the crest of the embankment, experienced more settlement than the outer slope area. The results of the total displacements that occurred in the embankment are shown in Figure 8.18.

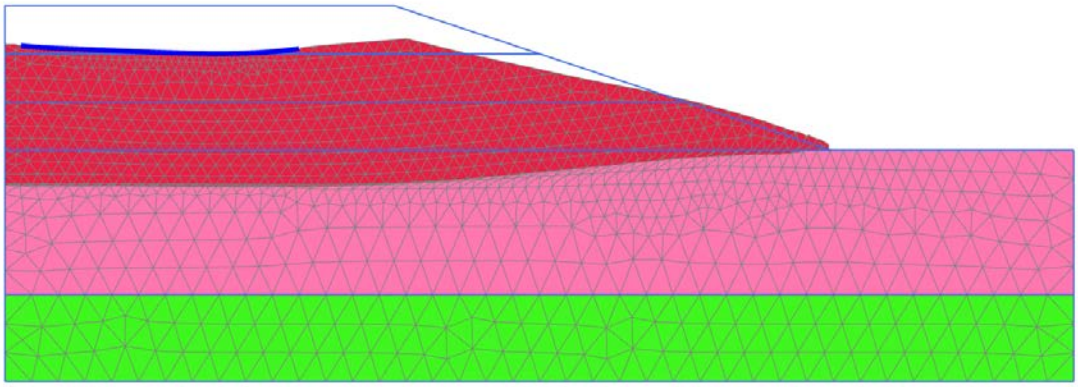

Figure 8.18. Deformed Mesh of the Model (Magnified 50 Times).

In Figure 8.19, the maximum total displacement occurred at the top right corner of the embankment and the influenced or stressed area starts from the top of the embankment to a depth of 20 ft (6 m) below the surface of the natural subgrade. This observation is similar to the one noted from the treated section analysis. In addition, the affected area is mostly located underneath the embankment, while the soft subgrade beyond the embankment location has been influenced less.

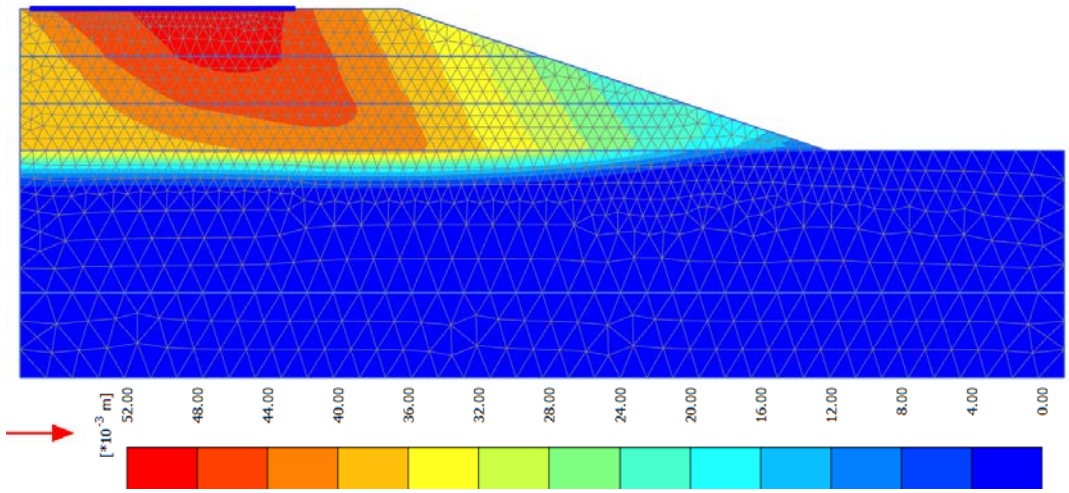

Figure 8.19. Total Displacements in the Embankment.

Figure 8.20 presents the horizontal soil movements within and outside the control untreated embankment section. From the plot, large horizontal soil movements occurred near the outer slope whereas small movements are shown in the area close to the center line. Figure 8.21 presents the results of the vertical soil displacements that show that they look similar to the

results of the total movements in Figure 8.19. The similarity of those two figures signifies that the vertical displacement is a predominant factor in the study.

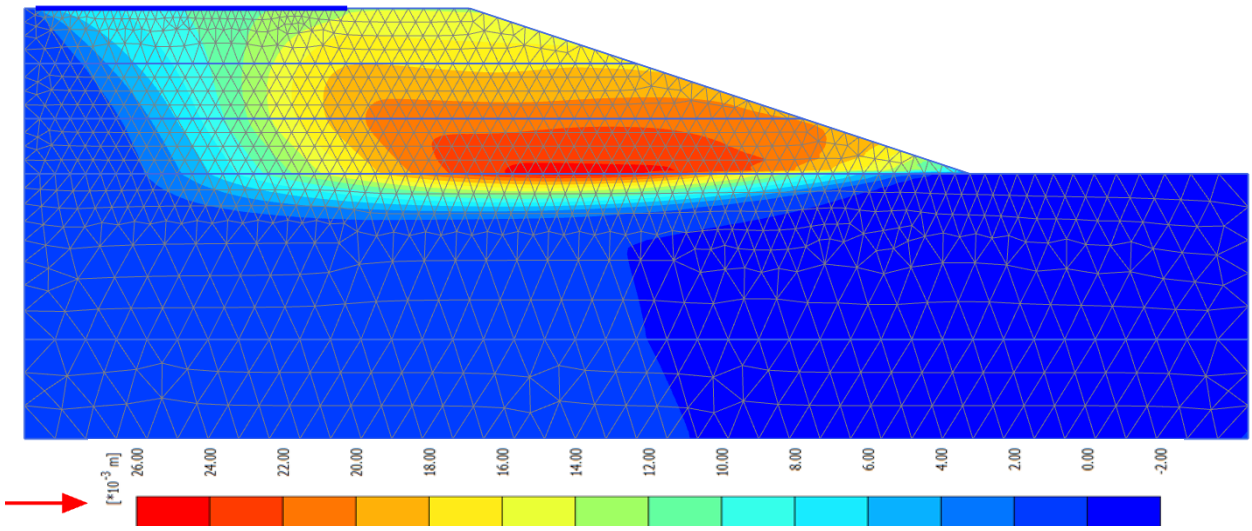

Figure 8.20. Horizontal Displacements of the Model.

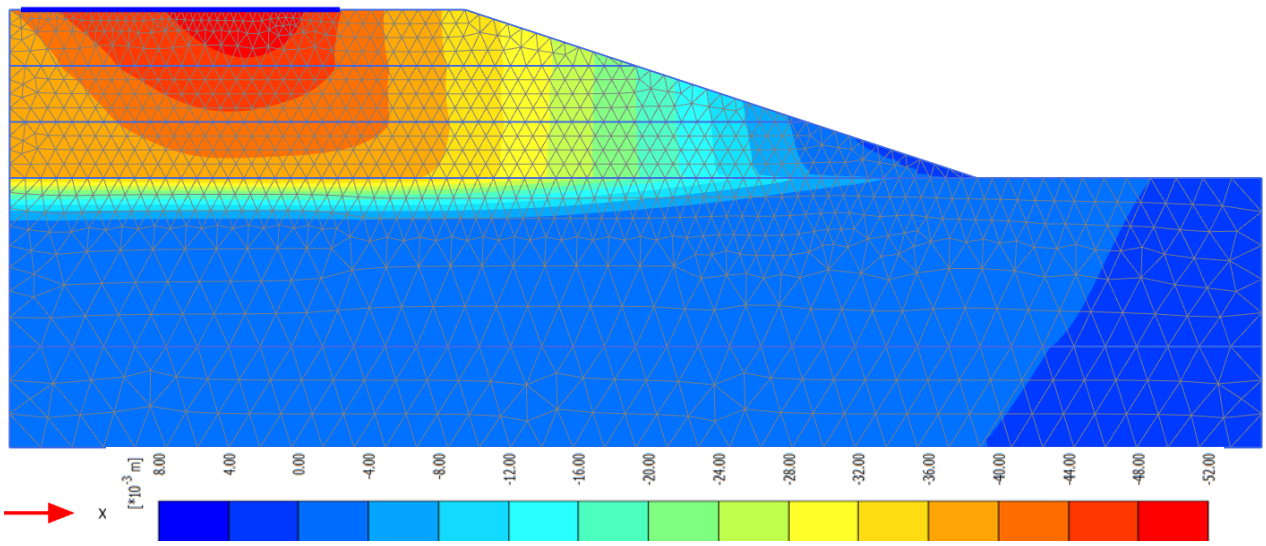

Figure 8.21. Vertical Displacements of the Model.

8.3.2.4 Validation

The results from the numerical analysis are compared with the monitored data from the field to evaluate whether the numerical model, including its parameters, are in agreement with the soil movement behavior seen in the field. The same data from the elevation surveys and Sondex in the treated section were used to compare against the results of the vertical soil

movements from the FEM model. The data recorded from the vertical inclinometer were compared with the lateral soil displacements. The data comparisons are presented in Figures 8.22 and 8.23. Figure 8.22 shows the graph plotted between the vertical displacements from elevation surveys and the results from the numerical model. The comparison of the lateral soil displacements is shown in Figure 8.23, which shows the monitoring data and the movements obtained from the numerical modeling using the FEM software.

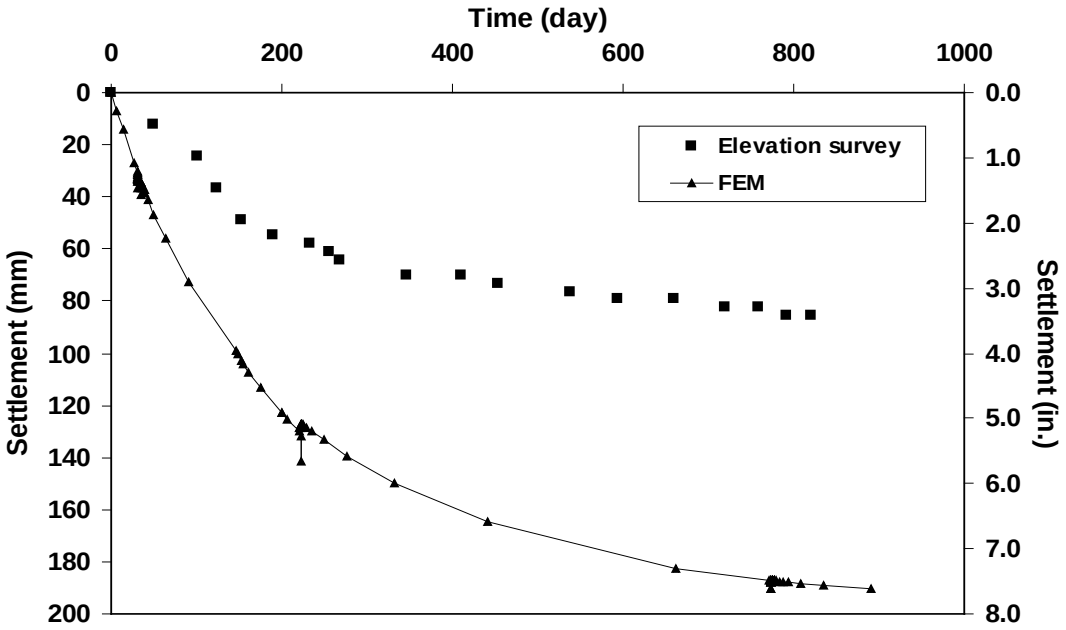

Figure 8.22. Comparison of the Control Section Vertical Displacement Values and the Data Obtained from the Elevation Surveys and Results of the Numerical Analysis.

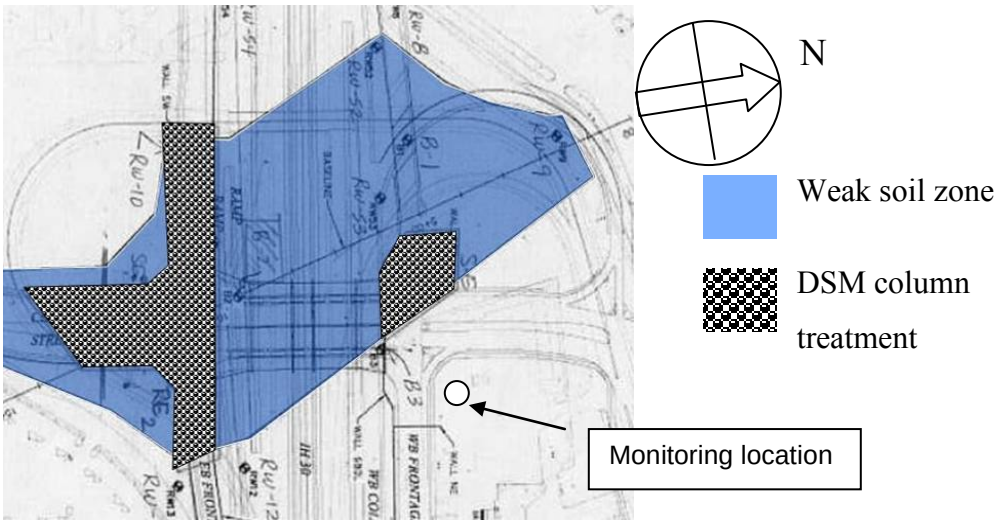

Figure 8.23. The Monitoring Location in the Control Section.

8.3.2.5 Comparisons in the Vertical Displacements

8.3.2.5.1 Data Comparisons with the Elevation Surveys

The data from the elevation surveys shown in Table 7.2 were plotted against the results of the vertical soil displacements from the FEM model as shown in Figure 8.22. The time-settlement relationship from the numerical analysis is much higher than the time-settlement curve from the elevation survey. This result reveals that the numerical model used to predict the soil displacement in the control section was not an excellent match possibly due to the control section soil properties being different from the assumptions used in the analysis. The location chosen for the control section is not located in a weak soil zone as per the site characterizations. The subgrade soil in this area has better engineering properties than the subgrade soil in the DSM treated section. However this section was chosen as a reference since this site was not underlain by the DSM columns. The settlement values from the elevation surveys at this site are small when compared with the results from the numerical analysis, which used weaker soil properties in the analysis. However, if the south embankment was constructed without the DSM columns, large vertical displacement of 7.1 in. (0.18 m) would have been experienced resulting in the settlements at the bridge approach sections.

8.3.2.5.2 Data Comparisons with the Sondex

The untreated section has settlement values less than the amount of the DSM treated section due to stronger properties of the subgrade soil in the area. Therefore, no comparison is presented and the data from the Sondex readings reported in Chapter 7 revealed that even without the DSM columns, the vertical soil movements monitored in the field fluctuated in a range of ±0.6 in. (1.5 cm), which is attributed to stronger foundation soil in the north embankment.

8.3.2.6 Comparisons in the Horizontal Displacements

8.3.2.6.1 Data Comparisons with the Vertical Inclinometer

Figures 8.24a and b show the lateral movements measured in the vertical inclinometer and the results of the lateral movements from the numerical analysis, respectively. In this analysis, the lateral displacements in the A-axis from the vertical inclinometer were chosen since it has the same movement direction as in the cross-section. Although the magnitude of the lateral

displacements in both figures are almost the same at 0.1 in. (2.54 mm) and 0.12 in. (2.99 mm), the comparison of them to validate the numerical model can be disregarded. These two small displacement values reveal that the horizontal displacements are insignificant in this study.

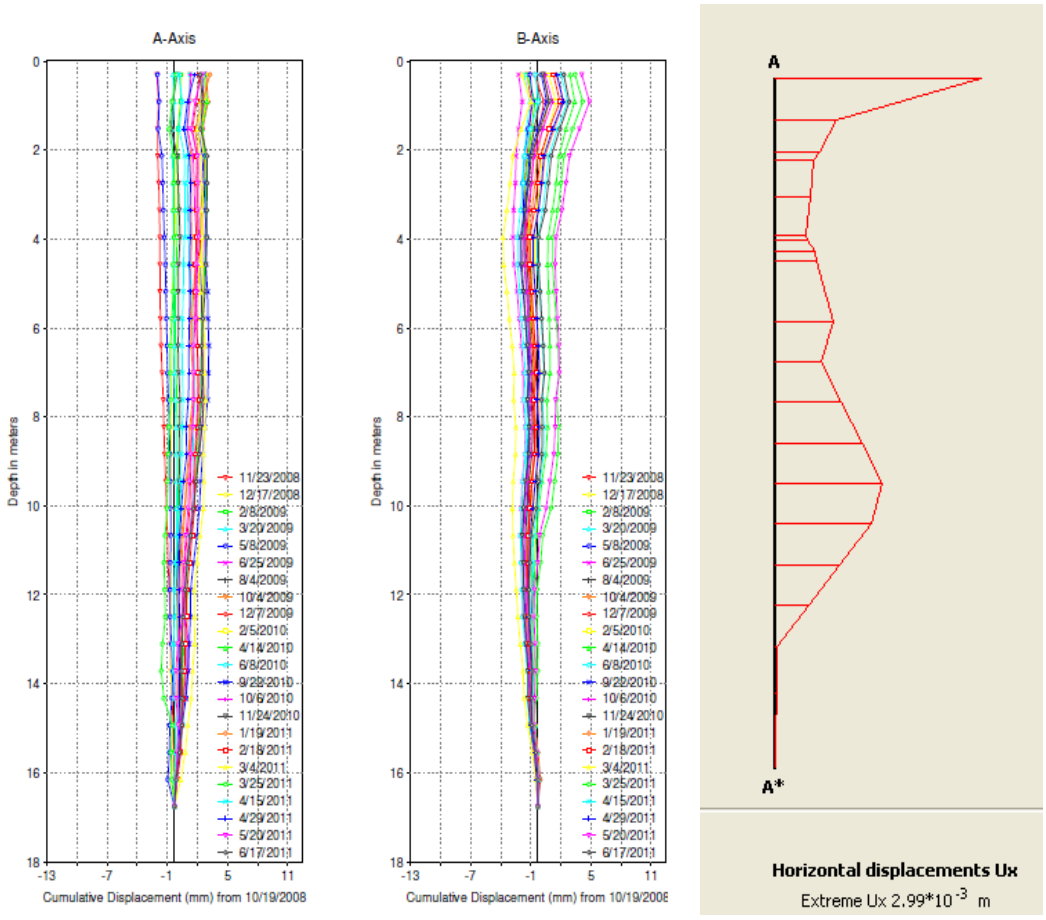

(a) (b)

Figure 8.24. Lateral Soil Movements (a) from the Vertical Inclinometer (b) from Results of the Numerical Analysis at the Section of the Inclinometer.

8.3.3 Comparisons of the Vertical Soil Movements that Occurred between the Treated and the Untreated Embankments

From the previous subsection, the horizontal soil movements were not significant in the study of the DSM treated section. Therefore, only the soil movements in the vertical direction were considered. Since the subgrade soil in the control section was different from the soil in the DSM test section, the comparison between the soil movements between both sections was meaningless. Therefore, to determine the effectiveness of the DSM columns in mitigating the

settlement that occurred in the embankment, the data from the elevation surveys on the treated embankment were used to compare with the results from the numerical analysis performed on the control section. To do that, the vertical displacements at Point A as shown in Figure 8.6 were compared with the displacement values at Point E as shown in Figure 8.17, and the comparison of the vertical soil movements is presented in Figure 8.25. The embankment with the DSM columns experienced only one-fourth the magnitude of the settlement that occurred in the untreated embankment. This smaller settlement can reduce the bump problem that might occur at the bridge approach area.

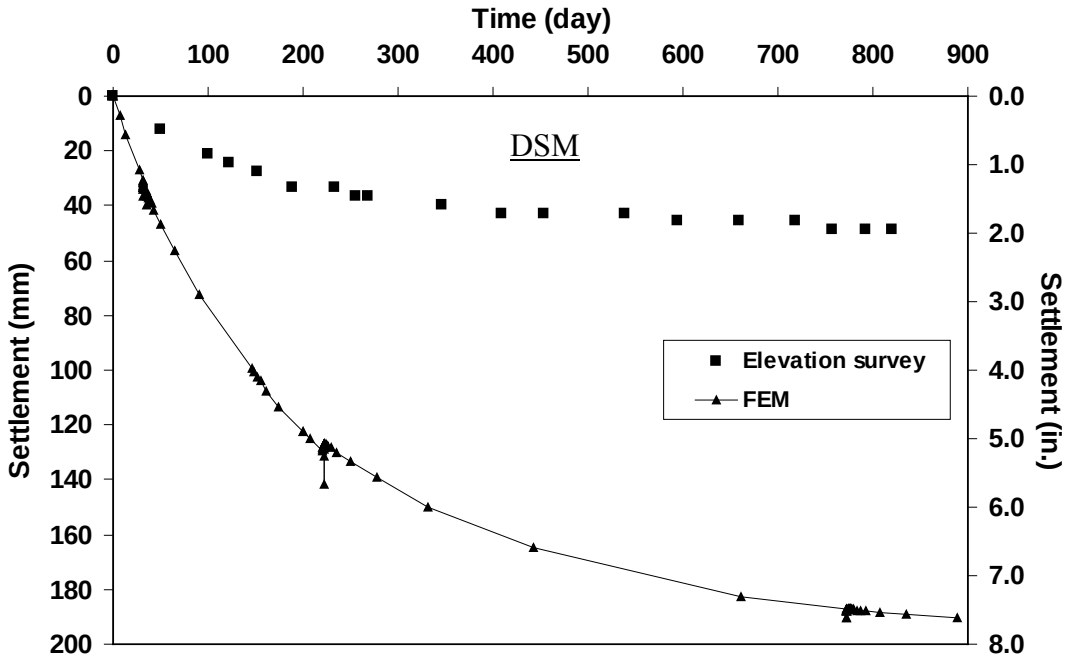

Figure 8.25. Comparison of the Vertical Displacements between the Data Obtained from the Elevation Surveys in the Treated Section and the Results from the Numerical Analysis in the Untreated Section.

8.3.4 Analysis of Vertical Soil Movements

To predict the long-term settlement, a hyperbolic method developed by Lin and Wong (1999) was used in this study with the hyperbolic equation shown as follows:

$$\frac{t}{s} = \alpha + \beta t \qquad (8.4)$$

where t = time from the start of embankment fill (day).

s = measured settlement as any specific time t (mm).

α = gradient of the straight line between t and t/s.

β = intersection of the straight line on the t/s axis.

According to Eq. 8.4, the elevation survey data from both the control and test sections were plotted with a function of time-settlement ratio as shown in Figure 8.26.

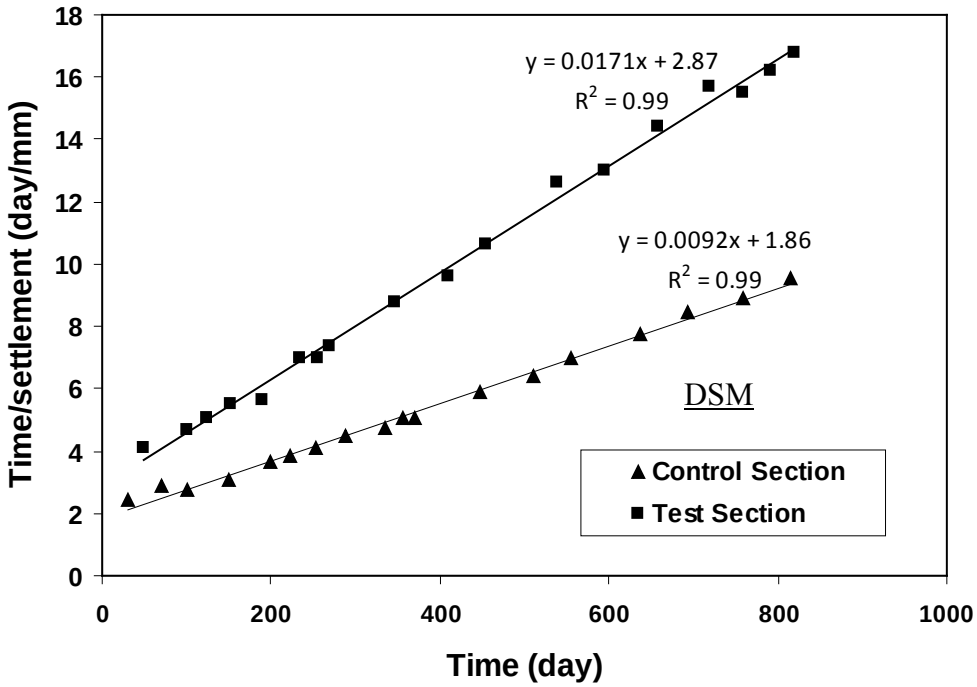

Figure 8.26. Regression Equations from the Hyperbolic Model Used to Predict the Soil Settlement Values in Both the Treated (Test) and the Untreated (Control) Sections.

Using the regression equations shown in Figure 8.26 and the hyperbolic equation in Eq. 8.4, the magnitude of the soil settlements at a specific time (t) in the embankments can be obtained from the following Eq. 8.5.

$$s = \frac{t}{(\alpha + \beta t)} \tag{8.5}$$

Therefore, the soil settlement occurring at time (t) in the treated section is equal to:

$$s = \frac{t}{(2.87 + 0.0171t)} \quad \text{mm} \tag{8.6}$$

and the soil settlement occurring at time (t) in the untreated section is equal to:

$$s = \frac{t}{(1.86 + 0.0092t)} \quad \text{mm} \tag{8.7}$$

By solving Eqs.8.6 and 8.7 and with a time increment of 10 days, the soil settlement that occurred in both embankments at any specific time interval can be calculated. The results of the settlement prediction from the hyperbolic model and the FEM are shown in Table 8.2. From the table, if the settlement predictions are performed for 10 years, the settlement values in the treated section are found to be 2.20 in. (56 mm) in the hyperbolic model and 2.52 in. (64 mm) in the FEM. The settlement values in the control section are equal to 4.06 in. (103 mm) in the hyperbolic model and 10.63 in. (270 mm) in the FEM. The settlement value in the control section was obtained when soft foundation soil, as placed in the test section, was used for the simulation. However, in the field, the foundation soil in the control section is stiffer than in the test section; therefore, the predicted settlement values from the FEM are higher than the values from the elevation surveys and the extrapolated data as seen in Table 8.2.

Table 8.2. Settlement Predictions from the Hyperbolic Model and the FEM.

Settlements at year (in.)	Elevation surveys*	Hyperbolic model (extrapolated data)				FEM			
	2	2	10	20	30	2	10	20	30
Treated Section	1.93	1.93	2.20	2.24	2.24	1.57	2.52	2.56	2.60
Control Section	3.35	3.35	4.06	4.17	4.21	9.45**	10.63**	10.83**	10.91**

Noted : * Measured Data

** Results from the simulation based on soil foundation in the treated section

From Figure 8.27, the results from the extrapolated data and the FEM for the test embankment are in agreement while the results for the control embankment are quite different according to the aforementioned reason.

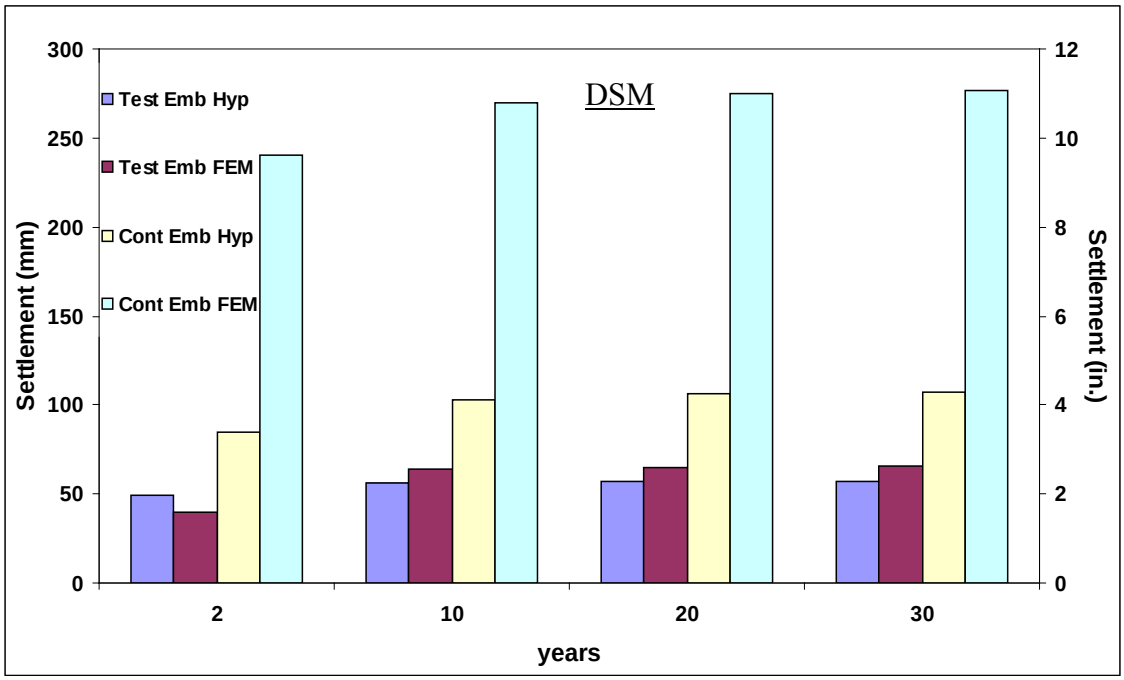

Figure 8.27. Settlement Values from Data Extrapolation and FEM.

8.3.5 Prediction of Soil Movements Occurred in the Treated Section with Variations of Embankment and DSM Configurations

To investigate the effects of the settlement on the embankment and foundation configurations, parameters such as the area-ratio (a_r) between the DSM and the natural soil, slope and height of the embankment were varied to produce results from different scenarios.

8.3.5.1 Influence of Area-Ratio (a_r) between the DSM and the Natural Subgrade

The a_r between the DSM and the natural soil is an important factor in reducing the settlements occurring underneath an embankment. Therefore, various values of the a_r were used in the numerical analysis. Area-ratios of 0.3, 0.4, 0.6, 0.7, and 0.8 were input into the original embankment model having a height of 18 ft (5.5 m) and a side slope (V:H) of 1:4. Figure 8.28 shows monitored point A and the embankment model with an area-ratio of 0.3.

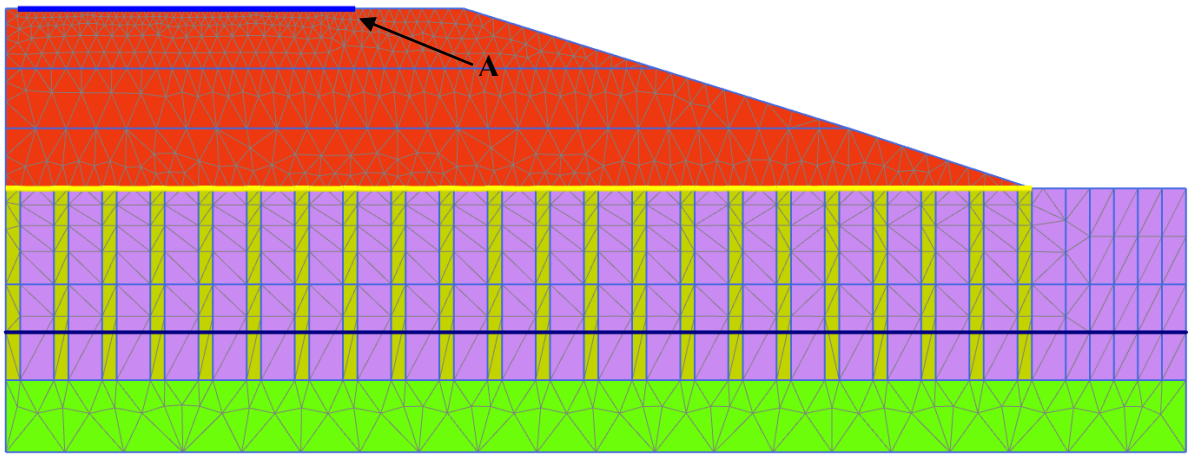

Figure 8.28. Nodes and Elements in the DSM Treated Section with an Area-Ratio (a_r) of 0.3.

The results from the FEM analysis are presented in Figures 8.29–8.31. Figure 8.29 shows the deformed mesh of the embankment by magnifying it 50 times. The maximum vertical displacement in this analysis is equal to 4.7 in. (0.12 m) and this occurred in the right side of the pavement slab as shown in Figure 8.30. Figure 8.31 shows the horizontal displacement; it is seen that the movements mostly occurred in the slope except for a small displacement of 0.015 in. (0.4 mm).

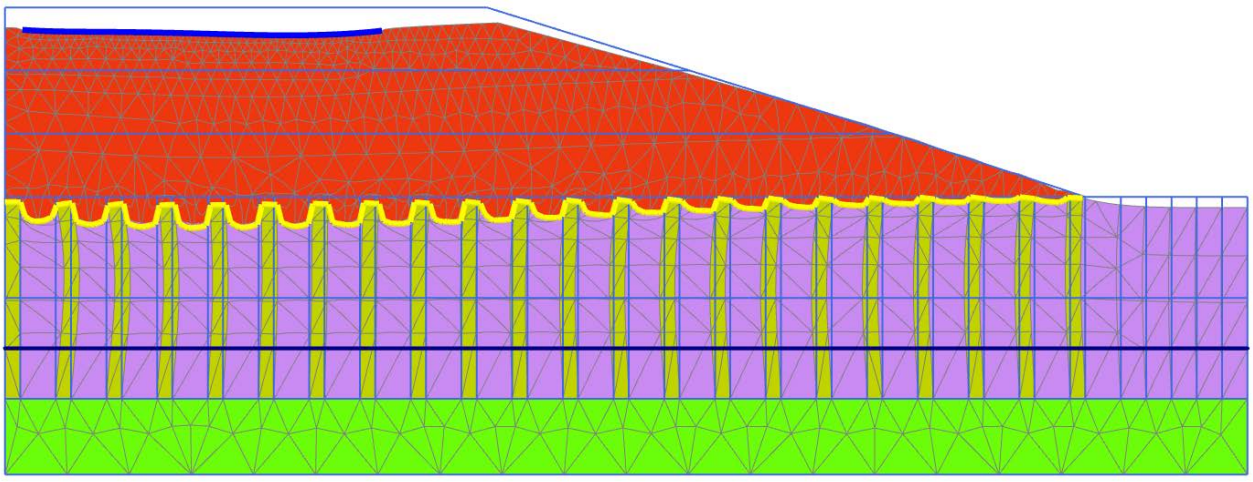

Figure 8.29. Deformed Mesh of the DSM Treated Section with the Area-Ratio (a_r) of 0.3 (Magnified 50 Times).

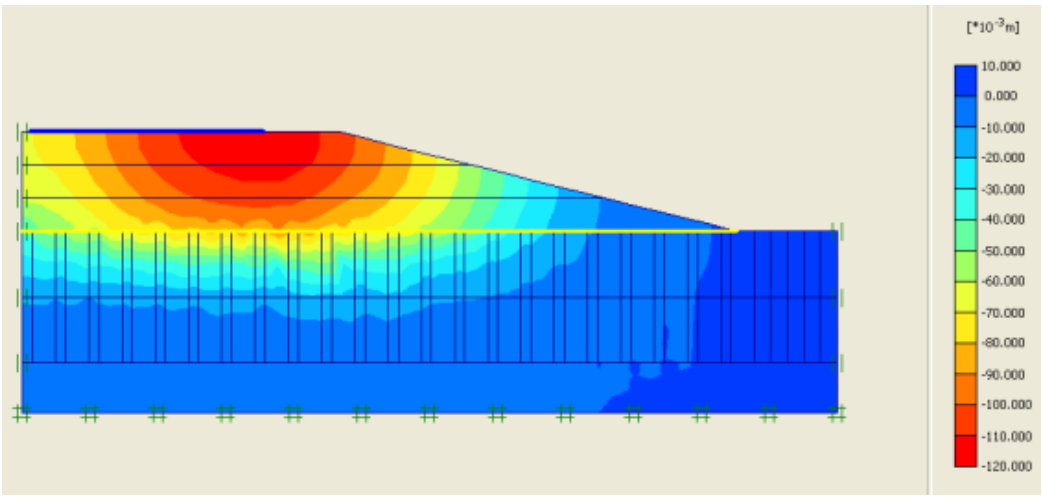

Figure 8.30. Vertical Soil Movements in the DSM Treated Section with an Area-Ratio (a_r) of 0.3.

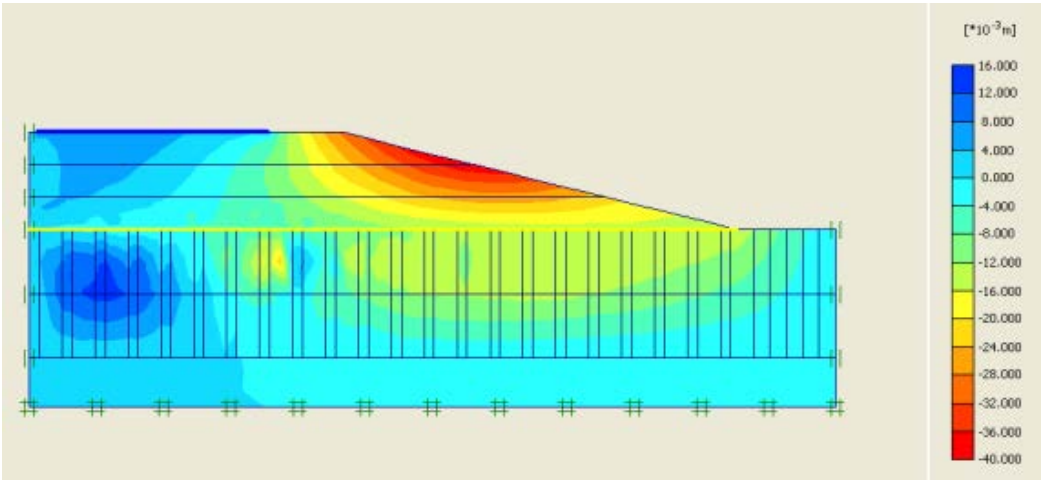

Figure 8.31. Horizontal Soil Movements in the DSM Treated Section with an Area-Ratio (a_r) of 0.3.

The same procedure was also performed to find the vertical and horizontal soil displacements for the area-ratios (a_r) of 0.4, 0.5, 0.6, 0.7, and 0.8. The results of the maximum displacements from the numerical analyses with all of the area-ratios (a_r) are presented in Table 8.3. The presented displacement values are the maximum soil movements occurring in any location in the embankment that are different from the settlement values monitored on the pavement surface. Figure 8.32 shows a relationship between the soil settlement monitored at Point A and the elapsed time period. The settlement can be reduced with an increase of the area-ratio of the treated soil.

Table 8.3. Maximum Soil Displacement of an Embankment with Various a_r.

Area-ratio	Vertical displacement		Horizontal displacement	
	in.	mm	in.	mm
0.3	4.70	119.28	1.55	39.32
0.4	3.15	80.09	1.93	49.08
0.5	1.66	42.25	0.67	16.95
0.6	1.41	35.89	0.48	12.31
0.7	0.76	19.41	0.30	7.75
0.8	0.67	17.06	0.25	6.43

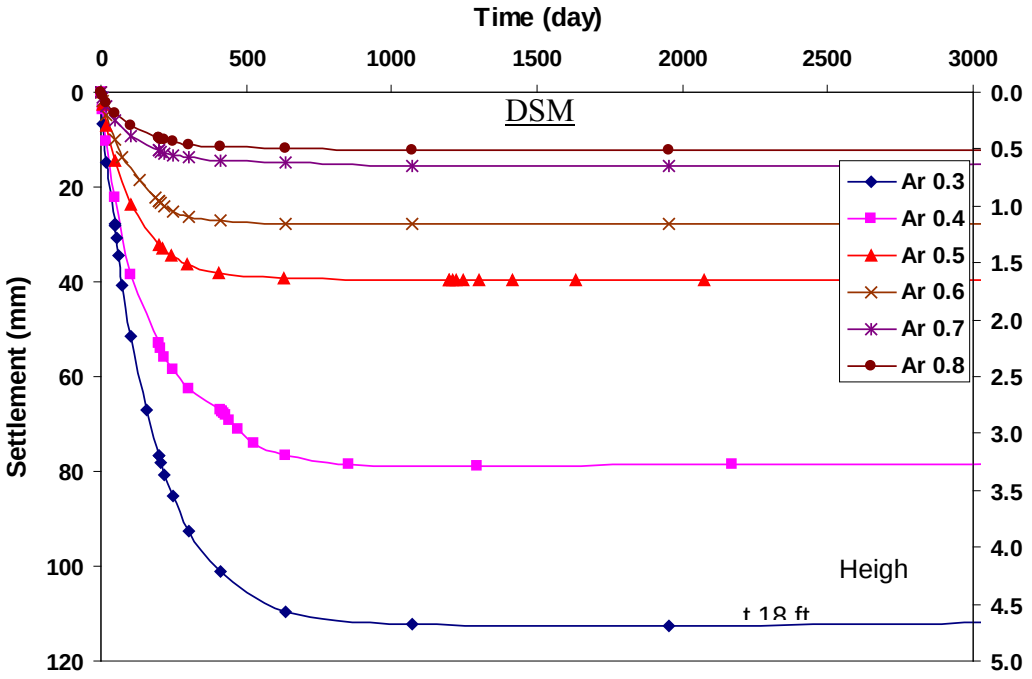

Figure 8.32. Time-Settlement in the DSM Treated Section with Various Area-Ratios (a_r) from 0.3 to 0.8.

Figure 8.33 shows the relationship between the soil settlements that occurred in the DSM treated section with various area-ratios from 0.3 to 0.8. The settlements are reduced in the

hyperbolic shape when the area-ratios increase from 0.3 to 0.8. The settlement has sharply decreased when the area-ratio increases from 0.3 to 0.5 but thereafter, the decrease is small. Therefore, the most effective area-ratio in the DSM design should be between 0.5 and 0.7 for mitigating soil settlements in the embankments when DSM is used for soil treatment.

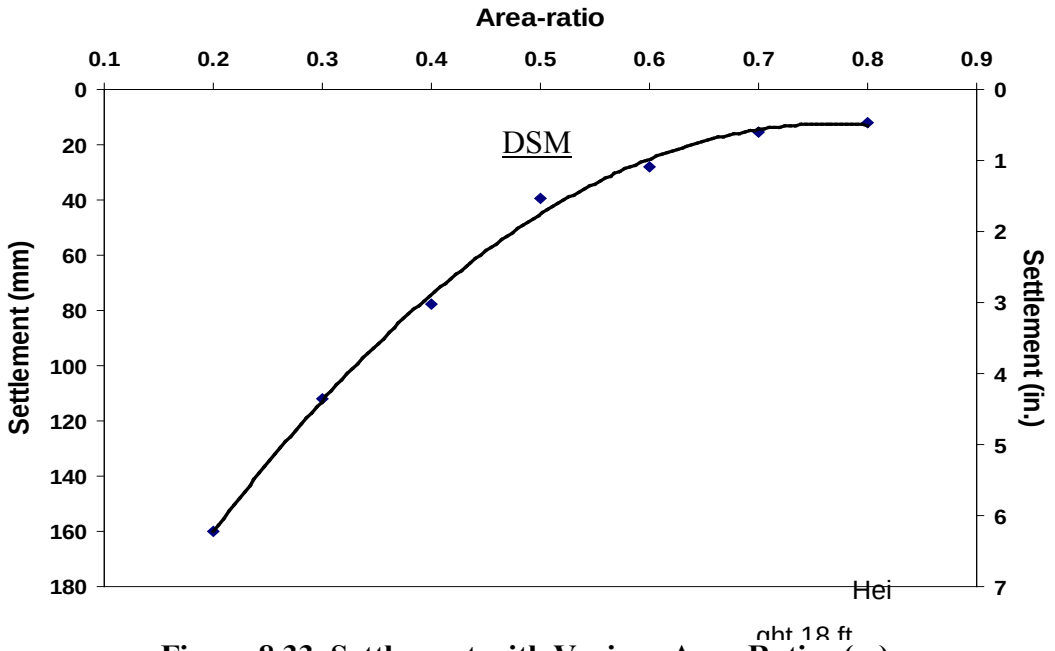

Figure 8.33. Settlement with Various Area-Ratios (a_r).

8.3.5.2 Influence of Embankment Slope

The stability of slopes is another factor that can influence the movements of soils in the embankment. With an embankment of good stability and no failure plane occurring in the slope, the soil movements will depend solely on consolidation. On the contrary, instability of an embankment can induce more settlement due to soil movements caused by the slope failure. Therefore, in order to study the effect of the embankment slopes on the amount of the settlement in the embankment, the gradient of the embankment was changed in the models with various V:H ratios of 1:1, 1:2, 1:3, 1:4, and 1:5. The embankment model in these analyses has a height of 18 ft (5.5 m) and the area-ratio of 0.5. The width of the DSM columns treated area was changed depending on the distance from the center line to the toe of the embankment slope.

The results from the numerical analysis are shown in Table 8.4. The soil displacements, both in the vertical and the horizontal directions, have small differences when the embankment slope changes from 1:1 to 1:5.

Table 8.4. The Maximum Soil Displacements with Various Embankment Slopes.

Slope (V:H)	Vertical displacement		Horizontal displacement	
	in.	mm	in.	mm
1:1	1.27	32.27	0.60	15.28
1:2	1.47	37.37	0.63	16.08
1:3	1.58	40.20	0.65	16.53
1:4	1.62	41.20	0.67	16.95
1:5	1.66	42.11	0.52	13.15

From this analysis, no slope failure is possible in any slope ratio configuration. As a result, the soil movement depends mostly on the weight of the embankment. Researchers conclude the slope of the embankment does not affect the magnitude of the soil settlement in the treated embankment.

8.3.5.3 Influence of Embankment Height

Another analysis was performed to investigate the changes in the height of embankment that affect the soil settlement. Various embankment heights were used for study starting from 16, 18, 20, 22, 24, and 26 ft (5.5, 6.0, 6.5, 7.0, 7.5, and 8.0 m) Other parameters, slope and the area-ratio, were maintained at 1:4 (V:H) and 0.5, respectively, throughout the study. Figure 8.34 shows monitored Point A and the embankment model with a height of 24 ft (7.5 m) and slope of 1:4 (V: H). The width of the embankment at its base and the width of the DSM columns treated area must be changed from case to case in order to maintain the slope value at 1:4.

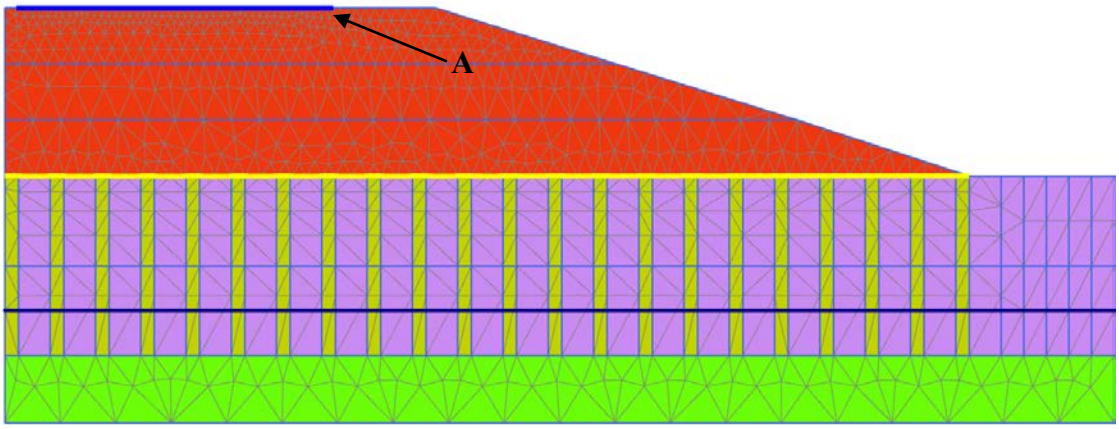

Figure 8.34. Geometry of the DSM Treated Section with a Height of 24 ft (7.5 m).

Figure 8.35 demonstrates how the height of the embankment affects the settlement at Point A in the treated section. The higher the embankment, the more soil settlements occur since the embankment height contributes to the increase in the overburden stress that induces soil settlements.

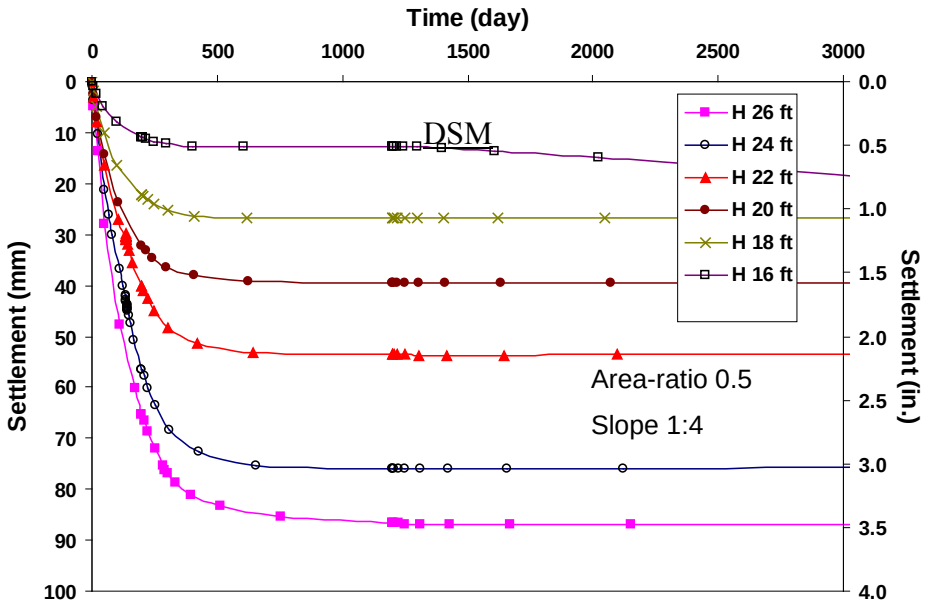

Figure 8.35. Time-Settlement in the DSM Treated Section with Various Heights of Embankment.

8.3.5.4 Conclusion from Variable Studies

Researchers concluded from the variable studies that two factors influencing the amount of the settlement in the embankment are the area-ratio of the DSM columns and the height of the embankment. With the same embankment geometry, the area-ratio can reduce the settlement that

occurs in the approach slab structures. Though area-ratio values less than 0.5 can be used to reduce the settlement, the magnitude of the settlement reductions will not be sufficient for the approach slabs. Hence larger ratios may be needed. However, if area-ratio values are higher than 0.7, then the cost of the area treatment will be high and may not result in a cost effective solution.

8.3.5.5 Design Chart for the DSM Columns

From the variable studies, the most influent factors for the settlement control in the DSM treated section are the area-ratio and height of the embankment. Design charts were developed for different area-ratios and heights of embankments. Along with these two variables, the thickness and the compression index of the subgrade layer were also varied in order to establish design charts that could be used under different scenarios. The heights of the embankment ranged from 15 to 30 ft (4.5 to 9 m) while the thicknesses and the compression indices of the subgrade ranged from 15 to 25 ft (4.5 to 7.5 m) and 0.34 to 0.40, respectively. Figure 8.36 presents a typical design chart for a subgrade thickness of 25 ft (7.5 m) and having a compression index of 0.4. A step-by-step design procedure is presented in the following:

1. Establish the height of embankment required for the DSM treatment.
2. Predict the settlement that may occur in the embankment with no foundation treatment.
3. From the predicted settlement value, draw another hypothetical line by interpolation to produce another curve using the existing curves as shown in Figures 8.36 through 8.38.
4. Establish a tolerable settlement value for the embankment system.
5. Using the tolerable settlement value, draw a line parallel to the x-axis until it reaches a curve of the embankment height under consideration.
6. From the intercept point, determine the required area-ratio from the figure.
7. Establish the length of the DSM columns such that the DSM columns are placed over the strong soil layer.
8. Design the diameter and arrangement of the DSM columns per the design guidelines and area-ratios.
9. Determine the number of DSM columns from the numbers obtained in Step 8.

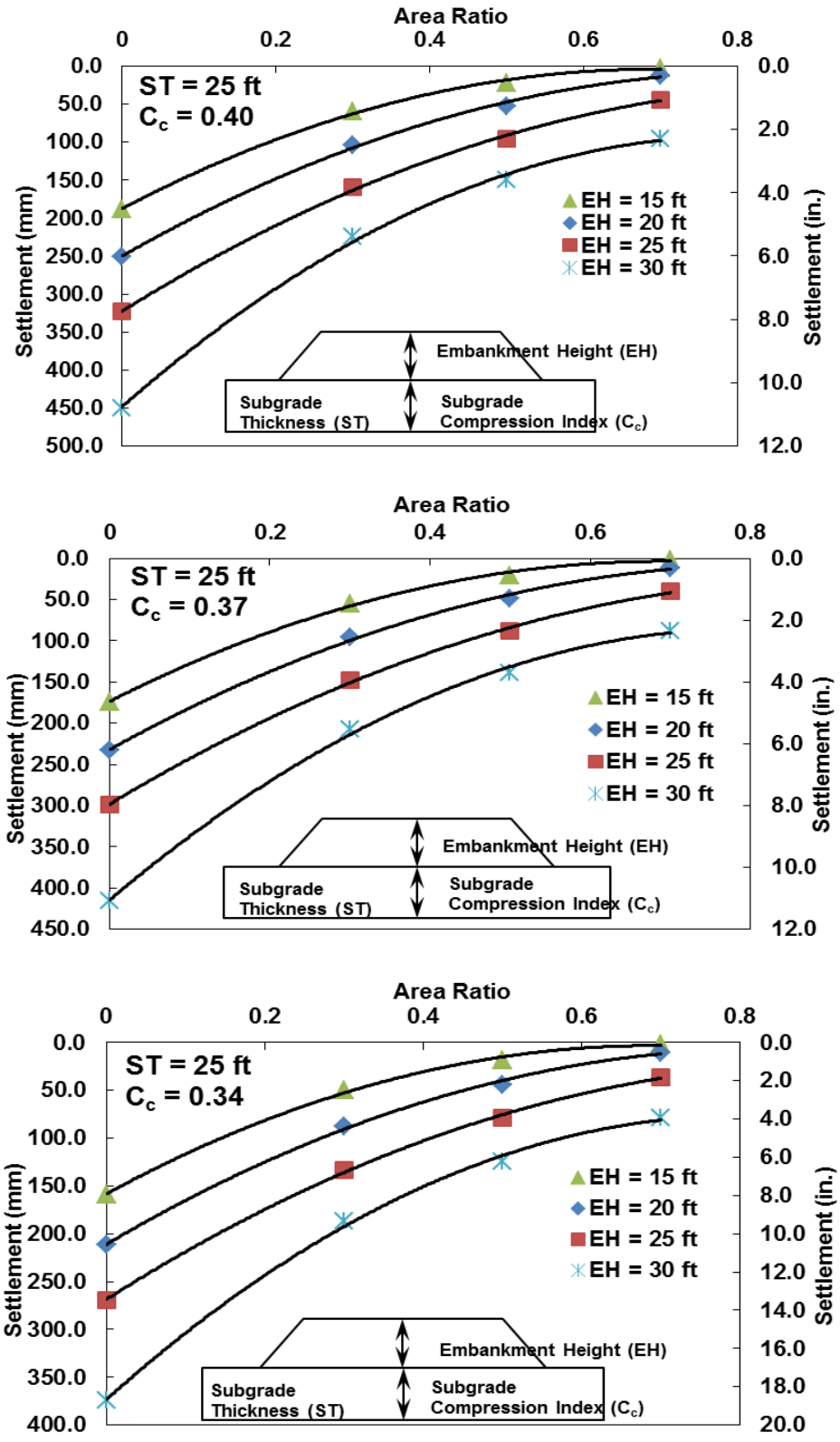

Figure 8.36. Design Chart for DSM Columns with Various Area-Ratios and Heights of Embankments for a Subgrade Thickness of 25 ft. and Varying Compression Indices.

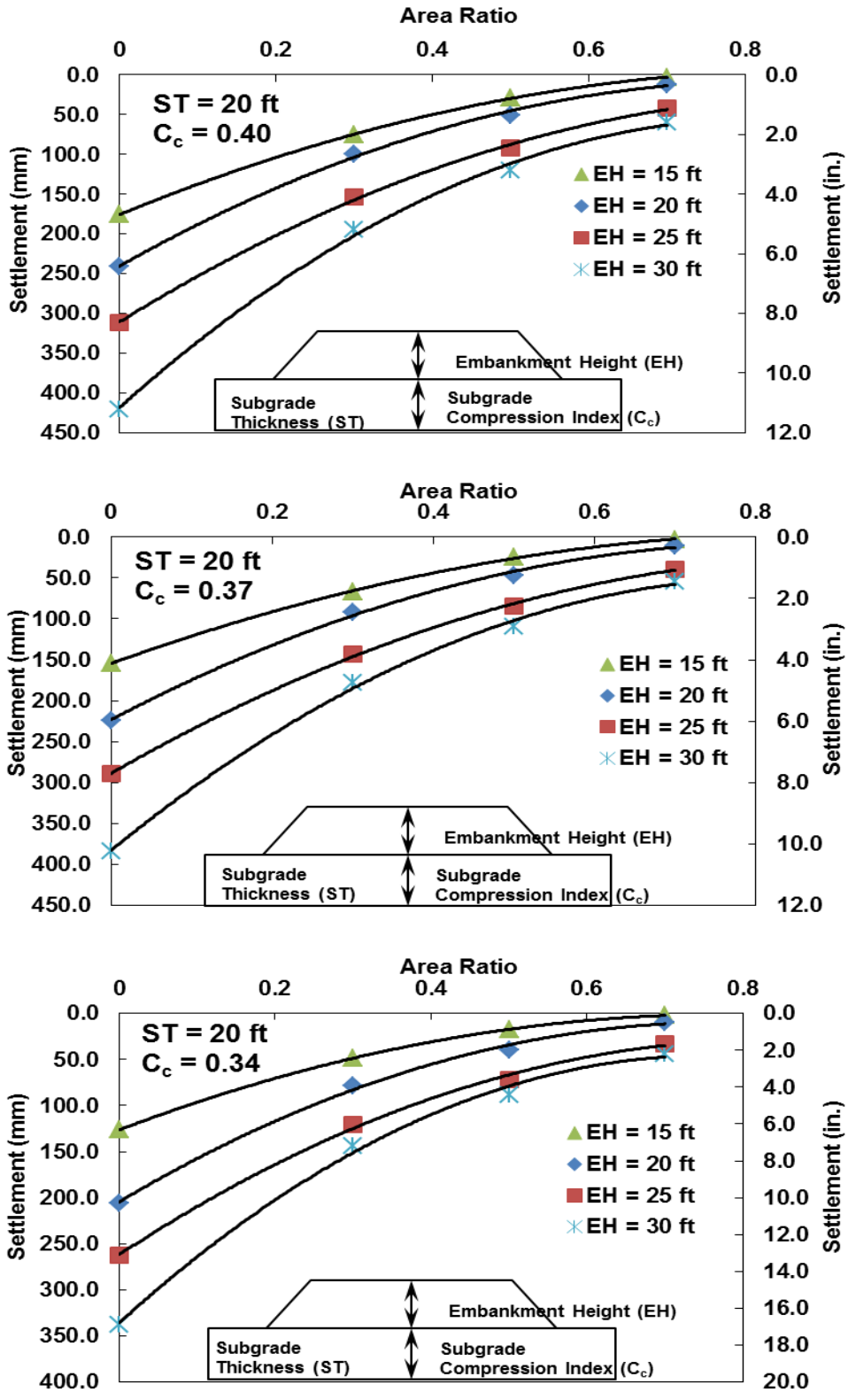

Figure 8.37. Design Chart for DSM Columns with Various Area-Ratios and Heights of Embankments for a Subgrade Thickness of 20 ft and Varying Compression Indices.

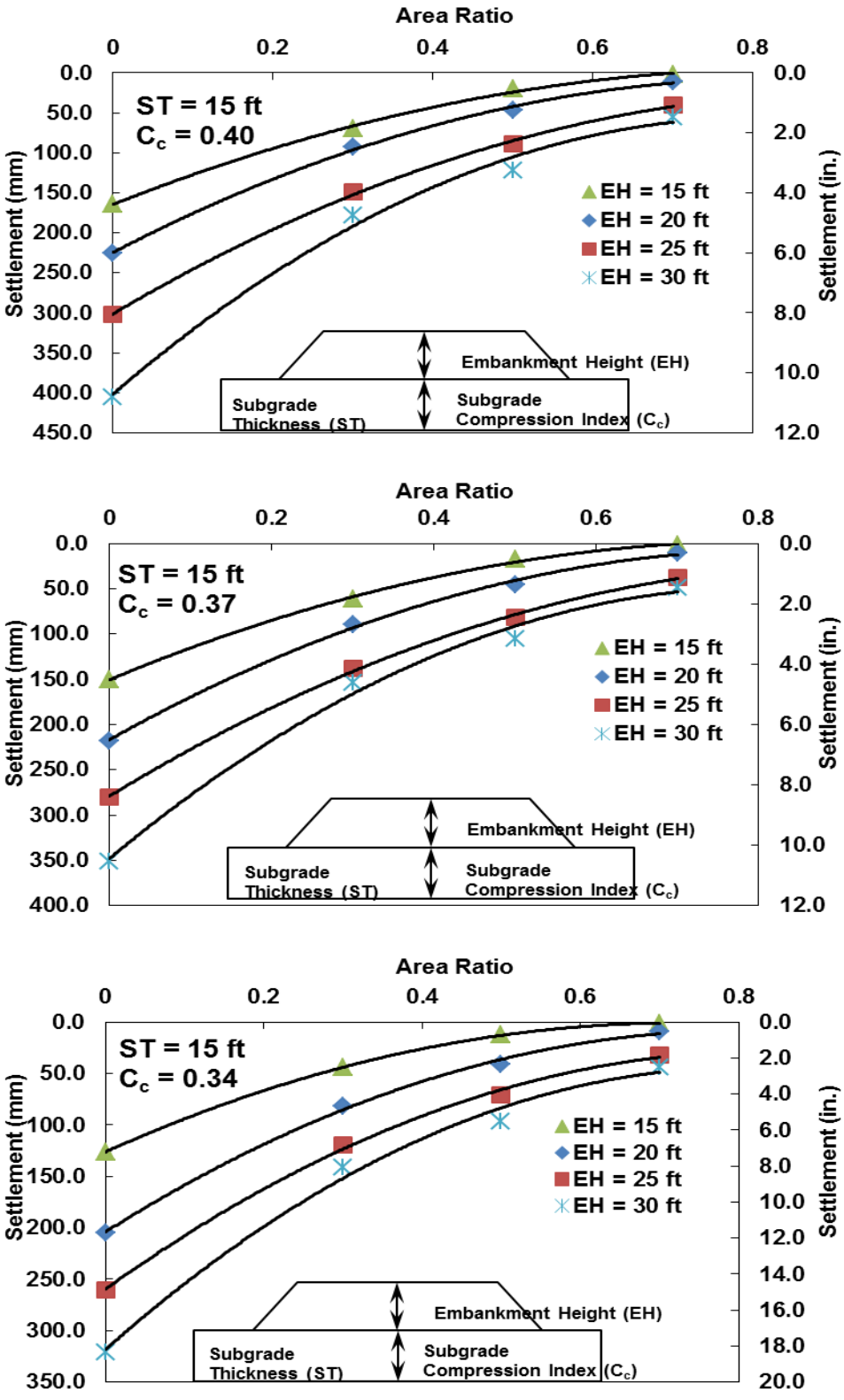

Figure 8.38. Design Chart for DSM Columns with Various Area-Ratios and Heights of Embankments for a Subgrade Thickness of 15 ft and Varying Compression Indices.

8.4 MODELING OF A LIGHTWEIGHT EMBANKMENT SYSTEM

8.4.1 ECS Embankment Section

8.4.1.1 Geometry and Boundary Conditions of the Test Section

A cross-section and subsurface profile of the ECS lightweight fill embankment constructed on SH 360 is shown in Figure 8.39. The embankment has a total height of 30 ft (9 m) from the existing ground and a side slope of 2H:1V. The embankment is constructed on a soft clay layer with a thickness of 16 ft (5 m) and underlain by a 10 ft (3 m) sand layer.

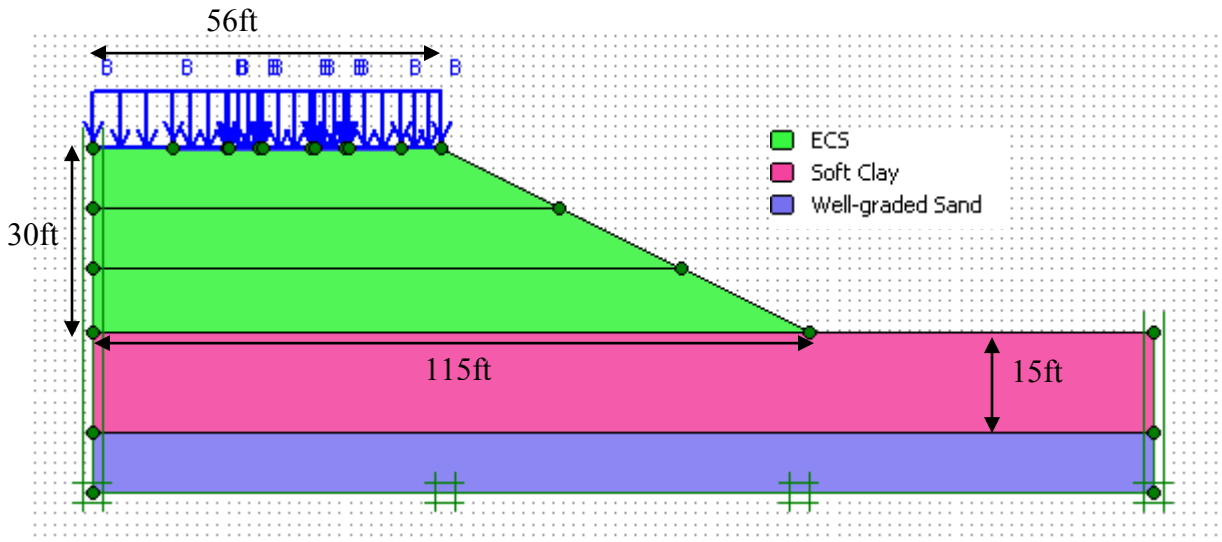

Figure 8.39. Geometry and Boundary Conditions of the ECS Test Section.

8.4.1.2 Material Property Values in a Numerical Analysis

In this model analyses, a soft soil model is used to simulate the soft clay material while a Mohr-Coulomb model is used to simulate the ECS and well-graded sand materials. The strength parameters used in this analysis were derived from the laboratory study results as presented in Chapter 5.

The analyses were performed to study the settlement behavior for a long-term duration. Therefore, the settlements that were calculated to occur during the construction phase using a plastic model are disregarded. The long-term settlement analyses were performed with a consolidation based model and were carried out until the ultimate pore pressure state was reached. The displacement of the boundary at x=0, y=0 was restricted in all directions as well as

the boundaries at the points of the base. The material properties used in the analyses are given in Table 8.5.

Table 8.5. Properties and Model Type of the Materials Used in the Test Section Model Analysis.

	Unit	ECS	Soft clay	Well-graded Sand
Model type		Mohr-Coulomb	Soft soil	Mohr-Coulomb
Moist density, γ_m	pcf	39.8	91	96.7
Saturated density, γ_s	pcf	50	109.5	109.9
Elastic modulus, E^{50}_{ref}	psf	1×10^{8}	-	3.8×10^{8}
Poisson's Ratio	-	0.15	-	0.15
Cohesion, c	psf	1570	940	0
Friction Angle, φ	°	49.5	5	33
Permeability, k	ft/min	2×10^{-3}	2×10^{-8}	1.2×10^{-4}
Compression Index, C_c	-	-	0.34	-
Recompression Index, C_r	-	-	0.023	-
Over Consolidation Ratio, OCR	-	-	3	-
Initial void ratio, e_o	-	-	0.80	-

8.4.1.3 Discretization of the Test Section

A two-dimensional plain-strain model with 15-node triangular elements was used to model the test embankment as shown in Figure 8.40. The embankment in the model consists of three types of materials: ECS, clay, and sand. In Figure 8.40, the highway pavement is also seen on the top of the embankment model, as a blue line that has a length equal to the width of the pavement in the field.

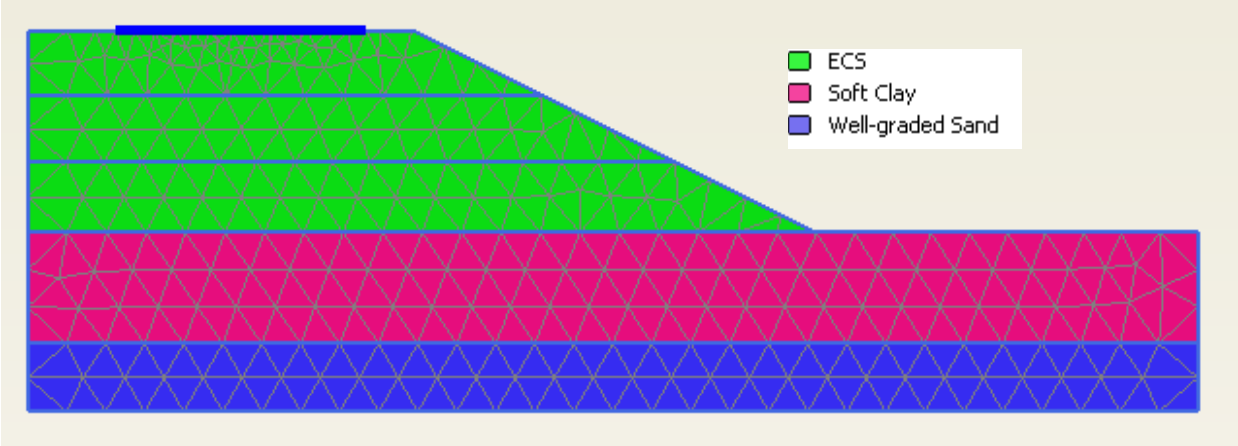

Figure 8.40. Nodes and Elements in the Test Section.

8.4.1.4 Settlement Analyses

The total height of the 30 ft (9 m) embankment was divided into 3 layers to simulate embankment construction phases in the analyses as shown in Figure 8.40. Figure 8.41 presents the construction phases in the numerical analyses. The duration of the embankment construction in each layer was close to 25 days, and thereafter, the embankment was left to be consolidated for another 25 days. In an initial stage, the soil weight was used as a parameter that induced soil stress.

In the second stage, each layer in the embankment was modeled for consolidation. The embankment construction was simulated in that way until the whole embankment construction was completed. The simulation was done such that it replicates the compaction effort performed in real practice. After the completion of the last layer of the embankment, the whole embankment was compacted by applying uniform load in Phase Number 8. The calculation of the settlement was reset after the construction of the highway pavement had been completed in Phase Number 9. The model analyzed used a combined gravity load of the material and the traffic load of 80 kN/m^2.

Since only elevation surveys and vertical inclinometer monitoring were performed at the ECS site at the locations shown in Figure 8.42 (Points A and B), only these two points were selected to investigate the soil movements and to validate the results of the numerical analysis in this study.

Identification	Phase no.	Start from	Calculation	Loading input	Time	Wa...	First	Last
Initial phase	0	0	N/A	N/A	0.00 ...	0	0	0
<Phase 2>	2	0	Consolidation ana...	Staged construction	25.0...	2	1	5
<Phase 3>	3	2	Consolidation ana...	Staged construction	25.0...	3	6	7
<Phase 4>	4	3	Plastic analysis	Staged construction	25.0...	4	8	21
<Phase 5>	5	4	Consolidation ana...	Staged construction	25.0...	5	22	33
<Phase 6>	6	5	Plastic analysis	Staged construction	25.0...	6	34	38
<Phase 7>	7	6	Consolidation ana...	Staged construction	25.0...	7	39	61
<Phase 8>	8	7	Consolidation ana...	Staged construction	70.0...	8	62	108
<Phase 9>	9	8	Consolidation ana...	Staged construction	50.0...	9	109	146
<Phase 13>	13	9	Consolidation ana...	Staged construction	1000...	13	147	276
<Phase 12>	12	13	Consolidation ana...	Minimum pore pressure	1000...	13	277	277

Figure 8.41. Calculation Phase in the Settlement Analyses.

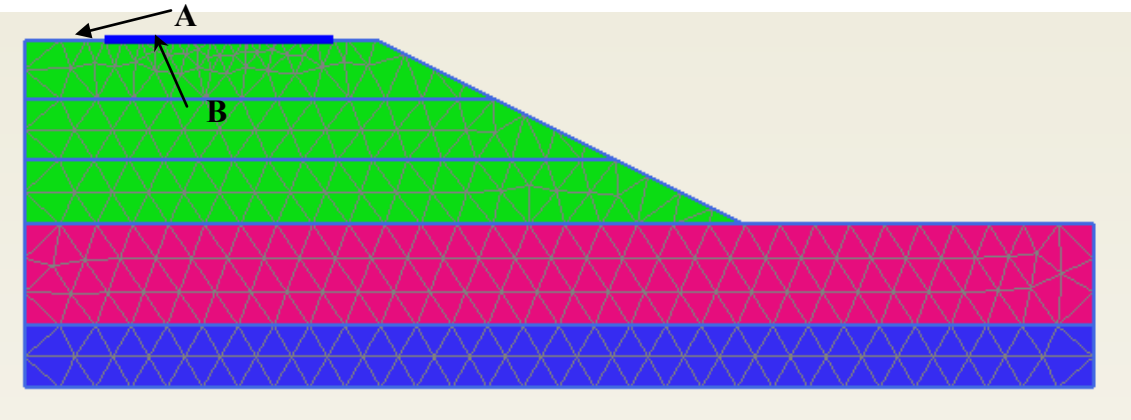

Figure 8.42. Observation Points in the Settlement Calculation.

8.4.1.5 Results of the Numerical Modeling Analysis

The results from the FEM analysis are presented in Figures 8.43 through 8.46. Figure 8.43 shows the deformed mesh of the embankment with a displacement magnification scale of 1:50. The maximum long-term displacement in this analysis is equal to 1.89 in. (48 mm) and occurred in the left side of the embankment as seen in Figure 8.43. The soft clay is the layer that experienced the highest amount of settlement due to the consolidation, which induces the settlement occurring in the ECS embankment.

Figure 8.44 shows the results of the total displacements that occurred in the embankment. Most of the consolidation occurred in the soft clay layer but the maximum total displacement occurred in the ECS layer. Figure 8.45 shows the horizontal soil movements that occurred in the embankment. Most of the lateral movements occurred at the toe of the slope and on the right side of the embankment while at the top of the slope and on the left side, only a small amount of

movements were noticed. The vertical soil displacements are presented in Figure 8.46. The pattern of color shades from the vertical movement results shown in Figure 8.46 is quite similar to the pattern of total movements shown in Figure 8.44, which means that the vertical movement is still a predominant factor in this study.

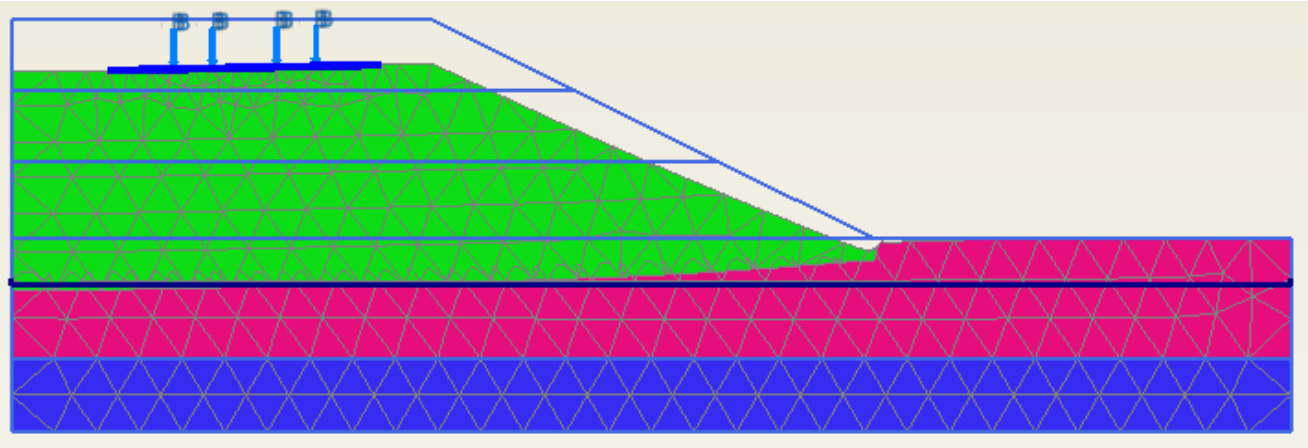

Figure 8.43. Deformed Mesh of the Test Section (Magnified 50 Times).

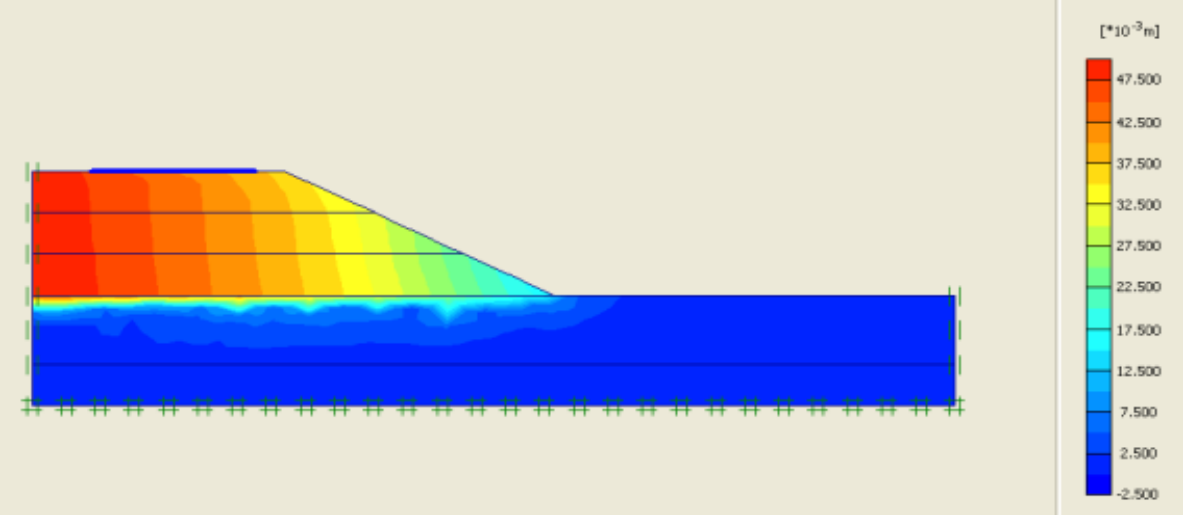

Figure 8.44. Total Displacements in the Test Section.

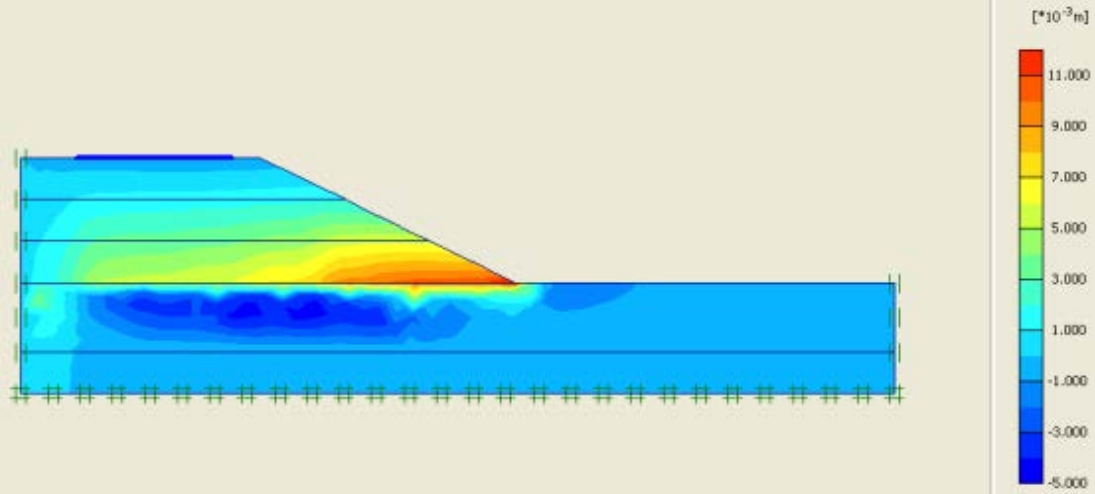

Figure 8.45. Horizontal Displacements in the Test Section.

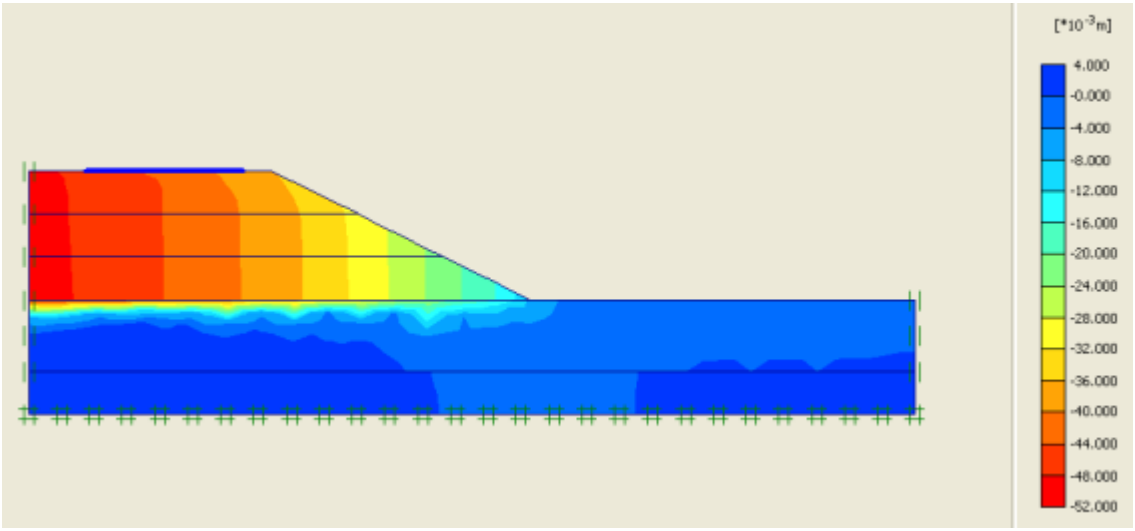

Figure 8.46. Vertical Displacements in the Test Section.

8.4.1.6 Model Validation

To validate the parameters used in the model, the results obtained from the above model analysis were used to compare with the monitoring data from the field. The comparisons were performed using the data from the elevation surveys to investigate the vertical soil displacements. The comparisons are presented in following subsections.

8.4.1.6.1 Comparison of the Numerical Analysis Results of the Vertical Displacements with the Elevation Surveys

The elevation surveys from Table 7.7 were plotted with the results of the numerical analysis as shown in Figure 8.47. The amount of settlement with time from both sources are not different and the prediction shows a good match.

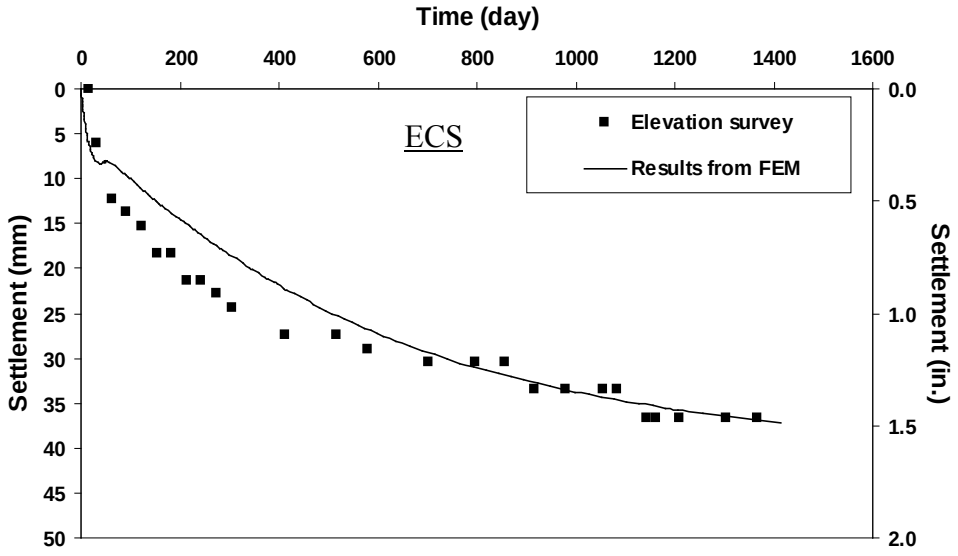

Figure 8.47. Comparison of the Vertical Displacements in the Test Section between Data Obtained from the Elevation Surveys and the Results from the Numerical Analysis.

8.4.1.6.2 Comparison of the Horizontal Displacement Results with the Vertical Inclinometer Data

No data were collected that were useful to perform a validation of the horizontal soil displacement. From Figure 8.48, there is no vertical inclinometer casing in the embankment that can provide suitable lateral movement data for model validation. Inclinometers V1 and V2 are located where the lateral movements can be influenced by different types of embankment fill materials such as reclaimed asphalt pavement (RAP) material in the north embankment and ECS material in the south embankment. The lateral soil movements measured in Inclinometers V1 and V4 are plotted and presented as shown in Figures 8.49 and 8.50. Inclinometer V2 is too close to the RAP embankment making the soil movements affected more predominately by the RAP rather than the ECS and hence these data were not used for comparisons.

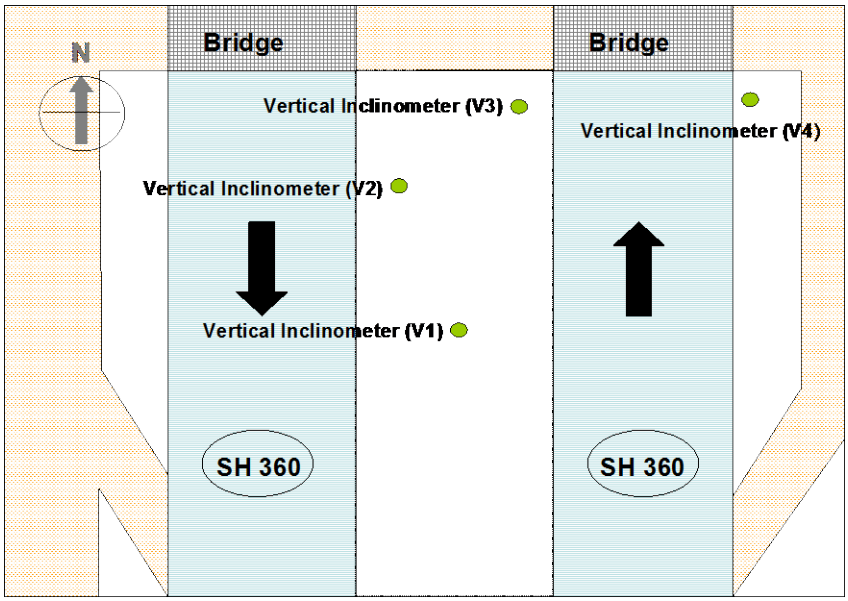

Figure 8.48. Locations of the Vertical Inclinometers Installed in the ECS Embankment on SH 360.

Figures 8.49a and b reveal the horizontal soil movements in Inclinometers V1 and V4, respectively. In Figure 8.49a, only the movements along the embankment cross-section (B-axis) are presented here since the movement in the A-axis cannot be modeled in this analysis. Figure 8.49a shows that the horizontal displacements monitored from Inclinometer V1 move toward the left while the results from the analysis are extremely small showing a displacement pattern different from the monitored data.

As already discussed in Chapter 7, the inclinometers located in the middle of the highway median (V1 and V3) recorded very small displacements that are close to the results from the numerical analysis. Figure 8.49b shows the horizontal soil displacements in the direction of the cross-section of the embankment. The displacement profile from the monitored data has a large displacement at the top and a low displacement at the bottom of the embankment that is different from the displacement profile that resulted from the numerical analysis. This can be evidence that, apart from the consolidation process, the lateral movements that occurred in the field could be the result of another reason like soil erosion as suspected in the previous chapter. However, the soil erosion phenomenon is very complicated and was not able to be modeled in the Plaxis program. The monitored horizontal soil movements from Inclinometer V3 are not presented because the soil movements were influenced from the movement that occurred around Inclinometer V4 and are too complex for the analysis.

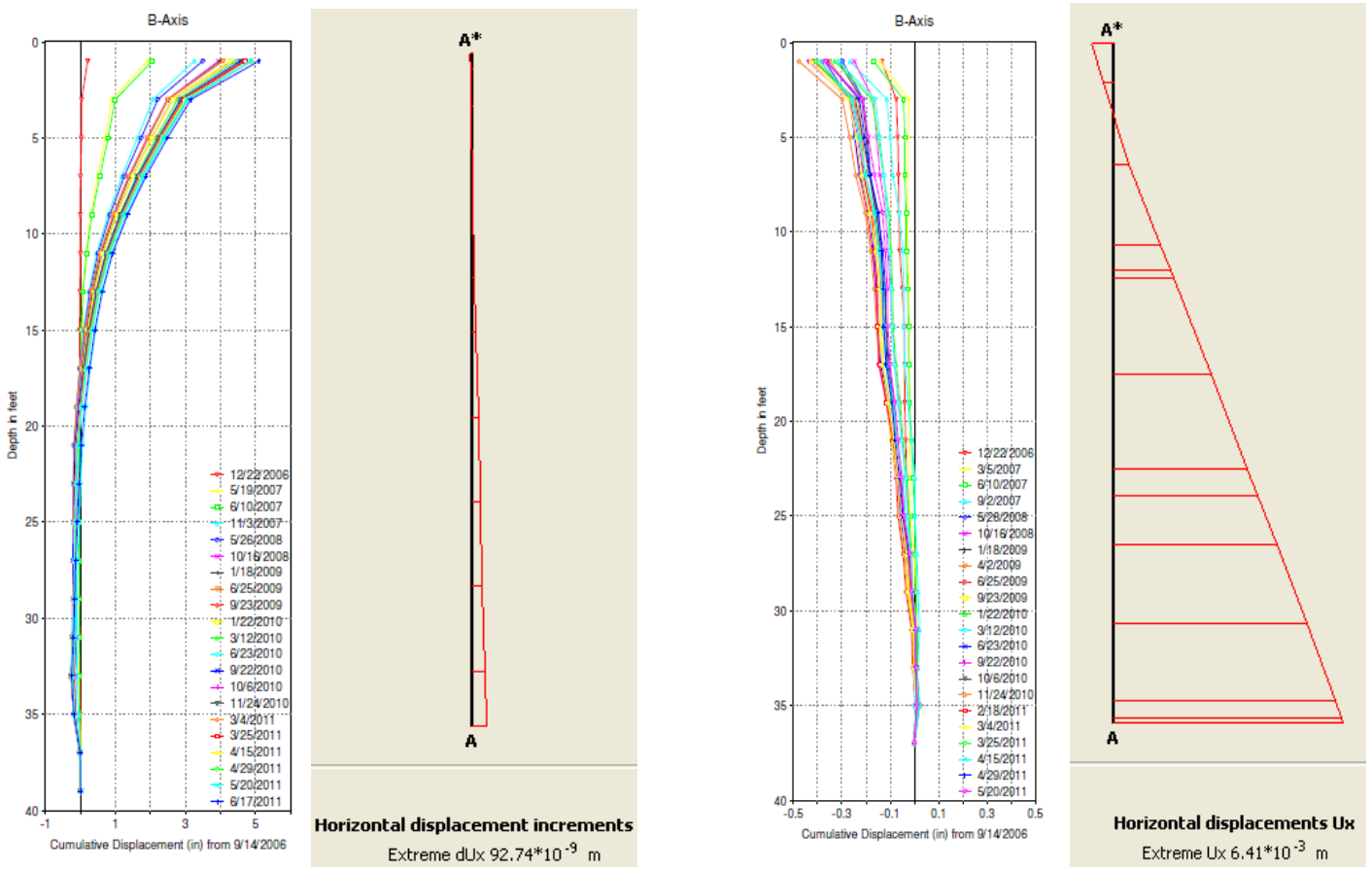

(a) (b)

Figure 8.49. Comparisons of the Horizontal Soil Movements between the Monitored Data and the Numerical Results in Inclinometers (a) V1 and (b) V4.

8.4.2 Control Embankment Section

The control section was an embankment section constructed with local select fill located on the north side of the Center Street bridge over IH 30. The settlement investigations, using both elevation surveys in the field and numerical analysis, were performed and used further to compare with the values from the ECS embankment test section to evaluate how ECS material can mitigate the settlement problem that can occurs in bridge approach embankment sections. The geometry, boundary conditions, and discretization of the control section are the same as the ones used in the ECS test section by replacing the embankment ECS fill material with sandy clay fill material as shown in Figure 8.50.

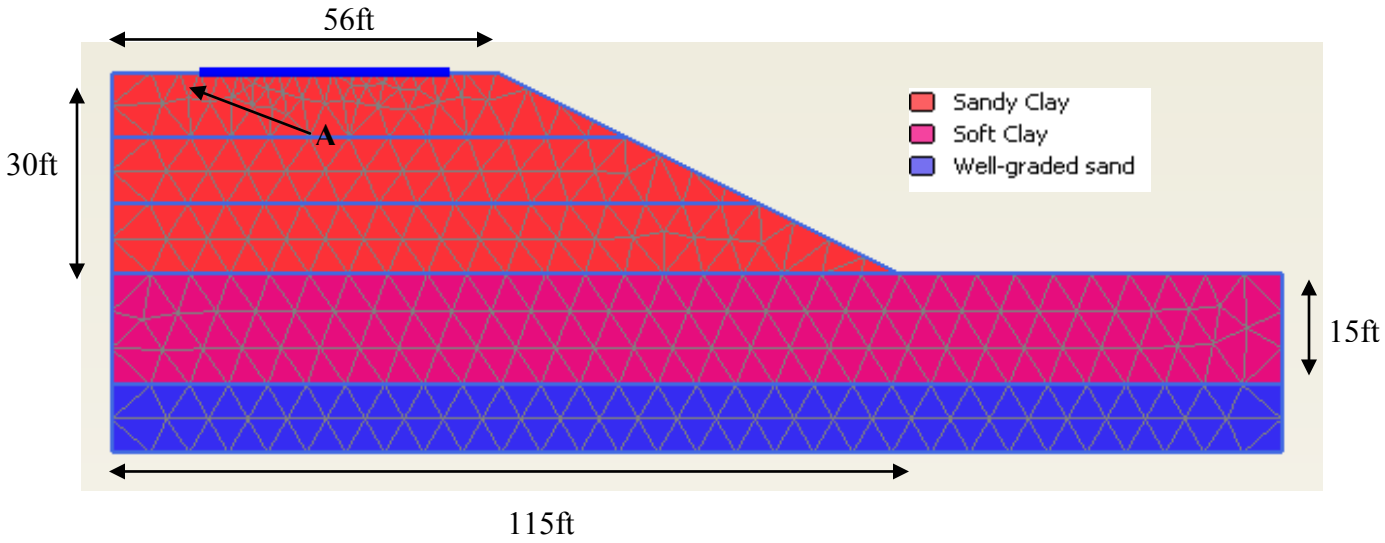

Figure 8.50. Nodes and Elements in the Control Section.

8.4.2.1 Settlement Analyses

The settlement numerical analysis on the control section at Point A was performed in the same way as was done on the ECS test section. The total embankment of 30 ft (9 m) high was divided into three layers with the same duration of construction phases, load multiplier factor, and traffic load as in the ECS test section analyses. Material properties used in the analysis are given in Table 8.6.

Table 8.6. Properties and Model Type of the Materials Used in the Control Section Model Analysis.

	Unit	Sandy clay	Soft clay	Well-graded Sand
Model type		Soft soil	Soft soil	Mohr-Coulomb
Moist density, γ_m	pcf	94.2	89.3	96.7
Saturated density, γ_s	pcf	109.5	107.4	109.9
Elastic modulus, E^{50}_{ref}	psf	-	-	3.8×10^{8}
Poisson's Ratio	-	-	-	0.15
Cohesion, c	psf	420	940	0
Friction Angle, φ	°	18	5	33
Permeability, k	ft/min	1×10^{-6}	2×10^{-8}	1.2×10^{-4}
Compression Index, C_c	-	0.12	0.34	-
Recompression Index, C_r	-	.030	0.023	-
Over Consolidation Ratio, OCR	-	3	3	-
Initial void ratio, e_o	-	0.55	0.80	-

8.4.2.2 Results of the Model Analysis

Figures 8.51 through 8.54 show the results from the numerical analysis in the control section. Figure 8.51 presents the deformed mesh of the embankment with a displacement scale enlarged to 20 times. The maximum settlement of the embankment of 0.55 in. (0.14 m) occurred evenly in the area under the embankment crest. The results of the total displacements that occurred in the embankment are presented in Figure 8.52. The figure reveals that consolidation mostly occurred in the subgrade layer and that consolidation also resulted within the embankment. Figures 8.53 and 8.54 show the horizontal and vertical soil movements that occurred in the control embankment, respectively. The vertical movement is still a predominant factor in the control embankment section.

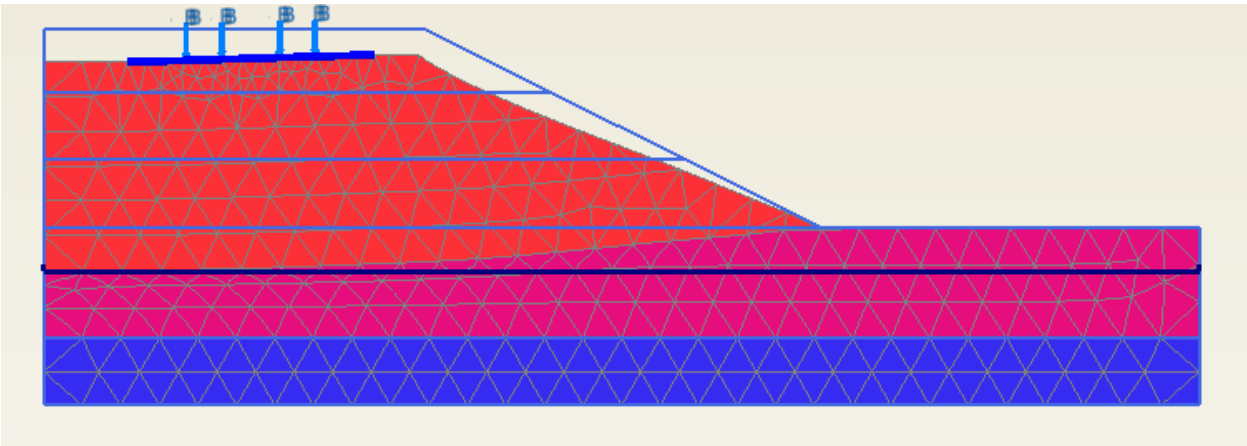

Figure 8.51. Deformed Mesh of the Control Section (Displacement Magnified 20 Times).

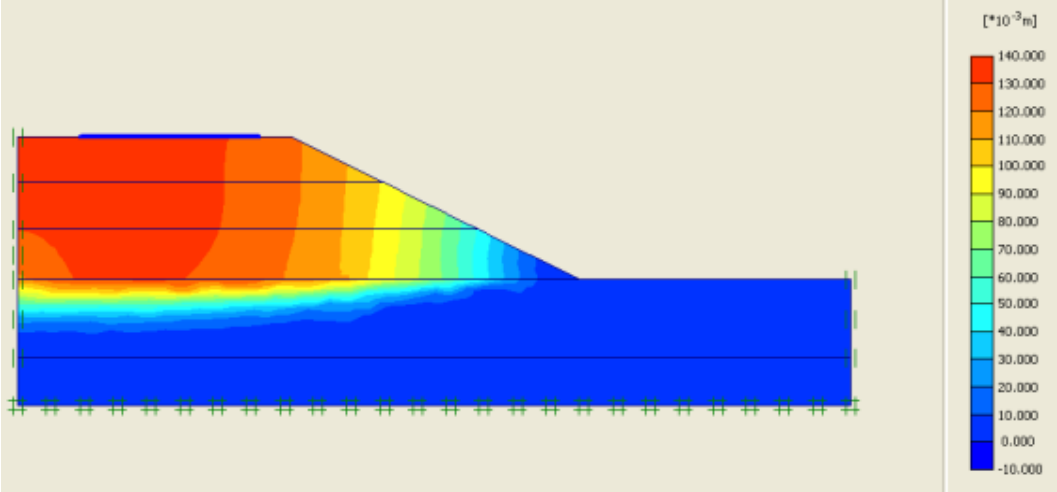

Figure 8.52. Total Displacements in the Control Section.

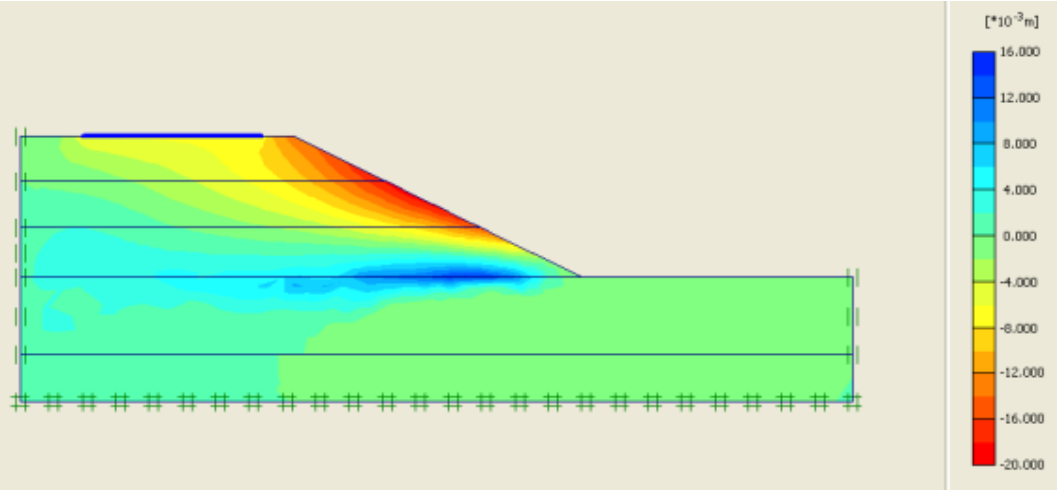

Figure 8.53. Horizontal Displacements in the Control Section.

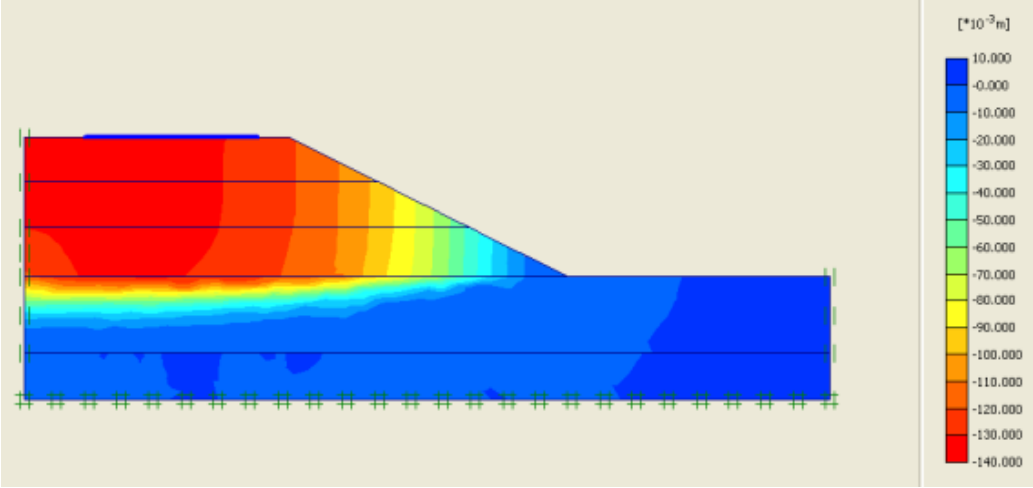

Figure 8.54. Vertical Displacements in the Control Section.

8.4.2.3 Validation

To validate the parameters used in the model, the results obtained from the above model analysis were used to compare with the elevation surveys from the field. The elevation surveys from Table 7.8 were plotted against the results of the numerical analysis shown in Figure 8.55. Time-settlement curves of both data are in agreement.

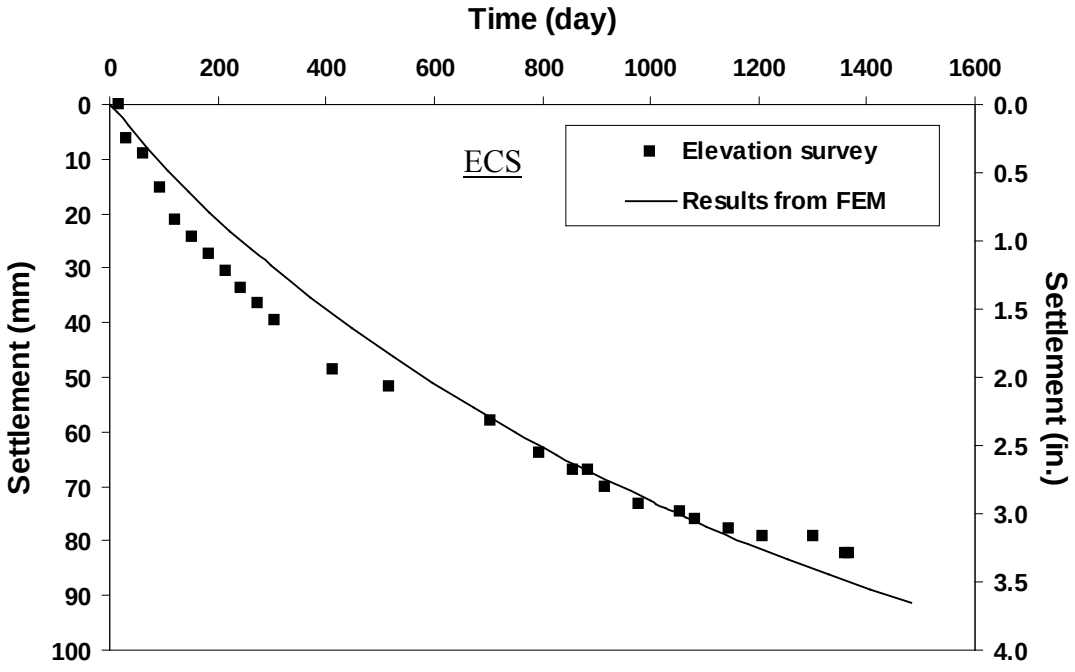

Figure 8.55. Comparison of the Vertical Displacements in the Test Section between the Data Obtained from the Elevation Surveys and the Results from the Numerical Analysis.

8.4.3 Analysis of the Vertical Soil Movements

A hyperbolic method as formulated by Lin and Wong (1999) was used to predict the long-term settlements of the test and control sections. According to Eq. 8.4, the elevation survey data from both the control and test sections were plotted against a function of time-settlement ratio as shown in Figure 8.56.

Using the regression equations obtained from Figure 8.56, the magnitude of the soil settlements at any specific time (t) in the embankments can be obtained. Therefore, the soil settlement that occurred at time (t) in the test section is equal to:

$$s = \frac{t}{(5.1468 + 0.0243t)} \text{ mm} \qquad (8.8)$$

and the soil settlement that occurred at time (t) in the control section is equal to:

$$s = \frac{t}{(5.2608 + 0.0085t)} \text{ mm} \qquad (8.9)$$

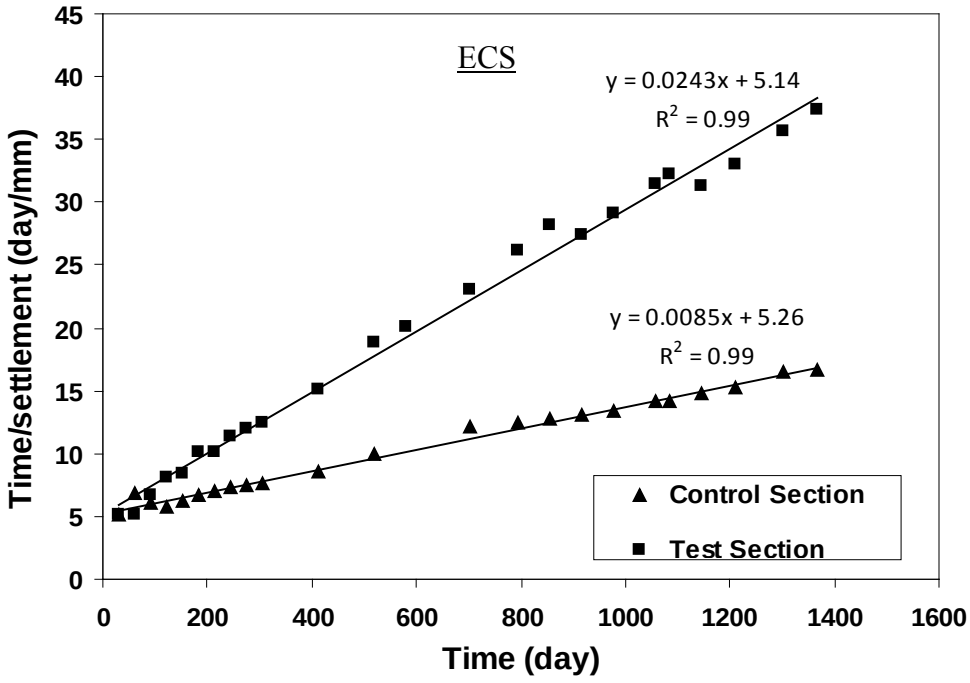

Figure 8.56. Regression Equations from the Hyperbolic Model to Predict the Soil Settlement Values in Both the Test and Control Sections.

By solving Equations 8.8 and 8.9 and with the time increment of 20 days, the soil settlement that occurred in both embankments at this specific time interval were plotted against data from the elevation surveys and the results from the numerical model, which are presented in

Figures 8.57 and 8.58. From both figures, the predicted soil settlements from the hyperbolic model and the FEM models are in agreement with the measured values from the elevation surveys. This means that the numerical model in the FEM and the hyperbolic equation from Eqs. 8.8 and 8.9 can be used to predict the settlements that occurred in both embankments with the results of the prediction shown in Table 8.7.

Table 8.7 Settlement Predictions from the Hyperbolic and FEM Models for the Test Section.

Settlements at year (in.)	Elevation surveys*	Hyperbolic model (extrapolated data)				FEM Model			
	4	4	10	20	30	4	10	20	30
Test Section	1.44	1.41	1.53	1.58	1.59	1.46	1.62	1.75	1.91
Control Section	3.36	3.22	3.94	4.25	4.37	3.50	4.76	5.31	5.35

Note: * - Measured Data

From Figure 8.57, the results from the extrapolated data and the FEM in both of the test and control embankments are in agreement.

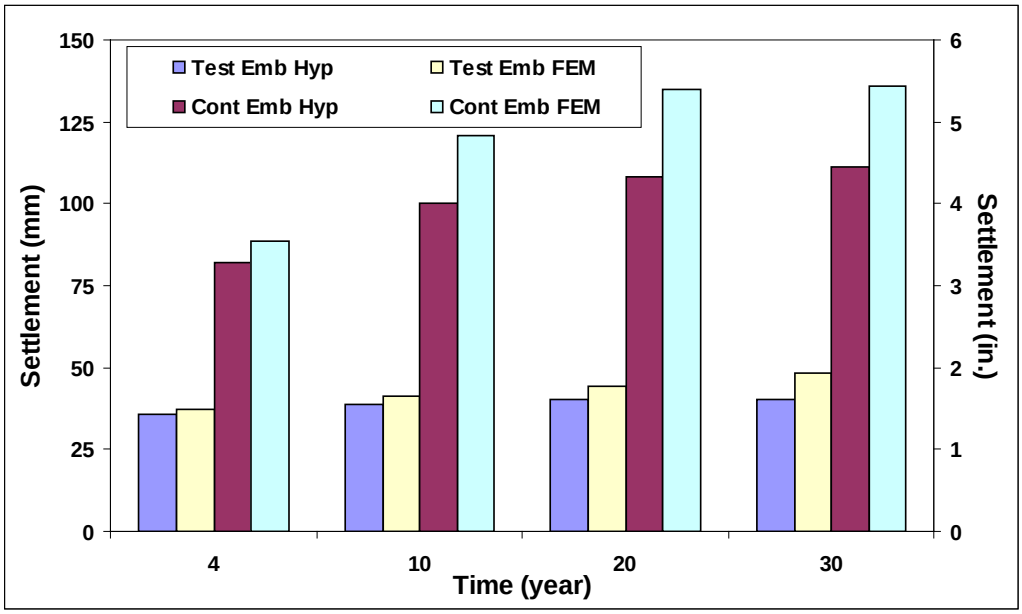

Figure 8.57. Settlement Values from the Data Extrapolation and FEM.

8.4.4 Prediction of the Soil Movements That Occurred in the ECS Section with Variations of Embankment Configurations

To investigate the effects of slope and height of the embankment configurations on the settlement, these two parameters were varied for different scenarios in this study.

8.4.4.1 Influence of Embankment Slope

In order to study the effect of the slope on the amount of the settlement that occurred in the embankment, as already performed in Section 8.3.5.2, the gradient of the embankment was changed with various V:H ratios of 1:1, 1:2, 1:3, and 1:4 while the height of the embankment was kept constant at 30 ft (9 m). Figure 8.58 shows monitored Point A and the embankment model with a slope of 1:1 (V:H).

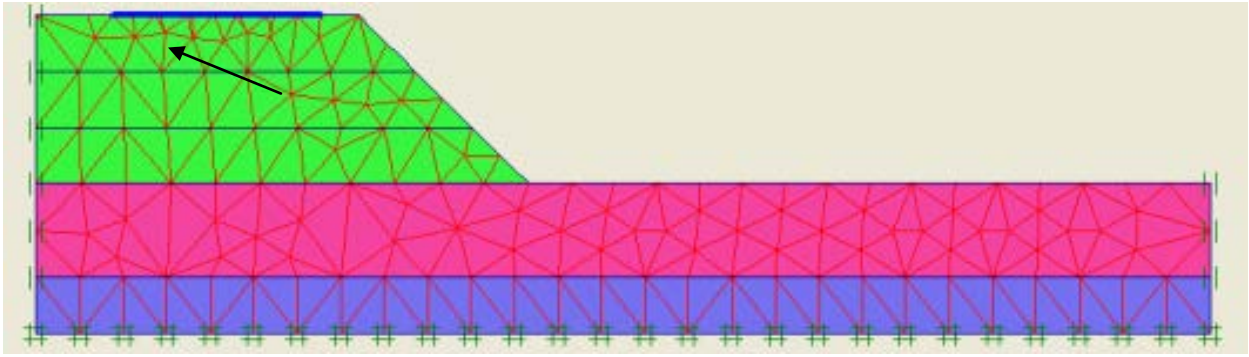

Figure 8.58. Geometry of the Test Section with a Slope of 1:1 (V:H).

The results from the numerical analysis are shown in Table 8.8. Both the horizontal and vertical soil displacement values that occurred in the embankment with the various slopes are not significantly different.

Table 8.8. Maximum Soil Displacements with Various Embankment Slopes.

Slope (V:H)	Vertical displacement		Horizontal displacement	
	in.	mm	in.	mm
1:1	1.73	43.95	0.68	17.23
1:2	1.91	48.63	0.47	11.91
1:3	1.96	49.70	0.38	9.55
1:4	2.16	54.80	0.35	8.80

Figure 8.59 shows the deformed mesh of the embankment with a various slope by magnifying it 50 times. As shown in Figure 8.59, the weight of the embankment structure can affect the extent of the consolidated area in the soft clay layer. With the milder slope, the settlement can be found in a wider area. If the slope stability is not problematic, more settlement can be induced by the wider slope. The gravity load of the embankment was considered as a main factor in this case.

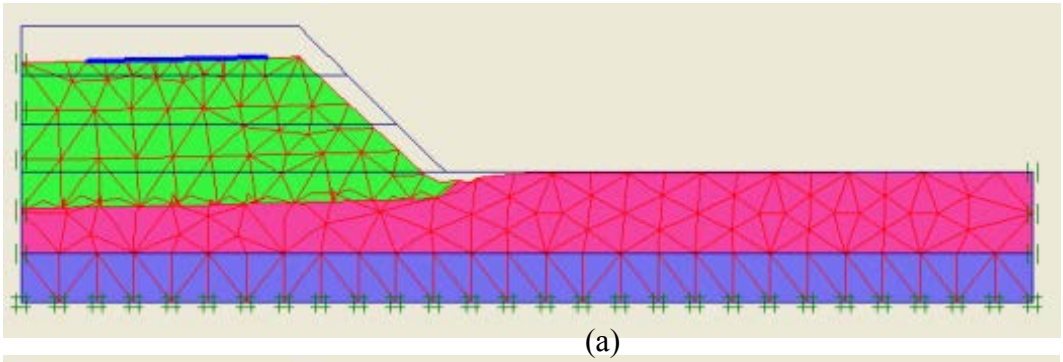

(a)

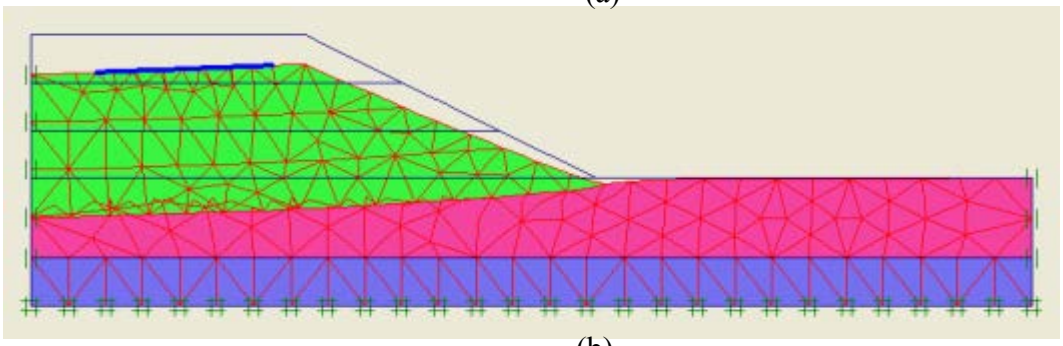

(b)

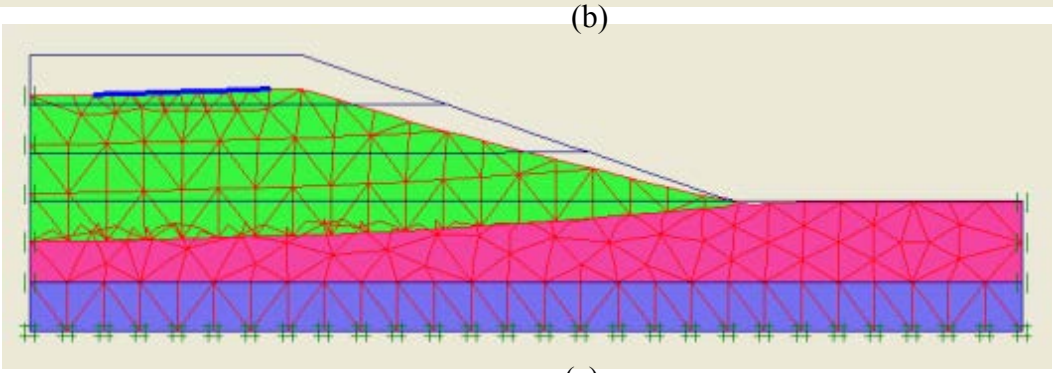

(c)

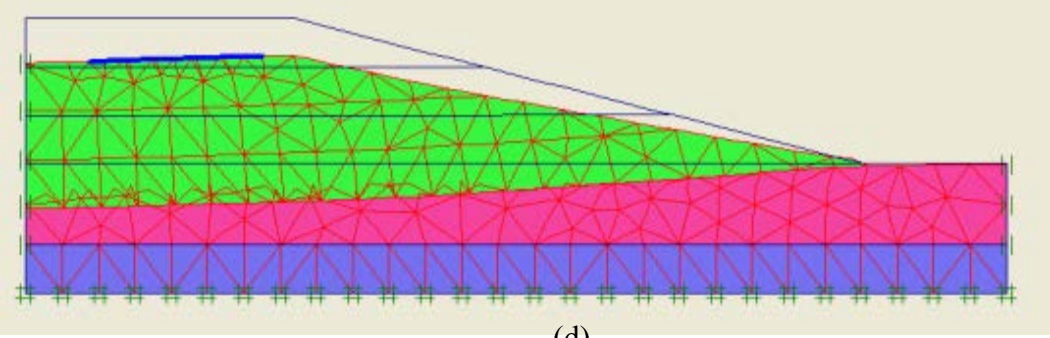

(d)

Figure 8.59. Deformed Mesh Showing Total Settlements in the Embankments with Various Slopes of a) 1:1, b) 1:2, c) 1:3, and d) 1:4 (V:H).

8.4.4.2 Influence of the Embankment Height

Another analysis was performed to examine the effect of the embankment height on the soil settlement. The heights of the embankment were varied from 20 to 40 ft (6.0 to 12.0 m) while the slope ratio was kept constant at 1:2 (V:H). Figure 8.60 shows Point A, which was selected to study in these analyses. The embankment model used a height of 20 ft (6.0 m) and slope of 1:2 (V:H). The width of the embankment at its base also varied according to the height of the embankment from case to case in order to maintain the slope value at 1:2.

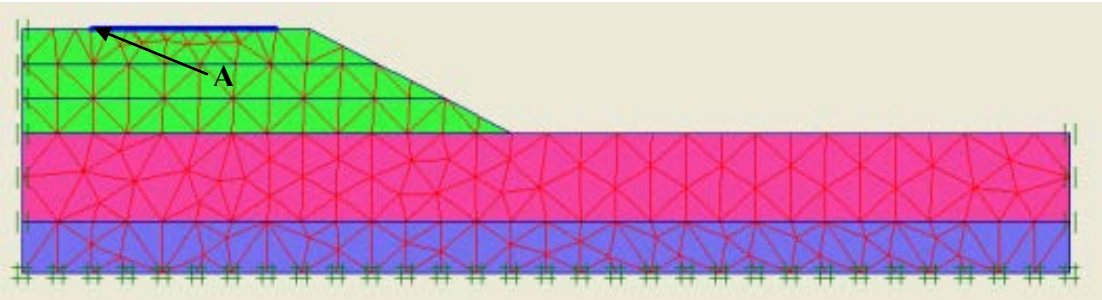

Figure 8.60. Geometry of the Test Section with a Height of 20 ft (6.0 m).

Figure 8.61 shows the time-settlement curves from the different heights of embankment at Point A in the test section. The highest settlement value is 2.8 in. (71 mm) when the height of the embankment is 40 ft (12 m) and the lowest value is 0.27 in. (7 mm) when the height is 20 ft (6 m). That means that the magnitudes of the soil settlements are influenced by the height of the embankment, i.e., the self weight load exerted from the embankment.

8.4.4.3 Conclusion from the Variable Studies

The height of the embankment has a great influence on the amount of settlement in the test section in this study. On the contrary, the slope of the embankment has not influenced the

magnitudes of the settlements but rather on the coverage of the consolidated area in the soft clay layer as seen in Figure 8.59. Overall the weight of the embankment has more influence on the settlements of the embankment. When the weight of embankment is increased due to the height of the embankment, the more settlement can be expected.

8.4.4.4 Design Chart for the Embankment Filled with ECS

From the variable studies, the most influent factor for the settlement control in the embankment constructed with the ECS is the height of the embankment. Therefore, a design chart was developed taking into account the different heights of embankment ranging from 15 to 40 ft (5 to 12 m). In addition, the thickness and the compression indices of the subgrade were also varied. The thickness of the subgrade ranged from 10 to 20 ft (3.0 to 6.0 m) and the compression indices from 0.34 to 0.40. According to the following design procedure, the ECS embankment design charts shown in Figure 8.61 can be interpreted.

1. Establish the height of the embankment.
2. Select the appropriate chart from Figure 8.61 based on the thickness of the subgrade.
3. For the given compression index of the subgrade, compare the settlement from the ECS fill embankment section to the local fill embankment section.
4. Select the fill with a settlement most near to the allowable settlement requirement.

8.5 SUMMARY

This chapter presents the details of the numerical analysis. The data from the laboratory studies in Chapter 5 and from the site monitored data presented in Chapter 7 were used as input data for the numerical analysis in the FEM model and in the hyperbolic model shown in Lin and Wong (1999) to determine the settlement values that occurred in the embankments at various time periods. In this study, the analyses were performed on two bridge sites: the DSM site on IH 30 and the ECS site on SH 360, both in Arlington, Texas. Each bridge site had a control and a test section to compare the effectiveness of each mitigation method, i.e., deep soil mixing for foundation soil improvement and lightweight fill embankment section.

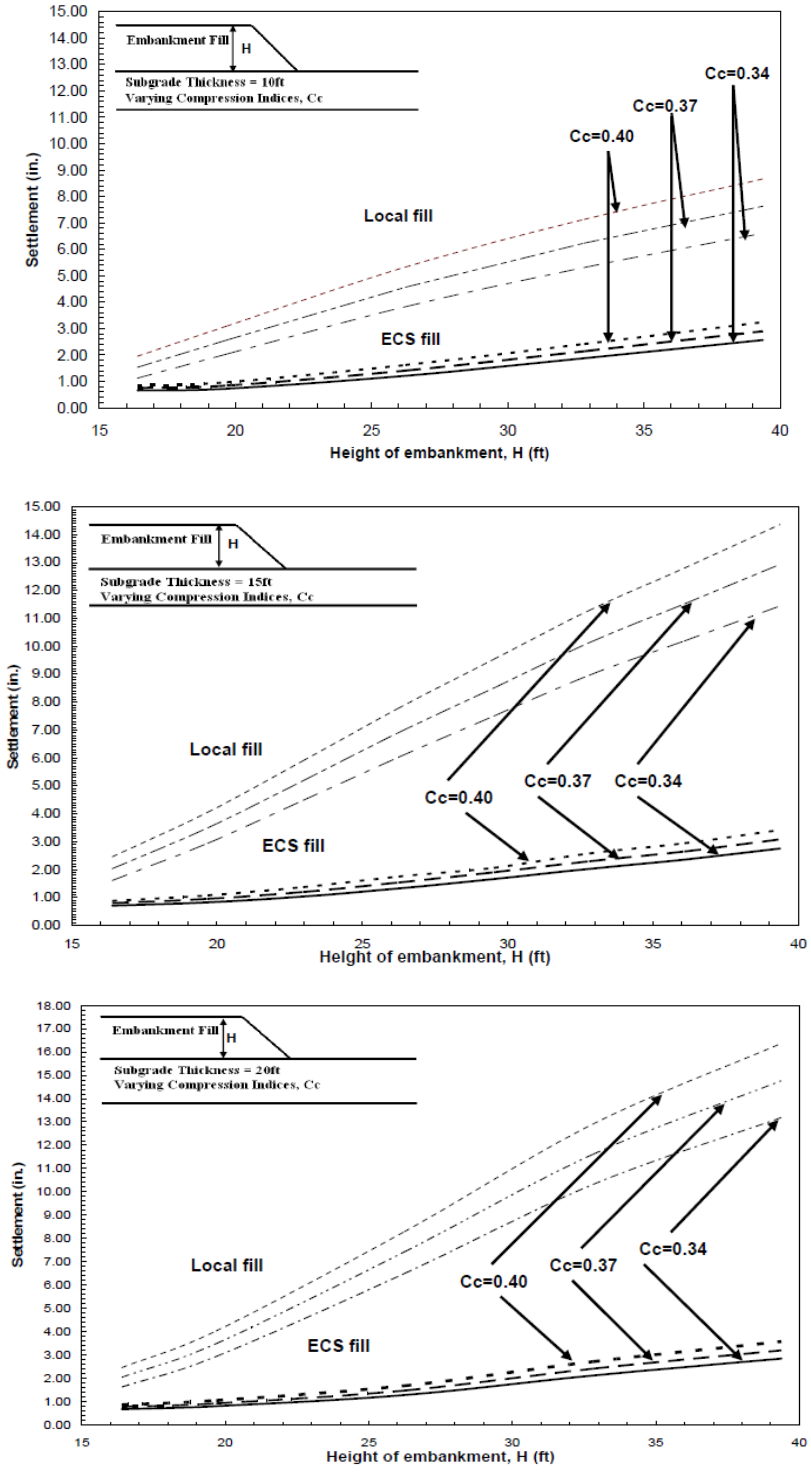

Figure 8.61. Design Charts for ECS Embankment.

To perform the analyses, three tasks were performed on modeling and validation, settlement prediction and comparisons, and modeling with various embankment configurations. For the model validation, the soil parameters and embankment geometry were used as the input

parameters in the model. In this task, after the numerical model had been completely executed, the results from the numerical analyses were compared with the monitored data from the field to validate the model. The second task, settlement prediction, was performed after the model validation in the first task had been satisfied. In this task, the predictions were forecasted to obtain the settlements that might occur in longer time durations of 10, 20, and 30 years using the hyperbolic model. The results from the analyses performed on both the test and control sections were then compared to evaluate the effectiveness of the embankment constructed with and without these mitigation methods. The last task was performed to understand how the amount of settlement that occurred in the treated embankment was affected by various embankment geometries.

For the DSM site, the long-term settlement predictions were performed, and the results showed that the DSM can be a viable technique to use as a mitigation method for the bump problem. The DSM can lessen the settlement magnitude from 9.5 to 1.6 in. (240 to 40 mm) within 2 years and from 10.6 to 2.5 in. (270 to 64 mm) within 10 years. Moreover, two other conclusions can be drawn from the variation of embankment configurations study. First, the area-ratio between the DSM and subgrade soil, with the most preferable values between 0.5 and 0.6, is a major factor in decreasing the amount of settlement that can occur in the embankment. Second, without the subgrade improvement technique, the weight of the embankment governs the amount of settlement. As seen from the factor study in the variance of height and slope of the embankment, the higher settlement can be expected from the higher embankment and the size of the consolidation area is influenced by the extension of the slope.

For the ECS site, researchers concluded that using lightweight as a backfill material can reduce the predicted settlement in the embankment. Since the gravity load exerted on the subgrade by the embankment is a main factor governing the settlement in the ECS site, the embankment constructed with the lightweight ECS has the least amount of settlement than the one constructed with a normal soil and the higher embankment experiences more settlements than the lower one. However, using ECS as a backfill material is not a foolproof technique to reduce the settlement. Although 30-year calculations using lightweight fill can reduce the settlement by 30%, this method does not impede the consolidation. Nevertheless, the settlement in the embankment, which is induced by the consolidation, will still exist and remedial techniques are necessary in the long-term.

In conclusion, based on the study, the DSM technique is considered an effective method. It can reduce the amount of settlement that may occur in the embankment and also impede the consolidation from occurring in the soft subgrade soil layer. Therefore, the settlements that occurred in the DSM site were not only small but also will be terminated in a short duration. Another mitigation method investigated in this study was using lightweight material as an embankment fill. This technique can reduce the settlement in the embankment also. However, according to the previous discussion, maintenance repairs are still necessary in this type of embankment for long-term service.

CHAPTER 9

MAINTENANCE MEASURES FOR DISTRESSED APPROACH SLABS

9.1 INTRODUCTION

Bridge approach maintenance costs in the United States are estimated to be at least $100 million per year (Briaud et al., 1997; Nassif, 2002). The best practice to minimize the occurrence of bridge bumps is to establish up-to-date maintenance activities and by scheduling periodic repair activities in addition to the required occasional maintenance (Dupont and Allen, 2002). Hence, it is important to understand the different mitigation techniques available to repair the distressed bridge approach slabs. This chapter presents an overview of the repair methods adopted for treatment of settled bridge approach slabs in various districts in Texas. Also, the results and details of the geophysical studies performed to implement a few of these technologies are summarized.

9.2 BRIDGE IDENTIFICATION AND REPAIR

A total of four bridges with distressed approach slabs in Texas were identified. Table 9.1 gives the identification and location of the bridges along with the mitigation technique either adapted or proposed as a part of this research project.

Table 9.1. Distressed Bridges and Mitigation Techniques Adopted.

Site No.	Identification	Location	Mitigation Technique Proposed
1	FM 1947	Hillsboro Waco District	Urethane Injection
2	US67 at SH 174	Cleburne Fort Worth District	Soil Nailing
3*	SH 6	Quanah Childress District	Geo Foams and Flowable Fills
4*	IH 410	San Antonio San Antonio District	Flowable fills

* Repair solution recommended but not implemented

Each subsection in the chapter presents the repair solutions and geophysical studies performed.

9.2.1 FM 1947 near Hillsboro, Waco District, Texas

A bridge approach slab repair at a bridge crossing Aquilla Lake on FM 1947 near Hillsboro in the Waco District was the first one studied as a part of this research. The location of the bridge is shown in Figure 9.1. At this bridge site, a polyurethane injection technique was used to lift the settled bridge approach slab.

Figure 9.1. Bridge Site Location, FM 1947 near Hillsboro.

Polyurethane is a high density polymer resin. For roadway repairs, tiny holes (usually 5/8 in. (15.86 mm) diameter) are drilled through the pavement slabs. The polyurethane is injected through a wand into the void spaces beneath the pavement. Once injected, the polyurethane expands into a foam-like structure filling in more than 90% of the void space and hardening in a very short period of time (usually 15 min. or less). This technique is usually performed in a square or triangular pattern to lift the pavement structures into their original position. Figure 9.2 presents a sketch of the pavement and bridge section observed in this study.

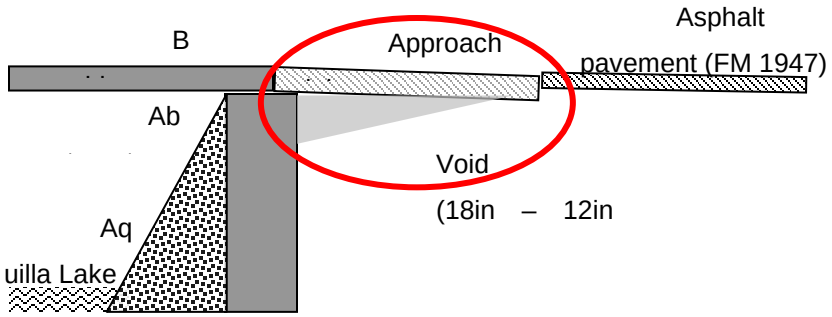

Figure 9.2. Problem Definition Sketch of the FM 1947 Bridge Site.

The polyurethane injection work at this site was carried out by the URETEK Company, USA. Before the actual injection process began, an elevation was performed on the bridge deck pavement and on the settled approach slab. A leveling thread was run over both pavements to determine the required amount of lift of the approach slab. The total settlement of the approach slab was around 4 in. (102 mm) before the repair. The depth of the void adjacent to the bridge abutment varied from 2 in. to 18 in. (56 to 457 mm) and gradually increased toward the abutment backwall. Figures 9.3 and 9.4 show the settlement and void formation, respectively. Figure 9.5 gives a closer view of the void under the slab.

Figure 9.3. Settlement of the Approach Slab.

Figure 9.4. Void Formation Adjacent to the Abutment.

Figure 9.5. Closer View of the Void.

The actual injection process began with drilling 5/8 in. (15.86 mm) diameter holes into the approach slab in a rectangular pattern to inject the polyurethane. The polyurethane expanded into a foam, lifted the settled approach slab to the required elevation, and hardened in place in less than 15 min. The principle benefit of this process was that this complex material is very light weight and the pressure against the subsoil due to the expanded foam was expected to be very low. A secondary benefit was that the time required for this treatment process was very short (total process time is in hours) when compared to the other conventional treatment techniques

such as cement grouting, asphalt overlay, or complete excavation and replacement of existing approach slabs. Figures 9.6 through 9.12 show the sequential process of the polyurethane injection beginning from the drilling of the holes to the final elevation of the approach slabs after the lifting process was completed.

Figure 9.6. Drilling Holes into the Approach Slab.

Figure 9.7. Another View of Drilling Holes.

Figure 9.8. Sealing the Void from the Exterior Face to Protect Loss of the Injected Polyurethane.

Figure 9.9. Taking Elevations during the Injection Process to Check for Extra Injection.

Figure 9.10. Pavement Differential of the Lifted Approach Slab during the Injection Process.

Figure 9.11. Another View of the Pavement Differential of the Approach Slab.

Figure 9.12. Level-Up of Uneven Sections with Cold Asphalt Mix.

Though there are no technical data readily available on this technique such as quality assessment and quality control studies, the post-performance of the approach slabs was found to be good. Further investigation into the use of this technique throughout TxDOT revealed that there are a few bridges that were repaired in the Houston District more than 10 years ago and they are satisfied with the performance of the polyurethane. One important item of interest that was discovered when investigating this product is that when using polyurethane injection, one must determine the amount of polyurethane that needs to be injected as this estimation is important in the cost analysis of the repair options. Considering this important fact, TXDOT amended its Special Specification 3043 using Special Provision 3043-001 "Raising and Undersealing Concrete Slabs" to calculate the quantity of polymer resin utilized by one of the following methods:

1. Payment will be made according to the actual quantity of polymer resin used in the work by weighing each holding tank with components by certified scales before and after each day's work.
2. Payment will be made according to the actual quantity of polymer resin used in the work by determining the weight of material placed by measuring the depth of polymer resin in the holding tanks before and after each day's work. A professional engineer and a site engineer must approve the calculation method that is based on

certified tank measurements, unit weight of each component of resins used in the work.

The repaired bridge approach slabs on FM 1947 were monitored for three years and the final settlement of the slab was less than ¼ in. (6.35 mm). However, it was discovered during a trip to the site in June 2011 that an overlay had been placed on the roadway, including the approach slabs, along several miles of FM 1947. Hence, additional observations will not be visible for a long time when significant differential settlement will reflect through the new pavement surface layer.

9.2.2 US 67 at SH 174 near Cleburne, Fort Worth District, Texas

Major repair work for the severely distressed bridge approach slabs on both ends of the US 67 bridge crossing over SH 174 was performed recently. The roadway has concrete approach slabs placed on embankments whose heights are around 35 ft (11 m). The location and elevation view are shown in Figures 9.13 and 9.14, respectively.

Figure 9.13. Bridge Site at US 67 over SH 174.

Figure 9.14. Existing Bridge along US 67 Crossing over SH 174.

The bridge was reported to be one of the earliest ones in Texas using the modular block walls with geogrids used as reinforcing elements. Since 1995 when the bridge and roadway were constructed, the approach slabs have settled as much as 17 in. (43 cm). Several mitigation methods were attempted to correct the ride and these methods included multiple HMAC overlays, two slab jacking attempts, and one compaction grouting installation directly under the approach slabs on each end of the bridge. These were not successful, as shown in Figure 9.15.

As a part of the research, laboratory tests were performed on the soil fill material under the approach slabs. This material was classified as non-plastic (NP) and poorly graded sand (SP). The problems associated with the distress in the approach slabs are also attributed to the erosion of the fill material underneath the slab and the settlement of the underlying foundation. The failure of the modular block wall and the erosion of the soil under the slab are shown in Figures 9.15 and 9.16.

Figure 9.15. Failure of the Modular Block Wall.

Figure 9.16. Erosion of the Soil under the Slab.

In order to address the observed movements of the modular block wall and correct its stability, the soil nailing technique was recently employed by the Area Office. Soil nails are slender reinforcement elements, generally rebar, inserted into the soil at predetermined locations based on a design to provide shoring and stability. Holes are drilled for placing the reinforcement and once placed, filled with grout. The rebars are placed at a slightly downward inclination to the ground surface and are placed at regularly spaced intervals. Once the rebars are placed, a wire mesh is placed on the soil face and is shotcreted from the exterior to tie the entire system together.

The soil nailing technique for this project was carried out by Olden Inc. Reinforcement bars conforming to ASTM A615, Grade 60 (#6 rebars) with a square head plate 5 in. × 5 in.

(127 ×127 mm) and a thickness of ⅜ in. (9.525 mm) conforming to ASTM A36 were used as soil nails. A Coinc 528NS brand grout with a compressive strength of 3000 psi (20684.25 kpa) after a 7 day curing period was used to fill in the annular space between the rebar and the soil wall. The drilling of the holes for placing the soil nails is shown in Figure 9.17.

Figure 9.17. Drilling of Holes to Place the Soil Nails.

The soil nails were placed at a spacing of 6 ft (1.83 m) horizontal and 4 ft (1.22 m) vertical. The length of each nail was 16 ft (4.88 m). After the placement of the nails, the hole was completely grouted. Samples of the grout were collected to test for the compressive strength. The installation of the soil nails and the grouting of the drilled holes is shown in Figure 9.18.

Figure 9.18. Placing of Nails and Grouting the Holes.

A welded wire fabric reinforcement, conforming to ASTM A185 with dimensions of 4 in. × 4 in. (W1.4 × W1.4 10GA) was placed along the soil face and shotcreted with a cement-based grout strength of 4000 psi (27,579 kpa) after a 28 day curing period. The shotcreted exterior is shown in Figure 9.19. The total soil nailing process on both ends of the bridge was completed in 10 days.

Figure 9.19. Shotcreting the Exterior Soil Face.

Since the soil nailing technique was recently completed in early summer 2011, further monitoring of the bridge by the researcher was not performed to the contract expiration. A recommendation was made to TxDOT on what types of monitoring should be used and the frequency required as this is needed to address the use of this technique to control approach slab settlement that is induced by modular block wall fill erosion and potential settlement of the foundation subgrade.

In the following sections, comprehensive geophysical and geotechnical explorations were performed to understand the causes of settlements of slabs at two additional locations in the state. A few treatment methods were suggested; however, they were not implemented due to circumstances beyond the control of the project monitoring committee.

9.2.3 SH 6, Quanah, Childress District, Texas

A series of field tests were carried out by the University of Texas at El Paso (UTEP) research team to assess the condition of the bridge approaches on SH 6 just north of Quanah, in the Childress District. A Ground Penetrating Radar (GPR) system was used to evaluate the bridge approaches and embankments to detect potential voids or anomalies below the surface. Field tests were conducted on the northbound and southbound lanes. Figure 9.20 gives the location of the bridge site.

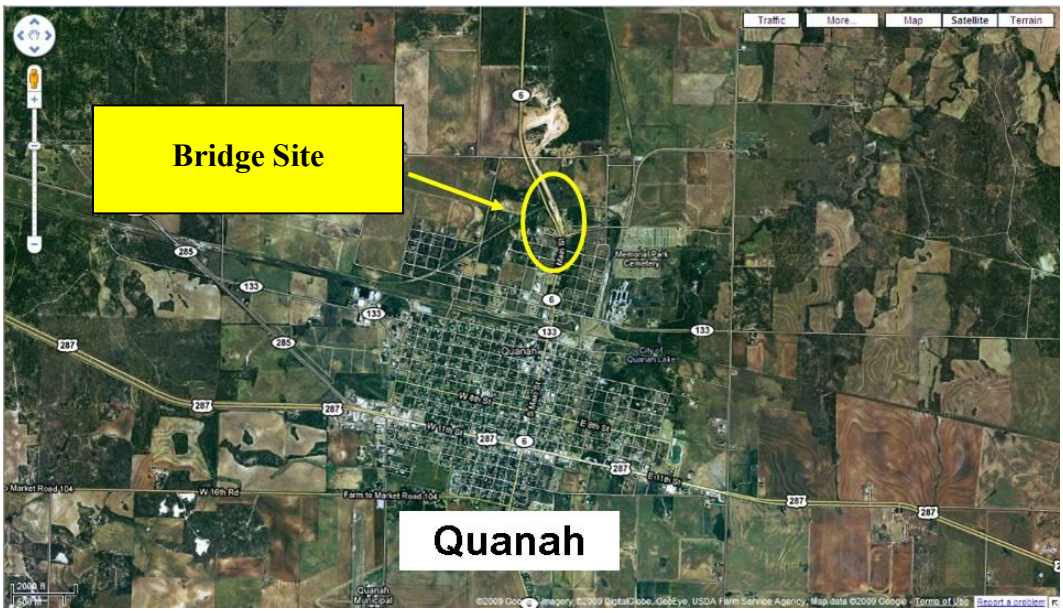

Figure 9.20. Bridge Site, SH 6, Quanah, Childress District.

GPR is a geophysical nondestructive technique that uses electromagnetic pulses to test, characterize, or detect subsurface materials based on changes in electrical and magnetic properties of the subsurface layers. GPR works using short electromagnetic pulses radiated by an antenna that transmits these pulses and receives reflected returns from the pavement layers. The reflected pulses are received by the antenna and recorded as a waveform. As the equipment travels along the pavement, it generates a sequence of waveforms or linescans. These waveforms are digitized and interpreted by computing the amplitude and arrival times from each main reflection. The reflections of these waves at the interfaces and objects within the material are analyzed to determine the location or depth of these interfaces and buried objects and to determine the properties of the materials. Whenever applicable, GPR can be employed as a rapid nondestructive tool for the evaluation of geometrical and material properties of structural components.

The test setup used in this study is shown in Figure 9.21. The equipment used for the GPR survey consists of a GSSI SIR-20 (SIRveyor) two-channel data acquisition unit controlled by a laptop computer, a ground-coupled antenna, and a survey wheel attached to the antenna. For this study, three different antennas were used: a 1.6 GHz (GSSI Model 5100), a 400 MHz (GSSI Model 5103), and a 200 MHz (GSSI Model 5106). The three antennas were used to cover different penetration depths, identify precisely pavement interfaces, and also detect the presence of utilities or anomalies at different depths. The maximum depth of penetration of each antenna

reaches to about 18 in., 4 ft, and 8 ft (0.46, 1.22, and 2.44 m), respectively, depending on the conductivity of the materials underneath.

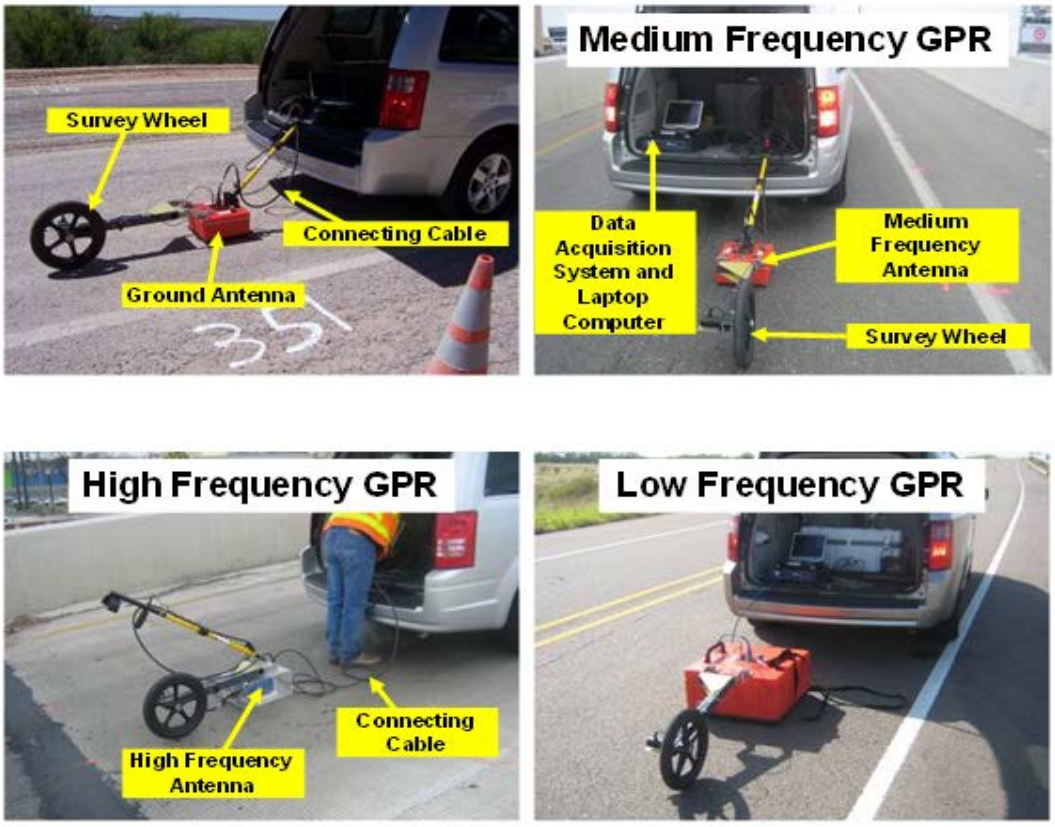

Figure 9.21. GSSI GPR System and Antennas Used in This Study.

The schematic of the test section at this site is shown in Figure 9.22, and the views from both ends of the section and north and south approach slabs are illustrated in Figure 9.23. The shoulders, main lanes, and selected concrete riprap plating the sideslopes were investigated. Linescans with the low (200 MHz) and high (1.6 GHz) frequency antennas were obtained along the center of the shoulder and main lanes in both directions. The lengths of the survey lines past the north end of the bridge were 1600 ft (487.68 m) while the survey lines past the south end of the bridge were 800 ft (243.84 m) long. In addition, four linescans with the high frequency antenna were obtained on each of the four embankment slopes (identified from 1 to 4) to evaluate the presence and extent of anomalies and voids under these selected slabs. Linescans of two of the four lanes were obtained on the outer edges of the slopes and the other two were equally distributed on the radial direction of each slope.

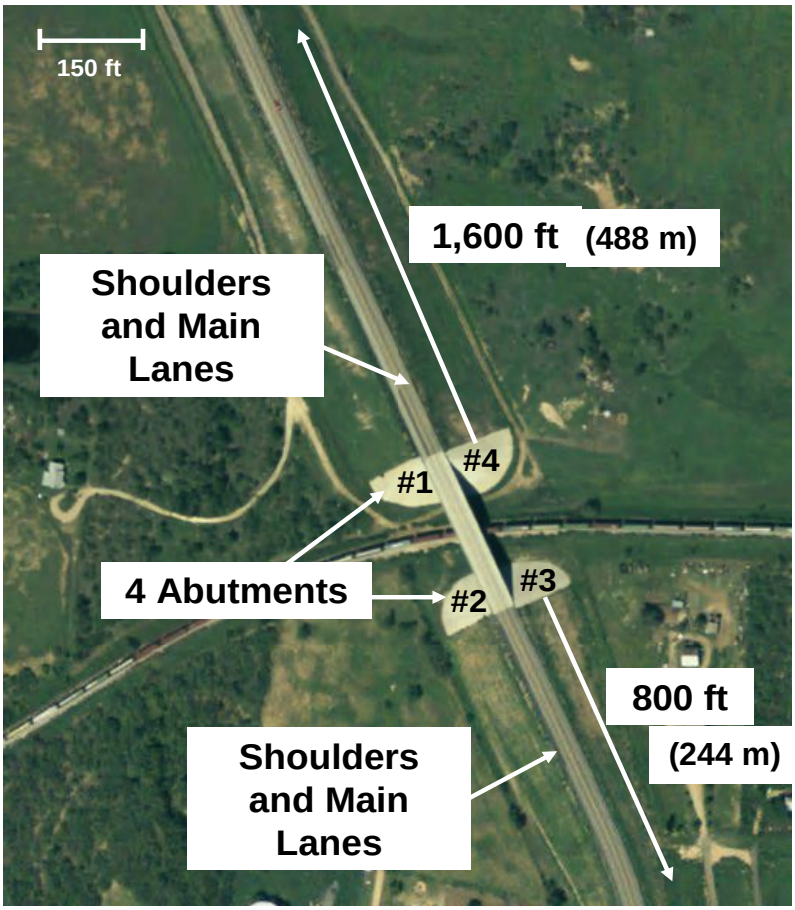

Figure 9.22. Test Section along SH 6.

a) North End b) South End

c) North approach Slab d) South approach Slab

Figure 9.23. Field Pictures.

A typical linescan for the test conducted on the southbound lanes obtained with the high frequency GPR antenna is shown in Figure 9.24. The horizontal axis relates to the distance measured from the start point (ft) and the vertical axis indicates the estimated depth using a typical dielectric constant of 6.5. This 30 ft (9.2 m) linescan shows the 20 ft (6 m) approach slab and the next 10 ft (3 m) of the pavement structure away from the bridge end. The pavement structure on the approach slab consisted of a hot mix asphalt (HMA) layer on top of a concrete slab of about 10 in. (25.4 cm) thick. The approach slab, HMA-base interface, and subgrade-base interface are identified in the figure. For the approach slab, the bottom of the HMA and the transverse reinforcement within the slab are marked. Based on the linescan, the thickness of the HMA was approximately 2.5 in (6.35 cm) and the steel rebar reinforcement appeared about 5 in. (12.7 cm) below that.

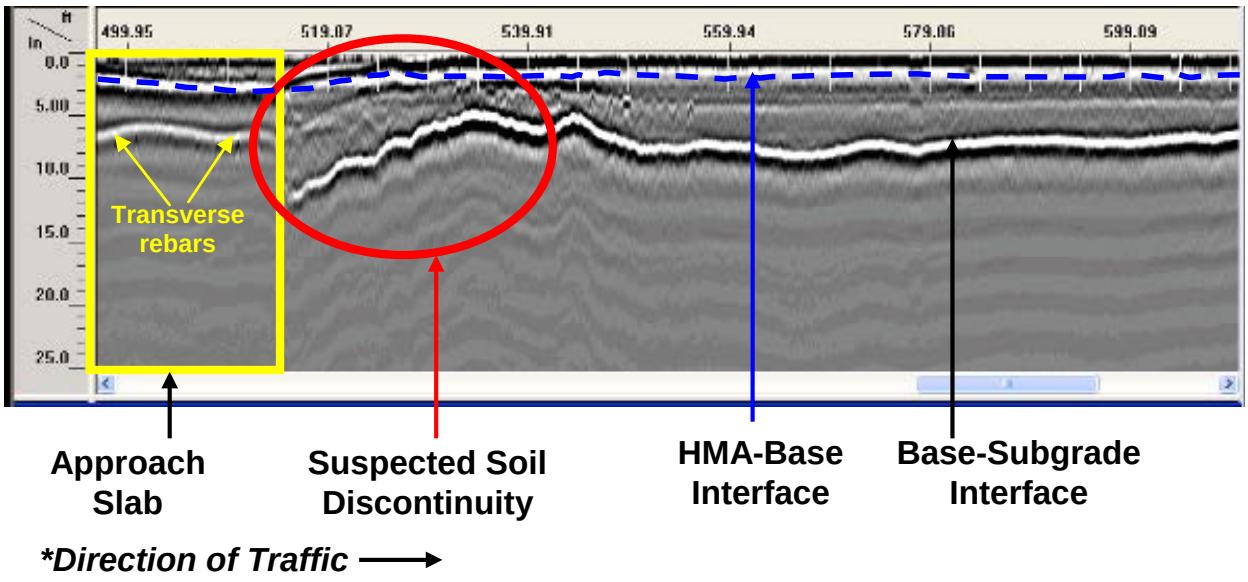

Figure 9.24. Typical Linescans with High Frequency Antenna.

In addition, an area of discontinuity immediately after the approach slab is highlighted. This area was approximately 40 ft (12.2 m) long and showed an erratic base-subgrade interface depth that ranged from 5 to 13 in. (12.7 to 33.02 cm). For the rest of the linescan, this interface appears at about an 8 in. (20.32 cm) depth The HMA-base interface appears to be at a depth of approximately 2.5 in. (6.35 cm). Under these layers, several other horizontal interfaces are dimly observed. These other layers are assumed as different layers within the subgrade.

Similar to the high frequency antenna, a typical linescan obtained with the low frequency antenna along the same area is shown in Figure 9.25. In this case, the horizontal scale is different because the starting point was located a few feet before the approach slab. Strong reflections were observed at the beginning of the linescan that corresponds to the bridge slab. Due to the lower frequency of the antenna, details of the approach slab are not as clearly identified as with the other antenna. The suspected soil discontinuity is also present that extends deeper than the previous linescan. Like the high frequency antenna, several other horizontal interfaces are observed but with stronger reflections. Similarly, these layers are assumed as different layers within the subgrade.

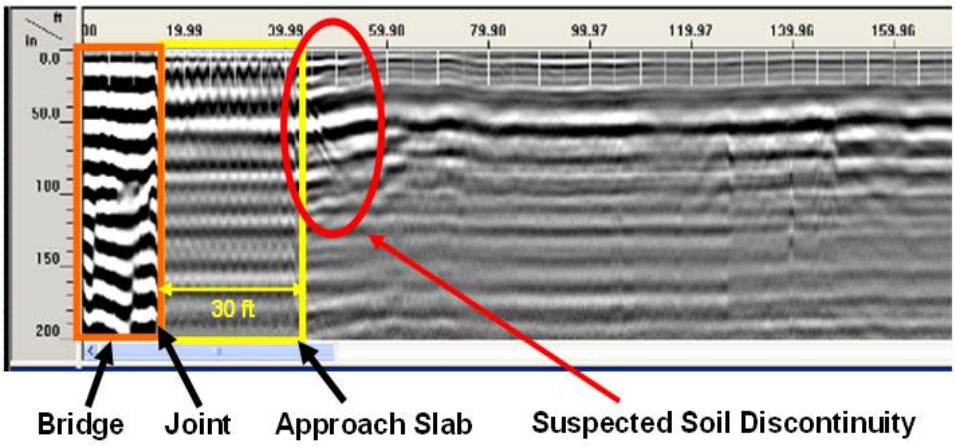

Figure 9.25. Typical Linescans with Low Frequency Antenna.

A sample linescan along the second slab of Slope 3 is shown in Figure 9.26. Some anomalies along the last 10 ft (3.0 m) (closer to the top of the slope) were observed. These may reveal the presence of voids or areas of concerns.

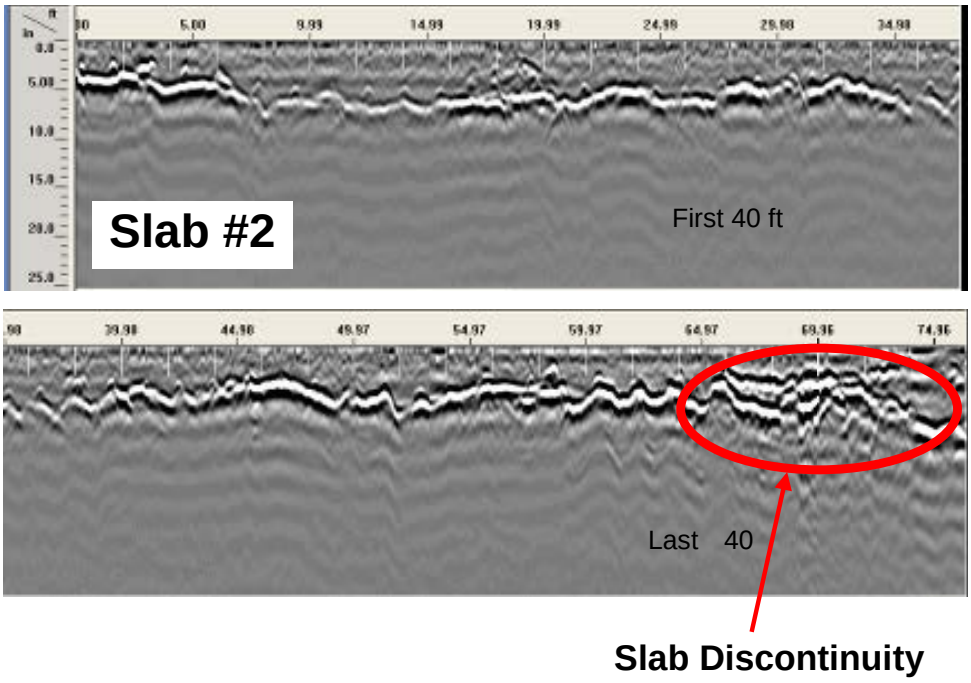

Figure 9.26. Typical Linescans from Slope 3.

The overall results from this survey are summarized in Figures 9.27 and 9.28 for the north and south sides of the bridge, respectively. GPR scans on the most critical areas are also

shown. The locations of possible void areas on the concrete slopes are also depicted. Based on the GPR data, areas of concern along the north side are located mainly on the southbound shoulder and lane and also about 30 ft (9.0 m) from the approach slab. Only one area on the south side, contiguous to the approach slab, seems to show some anomalies. For the case of the concrete slopes, the outer lines of Slopes 1 and 2 appear to have the longest void areas.

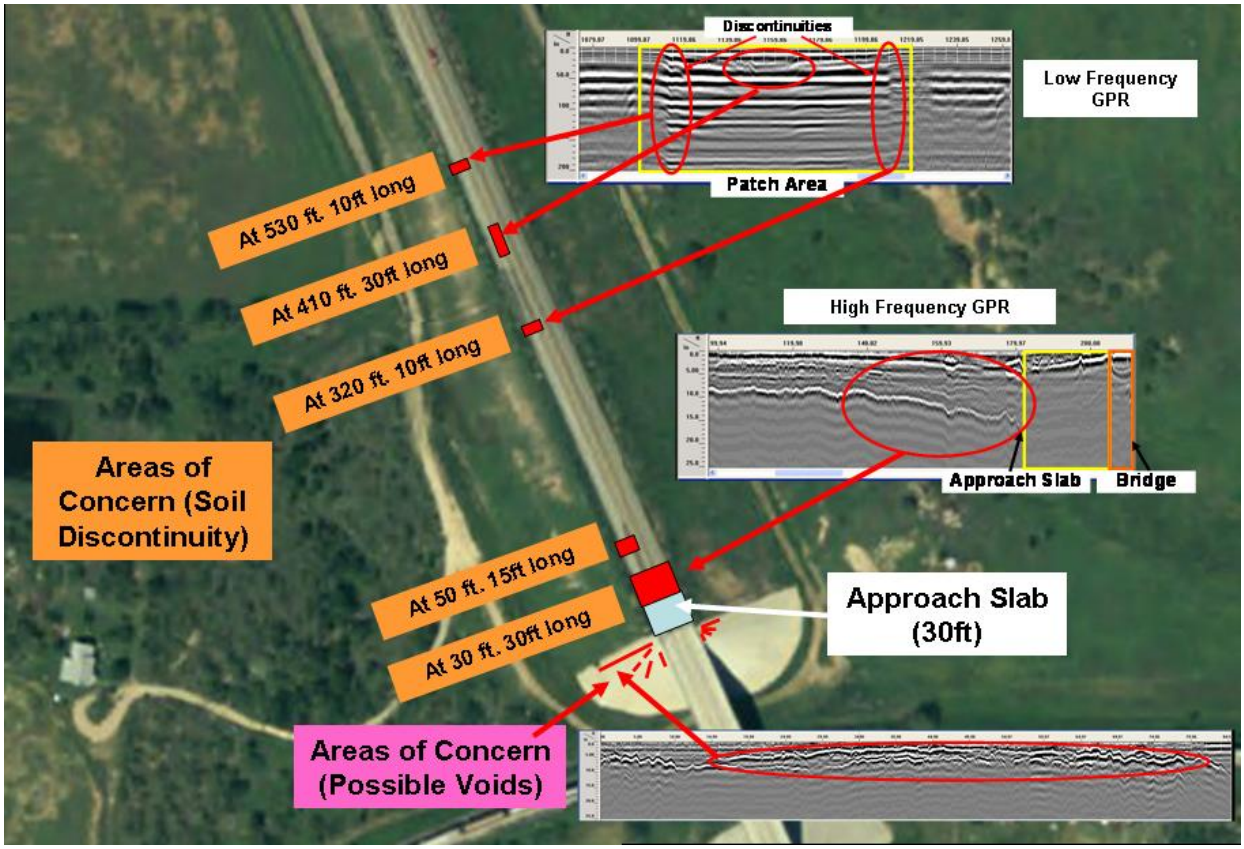

Figure 9.27. Overall Results (North Side).

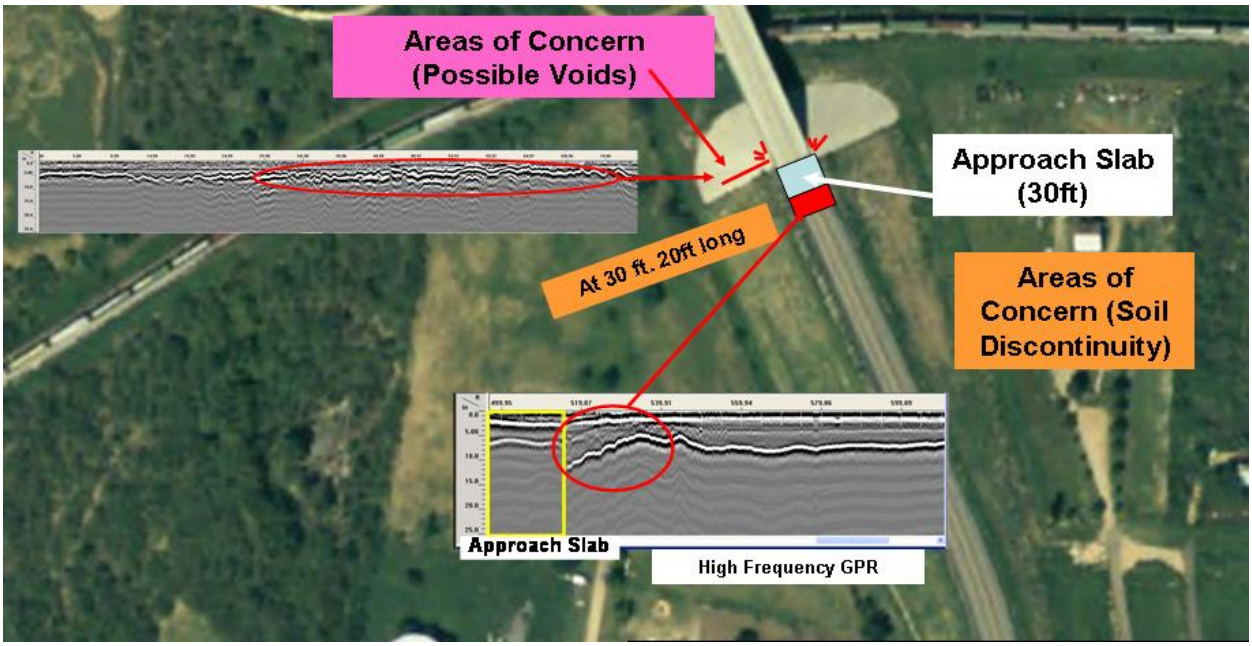

Figure 9.28 Overall Results (South Side).

9.2.3.1 Potential Void Volume Estimation under the Approach Slabs

An estimation of the suspected voids under the approach slabs, immediately before the bridge deck, was carried out. For this estimation, detailed GPR scans on the approach slabs were evaluated. As an example, Figure 9.29 shows a linescan of the southbound shoulder. The HMA-concrete interface, transverse rebars, and the bottom of the approach slab are identified at several selected points. With the assumed dielectric constant of the pavement structure, estimated depths were obtained and are presented in Figure 9.30. The suspected void under the approach slab adjacent to the bridge joint is also depicted. This suspected void area was measured by calculating the compound average difference of the bottom of the approach slab away from the bridge joint and from the linescan adjacent to the bridge joint.

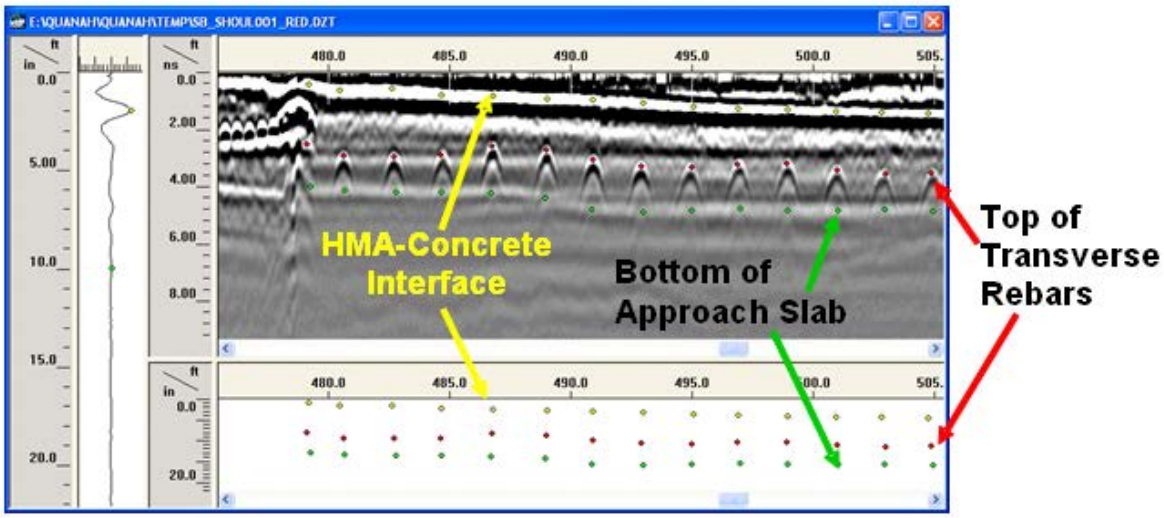

Figure 9.29. Selection of Points from the GPR Linescan.

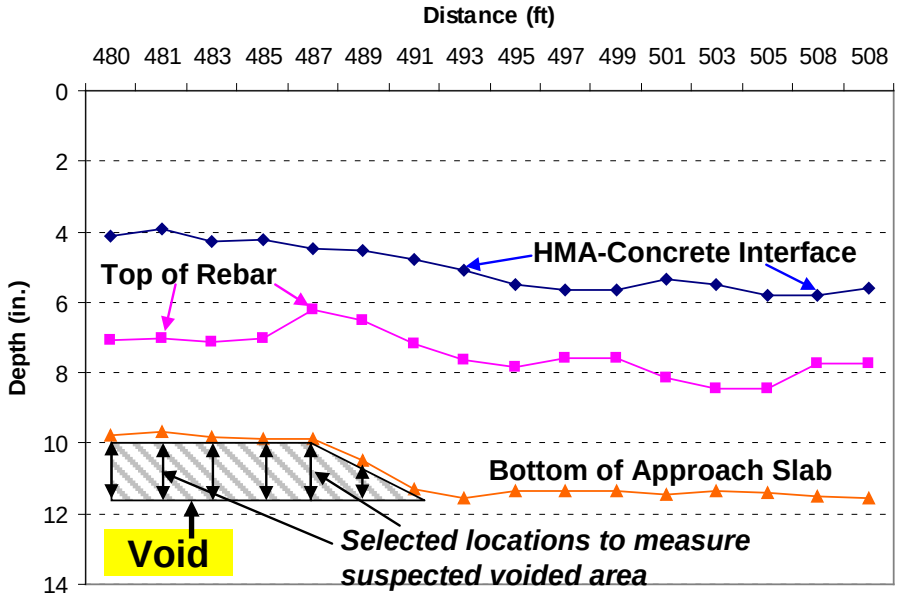

Figure 9.30. Estimated Depth Profile.

In the case shown above in Figure 9.30, the void area extends about 11 ft (3.35 m) from the bridge joint with a trapezoidal shape. The estimated volume was obtained by multiplying this area by the width of the shoulder (8 ft [2.44 m] in this case). The same process was implemented on the rest of the shoulders and main lanes and final void volumes were obtained and

summarized in Table 9.2. A width of 12 ft (3.66 m) was used for the case of the main lanes. From Table 9.2, the region under the southbound lane seems to have larger void areas.

Table 9.2. Voids under Approach Slabs.

	Estimated Void Volume (ft3)	
	Before Bridge	After Bridge
SHOULDER SB	3.7	7.8
LANE SB	23.5	15.4
SHOULDER NB	10.4	6.5
LANE NB	13.9	15.5

The same study was conducted for the four concrete slabs investigated on each slope. Estimated void volumes are presented in Table 9.3. A width of 4 ft (1.22 m) was assumed for each slab to obtain the volume. Slopes 1 and 4 exhibit larger void volume under the concrete slabs.

Table 9.3. Voids under Abutment Slabs.

	Estimated Void Volume (ft3)				
	Slab 1	Slab 2	Slab 3	Slab 4	
Abutment 1	1.9	3.3	8.6	10.8	*North Side SB Lane*
Abutment 2	1.2	1.9	3.0	5.4	*South Side SB Lane*
Abutment 3	0.0	8.4	3.0	3.5	*South Side NB Lane*
Abutment 4	8.0	3.8	2.4	5.9	*Noth Side NB Lane*

Based on the estimated void volume, the use of geofoam blocks covered with a geomembrane to protect from leaching oils on the north side of the bridge and use of flowable fill on the south side of the bridge is proposed. The proposed mitigation techniques were not implemented as the long-term performance of these techniques is still in the research phase and the local district is exploring for permanent solutions.

9.2.4 IH 410 Site in San Antonio, San Antonio District, Texas

A series of field tests, similar to the tests conducted on SH 6 in Quanah, using a Ground Penetration Radar were carried out to assess the condition of a bridge approach on IH 410 in San Antonio. In addition, cores were collected from the test locations and Dynamic Cone Penetration (DCP) tests were conducted at the core locations. The results of the GPR system and DCP test are presented and the volume of voids under the approach slabs is estimated. The location of the identified bridge is given in Figure 9.31.

Figure 9.31. Bridge Site on IH 410 in San Antonio.

The overall view of the section is shown in Figure 9.32, and the views of the investigated west and east approach slabs are illustrated in Figure 9.33. Both slabs were 20 ft (6.0 m) in length. Five longitudinal and five transverse linescans were obtained per each approach slab. The location of each line is detailed in Figure 9.34. GPR surveys were performed with a medium (400 MHz) and a high (1.6 GHz) frequency antenna. The longitudinal surveys were carried out on the approach slab and also on 50 ft (15.24 m) of the bridge ramp.

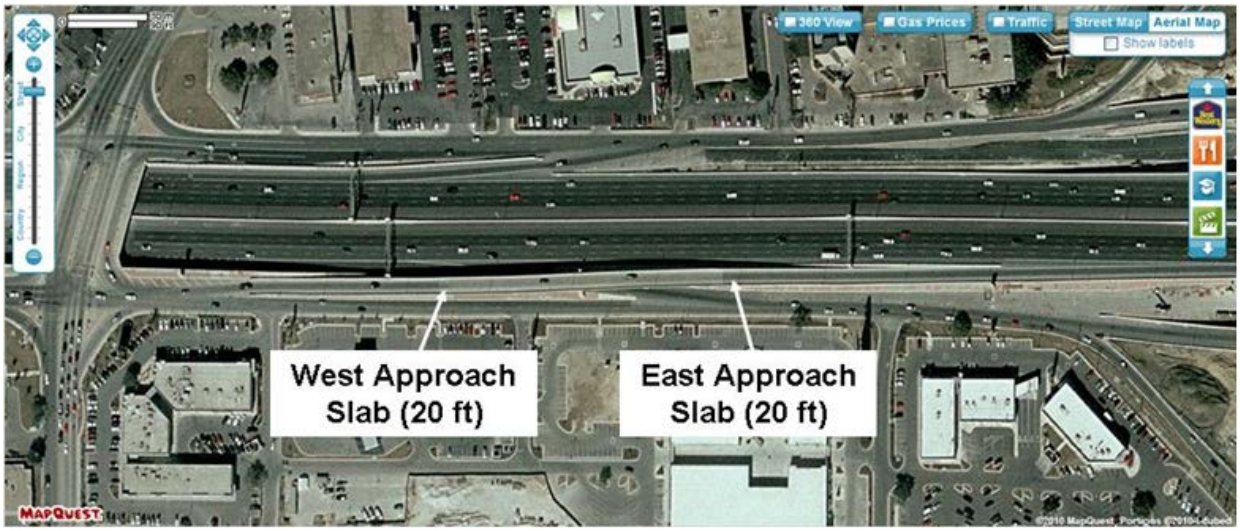

Figure 9.32. Overall Section View of the San Antonio Site.

Figure 9.33. Sectional Views of the West and East Approach Slabs.

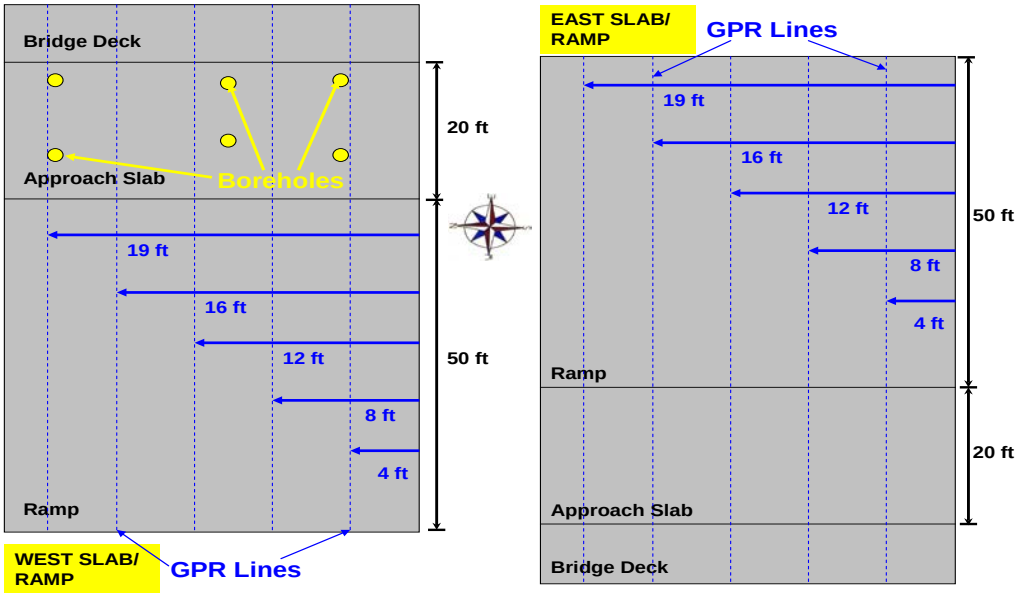

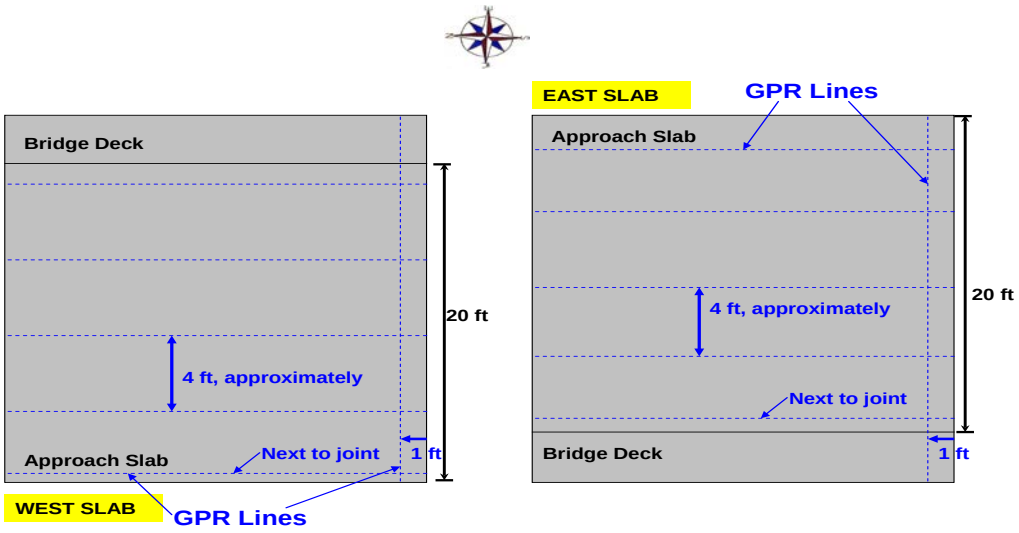

Figure 9.34. Detailed Location of Each Line.

A typical linescan obtained with the high frequency GPR antenna is shown in Figure 9.35 for the test conducted on the west approach slab. The bridge, approach slab, and ramp were clearly identified on the linescan. For the ramp, several layers at depths of about 2.5 (0.06 m), 5 in. (0.12 m), 8 in. (0.20 m), and 12 in. (0.30 m) from the top can be observed. A stronger reflection is also detected at about 18 in. (0.46 m).

The first four reflections were attributed to different HMA interfaces that might represent several asphalt layers. What appears to be the HMA-embankment interface turns up at a depth of about 18 in. (0.46 m). Some anomalies adjacent to the approach slab were also observed. For the approach slab, the transverse reinforcement is clearly detected at two different depths: between 4 (0.10 m) and 6 in. (0.15 m) and at 14 in. (0.36 m) approximately. The bottom of the pavement structure was detected at about 18 in. (0.46 m).

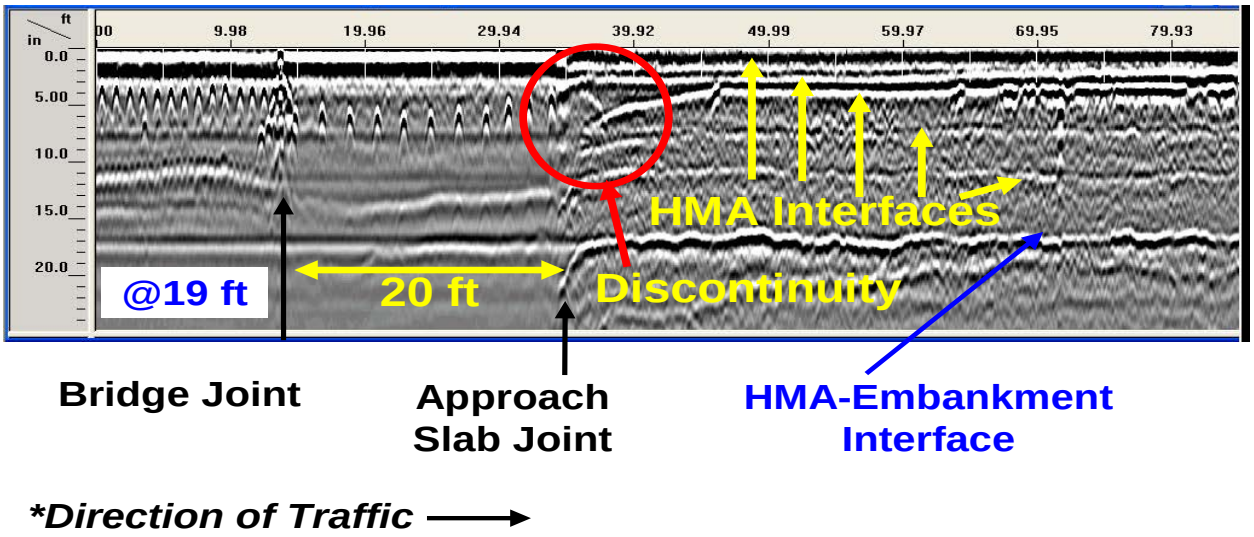

Figure 9.35. Typical Linescan of the West Approach Slab with the High Frequency Antenna.

GPR results from the medium frequency antenna are presented in Figure 9.36. Similar to the high frequency antenna, the bridge, approach slab, and ramp are clearly identified. In this case, the HMA interfaces are not as visible as with the high frequency antenna but the HMA-embankment interface is easy to distinguish. Under this layer, several other horizontal interfaces were observed. These other layers are assumed as different layers within the subgrade. On the approach slab, the first level of transverse reinforcement is easy to identify but not for the deeper level. In addition, an anomaly in the subgrade material immediately after the approach slab is highlighted. This area was approximately 30 ft (9.0 m) long and showed erratic interfaces at depths of 75 in. (1.91 m) approximately.

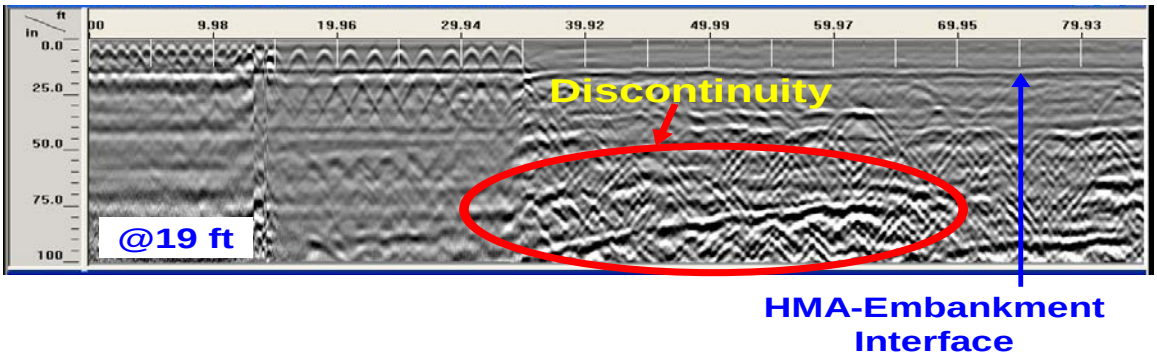

Figure 9.36. Typical Linescan of the West Approach Slab with the Medium Frequency Antenna.

From the GPR information, a core plan was established for the two approach slabs and is presented in Figure 9.37. Six cores per slab were identified on intact and anomalous areas as detailed in Figure 9.37. On the west slab, cores were designated from W1 to W2 and on the east slab from E1 to E6. From these six cores, four were marked on the approach slab and two on the asphalt roadway pavement.

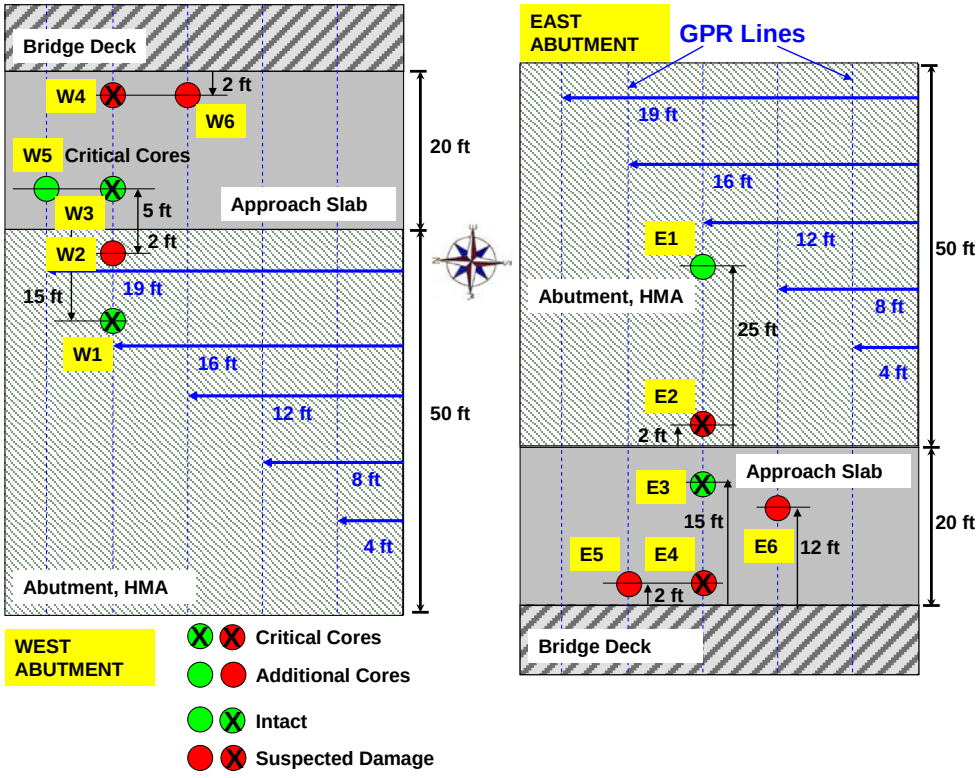

Figure 9.37. Proposed Core Layout for the San Antonio Bridge.

Detailed views from some of the cores retrieved on the west and east approach slabs are presented in Figures 9.38 and 9.39, respectively. Cores W1 and W2 (on the HMA ramp) were about 18 in. (0.46 m) long. Core W1 was cracked at depths of 6.5 in. (0.17 m) and 12 in. (0.30 m) while Core W2 showed severe stripping at depths ranging from 10 in. (0.25 m) to 15 in. (0.38 m). On the approach slab, cores W3 to W5 presented a concrete thickness of about 14 in (0.35 m), over a 2 in. (0.05 m) thick HMA layer. A 2 in. (0.05 m) to 4 in. (0.10 m) void was observed underneath the HMA. On the east approach slab, Core E2 had a thickness of 18 in. (0.45 m) with no indications of damage. Core E3 had a concrete layer of 13 in. (0.33 m) that cracked at about 3 in. (0.08 m) from the top, had a void of about 1 in. (0.03 m) to 2 in. (0.05 m) and a layer of stripped asphalt about 4 in. (0.10 m) thick.

Core E4 was intact and was 14 in. (0.35 m) thick with a void of about 5 in. (0.13 m) that appeared with some stripped asphalt underneath. Core E5 was 12.5 in. (0.32 m) thick that had some stripped asphalt as well. Core E6 was not feasible to obtain. The summary of results from the 12 cores retrieved and the comparison with the GPR results is presented in Table 9.4. Estimated depths to the bottom layers of the PCC or HMA are highlighted. In general, the GPR depth estimation compared favorably well with the ground-truth data since measured and estimated depths only differed by less than 1 in. The only outlier was Core W5 where the estimated depth was about 12.1 in. (0.307 m) and the actual depth from retrieved core was 14 in. (0.356 m).

In addition to the cores, Dynamic Cone Penetrometer (DCP) tests were carried out on the embankment at some of the core locations. As an example, results from Core W2 (on the west HMA ramp) and Core E4 (on the east approach slab) are presented in Figure 9.40. The accumulated blow counts and the corresponding moduli values versus depth are shown. In both cases, two different soil layers were identified. For Core W2, an interface seems to appear at a depth of 22 in. (0.56 m) and for Core E4, this interface materializes approximately at 35 in. (0.89 m). This top layer in both cases is softer than the bottom. Similar observations were obtained for all DCP tests conducted. Overall results are are summarized in Table 9.5.

W1

W1

W2

W2

W3

W3

Figure 9.38. Retrieved Cores from the West Slab.

E2

E3

E4

E4

E5

Figure 9.39. Retrieved Cores from the East Slab.

Table 9.4. Comparison of Retrieved Cores with the GPR Data.

Core Designation	Location	Core Results	Interfaces f rom High F requency GPR Data
W1	HMA ramp, at 16 ft from south edge, 2 ft from approach slab joint	18 in. of ACP over Base/embankment	1.77, 3.46, 5.40, 8.10, 12.30, **17.70**
W2	HMA ramp, at 16 ft from south edge, 15 ft from approach slab joint	17 in. of ACP over Base/embankment	1.86, 3.54, 5.74, 8.40, 11.30, **17.38**
W3	Approach slab, at 16 ft from south edge, 5 ft from approach slab joint	13 in. of PCC, 2 in. of Void/AC	4.47, **12.74**, 16.96
W4	Approach slab, at 16 ft from south edge, 2 ft from bridge joint	14 in. of PCC, 2 in. of AC/ 3 in. of Voids	4.89, **14.85**, 16.70
W5	Approach slab, at 19 ft from south edge, 5 ft from HMA ramp joint	14 in. of PCC, 1 in. of AC/ 4 in. of Voids	3.88, **12.15**, 16.20, 17.63, 18.98
W6	Approach slab, at 12 ft from south edge, 2 ft from bridge joint	N/A	3.54, 5.23, 11.73, 13.08, 14.68, 18.98
E1	HMA ramp, at 12 ft from south edge, 25 ft from approach slab joint	N/A	1.94, 2.70, 4.13, 6.83, 9.11, 12.57, 17.63
E2	HMA ramp, at 12 ft from south edge, 2 ft from approach slab joint	17.5 in. of ACP	2.45, 4.98, 8.44, 12.49, **17.72**
E3	Approach slab, at 12 ft from south edge, 15 ft from bridge joint	13 in. of PCC, 1-2 in. Void, ACP 4 in., stripped materials	2.70, 11.05, **13.58**, 16.03, 18.64
E4	Approach slab, at 12 ft from south edge, 2 ft from bridge joint	14 in. of PCC, 5 in. Void, stripped AC	2.62, **13.08**, 18.48
E5	Approach slab, at 16 ft from south edge, 2 ft from bridge joint	12.5 in. PCC, 0.5 in. AC, stripped material	3.71, 6.75, **12.15**, 13.33, 17.55
E6	Approach slab, at 8 ft from south edge, 12 ft from bridge joint	N/A	3.54, 5.57, 10.71, 11.98, 15.69, 18.39

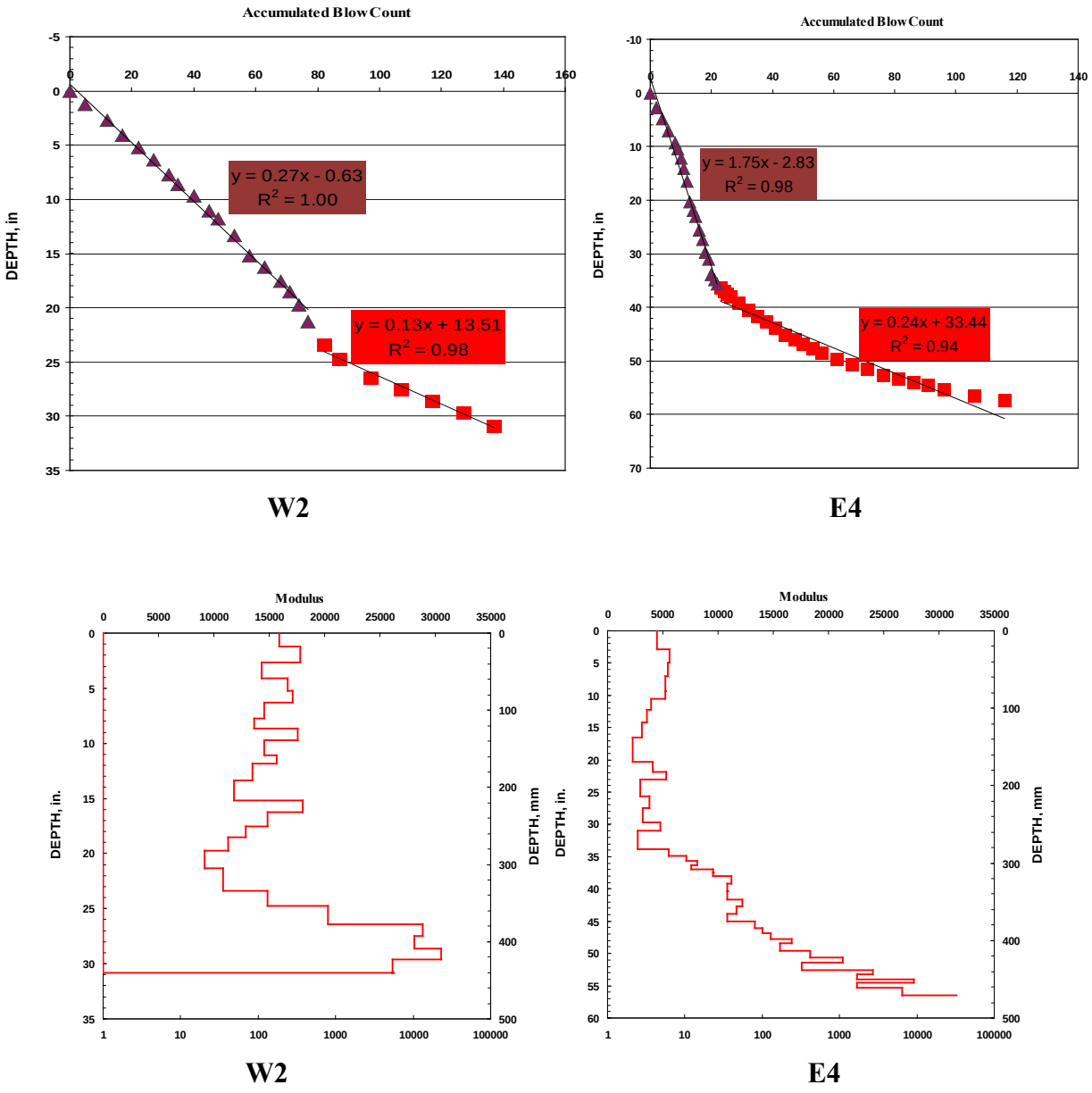

Figure 9.40. DCP Sample Results.

Table 9.5. Summary of DCP Results.

DCP Location	Slope Layer 1	Slope Layer 2	Approximate Interface Depth (in.)	Initial Modulus (ksi)	Modulus at Interface (ksi)	Final Modulus (ksi)
W1	0.22	0.08	25	15	11	37
W2	0.27	0.13	22	16	9	30
W3	0.21	0.39	6	23	14	23
W4	0.87	0.80	8	11	4	7
W5	1.73	0.24	65	10	3	23
W6	N/A					
E1	N/A					
E2	0.43	0.17	27	21	7	22
E3	0.31	0.21	17-26	11	4	22
E4	1.75	0.24	35	5	3	31
E5	0.27	0.18	20	18	11	21
E6	N/A					

In general, the slope of Layer 2 is more horizontal than Layer 1, indicating a stiffer layer when depth increases. However, for W3, the slope value for Layer 2 is larger but in this case the interface appears to be at a very shallow depth of 6 in. (0.15 m). For W4, the interface also manifests itself close to the top of the soil layer (8 in. [0.20 m]) and both slopes have very similar values. For the rest of the tests on the west slab, cores on the HMA ramp (W1 and W2) had an interface of about 20 in. (0.51 m) and for the case of W5, it appeared at 65 in. (1.65 m). On the east slab, the approximate soil interface was between 17 to 35 in. (0.43 to 0.89 m), and for E3, it is not clear since a void was found between 17 and 26 in. (0.43 to 0.66 m). Initial modulus widely ranged between 5 and 23, decreased always with depth until the interface was more or less reached and then increased to a value larger than the initial for all cases except W4.

9.2.4.1 Potential Void Volume Estimation under the Approach Slabs

Similar to the Quanah site, an estimation of the suspected voids under the approach slabs was carried out. As an example, Figure 9.41 shows a linescan of the west approach slab and at a

distance of 16 ft (4.88 m) from the south edge of the slab. In this case, the pavement structure was comprised of a concrete slab on top of a HMA layer and the embankment underneath. The bottom of the approach slab, bottom of the HMA-embankment interface, and the suspected void interface were identified at several selected points. With the assumed dielectric constant, estimated depths were obtained and are presented in Figure 9.42. The suspected void under the approach slab adjacent to the bridge joint is also depicted. This suspected void area was measured by calculating the compound average difference of the bottom of the approach slab and the suspected void at selected locations. For the case shown in Figure 9.42, the void area extends about 8 ft (2.44 m) from the bridge joint with a somewhat triangular shape. The estimated void area for this location was about 1.30 ft^2 (0.12 m^2).

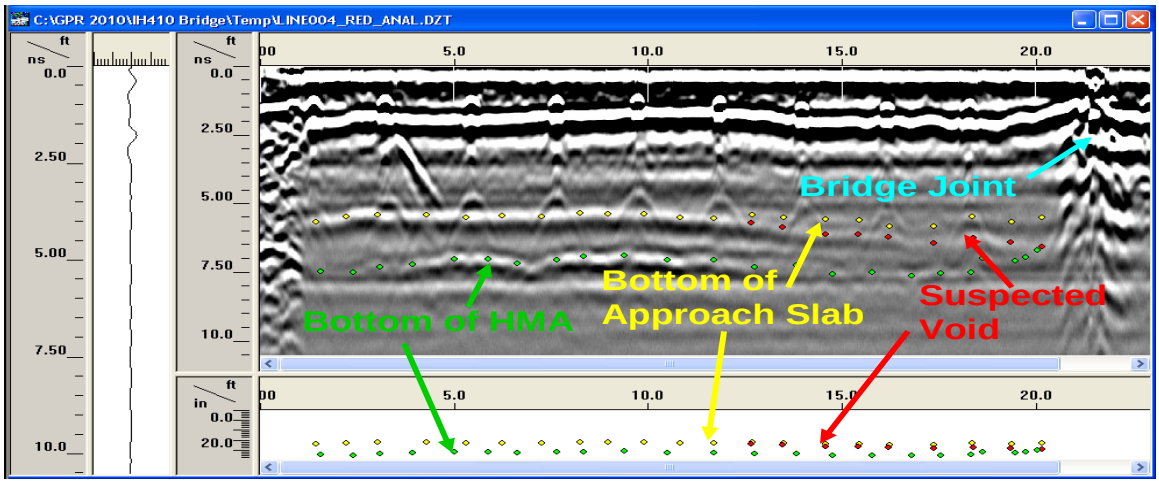

Figure 9.41. Selection of Points from the GPR Linescan.

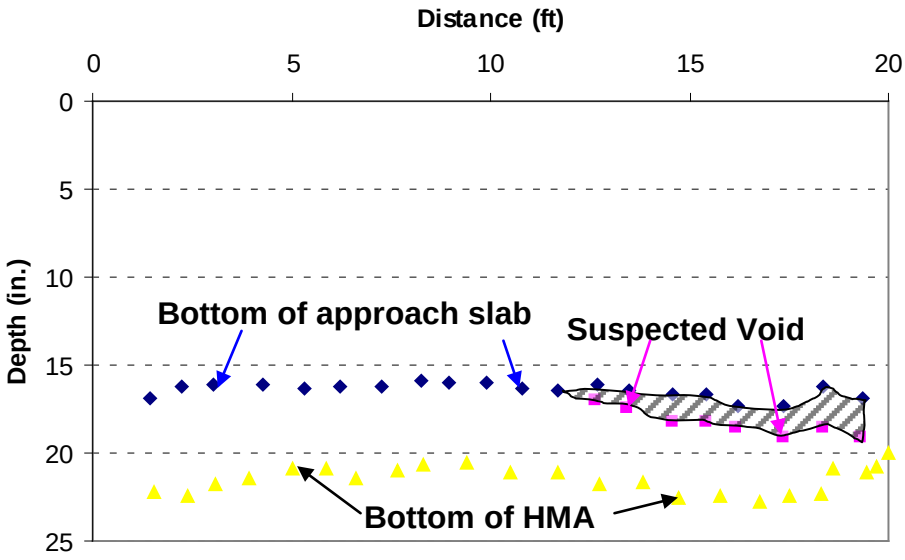

Figure 9.42. Estimated Depth Profile.

The same process was implemented on the rest of the four longitudinal lines obtained for each slab (see Figure 9.33 for details). Results for the west slab are summarized in Table 9.6. The region at 19 ft (5.8 m) from the south edge seems to have largest void area (2.02 ft^2 [0.19 m^2]) and the smallest (0.44 ft^2 [0.04 m^2]) was obtained at 12 ft (3.66 m). Moreover, the estimated void volume was obtained by measuring the average of the void area at the five locations and multiplying this area by the width of the lane (24 ft [7.32 m]). For this slab, the approximate void volume was 27 ft^3 (0.77 m^3). Similarly, the same procedure was conducted for the east approach slab and the estimated void areas and volume are presented in Table 9.7. For all locations in the east slab, the void area was about 2 ft^2 (0.19 m^2) and the final volume was 53 ft^3 (1.50 m^3), twice the volume than on the west slab.

Table 9.6. Void Area and Volume under the West Approach Slab.

	West Slab				
Distance from South Edge (ft)	@4ft	@8ft	@12ft	@16ft	@19ft
Void area (ft2)	0.87	0.93	0.44	1.30	2.02
Void Volume (ft3)	26.7				

Table 9.7. Void Area and Volume under the East Approach Slab.

	East Slab				
Distance from South Edge (ft)	@4ft	@8ft	@12ft	@16ft	@19ft
Void area (ft2)	2.30	1.53	2.69	2.39	2.11
Void Volume (ft3)	52.9				

Based on the estimated volume of voids, use of flowable fills was proposed as a suitable mitigation method. However the proposed solution was not implemented due to the uncertainty in the long-term performance of the approach slabs repaired using this technique. These distressed approach slabs are yet to be repaired.

9.3 SUMMARY

This chapter mainly presented the maintenance measures that are used as remedial methods after the settlement problems are detected. A brief introduction to the need and importance of adopting suitable remedial measures to mitigate the settlement related problems in distressed bridge approach slabs was presented.

This chapter provided appropriate mitigation techniques that can be investigated to treat the distressed bridge approach slabs. Hence, four bridge locations with settlement related problems were identified and investigated. The location of the bridges, the corrective methods employed, procedure of the method used, and the geophysical studies performed on the bridges along with recommendations were discussed. The corrective methods, both proposed and recommended, included polyurethane injection, soil nailing, flowable fills, and the use of lightweight geofoam blocks. Among these methods, polyurethane injection has provided some enhancements. However, void estimation is needed prior to selecting this method. Also, a few quality control measures need to be established and implemented when using this method. In the case of soil nailing, the method was mainly used to enhance the stability of the modular block wall, which in turn can control erosion thereby enhancing the stability of the approach slabs at both ends. Two additional sites were also studied for potential implementation of lightweight geofoam blocks and the use of flowable fills. Both methods are considered to have high potential to mitigate settlements. However, these methods were not implemented for monitoring and need to be investigated in future studies.

CHAPTER 10

SUMMARY AND CONCLUSIONS

10.1 GENERAL

The differential settlements between the roadway approach and bridge deck is termed as the bump and is considered as one of the major maintenance problems that affects the performance of the roadway. Many state highway agencies in the United States reported this as one of their major maintenance problems as every year; these agencies have been spending over $100 million on maintenance and repairs to the bridges and highways damaged by this bump problem. In addition, this bump causes a rough ride to traveling passengers. Recently, there have been several methods utilized to mitigate this settlement problem such as using driven piles, drilled shafts, flowable fill, ECS, DSM columns, geosynthetics, and others. In this research, two treatment methods were considered for the subgrade and embankment fill conditions in the north Texas region for potential reduction in overall settlements. The two mitigation methods researched were the use of DSM columns and ECS. Additionally, another method of using deep foundations with geopier was also investigated, however with limited focus.

One method to study the effectiveness of mitigation methods in reducing the settlements at the bridge approach was to study and investigate the settlements that have occurred in bridge embankments in real field conditions. Therefore, three bridge sites were selected in this research and these include the DSM site on IH 30 in Arlington, the ECS site on SH 360 in Arlington, and the geopier site on SH 6 in Houston. Field visits were made to observe the soil settlements occurring in the embankments on a periodic basis, every fortnight for the DSM and ECS sites, and every six months for the geopier site. In general, each site had the test (treated) and control (untreated) sections. The settlement data observed from both sections were then compared to evaluate the efficiencies of each mitigation method in decreasing the amount of settlement.

The data collected in the field were used not only for the mitigation settlement efficiency evaluation but also for a settlement analysis study. Two numerical models, FEM and a hyperbolic model for time scale extension, were used in this research. For the FEM, the data collected from the field instrumentation were employed to validate the model with the results

from the FEM. The hyperbolic model formulated by Lin and Wong (1999) used the observed field data to establish the time-settlement equation for each embankment. Once validations were done, the models were used for further modeling for hypothetical embankment sections. After the FEM model validation, the model was used to predict the settlement occurring in the embankments in the 10, 20, and 30 years of service life.

Both the test and control sections were simulated in the FEM model changing the embankment geometry and surcharge loading from traffic and using different DSM and ECS values. These results were used to develop design methods for the DSM and ECS fill material options.

10.2 SUMMARY AND CONCLUSIONS

The major objective of the research was to address the effectiveness of each mitigation method in reducing the settlement occurring in the embankment. The following conclusions are offered for each method considered in the research.

Efficiency of the DSM columns in reducing settlements in the embankment

I. Field Instrumentation and Monitoring Studies

a) The monitored data from the horizontal inclinometer show that the DSM method was successful in mitigating the settlement underneath the approach slab induced from the traffic load. The settlement that occurred under the approach slab section (0.1 in. [2.5 mm]) was lower than the values under the roadway pavement (0.5 in. [12.7 mm]) and slope fill (0.75 in. [19.0 mm]).

b) Vertical soil movements monitored from extensometers reveal that the settlement values in the embankment at the depth of 10 ft (3.0 m), 20 ft (6.0 m), and 40 ft (12.0 m) were equal to 0.20, 0.13, and 0.05 in. (5.1, 3.3, 1.3 mm.), respectively. These results show that the monitored settlement values are very small at different depths throughout the embankment; therefore, the DSM is an effective method to reduce the settlements. The same trend was also shown in the results of the Sondex; the sensor rings moved within a very small range (±0.15 in. [3.8 mm]).

c) Data from the elevation surveys show that the amount of the settlement that occurred in the control section was more than in the test section. The reduction in the surface movement in the DSM treated embankment was attributed to the enhancement of the subgrade soil foundation achieved through the DSM technique. This indicates the effectiveness of the DSM in improving the performance of the embankments settle less.

d) The horizontal movements monitored in both the DSM and control sections were very low. With the variations of the casing profiles showing a small movement less than 0.1 in. (2.5 mm), it indicates that the horizontal movements are not critical in the assessment of deep soil treatment methods in mitigating approach slab settlements.

II. Numerical Analysis Studies, Results, and Comparison Studies with the Field Data

a) The analytical predictions of soil movements in the DSM treated section are in good agreement with the field observation data monitored from all instruments including the horizontal inclinometer, total station, rod extensometer, and Sondex devices. Also, a hyperbolic model was used to take the initial settlements and then extend to interpret the long-term settlements. Overall, these analyses indicate that the accuracy of the model was valid not only for calculating the settlement in the present conditions but also for predicting the settlement over a long-term time frame.

b) When comparing the settlement values between the treated and untreated sections from the model analysis, it reveals that the DSM columns could reduce the settlement in the test section from 9.4 in. (240 mm) to 1.6 in. (40 mm) in 2 years and from 10.9 in. (277 mm) to 2.6 in. (66 mm) for the long-term duration.

c) Analyses were attempted using various 1) DSM area ratios, 2) embankment heights, and 3) slopes. The results from this study reveal that the most effective method in reducing the embankment settlement is by using a suitable area-ratio having a value between 0.5–0.6. Lowering the embankment height is also another effective method as it reduces gravity loads exerted on the subgrade soil. Hence, less settlement due to consolidation of the soft clay layer will occur. By lowering the height of the embankment, the approach slab will also experience less embankment settlement.

However, with using traffic weight related variables, an increase in the settlements may occur as stress transferred in the subsoils will be high and not desirable.

Efficiency of the ECS in reducing settlements in the embankment

III. Field Instrumentation and Monitoring Studies

a) By comparing the settlement values from the elevation surveys in both of the test and control sections, the ECS embankment experienced a settlement of only 1.44 in. (36 mm) while the control embankment experienced a total settlement of 3.36 in. (85 mm). This means that the ECS lightweight fill material can be used to mitigate the settlement at the bridge approach.

b) A wide opening between the highway pavement shoulder and the adjoining soil was seen during the site visits. This opening allowed more surface runoff to flow into the embankment raising the potential for erosion and making the settlement problem more severe.

c) A granular material with no cohesion between the particles, like ECS, could be easily eroded away by water intrusion, especially in the open area like the outer slope of the embankment. Consequently, that area will have lesser soil mass and lower density than at other locations. This occurrence was observed during the site visits in which the approach slab moved toward the outer slope where the soil has a lower soil density. In addition, the data monitored at Inclinometer V4 reveals slight erosion. Therefore, for the embankment constructed with a granular material, effective drainage and erosion control methods must be provided.

IV. Numerical Analysis Studies, Results, and Comparison Studies with the Field Data

a) The results from the vertical soil settlement analysis using the numerical modeling in the ECS test and the control sections are in accord with the elevation survey data performed in both sections. These signify that the models for both sections are accurate enough to estimate soil settlements in the future.

b) The results of the horizontal soil displacements from the numerical studies differ from the monitored data collected from the vertical inclinometers. This is a result from the

vertical inclinometers not installed at locations suitable for the data comparison. The vertical inclinometers installed in the inner side of the embankment yield lateral soil displacement data influenced by two embankments constructed with different fill materials, ECS, and RAP.

c) From the numerical analyses, the results show that the embankment constructed with the ECS will have a long-term settlement in 30 years of 1.89 in. (48 mm) while the embankment constructed with the local fill will have a settlement of 5.4 in. (136 mm) in the same time interval.

d) Although using the ECS lightweight fill material to construct an embankment can lessen the amount of the settlement to one-third compared with the values predicted in the normal fill embankment in this study, this technique does not impede the consolidation process from occurring in the clay layer. It is seen from the analysis results that the settlements in the test section are still increasing from 1.61, 1.77, 1.93 in. (41, 45, 48 mm) at years 10, 20, and 30, respectively. Therefore, maintenance applications are still necessary to be performed in this type of embankment throughout its long-term service.

The following flow chart (See Figure 10.1) describes the step-by-step process for selecting the appropriate mitigation method for new bridge approach settlement issues.

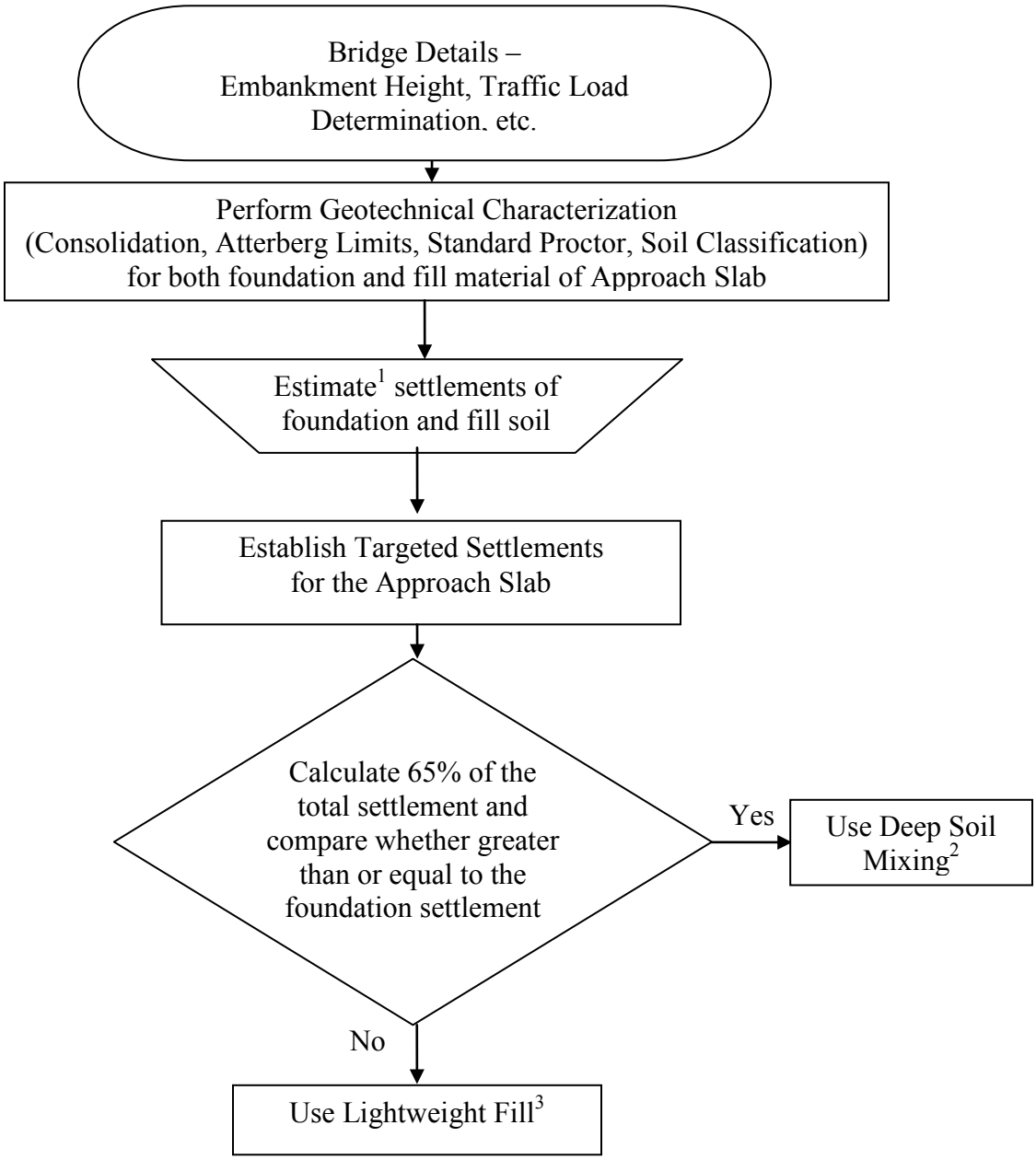

[1]Use analytical methods like design charts, FEM models, etc.
[2]Use Subchapter 8.3.5.4
[3]Use Subchapter 8.4.4.3

Figure 10.1. Flowchart Showing Step-by-Step Process for Selecting the Appropriate Mitigation Method for Bridge Approach Settlement Issues.

10.3 LIMITATIONS AND RECOMMENDATIONS

The Plaxis Finite Element Program used in the numerical analysis in this study still has its limitation in modeling soil erosion behavior. Therefore, this complicated phenomenon could not be simulated in the ECS site and the results from the numerical analysis did not actually match with the data from the field especially with the monitored horizontal soil displacement data.

REFERENCES

[1] Abendroth, R. E., Greimann, L.F., and LaViolette, M. D. (2007). "An Integral Abutment Bridge with Precast Concrete Piles." *Final Rep., IHRB Project TR-438, CTRE Project No. 99-48*, IOWA Department of Transportation, Center for Transportation Research and Education Report, Ames, Iowa.

[2] Aboshi, H. and Suematsu, N. (1985). "Sand Compaction Pile Method: State-of-the-Art Paper." *Proc. of 3rd International Geotechnical Seminar on Soil Improvement Methods*, Nanyang Technological University, Singapore.

[3] Abu al-Eis, K. and LaBarca, I. K. (2007). "Evaluation of the URETEK Method of Pavement Lifting." *Rep. No. WI-02-07*, Wisconsin Department of Transportation, Division of Transportation Systems Development, Madison, Wisconsin.

[4] Abu-Hejleh, N., Hanneman, D., White, D. J. and Ksouri, I. (2006). "Flowfill and MSE Bridge Approaches: Performance, Cost and Recommendations for Improvements." *Report No. CDOT-DTD-R-2006-2.* Colorado Department of Transportation, Denver.

[5] Abu-Hejleh, N., Wang, T., and Zornberg, J.G. (2000). "Performance of Geosynthetic-Reinforced Walls Supporting Bridge and Approaching Roadway Structures." *ASCE Geotechnical Special Publication No. 103*, Advances in Transportation and Geoenvironmental Systems Using Geosynthetics (2000) 218–243.

[6] Abu-Hejleh, N., Zornberg, J.G., Wang, T., and Watcharamonthein, J. (2003). "Design Assessment of Founders-Meadows GRS Abutment Structure." *Proc., 82nd Annual TRB Meeting.*

[7] Albajar, L., Gascón, C., Hernando, A., and Pacheco, J. (2005). "Transiciones de Obra de Paso-Terraplén. Aproximación al Estado del Arte y Experiencias Españolas." Asociación Técnica de Carreteras, Ministerio de Fomento.

[8] American Association of State Highway and Transportation Official AASHTO. (2004). *LRFD Bridge Design Specification, 3rd edition, with 2006 interim revisions,* Washington, D.C.

[9] Ardani, A. (1987). "Bridge Approach Settlement." *Report No. CDOT-DTP-R-87-06*, Colorado Department of Highways, Denver, Co.

[10] Arockiasamy, M., Butrieng, N., and Sivakumar, M. (2004). "State-of-the-Art of Integral Abutment Bridges: Design and Practice." *Journal of Bridge Engineering,* ASCE, September/October, 2004, 497–506.

[11] Arsoy, S., Barker, R. M., and Duncan, J. M. (1999). "The Behavior of Integral Abutment Bridges." *Rep. No. VTRC 00-CR3*, Virginia Transportation Research Council, Charlottesville, VA.

[12] Arsoy, S., Duncan, J. M., and Barker, R.M. (2002). "Performance of Piles Supporting Integral Bridges." *Transportation Research Record 1808*, Washington, D.C.

[13] ASCE Grouting Committee (1980). "Preliminary glossary of terms relating to grouting." ASCE Journal of Geotechnical Division, Vol. 106 (GT7), 803-815.

[14] Atkinson, M.S. and Eldred, P. (1981). "Consolidation of Soil Using Vertical Drains." *Geotechnique*, 31(1), 33–43.

[15] Bakeer, M., Shutt, M., Zhong, J., Das, S., and Morvant, M. (2005). "Performance of Pile-Supported Bridge Approach Slabs." *Journal of Bridge Engineering*, ASCE.

[16] Barksdale, R.D. and Bachus, R.C. (1983). "Design and Construction of Stone Columns, Vol. 1." *Rep. No. FHWA/RD-83/026*, Federal Highway Administration, Washington, D.C.

[17] Barron, R. A. (1948). "Consolidation of Fine-Grained Soils by Drain Wells." *Transactions of ASCE No. 2346*, pp. 718–754.

[18] Barron, R. F., Wright, J., Kramer, C., Andrew, W. H, Fung, H., and Liu, C. (2006). "Cement Deep Soil Mixing Remediation of Sunset North Basin Dam." *Dam Safety 2006*, Association of Dam Safety Officials.

[19] Bathe, K.-J. (2003). Finite Element Procedures, Prentice-Hall of India, New Delhi.

[20] Baumann, V. and Bauer, G.E.A. (1974). "The Performance of Foundations on Various Soils Stabilized by the Vibro-Compaction Method." *Canadian Geotechnical Journal*, 509–530.

[21] Bergado, D.T., and Patawaran, M.A.B. (2000). "Recent Developments of Ground Improvement with PVD on Soft Bangkok Clay." *Proc. Intl. seminar on Geotechnics in Kochi 2000*, Kochi, Japan, October, 2000.

[22] Bergado, D.T., Anderson, T.R., Miura, N., and Balasubramaniam, A.S. (1996). "Soft Ground Improvement in Lowland and Other Environments." ASCE, New York.

[23] Bergado, D.T., Miura, N., and Panichayatum, B. (1988). "Improvement of Soft Bangkok Clay using Vertical Band Drains Based on Full Scale Test." *Proc. of the International Conference on Engineering Problems of Regional Soils*, Beijing, China, 379–384.

[24] Bergado, D.T., Singh, N., Sim, S.H., Panichayatum, B., Sampaco, C.L., and Balasubramaniam, A.S. (1990). "Improvement of Soft Bangkok Clay Using Vertical Drains Compacted with Granular Piles." *Geotextiles and Geomembranes*, 9, 203–231.

[25] Bowders, J., Loehr, E., Luna, R., and Petry, T.M. (2002). "Determination and Prioritization of MoDOT Geotechnical Related Problems with Emphasis on Effectiveness of Designs for Bridge Approach Slabs and Pavement Edge Drains." *Project Rep. No. R199-029*, Missouri Department of Transportation, Jefferson.

[26] Bowles, J. E. (1988). *Foundation Analysis and Design*, McGraw-Hill, New York.

[27] Bozozuk, M. (1978). "Bridge Foundations Move." *Transportation Research Record 678*: Tolerable Movements of Bridge Foundations, Sand Drains, K-Test, Slopes, and Culverts, Transportation Research Board, National Research Council, Washington, D.C. 17–21.

[28] Brewer, W.E. (1992). "The Design and Construction of Small Span Bridges and Culvert Using Controlled Low Strength Material (CLSM)." *FHWA/OH-93/014*, Ohio Department of Transportation, Columbus, 129.

[29] Brewer, W. B., Hayes, C. J., and Sawyer, S. (1994). "URETEK Construction Report." *Construction Report*, Report Number OK 94(03), Oklahoma Department of Transportation.

[30] Briaud, J. L., James, R. W., and Hoffman, S. B. (1997). "NCHRP Synthesis 234: Settlement of Bridge Approaches (the bump at the end of the bridge)." Transportation Research Board, National Research Council, Washington, D.C., pp.75.

[31] Brown, D.A., Steve, D.D., Thompson, W.R., and Lazarte, C. A. (2007). "Design and Construction of Continuous Flight Auger (CFA) Piles." Geotechnical Engineering Circular No. 8, Federal Highway Administration, Washington, D. C.

[32] Bruce, D. (2001). "An Introduction to the Deep Mixing Methods as Used in Geotechnical Applications. Volume III. The Verification and Properties of Treated Ground." Report No. FHWA-RD-99-167, US Department of Transportation, Federal Highway Administration, 2001.

[33] Bugrov, A.K. (1975). "The Finite Element Method in Consolidation Analyses of Water-Saturated Soils." Power Technology and Engineering (Formerly Hydrotechnical Construction), Vol. 9, No. 7, 661–668.

[34] Burde, H.J. (2004). "FE in Geotechnical Engineering." Stichting Postcademish Onderwijs Civile Techniek en Bouwtechniek, Noordwijkerhout, The Netherlands, January, 2004.

[35] Burdette, E.G., Howard, S.C., Tidwell, J.B., Wasserman, E.P., Ingram, E.E., Deatherage, J.H., and Goodpasture, D.W. (2004). Lateral Load Tests on Prestressed Concrete Piles Supporting Integral Abutments. PCI Journal, 49(5), 70–77.

[36] Burke, M.P. (1987). "Bridge Approach Pavements, Integral Bridges, and Cycle-Control Joints." *Transportation Research Record 1113*, TRB, National Research Council, Washington D.C., 54–65.

[37] Burke, M.P. (1993). "Integral Bridges: Attributes and Limitations." *Transportation Research Record 1393*. p. 1–8. Transportation Research Board, 75th Annual Meeting.

[38] Burke, G. (2001). "Current Methods of Sampling and Testing of Soil Cement and Their Limitations." Proceedings of International Workshop on Deep Mixing Technology, Vol. 2, National Deep Mixing Program, Oakland, CA. 2001.

[39] Bush, D.I., Jenner, C.G., and Bassett, R.H. (1990). "The Design and Construction of Geocell Foundation Mattress Supporting Embankments over Soft Ground." Geotextiles and Geomembranes, 9: 83–98.

[40] Buss, W.E. (1989). "Iowa Flowable Mortar Saves Bridges and Culverts." *Transportation Research Record 1234*, TRB, National Research Council, Washington, D.C., pp. 30–34.

[41] Byle, M. J. (1997). "Limited Mobility Displacement Grouting - When 'Compaction Grout' is Not Compaction Grout." Grouting: Compaction, Remediation, Testing, Proceedings of GeoLogan GeoInstitute Conference, Geotechnical Special Publication No. 66, Logan, Utah, ASCE, p. 32–43.

[42] Byle, M. J. (2000). "An Approach to the Design of LMD Grouting." *Geotechnical Special Publication 104*, Advances in Grouting and Ground Modification, Proceedings of Sessions of Geo-Denver 2000, Wallace Baker Memorial Symposium, ASCE, Denver, Colorado, 94–110.

[43] Cai, C. S., Voyiadjis, G. Z., and Xiaomin, S. (2005). "Determination of Interaction between Bridges Concrete Approach Slab and Embankment Settlement." Department of Civil Engineering, Louisiana State University, Baton Rouge, La.

[44] Chini, S. A., Wolde-Tinsae, A. M., and Aggour, M. S. (1992). "Drainage and Backfill Provisions for Approaches to Bridges." University of Maryland, College Park.

[45] Cooper, M.R. and Rose, A.N. (1999). "Stone Column Support for an Embankment on Deep Alluvial Soils." *Proc of the Institution of Civil Enginee*rs, Geotechnical Engineering, 137(1), 15–25.

[46] Cotton, D. M., Kilian, A. P., and Allen, T. (1987). "Westbound Embankment Preload on Rainier Avenue, Seattle, Washington." *Transportation Research Record No. 1119*, Transportation Research Board, Washington, D.C., 61–75.

[47] Cowland. J.W. and Wong, S.C.K. (1993). "Performance of a Road Embankment on Soft Clay Supported on a Geocell Mattress Foundation." *Geotextiles and Geomembranes*, 12, 687–705.

[48] Das, S. C., Bakeer, R., Zhong, J., and Schutt, M. (1990). "Assessment of Mitigation Embankment Settlement with Pile Supported Approach Slabs." Louisiana Transportation and Research Center, Baton Rouge, LA.

[49] Das, B. M. (2008). *Fundamentals of Geotechnical Engineering*. 3rd Edition, Cengage Learning, Stamford, CT.

[50] DiMillio, A.F. (1982). "Performance of Highway Bridge Abutments Supported by Spread Footings on Compacted Fill." *Final Rep. No. FHWA/RD-81/184*, Federal Highway Administration, Washington, D.C.

[51] Du, L., Arellano, M., Folliard, K. J., Nazarian, S., and Trejo D. (2006). "Rapid-Setting CLSM for Bridge Approach Repair: A Case Study." ACI Material Journal, September-October 2006, pp. 312–318.

[52] Dunn, K. H., Anderson, G.H., Rodes, T.H., and Zieher, J.J. (1983). "Performance Evaluation of Bridge Approaches." Wisconsin Department of Transportation.

[53] Dunnicliff, J. (1988). Geotechnical Instrumentation for Monitoring Field Performance. Wiley and Sons, NY.

[54] Dupont, B. and Allen, D. (2002). "Movements and Settlements of Highway Bridge Approches." *Rep. No. KTC-02-18/SPR-220-00-1F*, Kentucky Transportation Center Report, Lexington, KY.

[55] EBA Engineering, Inc. (1992). *Final Report: Summary Results Obtained from the Auger Cast Piles Investigation.* Study DTFH 692-Q-00062. FHWA, U.S. Department of Transportation.

[56] Edgar, T. V., Puckett, J. A., and D'Spain, R. B. (1989). "Effect of Geotextile on Lateral Pressure and Deformation in Highway Embankments." *Geotextiles and Geomembranes*, 8(4), 275–306.

[57] Elias, V., Christopher, B. R., and Berg, R.R. (2001). "Mechanically Stabilized Earth Walls and Reinforced Soil Slopes Design and Construction Guidelines." FHWA NHI-00- 043.

[58] Federal Highway Administration (2000). "Priority, Market-Ready Technologies and Innovations." Rep. No. FHWA-HRT-04-053.

[59] Folliard, K. J., Du, L., Trejo, D., Halmen, C., Sabol, S., and Leshchinsky, D. (2008). "Development of a recommended practice for use of controlled low-strength material in highway construction." Report No. NCHRP 597, Transportation Research Board, Washington, D.C.

[60] Girton, D. D., Hawkinson, T.R., and Greimann, L.F. (1991). "Validation of Design Recommendations for Integral-Abutment Piles." *Journal of Structural Engineering*, ASCE, 117(7), 2117–2134.

[61] Goughnour, R. R. and Bayuk, A.A. (1979). "A Field Study of Long-term Settlement of Loads Supported by Stone Column in Soft Ground." *Proc of International Conference on Soil Reinforcement: Reinforced Earth and Other Techniques*, Vol. 1, Paris, 279–286.

[62] Greimann, L. F. and Wolde-Tinsae, A. M. (1988). "Design Model for Piles in Jointless Bridges." *Journal of Structural Engineering*, ASCE, 114(6), 1354–1371.

[63] Greimann, L. F., Abendroth, R.E., Johnson, D.E., and Ebner, P.B. (1987). "Pile Design and Tests for Integral Abutment Bridges." *Final Rep. Iowa DOT Project HR 273, ERI Project 1780, ISU-ERI-Ames-88060*, Ames, Iowa.

[64] Greimann, L. F., Yang, P-S., and Wolde-Tinsae, A. M. (1983). "Skewed Bridges with Integral Abutments." *Transportation Research Record 903*: Bridges and Culverts, Transportation Research Board, National Research Council, Washington, D.C., 64–72.

[65] Greimann, L. F., Yang, P-S., and Wolde-Tinsae, A. M. (1986). "Nonlinear Analysis of Integral Abutment Bridges." *Journal of Structural Engineering*, ASCE, 112(10), 2263–2280.

[66] Grover, R. A. (1978). "Movement of Bridge Abutments and Settlements of Approach Pavements in Ohio." *Transportation Research Record 678*, Washington, D.C.

[67] Ha, H., Seo, J., and Briaud, J-L. (2002). "Investigation of Settlement at Bridge Approach Slab Expansion Joint: Survey and Site Investigations." Report No. FHWA/TX-03/4147-1, Texas Transportation Institute, Texas A&M University, College Station, TX.

[68] Hansbo, S. (1979). "Consolidation of Clay by Bandshaped Prefabricated Drains." *Ground Engineering*, 12(5), 16–25.

[69] Hansbo, S. (1997a). "Aspects of Vertical Drain Design: Darcian or Non-Darcian Flow." *Geotechnique*, 47(5), 983–992.

[70] Hansbo, S. (1997b). "Practical Aspects of Vertical Drain Design." *Proceedings of 14th International Conference on Soil Mechanics and Foundation Engineering*, Vol. 3, Hamburg.

[71] Hansbo, S. (2001). "Consolidation Equation Valid for Both Darcian or Non-Darcian Flow." *Geotechnique*, 51(1), 51–54.

[72] Hartlen, J. (1985). "Pressure Berms, Soil Replacement and Lightweight Fills." *Soil Improvement Methods, Proceedings of the Third International Geotechnical Seminar*, Nangyang Technological Institute, Singapore, 101–111.

[73] Hausmann, M. R. (1990). "Engineering Principles of Ground Modification." McGraw-Hill Publishing Company, New York.

[74] Hopkins, T.C. (1969). "Settlement of Highway Bridge Approaches and Embankment Foundations." *Rep. No. KYHPR-64-17; HPR-1(4)*, Kentucky Transportation Center, Lexington, Kentucky.

[75] Hopkins, T. C. (1973). "Settlement of Highway Bridge Approaches and Embankment Foundations." *Rep. No. KYHPR-64-17; HPR-1(8)*, Kentucky Transportation Center, Lexington, Kentucky, 40.

[76] Hopkins, T.C. (1985). "Long-Term Movements of Highway Bridge Approach Embankments and Pavements." University of Kentucky, Transportation Research Program.

[77] Hopkins, T.C. and Deen, R.C. (1970). "The Bump at the End of the Bridge." *Highway Research Record No. 302*, Highway Research Board, National Research Council, Washington, D.C., 72–75.

[78] Hoppe, E. J. and Gomez, J. P. (1996). "Field Study of an Integral Backwall Bridge." *Report No. VTRC 97-R7*, Virginia Transportation Research Council, Charlottesville, VA.

[79] Hoppe, E.J. (1999). "Guidelines for the Use, Design, and Construction of Bridge Approach Slabs." *Rep. No. VTRC 00-R4*, Virginia Transportation Research Council, Charlottesville, VA.

[80] Horvath, J. (2000). "Integral Abutment Bridges: Problem and Innovative Solutions Using EPS Geofoam and Other Geosynthetics." Research *Report No. CE/GE-00-2*, Manhattan College, Bronx, New York.

[81] Horvath, J. S. (1991). "Using Geosynthetics to Reduce Surcharge-Induced Stresses on Rigid Earth Retaining Structures." *Transportation Research Record 1330*, 47–53.

[82] Horvath, J. S. (2005). "Integral-Abutment Bridges: Geotechnical Problems and Solutions Using Geosynthetics and Ground Improvement." *IAJB 2005 - The 2005 FHWA Conference on Integral Abutment and Jointless Bridges*. 16-18 March, Baltimore, Maryland, USA.

[83] Hsi, J. and Martin, J. (2005). "Soft Ground Treatment and Performance, Yelgun to Chinderah Freeway, New South Wales, Australia." *In Ground Improvement-Case Histories*, Elsevier Geo-Engineering Book Series, Volume 3, 563–599.

[84] Hsi, J. P. (2007). "Managing Difficult Ground-Case Studies." *Proceedings of First Sri Lankan Geotechnical Society International Conference on Soil and Rock Engineering*, Colombo.

[85] Hsi, J. P. (2008). "Bridge Approach Embankments Supported on Concrete Injected Columns." *Proceedings of the Challenge of Sustainability in the Geoenvironment*, ASCE, Geocongress 08, New Orleans, Louisiana.

[86] Indraratna, B., Balasubramaniam, A. S., and Ratnayake, P. (1994). "Performance of Embankment Stabilized with Vertical Drains on Soft Clay." *Journal of Geotechnical Engineering*, ASCE, 120(2), 257–273.

[87] James, R.W., Zhang, H., and Zollinger, D.G. (1991). "Observations of Severe Abutment Backwall Damage." *Transportation Research Record 1319*, Transportation Research Board, 55–61.

[88] Jamiolkowski, M., Lancellota, R., and Wolski, W. (1983). "Precompression and Speeding Up Consolidation." *Proceedings, Eight European Conference on Soil Mechanics and Foundation Engineering*, Vol 3, Helsinki.

[89] Japan Railway (JR) Technical Research Institute (1998). "Manual on Design and Construction of Geosynthetic-Reinforced Soil Retaining Wall."

[90] Jayawickrama, P., Nash, P., Leaverton, M., and Mishra, D. (2005). "Water Intrusion in Base/Subgrade Materials at Bridge Ends." *TxDOT Report, FHWA/TX-06/0-5096-1*, Texas Tech University, Lubbock, Texas.

[91] Jenner, C.G., Basset, R.H., and Bush, D.I. (1988). "The Use of Slip Line Fields to Assess the Improvement in Bearing Capacity of Soft Ground Given by Cellular Foundation Mattress Installed at the Base of an Embankment." *In Proceedings of the International Geotechnical Symposium on Theory and Practice of Earth Reinforcement*, Balkema, Rotterdam, 209–214.

[92] Kamel, M.R., Benak, J.V., Tadros, M.K., and Jamshidi, M. (1996). "Prestressed Concrete Piles in Jointless Bridges." *PCI Journal*, 41(2), 56–67.

[93] Kramer, S. L. and Sajer, P. (1991). "Bridge Approach Slab Effectiveness." *Final Report*, Washington State Department of Transportation, Olympia, Washington.

[94] Krishnaswamy, N.R., Rajagopal, K., and Madhavi Latha, G. (2000). "Model Studies on Geocell Supported Embankments Constructed over Soft Clay Foundation." *Geotechnical Testing Journal*, ASTM, 23: 45–54.

[95] Kunin, J. and Alampalli, S. (2000). "Integral Abutment Bridges: Current Practice in United States and Canada." *ASCE Journal of Performance of Constructed Facilities*, 14(3), 104–111.

[96] Laguros, J. G., Zaman, M. M., and Mahmood, I. U. (1990). "Evaluation of Causes of Excessive Settlements of Pavements Behind Bridge Abutments and their Remedies; Phase II. (Executive Summary)." *Rep. No. FHWA/OK 89 (07)*, Oklahoma Department of Transportation.

[97] Lawton, E.C., and Fox, N.S. (1994). "Settlement of Structures Supported on Marginal or Inadequate Soils Stiffened with Short Aggregate Piers." *ASCE GSP No. 40,* Vertical and Horizontal Deformations of Foundations and Embankments, ASCE, Vol. 2, 962–974.

[98] Lawver, A., French, C., and Shield, C. K. (2000). "Field Performance of an Integral Abutment Bridge." *Transportation Research Record*: Journal of the Transportation Research Board, 1740, 108–111.

[99] Lenke, L. R. (2006). "Settlement Issues-Bridge Approach Slabs." *Report No. NM04MNT-02*, New Mexico Department of Transportation.

[100] Lien, B. H. and Fox, N. S. (2001). "Case Histories of Geopier® Soil Reinforcement for Transportation Applications." Proc. of Asian Institute of Technology Conference, Bangkok, Thailand.

[101] Lin, Q.L. and Wong, I.H. (1999). "Use of Deep Cement Mixing to Reduce Settlements at Bridge Approaches." Journal of Geotechnical and Geoenvironmental Engineering, ASCE, Vol. 125(4), 309.

[102] Liu, H.L., Ng, C.W.W., and Fei, K. (2007). "Performance of a Geogrid-Reinforced and Pile-Supported Highway Embankment over Soft Clay: Case Study." *Journal of Geotechnical and Geoenvironmental Engineering*, ASCE, 133(12), 1483–1493.

[103] Long, J.H., Olson, S.M., and Stark, T.D. (1998). "Differential Movement at Embankment/Bridge Structure Interface in Illinois." *Transportation Research Record No. 1633*, Transportation Research Board, Washington, D.C., 53–60.

[104] Louisiana Department of Transportation and Development (LaDOTD, 2002). "Bridge Design Metric Manual."

[105] Lukas, R.G. (1986). "Dynamic Compaction for Highway Construction, Vol. 1, Design and Construction Guidelines." *Rep. No. FHWA/RD-86/133*, Federal Highway Administration, National Technical Information Service, Washington, D.C.

[106] Lukas, R.G. (1995). "Dynamic Compaction, Geotechnical Engineering Circular No. 1." *Report No. FHWA-SA-95-037*, Federal Highway Administration, Washington, D.C.

[107] Luna R., Jonathan, L. R., and Andrew, J. W. (2004). "Evaluation of Bridge Approach Slabs, Performance and Design." *Rep. No. RDT 04-010*, Department of Civil, Architectural and Environmental Engineering, University of Missouri, Rolla.

[108] Maddison, J. D., Jones, D. B., Bell, A. L., and Jenner, C. G. (1996). "Design and Performance of an Embankment Supported Using Low Strength Geogrids and Vibro Concrete Columns." *Geosynthetics: Applications, design and construction, De Groot, Den Hoedt, and Termaat, eds.*, Balkema, Rotterdam, The Netherlands, 325–332.

[109] Magnan, J. (1994). "Methods to Reduce the Settlement of Embankments on Soft Clay: A Review." *Proc., Vertical-Horizontal Deformations of Foundations and Embankments*, ASCE, New York, 77–91.

[110] Mahmood, I. U. (1990). "Evaluation of Causes of Bridge Approach Settlement and Development of Settlement Prediction Models." PhD Thesis, University of Oklahoma, Norman, Okla.

[111] McKenna, J.M., Eyre, W.A., and Wolstenholme, D. R. (1975). "Performance of an Embankment Supported by Stone Columns in Soft Ground." *Geotechnique*, 25(1), 51–59.

[112] McVay, M., Armaghani, B., and Casper, R. (1994). "Design and Construction of Auger-Cast Piles in Florida." *Transportation Research Record, 1447*, 10–18.

[113] Mekkawy, M., White, D.J., Souleiman, M.T., and Sritharan, S. (2005). "Simple Design Alternatives to Improve Drainage and Reduce Erosion at Bridge Abutments." *Proceedings of the 2005 Mid-Continent Transportation Research Symposium*, Ames, Iowa.

[114] Michell, J. K. and Huber, T.R (1985). "Performance of a Stone Column Foundation." *Journal of Geotechnical Engineering*, ASCE, 111(2), 205–223.

[115] Miller, E. A. and Roykroft, G. A., (2004). "Compaction Grouting Test Program for Liquefaction Control." *Journal of Geotechnical and Geoenvironmental Engineering*, ASCE, 355–361.

[116] Mimura, C.S. and Kimura, S.A. (1995). "A Light-Weight Solution." *Proceedings Geosynthetics '95*, Nashville, Tennessee, Vol. 1, 39–51.

[117] Minks, A.G., Wissmann, K.J., Caskey, J.M., and Pando, M.A. (2001). "Distribution of Stresses and Settlements below Floor Slabs Supported by Rammed Aggregate Piers." *Proceedings of 54th Canadian Geotechnical Conference*, Calgary, Alberta, Canada, 16–19.

[118] Missouri Department of Transportation (2003). http://www.modot.mo.gov/.

[119] Monley, GJ. and Wu, J. T. (1993). Tensile Reinforced Effects on Bridge Approach Settlement. *Journal of Geotechnical Engineering*, 119(4), 749–763.

[120] Munoz, A. and Mattox, M. (1977). "Vibroreplacement and Reinforced Earth Unite to Strengthen a Weak Foundation." Civil Engineering, ASCE, 58–62.

[121] Narsavage, P. (2007). "Downdrag in Foundation Design." Ohio Department of Transportation. www.odotnet.net/geotechnical/Web_Links/Docs/2007_Consult_Workshop/Downdrag.ppt.

[122] Nassif, H. (2002). "Finite Element Modeling of Bridge Approach and Transition Slabs." *Rep. No. FHWA-NJ-2002-007*, Department of Civil and Environmental Engineering, Center for Advanced Infrastructure & Transportation (CAIT), Rutgers, New Jersey.

[123] Neely, W. J. (1991). "Bearing Capacity of Auger-Cast Piles in Sand." *Journal of Geotechnical Engineering*, 117(2), 331–345.

[124] Nicholson D.P. and Jardine R.J. (1982). "Performance of Vertical Drains at Queenborough Bypass." Vertical Drains, the Institution of Civil Engineers: London, 67–90.

[125] O'Neill, M. W. (1994). "Review of Augered Pile Practice outside the United States." *Transportation Research Record, 1447*, 3–9.

[126] ODOT. (2005). "Bridge Foundation Design Practices and Procedures." Bridge Engineering Section, Oregon Department of Transportation, 20.

•

[127] Ohio Department of Transportation (2003). www.dot.state.oh.us

[128] Opland, W. H. and Barnhart, V. T. (1995). "Evaluation of The URETEK Method for Pavement Undersealing." *Research Rep. No. R-1340*, Michigan Department of Transportation in Cooperation with the U.S. Department of Transportation.

[129] PCI. (2001). "The State of the Art of Precast/Prestressed Integral Bridges." Precast/Prestressed Concrete Institute, Chicago, Illinois.

[130] Pierce, C. E., Baus, R. L., Harries, K. A., and Yang, W. (2001). "Investigation into Improvement of Bridge Approaches in South Carolina." *Summary Report, Report No. FHWA-SC-01-02*, South Carolina Department of Transportation.

[131] Plaxis Manual, (2008). Plaxis 2D (Version 8), Plaxis Inc., Delft, Netherlands.

[132] Porbaha, A. (1998). "State of the Art in Deep Mixing Technology, Part I: Basic Concepts and Overview of Technology." *Ground Improvement*, 2(2), 8–-92.

[133] Porbaha, A. (2000). "State of the Art in Deep Mixing Technology: Design Considerations." *Ground Improvement*, 4(3), 111–125.

[134] Porbaha, A. and Roblee, C. (2001). "Challenges for Implementation of Deep Mixing in the USA." *Proceedings of International Workshop on Deep Mixing Technology*, National Deep Mixing Program, Oakland, CA, 2 volumes.

[135] Rathmayer, H. (1996). "Deep Mixing Methods for Soft Subsoil Improvement in the Nordic Countries." *Proceedings of IS-Tokyo '96*, The 2nd International Conference on Ground Improvement Geosystems, 14-17 May 1996, Tokyo, 869–878.

[136] RECON (2007). DSM Work Plan Report for Project STP 2007 (165) MM, IH 30, Tarrant County, Arlington, Texas.

[137] Rixner, J.J., Kraemer, S.R., and Smith, A.D. (1986). "Prefabricated Vertical Drains, Vol. 1." *Rep. No. FHWA-RD-86/168*, Federal Highway Administration, Washington, D.C.

[138] Rama Rao, R., Rahardjo, H., and Fredlund, D. G. (1988). "Closed-Form Heave Solutions for Expansive Soils." Journal of Geotechnical Engineering, ASCE, 114 (5), 573-588.

[139] Rowe, R.K., Gnanendran, C.T., Landva, A.O., and Valsangkar, A.J. (1995). "Construction and Performance of a Full-Scale Geotextile Reinforced Test Embankment." *Canadian Geotechnical Journal*, 32(3), 512–534.

[140] Schaefer, V.R. and Koch, J.C. (1992). "Void Development under Bridge Approaches," *Report No. SD90-03*, South Dakota Department of Transportation.

[141] Seo, J. (2003). "The Bump at the End of the Bridge: An Investigation." Dissertation submitted in partial fulfillment of the requirements for the degree of the Doctor of Philosophy, Texas, A&M University, College Station, Texas.

[142] Seo, J., Ha, H. S., and Briaud, J.L. (2002). "Investigation of Settlement at Bridge Approach Slab Expansion Joint: Numerical Simulation and Model Tests." *Report No. FHWA/TX-03/4147-2*, Texas Transportation Institute, Texas A&M University, College Station, Texas.

[143] Serridge, C.J. and Synac, O. (2007). "Ground Improvement Solutions for Motorway Widening Schemes and New Highway Embankment Construction Over Soft Ground." *Ground Improvement Journal*, 11(4), 219–228.

[144] Shen, S.-L., Hong, Z.-S., and Xu, Y.-S. (2007). "Reducing Differential Settlements of Approach Embankments." *Proc. of Institute of Civil Engineers*, Geotechnical Engineering, Issue GE4, 215–226.

[145] Slope Indicator. (1997). Digitilt Inclinometer Probe. Slope Indicator Company, Mukilteo, Washington.

[146] Slope Indicator. (2004). Horizontal Digitilt Inclinometer Probe. Slope Indicator Company, Mukilteo, Washington.

[147] Sluz, A., Sussmann, T. R., and Samavedam, G. (2003). "Railroad Embankment Stabilization Demonstration for High-Speed Rail Corridors." *Grouting and Ground Treatment* (GSP No. 120). 3rd International Specialty Conference on Grouting and Ground Treatment. February 10–12, New Orleans, Louisiana, USA.

[148] Smadi, O. (2001). "The Strength of Flowable Mortar." http://www.ctre.iastate.edu/PUBS/tech_news/2001/julaug/flowable_mortar.pdf.

[149] Snethen, D. R. and Benson, J. M. (1998). "Construction of CLSM Approach Embankment to Minimize the Bump at the End of the Bridge." *The Design and Application of Controlled Low-Strength Materials (Flowable Fill)*, ASTM STP 1331.

[150] Soltesz, S. (2002). "Injected Polyurethane Slab Jacking." *Final Report*, Report No. FHWA-OR-RD-02-19, Oregon Department of Transportation Research Group.

[151] Stark, T. D., Olson, S. M., and Long, J. H. (1995). "Differential Movement at the Embankment/Structure Interface Mitigation and Rehabilitation." *Report No. IABH1, FY 93*, Illinois Department of Transportation, Springfield, Illinois.

[152] Stewart, C. F. (1985). "Highway Structure Approaches." California Department of Transportation, Sacramento, CA.

[153] Strauss, J., Dahnke, D., and Nonamaker, F. (2004). "Compaction Grouting to Mitigate Settlement Beneath Approach Fills, California State Route 73 at Laguna Canyon Road." *Geotechnical Engineering for Transportation Project*, ASCE, 1876–1883.

[154] Tadros, M.K. and Benak, J.V. (1989). "Bridge Abutment and Approach Slab Settlement (Phase I Final Report)." University of Nebraska, Lincoln.

[155] Terzaghi, K. (1943). "Theoretical Soil Mechanics." John Wiley and Sons, New York.

[156] Texas Department of Transportation (TxDOT) (2001). Bridge Design Manual. Texas Department of Transportation, December.

[157] Texas Department of Transportation (TxDOT) (2006). "Report on Texas Bridges." Prepared by the Bridge Division of the Texas Department of Transportation, Austin, Texas.

[158] Timmerman, D.H. (1976). "An Evaluation of Bridge Approach Design and Construction Techniques." *Final Report*, Rep. No. OHIODOT-03-77, Ohio Department of Transportation.

[159] Unified Facilities Criteria (UFC) (2004). "Pavement Design for Roads, Streets, Walk, and Open Storage Area." *Rep. No. UFC 3-250-01FA*, US Army Corps of Engineers.

[160] Vipulanandan, C., Kim, M.G., and O'Neill, M.W. (2004). "Axial Performance of Continuous Flight Auger Piles for Bearing." *Project Report No. 7-3940-2*, Texas Department of Transportation, Austin, Texas.

[161] Wahls, H. E. (1990). *NCHRP Synthesis of Highway Practice No. 159: Design and Construction of Bridge Approaches*. Transportation Research Board, National Research Council, Washington, D.C.

[162] Walkinshaw, J. L. (1978). "Survey of Bridge Movements in the Western United States." *Transportation Research Record 678: Tolerable Movements of Bridge Foundations, Sand Drains, K-Test, Slopes, and Culverts*, Transportation Research Board, National Research Council, Washington, D.C., 6–12.

[163] White, D. J. and Suleiman, M.T. (2004). "Design of Short Aggregate Piers to Support Highway Embankments." 83rd Annual Meeting Transportation Research Board, Washington, D.C.

[164] White, D., Mohamed, M., Sritharan, S., and Suleiman, M. (2007). "Underlying Causes for Settlement of Bridge Approach Pavement Systems." *Journal of Performance of Constructed Facilities*, ASCE, 273–282.

[165] White, D., Sritharan, S., Suleiman, M., Mohamed M., and Sudhar, C. (2005). "Identification of the Best Practices for Design, Construction, and Repair of Bridge Approaches." *CTRE. Project 02-118*, Iowa State University. Ames, Iowa.

[166] White, D.J., Wissman, K., Barnes, A.G., and Gaul, A.J. (2002). "Embankment Support: A Comparison of Stone Column and Rammed Aggregate Pier Soil Reinforcement." *Proc. 81st Annual TRB Meeting*, Washington, D. C.

[167] Wissmann, K. J. and Fox, N.S. (2000). "Design and Analysis of Short Aggregate Piers to Reinforce Soils." Preceedings, Geotechnical Colloquium, Technical University Darmstadt, Fermany, March 25, 2000.

[168] Wolde-Tinsae, A.M, Aggour, S.M., and Chini, S.A. (1987). "Structural and Soil Provisions for Approaches to Bridges." *Interim Report AW087-321-046*, Maryland Department of Transportation.

[169] Won, M. S. and Kim, Y. S. (2007). "Internal Deformation Behavior of Geosynthetic-Reinforced Soil Walls." *Geotextiles and Geomembranes*, 25(1), 10–22.

[170] Wong, H. K. W., and Small, J. C. (1994). "Effect of Orientation of Bridge Slabs on Pavement Deformation." *Journal of Transportation Engineering*, 120(4), 590–602.

[171] Wu, J.T.H., Lee, K.Z.Z., Helwany, B. S., and Ketchart, K. (2006). "Design and Construction Guidelines for Geosynthetic-Reinforced Soil Bridge Abutments with a Flexible Facing." *Proc. NCHRP Report 556*. Transportation Research Board, Washington, D.C.

[172] Wu, J.T.H., Lee, K.Z.Z., and Ketchart, K. (2003). "A Review of Case Histories on GRS Bridge-Supporting Structures with Flexible Facing." Proc. 82nd Annual TRB Meeting.

[173] Zelada, G. A. and Stephenson, R. W. (2000). "An Evaluation of Auger Cast-in-Place Pile Design Methodologies for Compression Loading." *Proc. of Int. Conf. on New Technological and Design Developments in Deep Foundations*, Geo-Denver 2000, ASCE, August 5–8, 2000, Denver.